UNIVERSITY OF CALGARY

Synthesis of Nitrogen Heterocycles Using Unsaturated Sulfones

by

Huimin Zhai

A THESIS

SUBMITTED TO THE FACULTY OF GRADUATE STUDIES

IN PARTIAL FULFILLMENT OF THE REQUIREMENTS FOR THE

DEGREE OF DOCTOR OF PHILOSOPHY

DEPARTMENT OF CHEMISTRY

CALGARY, ALBERTA

November, 2006

Your file Votre référence
ISBN: 978-0-494-25721-0
Our file Notre référence
ISBN: 978-0-494-25721-0

Abstract

Acetylenic sulfones are versatile synthetic reagents that undergo conjugate addition reactions with amine nucleophiles at the β-position. The α-protons of the resulting vinyl sulfones can then be deprotonated with a suitable base and the resulting anions can in turn react with a variety of electrophiles. If the amine also contains a suitable electrophilic substituent, intramolecular cyclization results in the formation of a nitrogen heterocycle. Acetylenic sulfones can also undergo a variety of Diels-Alder and 1,3-dipolar cycloadditions. Four applications of the previously developed addition-cyclization methodology and of other properties of acetylenic sulfones were further studied.

First, the methodology using acetylenic sulfones was extended toward the preparation of saturated sulfone products by conjugate additions of amino alcohols derived from α-amino acids to vinyl sulfones, followed by *N*-benzylation, chlorination and intramolecular alkylation. This approach to substituted pyrrolidines was accompanied by the stereospecific rearrangement of substituents from the α-position of the amine to the β-position of the product via aziridinium ion intermediates during the chlorination step. Another type of rearrangement was observed during the reaction of (2-piperidine)methanol or 2-(2-piperidine)ethanol with phenyl *trans*-1-propenyl sulfone, in which the methyl group appeared to migrate from the β- to the α-position of the sulfone moiety. This resulted from isomerization of the original sulfone to phenyl 2-propenyl sulfone via addition-elimination of sulfinate anion, followed by cyclization with the amino alcohol in the usual manner.

Secondly, the first syntheses of polymer-supported acetylenic sulfones were achieved and their applications to the preparation of various cyclized products were exploited.

Thirdly, several unexpected rearrangements were observed during the reaction of acetylenic sulfones with 1,3-diphenylisobenzofuran (DPIBF). The mechanisms of these rearrangements of the Diels-Alder cycloadducts were investigated under pyrolytic, acid-catalyzed and photolytic conditions. The mechanisms involved carbocation rearrangements or pericyclic processes, depending on the conditions.

In addition, the synthesis of (-)-julifloridine was accomplished from (2*S*,3*S*)-2-benzyloxy-3-benzylamino-1-chlorobutane and 3-(*t*-butyldimethylsilyloxy)-1-(*p*-toluenesulfonyl)-1-propyne in an overall 20% yield over seven steps. The established

conjugate addition and cyclization reactions yielded an enamine sulfone, which underwent acid-catalyzed desulfonylation to afford an enamine aldehyde. Stereoselective reduction, followed by a Swern oxidation constructed the 2,6-*trans* disubstituted piperidine. Chain extension and hydrogenation, followed by a Birch reduction, afforded the target alkaloid.

Acknowledgements

I sincerely thank my supervisor, Dr. Thomas G. Back for his encouragement and assistance over the course of my program.

I would like to acknowledge the assistance of Ms. Bonnie King for all the academic matters related to the graduate program. I also thank Ms. Dorothy Fox, Ms. Qiao Wu, Ms. Roxanna Smith, Ms. Olivera Blagojevic and Dr. Raghav Yamdagni for technical assistance, as well as Dr. Masood Parvez for X-ray crystallography.

I would also like to thank my fellow lab members Dr. Zhaohua Yan, Dr. Sultan Chowdhury, Dr. Ziad Moussa, Dr. Jeremy Wulff, Dr. Xianghui Wen, Dr. Srini Manivannan, Dr. Kannan Vembaiyan, Mike Hamilton, Jerry Taylor, Michael Bey, Stephanie Sibley, Vania Lim, Mitch Weston, Jovina Sorbetti, Dusan Kuzma, Danica Rankic, Amir Zuccolo, Detian Gao, Violeta Iosub, Kristine Clary, and David Press.

Finally, I would like to acknowledge the University of Calgary, NSERC, and Merck Frosst (Canada) Ltd. for their financial support.

For Cathy and my Family

Table of Contents

List of Tables

List of Schemes

List of Figures

List of Abbreviations

Å	Ångstroms
Ac	acetyl
Anal.	elemental analysis
AIBN	2,2'-azobis(2-isobutyronitrile)
Ar	aryl
aq.	aqueous
ax	axial
B^-	base
9-BBN	9-borabicyclo[3.3.1]nonane
BHA	benzhydrylamine
BHT	butylated hydroxytoluene
BOC	*t*-butoxycarbonyl
Bn	benzyl
br	broad
Bu	butyl
Bz	benzoyl
°C	degrees Celsius
c	concentration
ca.	circa
cat.	catalytic
Cbz	carbobenzyloxy
cm^{-1}	reciprocal centimeters – wavenumbers
^{13}C NMR	carbon-13 nuclear magnetic resonance
conc.	concentrated
COSY	^1H - ^1H correlation spectroscopy
d	doublet or days
δ	chemical shift in ppm downfield from tetramethylsilane
DBU	1,8-diazabicyclo(5.4.0)undec-7-ene
DCC	1,3-dicyclohexylcarbodiimide

DCM	dichloromethane
dd	doublet of doublets
DDQ	2,3-dichloro-5,6-dicyano-1,4-benzoquinone
dec.	decomposed
DIBAL-H	diisobutylaluminum hydride
DIPEA	diisopropylethylamine
DMAD	dimethyl acetylenedicarboxylate
DMAP	*N,N*-dimethyl-4-aminopyridine
DMDO	dimethyldioxirane
DME	dimethyl ether
DMF	*N,N*-dimethylformamide
DMSO	dimethyl sulfoxide
DPIBF	1,3-diphenylisobenzofuran
dppp	1,3-bis(diphenylphosphio)propane
dt	doublet of triplets
E^+	electrophile
e.e.	enantiomeric excess
e.g.	for example
equiv.	equivalents
ESI	electrospray ionization
Et	ethyl
eq	equatorial
g	grams
H^+	acid
h	hours
HMBC	heteronuclear multiple bond correlation
HMQC	heteronuclear multiple quantum coherence
^{1}H NMR	proton nuclear magnetic resonance
HPLC	high performance liquid chromatography
$h\nu$	light
Hz	Hertz

IR	infrared
Im	imidazale
i-Pr	*iso*-propyl
J	coupling constant
LAH	lithium aluminum hydride
LDA	lithium diisopropylamide
LDBB	p,p′-di-*tert*-butylbiphenyl lithium
LHMDS	lithium hexamethyldisilazide
LUMO	lowest unoccupied molecular orbital
lit.	literature
M	molar
MAS	magic angle spinning
m	multiplet
M^+	molecular ion
MALDI-TOF	matrix-assisted laser desorption/ ionization-time-of-flight
*m*CPBA	*m*-chloroperbenzoic acid
Me	methyl
Mes	mesityl
mg	milligrams
MHz	megahertz
min	minutes
mL	milliliters
mm	millimeters
mmol	millimoles
MOM	methoxymethyl
mp	melting point
MAS	magic angle spinning
MNDO	modified neglect of diatomic overlap
MS	mass spectrometry
Ms	methylsulfonyl
M.Sc.	Master of Science

m/z	mass to charge ratio
nm	nanometers
NMO	4-methylmorpholine *N*-oxide
NOE	nuclear overhauser effect
Nu	nucleophile
ORTEP	Oak Ridge Thermal Ellipsoid Plot
P	general protecting group or symbol for phosphorus
p-	para
Ph	phenyl
ppm	parts per million
psi	pounds/square inch
PTC	phase transfer catalyzed
q	quartet
R	generalized alkyl group or substituent
rt	room temperature
s	singlet
SPOS	solid-phase organic synthesis
t	triplet
td	triplet of doublets
t- or *tert*	tertiary
TBAF	tetrabutylammonium fluoride
TBDPS	*t*-butyldiphenylsilyl
TBS	*t*-butyldimethylsilyl
Tf	trifluoromethanesulfonyl
TFA	trifluoroacetic acid
THF	tetrahydrofuran
THP	tetrahydropyran
TLC	thin layer chromatography
TMEDA	*N,N,N',N'*-tetramethylethylenediamine
TMS	trimethylsilyl
Ts	*p*-toluenesulfonyl

Chapter 1
Introduction

1.0 Overview

Nitrogen hetereocycles occur in nature as alkaloids and these and numerous synthetic analogues are of importance in the pharmaceutical industry. As a result, the development of new synthetic methods to prepare existing compounds of this class more efficiently and to provide access to novel nitrogen hetereocycles for future applications is an area of intense activity. Our group recently developed several new protocols for the preparation of nitrogen hetereocycles via cyclization reactions of unsaturated sulfones. The present thesis describes several extensions of this work based on vinyl and acetylenic sulfones. These include the discovery of novel rearrangements during the use of vinyl sulfones for this purpose, the preparation of the first acetylenic sulfones attatched to solid supports and the total synthesis of (-)-julifloridine, a piperdine alkaloid. In order to place these results into an appropriate literature context, this chapter will provide a brief review of acetylenic and vinyl sulfones, as well as of solid phase organic synthesis. Several unexpected rearrangements were observed during the reaction of acetylenic sulfones with 1,3-diphenylisobenzofuran (DPIBF) in the course of the present work, and a survey of related chemistry that has been reported previously for the transformations of DPIBF and its cycloadducts will also be provided in this chapter. Finally, the properties and earlier syntheses of julifloridine and related piperidine alkaloids will be reviewed. Subsequent chapters will then describe our own results in each of these respective areas.

1.1 Acetylenic Sulfones

1.1.1 Background

The chemistry of unsaturated sulfones is a rich topic that has recently been thoroughly reviewed.[1] In particular the β–position of a typical acetylenic sulfone **1** is electrophilic, allowing it to react with nucleophiles (e.g. amines) via conjugate addition

reactions. Due to the sulfone's ability to stabilize α-anions, the vinyl sulfone intermediates may be deprotonated with strong bases. The resulting anions can in turn react with electrophiles to produce α,β-unsaturated sulfones **2**, as shown in Scheme 1.1. Since **2** are also electrophilic, they can undergo a second sequence of similar reactions to arrive at the saturated compound **3**. When an appropriately functionalized amine is tethered to the electrophile the overall process can proceed in an intramolecular fashion to give the corresponding nitrogen heterocycle. Acetylenic sulfones can also undergo a variety of Diels-Alder and 1,3-dipolar cycloadditions. These processes are illustrated in Scheme 1.1. Introduction of a sulfone group causes a substantial lowering of the LUMO energy level in an alkyne. Consequently the sulfone group increases the electrophilicity of the alkyne. Other notable features of sulfones, including their ease of handling (many are nicely crystalline) and general lack of offensive odours have added to the attractions of these compounds as synthetic intermediates. Moreover, the sulfone group can be removed at the end of a synthetic sequence by a variety of reductive, alkylative, or oxidative methods, where the sulfonyl moiety is replaced by hydrogen, an alkyl group from a suitable organometallic cross-coupling reagent, or an oxygen function, respectively.[2]

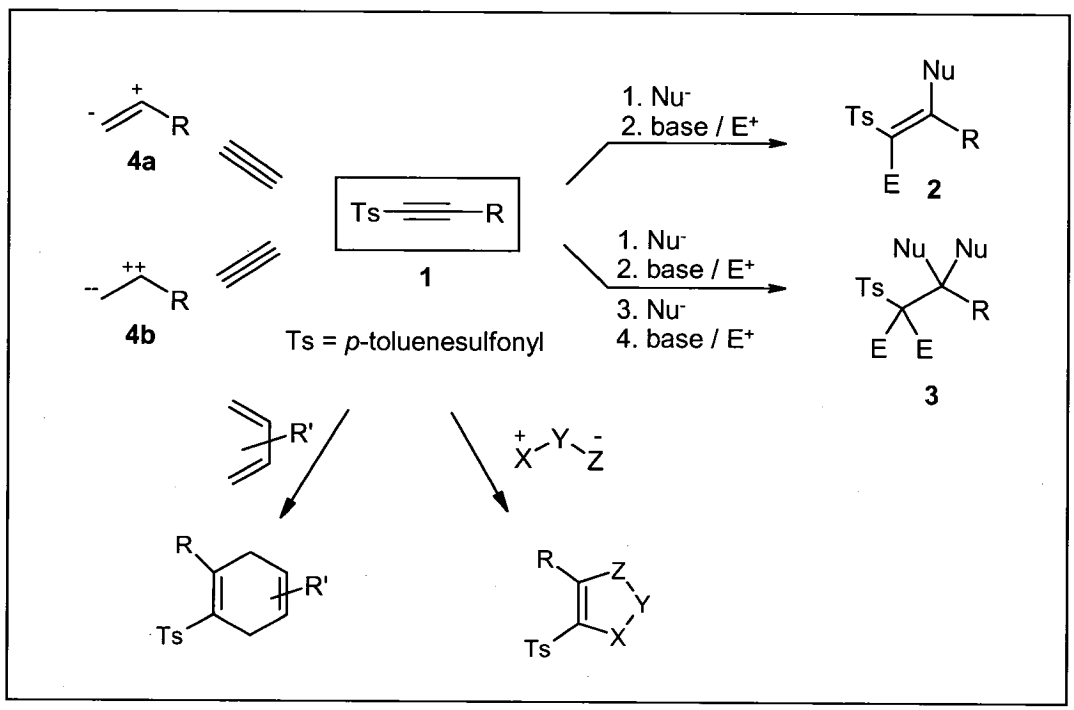

Scheme 1.1 Conceptual View of Acetylenic Sulfones

Overall, the acetylenic sulfone may be seen as a disposable activating group. Because of all these possible transformations, acetylenic sulfones can act as synthetic equivalents of hypothetical alkene dipoles **4a** or alkane multipoles **4b**.

1.1.2 Preparation of Acetylenic Sulfones

The synthesis of acetylenic sulfones has been extensively studied, and there exist a variety of methods to obtain these compounds.[1d] One of these methods was developed by our group, and involves a very straightforward and convenient process, based on the additions of selenosulfonates to unsaturated organic substrate,[3] named 'selenosulfonation' by Back and Collins (see Scheme 1.2).

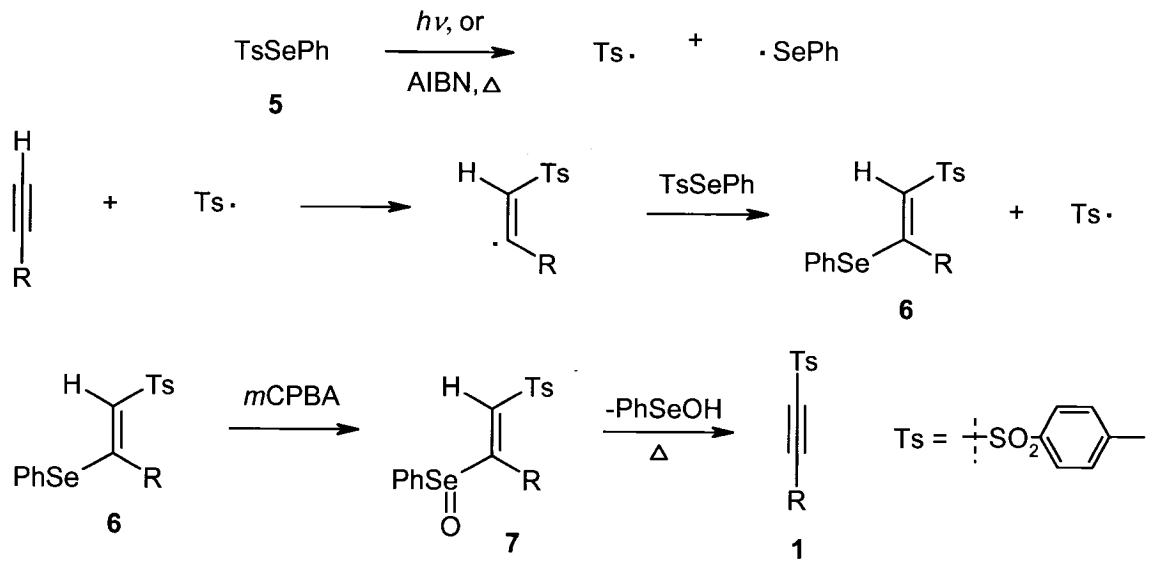

Scheme 1.2 Selenosulfonation of Acetylenes to Prepare Acetylenic Sulfones

The free-radical addition of selenosulfonate **5**[4] to acetylenes can be initiated by either photolysis or pyrolysis in the presence of a free-radical initiator such as AIBN. The first step is the homolytic cleavage of the selenosulfonate to give a phenylselenyl and a sulfonyl radical. Reaction between the sulfonyl radical and the terminus of the acetylene affords a vinyl radical which subsequently reacts with another selenosulfonate molecule to give the *anti*-addition product, while regenerating the sulfonyl radical that is required to

propagate the resulting chain reaction. An attractive feature of this reaction is that the addition of the selenosulfonate across the acetylene proceeds in a highly regio- and stereoselective manner. Thus, when the vinyl selenide **6** is oxidized to the selenoxide **7**, *syn*-elimination occurs to produce the corresponding acetylenic sulfone **1**.

Although there exist many other methods to prepare acetylenic sulfones,[1d] this procedure was the only one employed in the present work as it readily provided the required acetylenic sulfone starting materials.

1.1.3 Conjugate Additions of Amines to Acetylenic Sulfones

The use of acetylenic sulfones in cycloadditions, radical reactions, and various types of conjugate additions is well documented, and will not be explored in great depth here. It is the conjugate addition of amine nucleophiles containing pendant electrophilic groups, which is most pertinent to the discussion at hand. The utilization of amines as nucleophiles in conjugate addition reactions with acetylenic sulfones was explored thoroughly in the 1960's and 1970's by Stirling[5] and Truce.[6] Conjugate addition occurs at the electrophilic β-position to give the corresponding vinyl sulfone. In the case of a primary amine, both the *cis* and *trans* vinyl sulfones are produced, while when a secondary amine is employed, only the *trans* product is obtained (see Scheme 1.3).

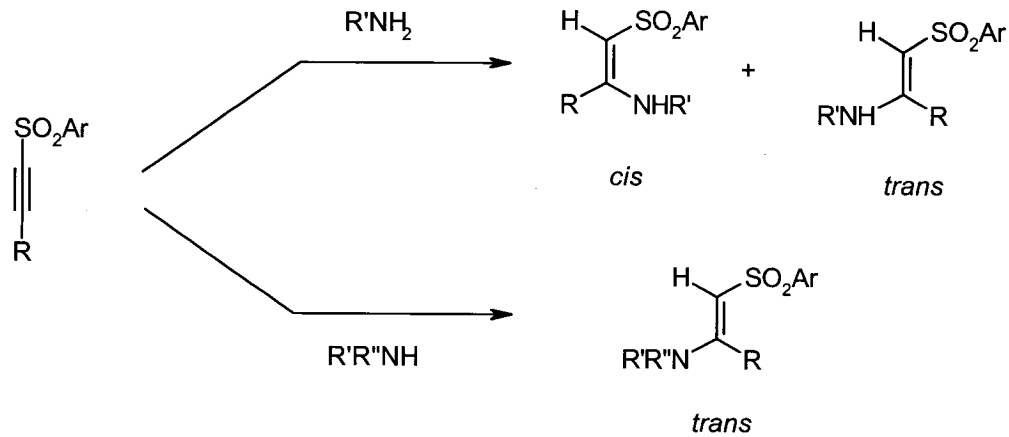

Scheme 1.3 Conjugate Additions of Amines to Acetylenic Sulfones

Further investigation by Stirling [7] and Truce[6] found that both primary and secondary amines react initially in an *anti* fashion to give the *cis* product. In the case of a primary amine, hydrogen bonding occurs between the remaining amine hydrogen atom and a sulfone oxygen to stabilize the *cis* isomer. The formation of the otherwise more thermodynamically favored *trans* isomer is a consequence of dipole repulsions between the amine and the sulfone moiety, and results in partial isomerization of the initially formed *cis* product via an iminium ion, thus giving a mixture of *cis*/*trans* products. When the amine is secondary, the stabilizing hydrogen bonding is absent, and therefore, the sole or main product is the *trans* adduct.

1.1.4 Cyclizations via Sulfone-Stabilized Carbanions

When the amine contains an appropriate leaving group, ring-closure via intramolecular alkylation or acylation of a sulfone-stabilized anion becomes possible.[8] There are three types of closures: if we start with a primary amine in the conjugate addition, the hydrogen of the NH group is acidic and, after deprotonation, the enamide anion **8** is generated. On the other hand, if we start with a secondary amine and there is no γ-hydrogen atom in the R substituent, the electron-withdrawing property of the sulfone group activates α-protons to abstraction by a suitable base. The resulting sulfone-stabilized vinyl carbanion **9** can undergo intramolecular alkylation. Finally if we start with a secondary amine where there exists a γ-hydrogen atom in the R substituent, then the allylic hydrogen atom will be deprotonated to form the allyl sulfone anion **10** rather than the vinyl sulfone anion **9**. Intramolecular alkylation at the α-position of the sulfone affords a similar product. These processes are shown in Scheme 1.4.

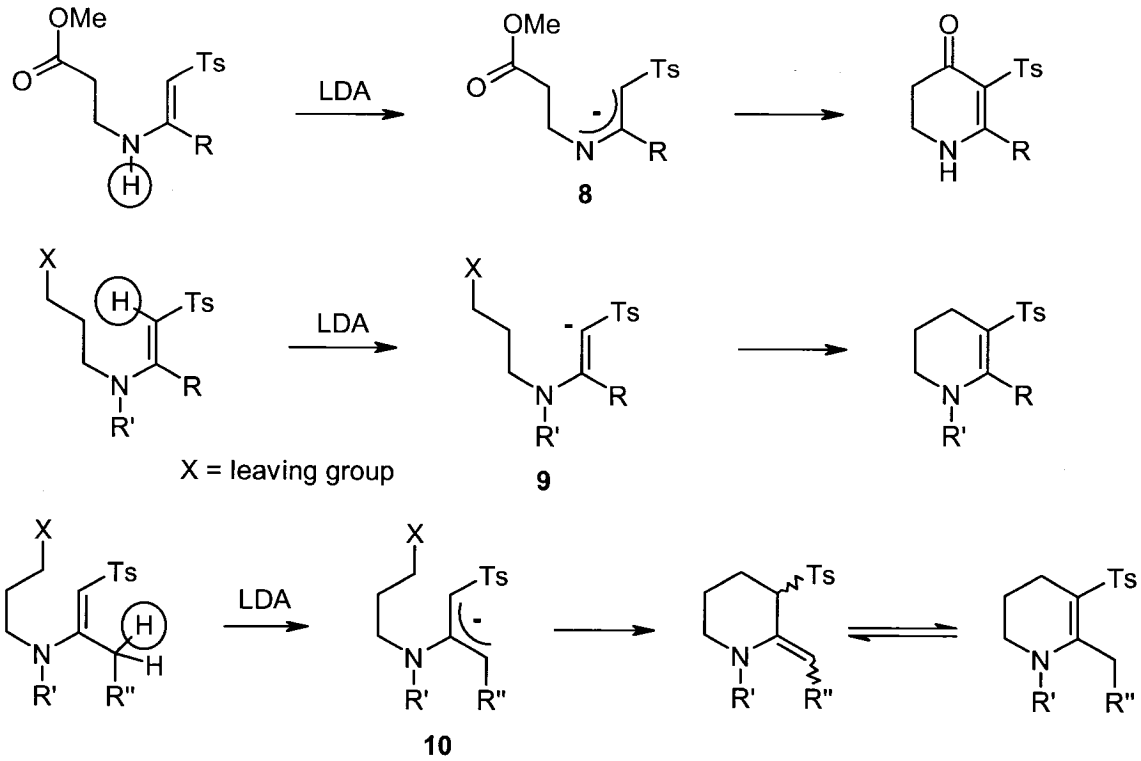

Scheme 1.4 Sulfone-Based Intramolecular Cyclizations

1.1.5 Reductive Desulfonylation

As mentioned previously, an advantage of the sulfone group is that it can be removed when it becomes no longer necessary. There exists a wide range of reductive procedures to effect this transformation selectively,[2] which often permits the removal of the sulfone group without affecting other existing functional groups. Some of the most common procedures call for the use of sodium[9] or aluminum[10] amalgams or dissolving metals in liquid ammonia (i.e. sodium, lithium). One of the mildest conditions uses magnesium in refluxing methanol.[11] A few examples are given in Scheme 1.5.[12]

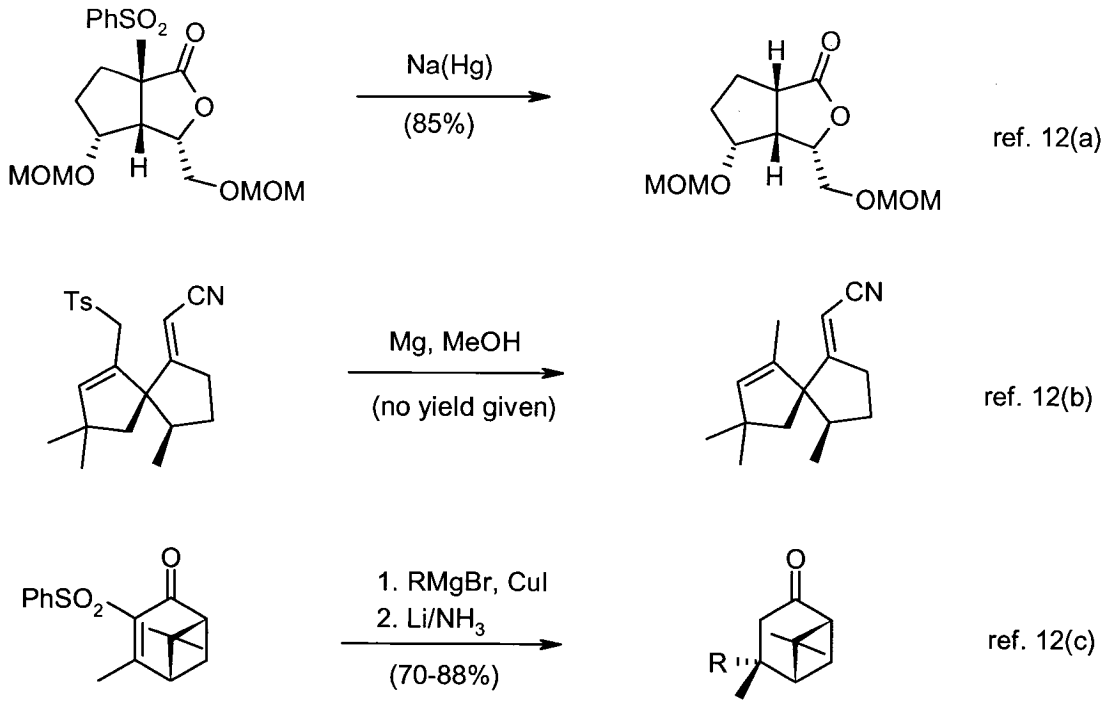

Scheme 1.5 Reductive Desulfonylations

1.1.6 Applications of the Acetylenic Sulfone-Based Cyclization Methodology to the Synthesis of Some Natural Products

In 1999, Back and Nakajima published a novel route to a variety of nitrogen-containing ring systems, based upon the conjugate additions of amino acid derivatives. Specifically, additions of **11** - **13** to a variety of acetylenic sulfones (see Scheme 1.6) afforded enamine sulfone intermediates, which were then treated with LDA to effect intramolecular acylation (in the case of **11**) or alkylation (in the case of **12** or **13**), providing access to cyclic enaminone or enamine targets **14** - **16**.[13]

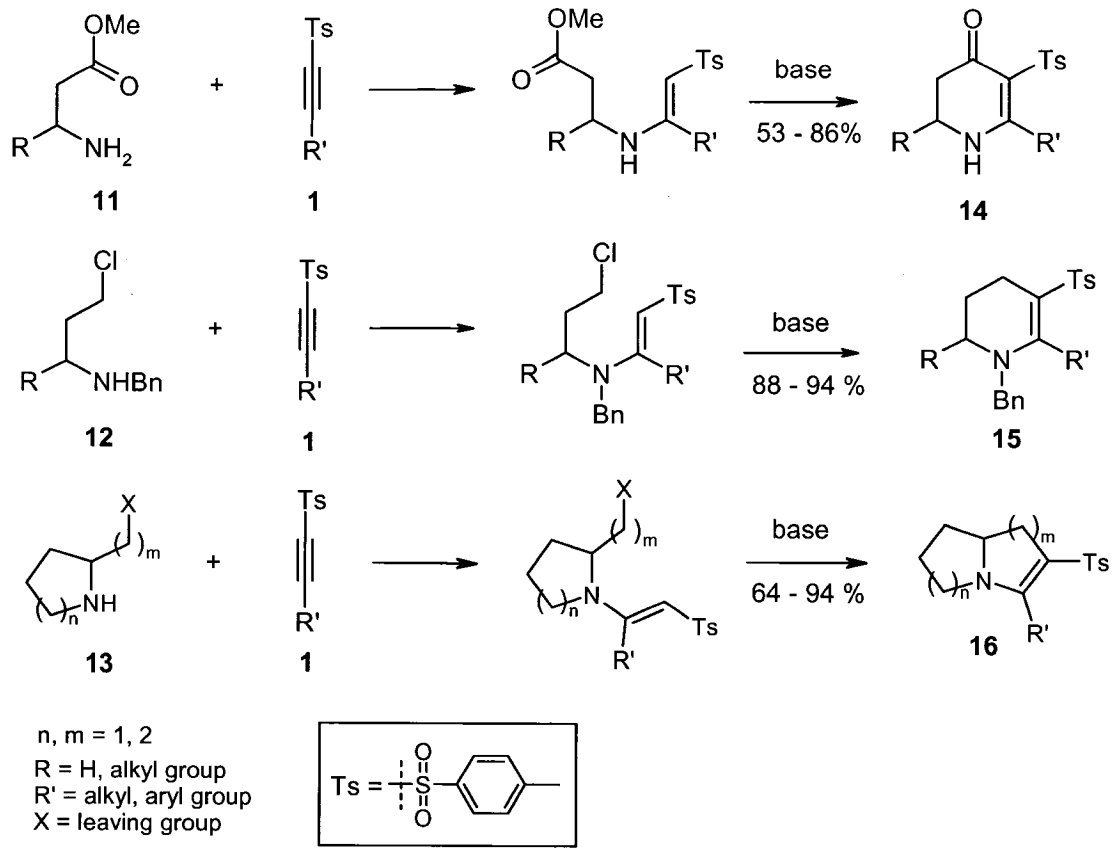

Scheme 1.6 Back and Nakajima's Approach to Nitrogen Heterocycles

There exists a great deal of flexibility in this two-step protocol in that the sizes and the number of rings formed can be adjusted by varying the starting materials. As well, cyclization can occur via either α-alkylation or α-acylation, thus providing variety in the products formed and in the types of transformations that could follow. As a result of this versatility, a whole host of nitrogen heterocycles becomes accessible through this methodology. Figure 1.1 shows the core structures of the types of target molecules that have been prepared by this method,[13b] following further functional group manipulation and reductive desulfonylation. The portion of the product originating from the acetylenic sulfone is shown in bold.

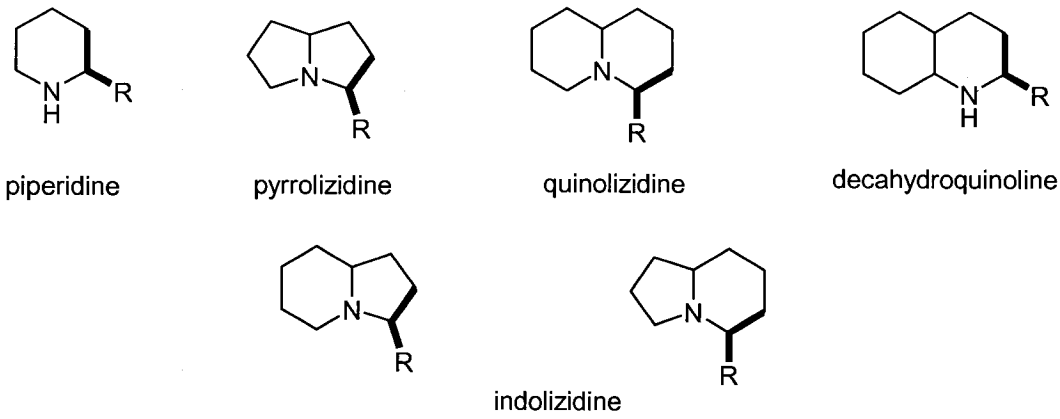

Fig. 1.1 Core Structures of Target Molecules

This protocol has been successfully applied to the synthesis of various alkaloids by our group over the past several years (Fig. 1.2). Thus, Back and Nakajima synthesized the dendrobatid alkaloids indolizidines (-)-167B, (-)-209D, (-)-209B, and (-)-207A.[13]

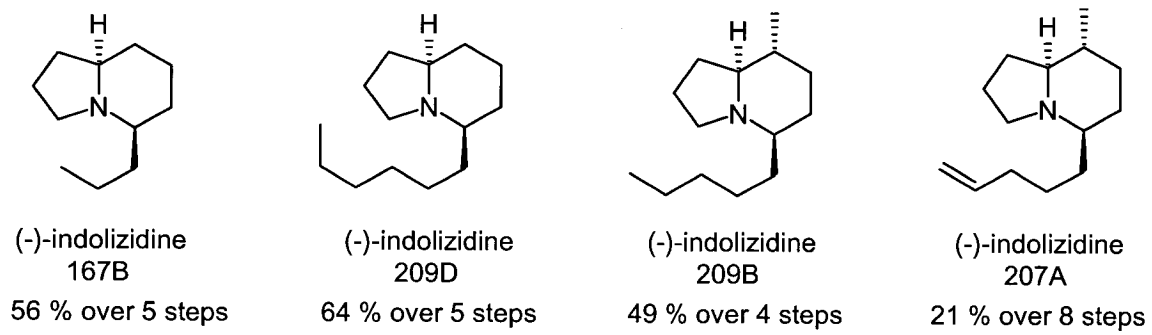

Fig. 1.2 Dendrobatid Alkaloids Prepared by Back and Nakajima

In a related approach to a somewhat more challenging natural product, Back and Nakajima completed an enantioselective total synthesis of (-)-pumiliotoxin C from enantiomerically pure amino ester **17** and acetylenic sulfone **18**, as shown in Scheme 1.7.[13c]

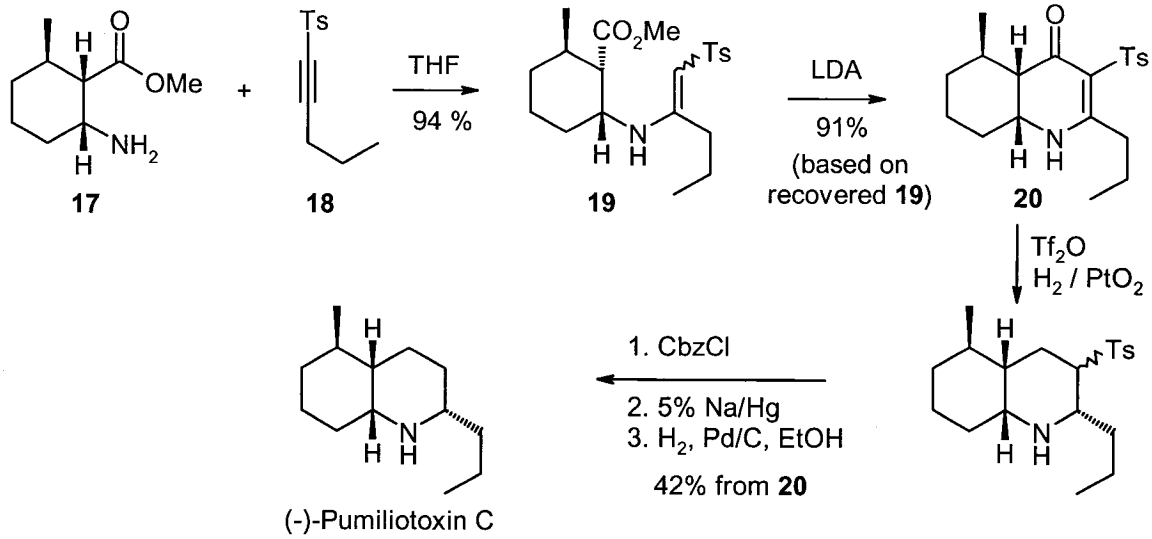

Scheme 1.7 Enantioselective Synthesis of (-)-Pumiliotoxin C

Back and Hamilton demonstrated the applicability of this methodology to the synthesis of α-aryl-substituted quinolizidine alkaloids, by completing an enantioselective synthesis of (-)-lasubine II, as shown in Scheme 1.8.[14]

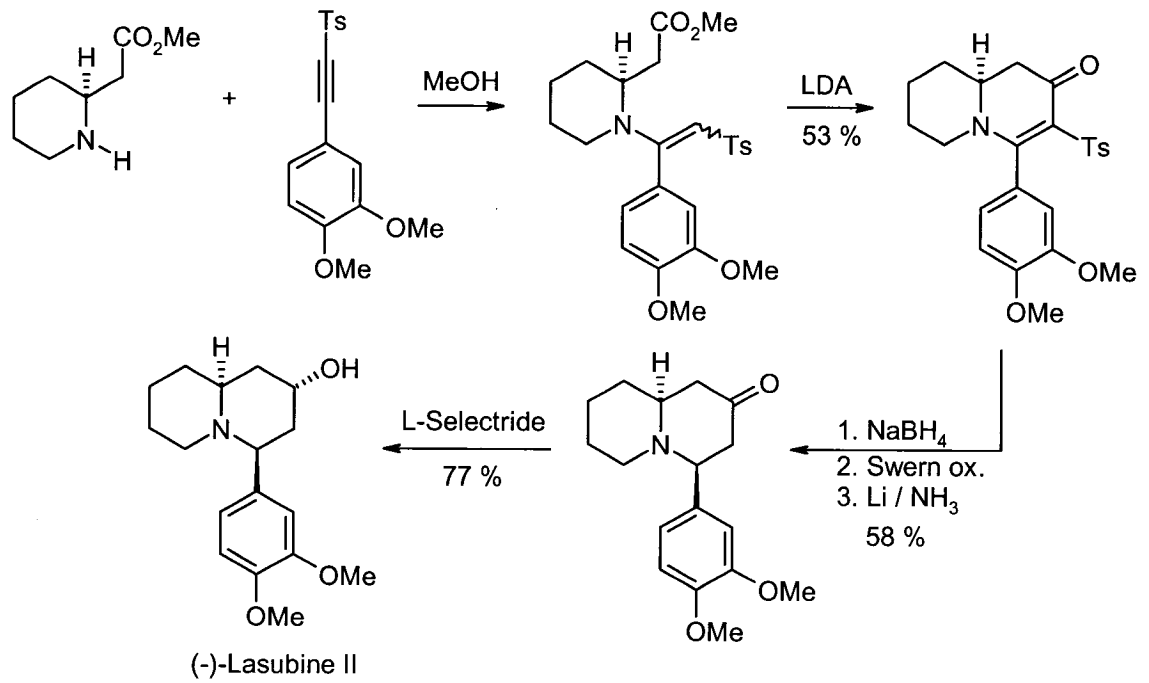

Scheme 1.8 Back and Hamilton's Synthesis of (-)-Lasubine II

More recently, Back and Lim reported the similar reaction of (2-piperidyl)acetate ester **(21)** with the appropriate acetylenic sulfone **22**, which provided a concise new route to the corresponding 4-substituted 2-ketoquinolizidine alkaloid (+/-)-myrtine (see Scheme 1.9).[15]

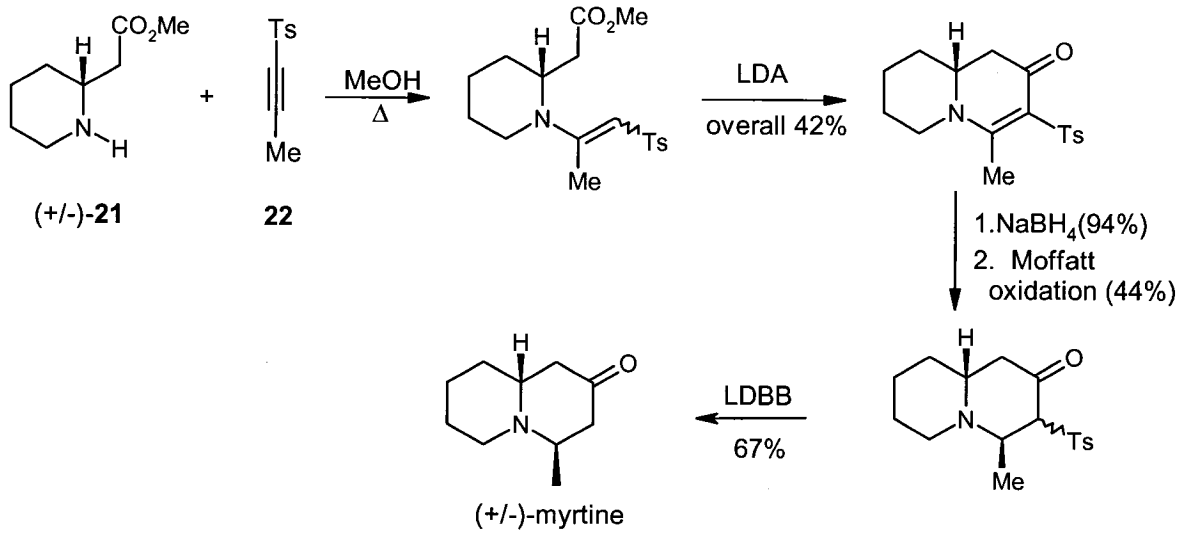

Scheme 1.9 Back and Lim's Synthesis of (+/-)-Myrtine

Additionally, the use of anilines instead of aliphatic amines as the nucleophiles in the conjugate addition reaction was demonstrated by Back and Wulff[16] to afford aromatic heterocycles such as 4-quinolones, quinolines, and tetrahydroquinolines (see scheme 1.10, where the bold part is used to indicate the molecular fragment originating from the acetylenic sulfone), which are known to possess useful biological activity. They reported the first syntheses of the quinolone alkaloids **23** and **24**, as shown in Scheme 1.10, which had been isolated from *Ruta chalepensis*, a shrub that grows in the northern Saudi desert and is used in local folk medicine.[17]

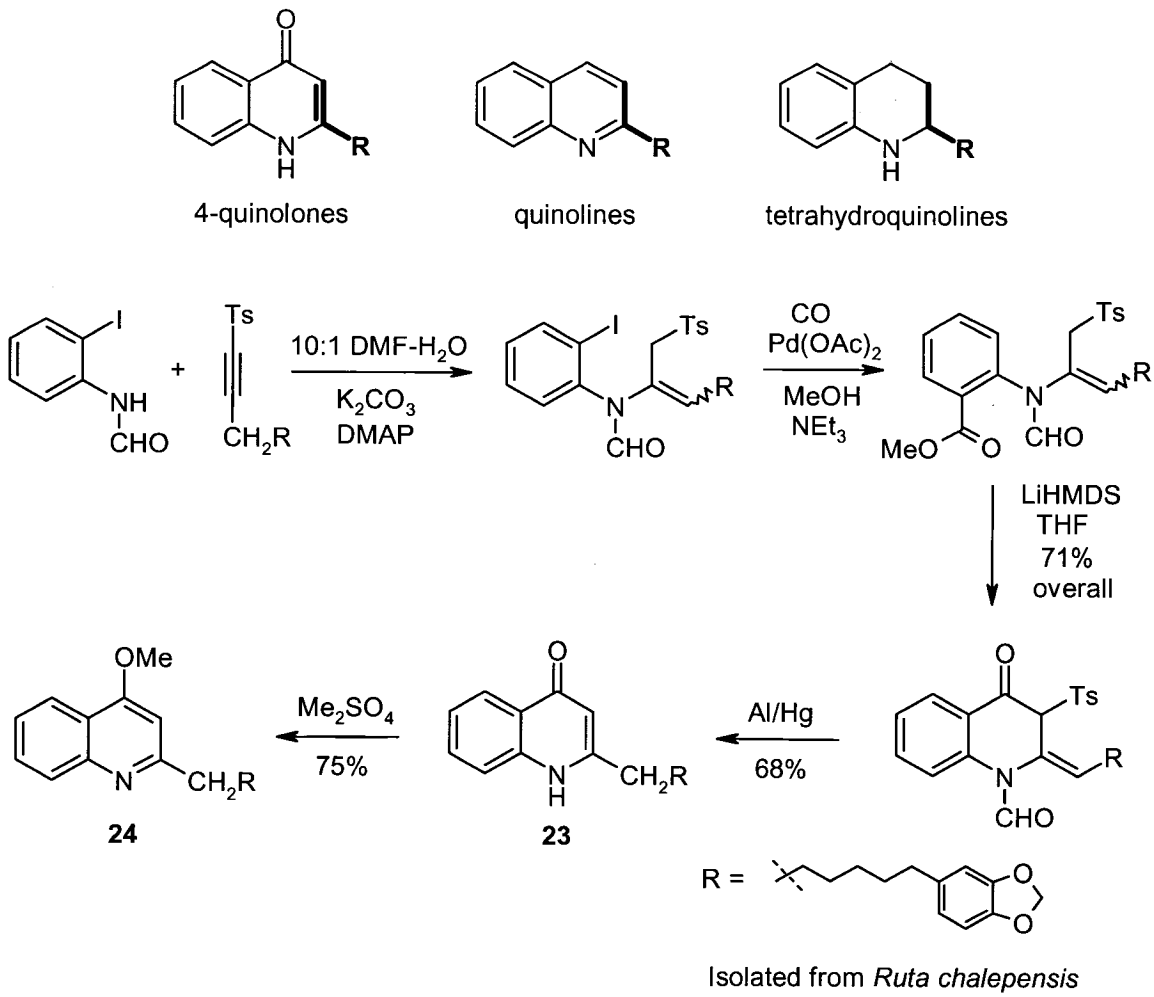

Scheme 1.10 Back and Wulff's Synthesis of Quinoline Alkaloids **23** and **24**

1.2 Vinyl Sulfones

1.2.1 Background

Like acetylenic sulfones, vinyl sulfones have also proven to be versatile synthetic reagents.[18] We wished to explore the possibility that the activating and electron-withdrawing effects of the sulfone moiety would enable these compounds to undergo conjugate additions and cycloadditions, as well as deprotonation and alkylation of the corresponding α-anions similar to those that had been previously established for acetylenic sulfones. Again, the sulfone group can be removed at the end of a synthetic sequence by a

variety of reductive, alkylative, or oxidative methods. Vinyl sulfones have now become generally accepted as useful intermediates in organic synthesis and many methods for preparing them are readily available, some of which provide a high degree of regio- and stereoselectivity. The preparation and synthetic applications of vinyl sulfones will be described in more detail in the following sections. This will provide a background and literature context for a description of our own work on cyclization reactions of vinyl sulfones, as well as some novel rearrangements discovered during the course of this work, that will be the subject of Chapter 2.

1.2.2 Preparation of Vinyl Sulfones

1.2.2.1 Oxidation of the Corresponding Sulfide

The simplest approach to the synthesis of vinyl sulfones is the oxidation of the corresponding sulfide. The most common oxidant is hydrogen peroxide, generally in acetic acid.

Paquette and Carr developed a synthesis of phenyl vinyl sulfone **(27)** which appeared in *Organic Syntheses*.[19] Controlled phase-transfer catalyzed (PTC) alkylation of benzenethiol with 1,2-dibromoethane under nitrogen furnished 2-bromoethyl phenyl sulfide **(25)**, treatment of which with sodium ethoxide gave phenyl vinyl sulfide **26** in 50-65% yield on a 1 mole scale (see Scheme 1.11). Hydrogen peroxide in acetic acid oxidized **26** to phenyl vinyl sulfone **(27)** in 74-78 % yield. This method can be applied to other vinyl sulfones and generally offers high yields, except where oxidation of the olefin moiety competes effectively. It's evident that this method is most useful in those cases where the vinyl sulfide precursor is itself readily available. Unfortunately, the last step requires handling of the unpleasant and unstable vinyl sulfide.

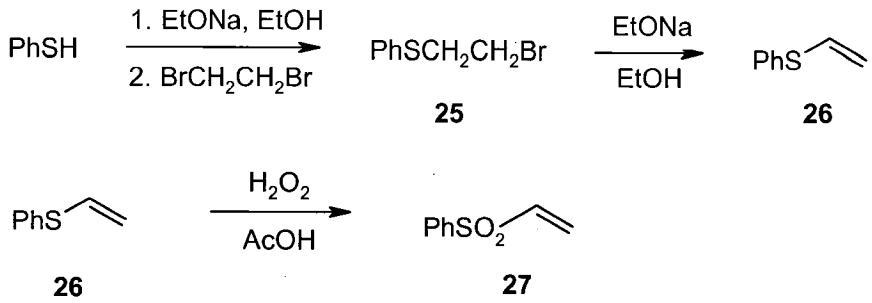

Scheme 1.11 Synthesis of Vinyl Sulfones via Oxidation of the Corresponding Sulfide

A few years later, Brace revised the above method, offering a more practical, versatile high-yielding synthesis of phenyl vinyl sulfones.[20] As shown in Scheme 1.12, the biphasic PTC reaction of benzenethiol in benzene solution with aqueous NaOH gave sulfide **28** in 88% yield. Then, oxidation of **28** with hydrogen peroxide in acetic acid afforded the corresponding alkyl sulfone **29**. Elimination of HCl from **29** occurred rapidly and **27** was isolated quantitatively.

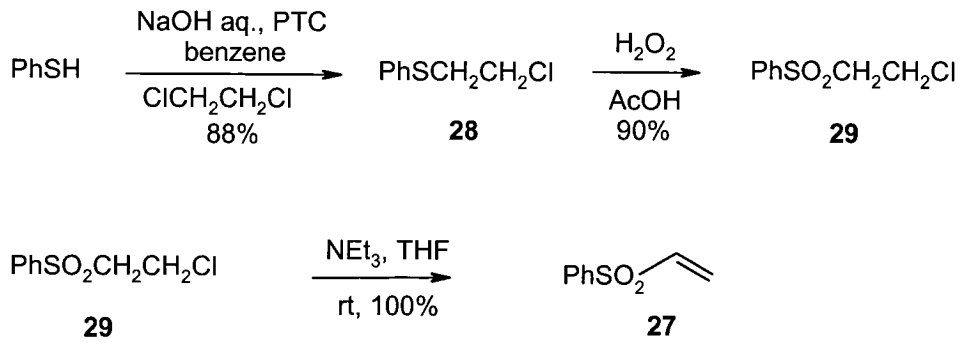

Scheme 1.12 Brace's Revised Synthesis of Vinyl Sulfones

1.2.2.2 Radical and Ionic Additions to Alkenes

Another very broadly applicable strategy for the preparation of vinyl sulfones involves the free radical addition of $ArSO_2X$ **(30)** to olefins. The resulting β-heterosubstituted sulfone **31** can then undergo elimination of HX to afford the desired vinyl sulfones **32** (see Scheme 1.13). The ideal reagent $ArSO_2X$ would undergo such

additions efficiently and with a high degree of control over the regio- and stereochemical outcome. Moreover, the group X should be readily eliminated, preferably without the need for extreme pH conditions.

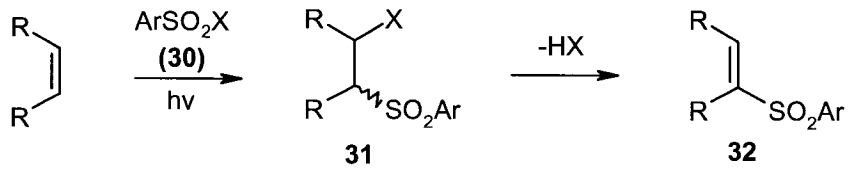

Scheme 1.13 Synthesis of Vinyl Sulfones via Radical Additions

Perhaps the most obvious choice of reagent for this purpose would be a sulfonyl halide. However, this approach lacks many of the desired features identified above. Addition reactions of sulfonyl chlorides and bromides generally proceed in low yield due to competing polymerization reactions and the stereo- and regioselectivity is often poor.[21] Sulfonyl iodides overcome some of these difficulties. Thus, Liu *et al.* carried out the radical addition of preformed $PhSO_2I$ or TsI to alkenes in the presence of catalytic amounts of $CuCl_2$.[22] Sulfonyl iodides, however, are themselves unstable and less easy to handle. An indirect but versatile approach involving electrophilic chlorosulfenylation-dehydrochlorination has been used by Fuchs to prepare a variety of cyclic vinyl sulfones (e.g. see Scheme 1.14).[23]

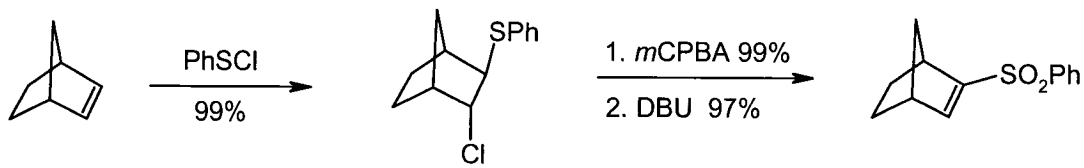

Scheme 1.14 Fuchs' Method to Synthesize Cyclic Vinyl Sulfones

An interesting alternative is to employ compounds $ArSO_2X$ **(30)** where X = SeR. As mentioned in section **1.1.2**, the synthetic importance of the selenosulfonation reaction

stems from its high regio- and stereoselectivity, and from the ability of the phenylseleno group to undergo facile selenoxide *syn*-elmination. The selenosulfonation of olefins can be performed by either heterolytic or homolytic cleavage of the Se-S bond. Electrophilic addition of the selenosulfonate[3b] requires catalysis by a Lewis acid such as boron trifluoride etherate. The reaction is believed to involve a seleniranium ion **33**, similar to that postulated in the electrophilic addition of selenenyl halides or pseudohalides to olefins.[24] As expected, the reaction is highly stereospecific, giving *anti*-adducts from 1,2-disubstituted alkenes, and highly regioselective favoring the Markovnikov products as in the case of **34**. Subsequent oxidation, followed by selenoxide elimination, then affords the corresponding vinyl sulfones **35** in excellent yields. Alternatively, the homolytic reaction can be performed thermally by refluxing the reactants in chloroform or benzene in the presence of a radical initiator such as AIBN,[25, 3b] or photochemically by irradiating with UV light.[26] The mechanism was determined to be a free radical chain reaction as shown in Scheme 1.15. The sulfonyl radical **36**, formed by the homolysis of the selenosulfonate, adds to the less substituted carbon atom of the olefin to generate the β-sulfonylalkyl radical **37**, which then attacks the selenium moiety of another molecule of the selenosulfonate. The chain transfer step affords the 1,2 adduct **38** and regenerates the sulfonyl radical. The product obtained has anti-Markovnikov orientation consistent with the indicated free radical addition mechanism. Oxidation, followed by selenoxide elimination, then affords the corresponding vinyl sulfones **39** in excellent yields. Thus, products with complementary regiochemistry can be obtained by carrying out the selenosulfonation under electrophilic or free radical conditions. Cyclic olefins afford products of *anti*-addition exclusively, under both electrophilic and free radical conditions (see Scheme 1.16),[3b] whereas the free radical selenosulfonation of acyclic olefins is nonstereospecific. Thus, *E* and *Z*-5-decenes gave identical mixtures of erythro and threo diastereomers of **40** (see Scheme 1.16).[3b]

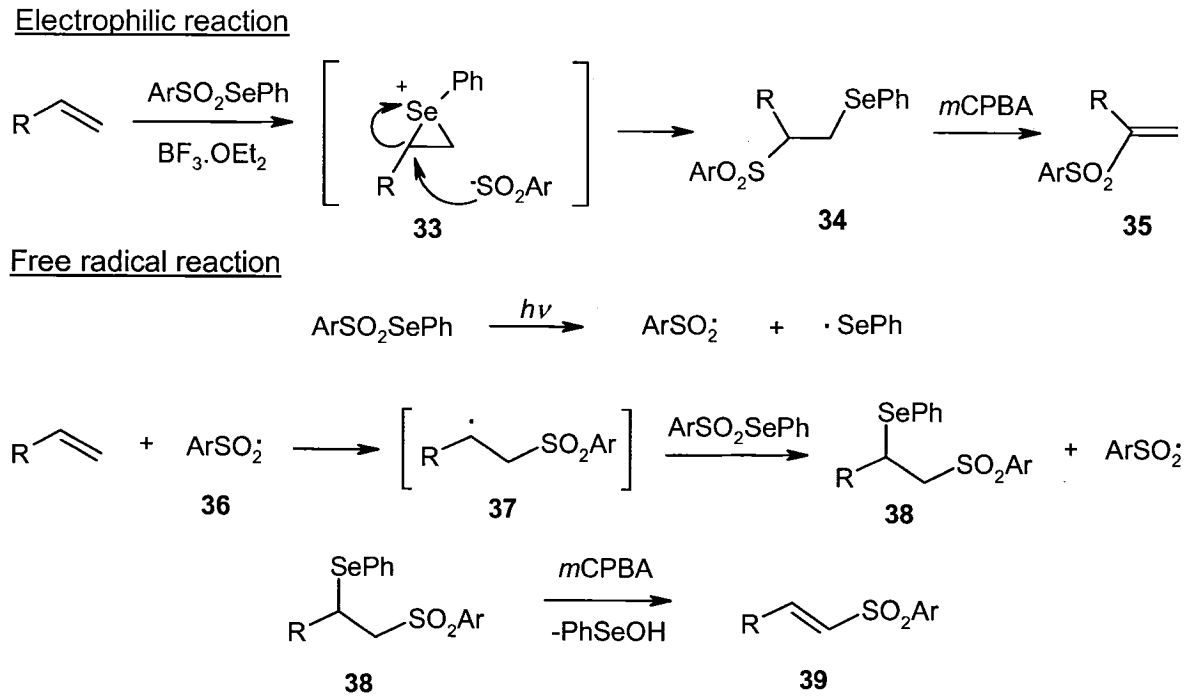

Scheme 1.15 Selenosulfonation of Olefins to Prepare Vinyl Sulfones

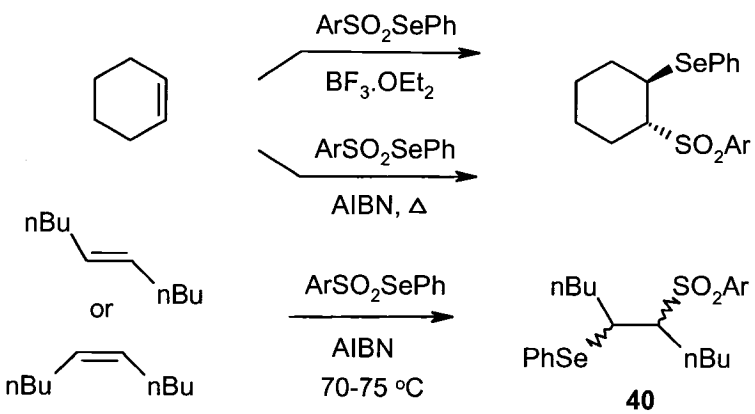

Scheme 1.16 Stereoselectivity of Selenosulfonation of Cyclic and Acyclic Olefins

Vinyl sulfones can also be synthesized by the addition of sulfinic acid salts **(41)** to olefins such as styrene **(42)** in the presence of certain electrophilic reagents, followed by a subsequent elimination step. Examples are the mercuriosulfonation and iodosulfonation reactions shown in Scheme 1.17. These reactions are only applicable to terminal olefins and the mechanisms are uncertain.[27]

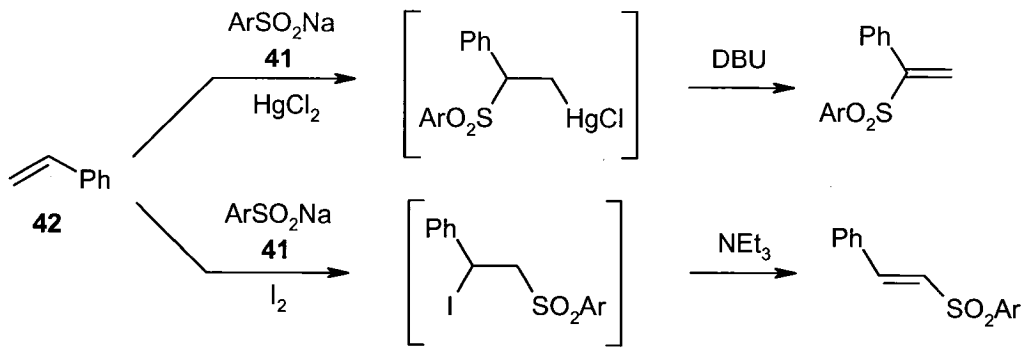

Scheme 1.17 Synthesis of Vinyl Sulfones by the Addition of Sulfinic Acid Salts

1.2.2.3 Aldol-Like, Wittig, Peterson and Related Reactions Using Sulfone-Stabilized Carbanions

Many variants of the syntheses of vinyl sulfones rely on the addition of a sulfone-stabilized carbanion **43** to a carbonyl compound **44**, followed by a subsequent elimination step (see Scheme 1.18)

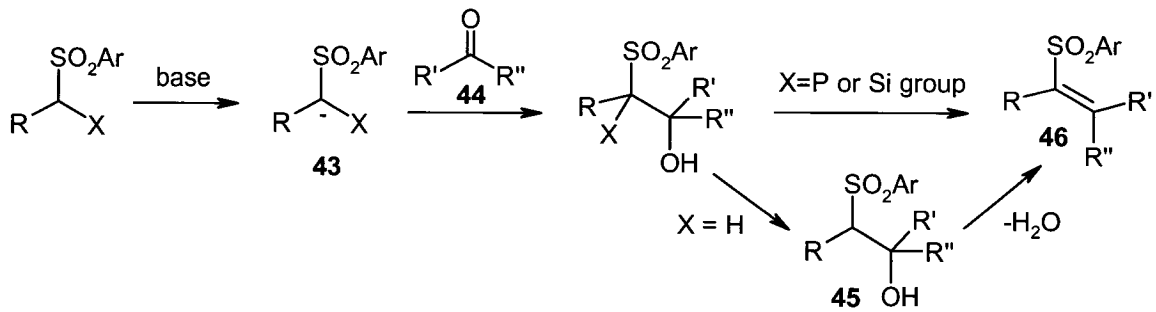

Scheme 1.18 Synthesis of Vinyl Sulfones via Aldol-Like Reactions

In the simplest case where X = H, dehydration of the intermediate hydroxysulfone **45** is necessary, usually in a separate step,[28] whereas the use of phosphorus (e.g. X = $P(O)(OR)_2$) or silicon (e.g. X = $SiMe_3$) groups allows direct *in situ* elimination to give the vinyl sulfone product **46**.

The sulfonylphosphonates **47**[29] and the silyl sulfones **48**[30] have proven useful in Wadsworth-Horner-Emmons and Peterson reactions respectively, each process giving

substituted vinyl sulfones (see Scheme 1.19).

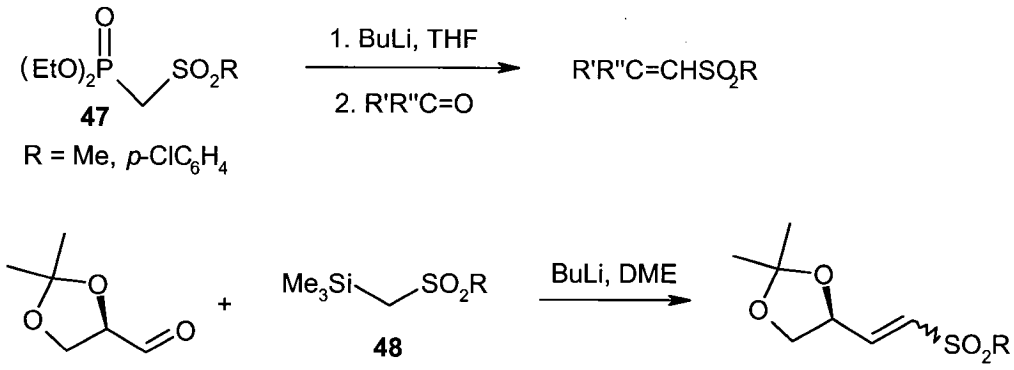

Scheme 1.19 Synthesis of Vinyl Sulfones via Wadsworth-Horner-Emmons and Peterson Reactions

This phosphonate method has the advantage that the products obtained from aldehydes are exclusively *trans*, whereas in the Peterson process mixtures of geometrical isomers are usually formed.

1.2.2.4 From Reactions of Acetylenic Sulfones

Mono-addition reactions of organocuprates **(49)** to acetylenic sulfones such as **50** afforded vinyl sulfones **(51)** mainly through *syn*-addition (see Scheme 1.20).[31]

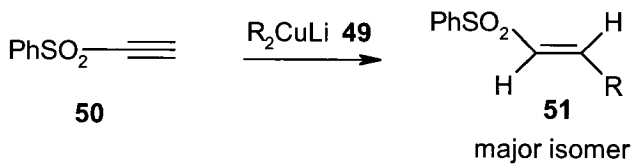

Scheme 1.20 Synthesis of Vinyl Sulfones through Organocuprate Additions to Acetylenic Sulfones

Ethynyl *p*-tolyl sulfone also undergoes Lewis acid-catalyzed ene reactions with electron-rich alkenes. This process introduces the vinyl sulfone moiety into the substrate

as shown in Scheme 1.21. The reaction is very sensitive to both the reaction conditions (the use of an aromatic solvent is important) and the substitution pattern of the starting olefin.[32]

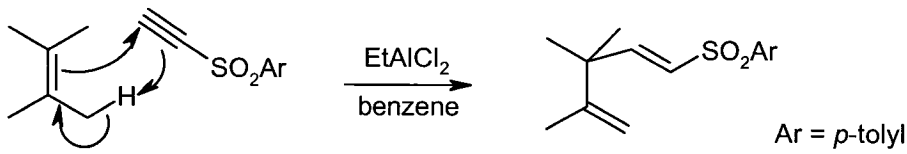

Scheme 1.21 Synthesis of Vinyl Sulfones through Ene Reactions with Acetylenic Sulfones

1.2.2.5 Cross-metathesis of Phenyl Vinyl Sulfone with Alkenes

Functionalized α,β-unsaturated sulfones can be synthesized in a single step through the cross-metathesis of readily available simple phenyl vinyl sulfone **27** with terminal olefins, catalyzed by the commercially available 'second generation' Grubbs' catalyst **52**.[33] The functionalized α,β-unsaturated sulfone products were obtained in high yield and with excellent stereoselectivity, as the (*E*)-isomers were the sole products (see Scheme 1.22).

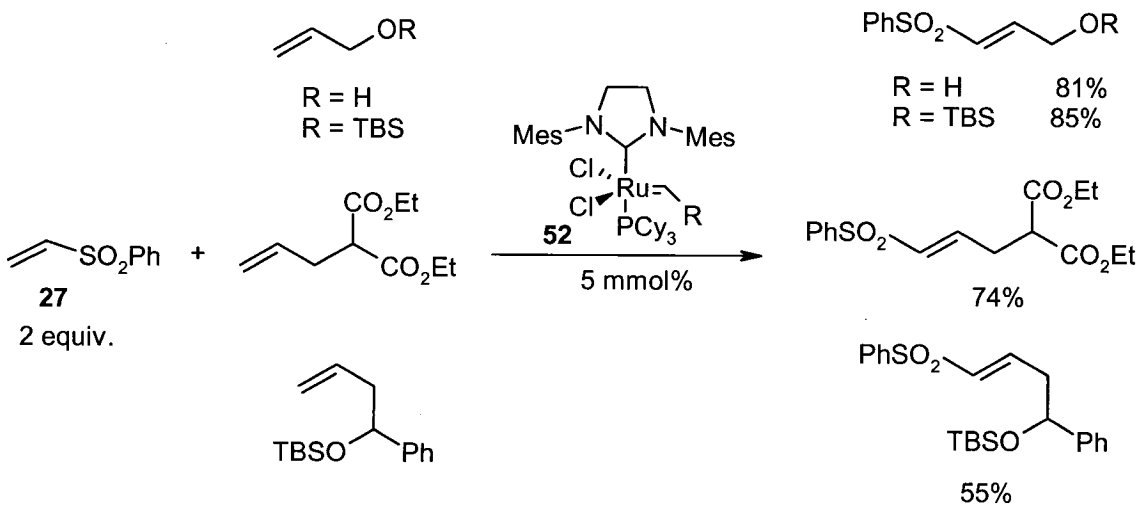

Scheme 1.22 Synthesis of Vinyl Sulfones through Cross-Metathesis

1.2.3 Synthetic Uses of Vinyl Sulfones

As mentioned in section **1.1.1**, the sulfone group can stabilize an α-carbanion. Moreover, the activating and electron-withdrawing effects of the sulfone moiety enable these compounds to serve efficiently as both Michael acceptors and as dienophiles and dipolarophiles in cycloaddition reactions.

Thus, Michael reactions of vinyl sulfones **39** allow for the introduction of nucleophilic substituents at the β-position, Various nucleophiles such as thiolates,[5a] enolates,[34] organometallic reagents,[35] and enamines[36] undergo conjugate additions to vinyl sulfones to afford synthetically valuable compounds. For example, the conjugate addition of cyclohexanone enolate **53** to methyl styryl sulfone **54**, and subsequent proton transfer and intramolecular addition of the resulting sulfone-stabilized carbanion to the carbonyl group, provides a synthetically useful method for the construction of bicyclic products such as **55** in Scheme 1.23.[37]

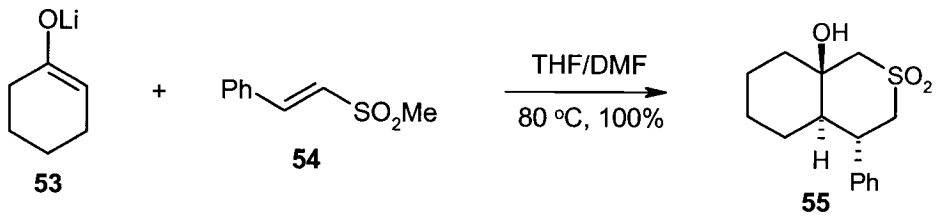

53 + **54** → **55**

Scheme 1.23 Application of a Conjugate Addition to a Vinyl Sulfone

Diels-Alder cycloaddition reactions of vinyl sulfones have also received considerable attention in the past decade. Calculations have shown that the introduction of a sulfone group causes a substantial lowering of the LUMO energy levels in olefins (ΔE = 3.07 eV).[38] Consequently, the sulfone group increases the electrophilicity of the olefin and enhances its reactivity as a dienophile. Vinyl sulfones, such as **27** react with many dienes to give excellent yields of the corresponding Diels-Alder adducts.[39] For example, the reaction of **27** with diene **56** proceeds to form **57** in 94% yield. Further transformation of the cycloadduct **57** into the corresponding alkene by reductive desulfonylation or into ketone **58** by oxidative desulfonylation makes **27** serve as the synthetic equivalent of ethylene **59** and ketene **60**. This is of special utility in view of the low reactivity of

ethylene as a dienophile and the difficulty in handing unstable ketene, as well as its tendency to undergo [2+2] cycloadditions preferentially.

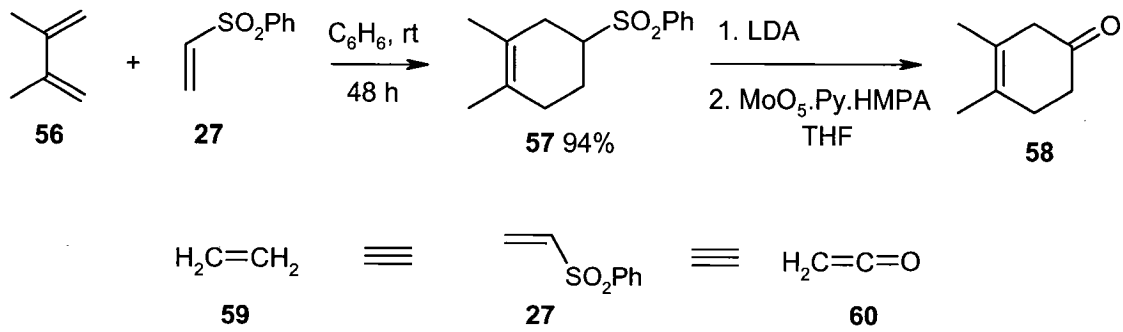

Scheme 1.24 Synthetic Equivalent of Ethylene and Ketene

1.2.4 Conjugate Addition of Amines to Vinyl Sulfones

Nitrogen heterocycles often demonstrate potentially useful bioactivity and it will be recalled that our group has reported the synthesis of various such products via conjugate additions of cyclic amines bearing chloro or ester substituents to acetylenic sulfones, followed by intramolecular alkylation or acylation. The success of these methods using acetylenic sulfones prompted us to investigate extension of this methodology to vinyl sulfones. When using vinyl sulfones, as shown in Scheme 1.25, we would expect to obtain the saturated sulfone products directly without the reduction of the enamine double bond that results when acetylenic sulfones are used. It would be of special interest to compare the resulting stereochemistry of the R group to that of the reduction product when acetylenic sulfones are used.

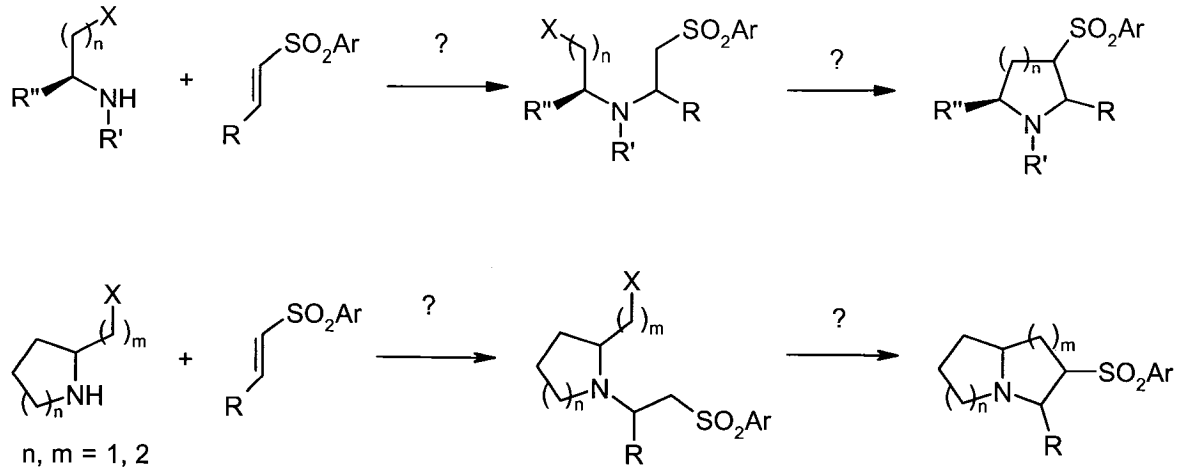

Scheme 1.25 Proposed Reaction of Vinyl Sulfone with Amines to Generate Nitrogen Heterocycles

As in the case of acetylenic sulfones, the utilization of amines as nucleophiles in conjugate addition reactions with vinyl sulfones was explored thoroughly in the 1960's by Stirling.[5a, 34, 40,] The reactivity of vinyl sulfones towards nucleophiles is lower than that of the corresponding acetylenic sulfones and, due to steric reasons, β-substituted vinyl sulfones react more slowly than unsubstituted vinyl sulfones.

1.3 Cyclizations and Cycloadditions of Acetylenic Sulfones on Solid Supports

Although syntheses such as those presented in section 1.1 clearly demonstrate the utility of acetylenic sulfones in the construction of natural products and other heterocycles, the real strength of the methodology may ultimately lie in its extension to solid phase, parallel synthesis strategies for the preparation of libraries of heterocyclic structures for bioasssay. An overview of general solid-phase organic synthesis (SPOS)[41] will therefore be discussed in the following sections.

1.3.1 Background

Even though we now have lots of excellent and efficient methods to construct the target molecules, we still need to find some new strategies, which are environmentally cleaner, more efficient and which lead to libraries in a shorter time. The use of solid-phase reagents and scavengers provides us a convenient and attractive method for the efficient preparation of chemical libraries with potential application in the pharmaceutical industries. These methods can be extended to some multi-step process, which provide some more complex structures, such as biologically active natural products.[42]

Synthetic chemists have to accelerate the rate of production of new products, because pharmaceutical industries have increasing demands to speed up the drug discovery process and to find the potential lead compounds by high-throughput screening. In response to this, new techniques using solid-phase synthesis emerged, which can simultaneously produce libraries of compounds instead of a single product. This strategy for the synthesis of large numbers of compounds forms the basis of combinatorial chemistry or combinatorial synthesis.[43] Nowadays, compound library generation needs well designed new methodology to produce sufficient amounts of pure and fully characterized compounds for initial bioassays.

1.3.2 Solid-Phase Organic Synthesis (SPOS)

The most familiar way of synthesizing organic compounds is with classical solution-phase synthesis in which all of the intermediates and products remain in solution. This is advantageous because the range of reactions that one can carry out in solution-phase is greater than that for the solid-phase. The major disadvantage of solution-phase chemistry lies in the fact that, relative to the time required to carry out a reaction, an excessively large amount of time is used for compound purification. Another main disadvantage is that sometimes, if we want to drive reactions to completion, more than one equivalent of reagent is necessary, but the use of excess reagents is often prohibitive because of the increasing cost and requirement for their eventual removal.

In order to overcome the problems associated with classical multi-step synthesis in solution and to produce large numbers of compounds in a parallel fashion, modifications of the techniques introduced by Merrifield[44] and Letsinger[45] have been extensively developed. Merrifield first used the term 'solid phase synthesis' in 1963 to illustrate the preparation of a peptide. This involved using polystyrene cross-linked with divinylbenzene as the polymeric support, with pendant chloromethyl groups. This material is known simply as Merrifield resin, and can be used to support a substrate, which is then elaborated using an excess of reagents and coupling components to drive reactions to completion. The desired peptide is then detached from the solid support and isolated by a simple filtration. Merrifield resin is still one of the most commonly used resins in SPOS to this day. This general process has become the backbone of modern combinatorial chemistry and is now a widely used technique.[46] Since then, solid-phase organic synthesis (SPOS) has become a very efficient method for production of combinatorial libraries, and with the accomplishment of high-throughput screening for biological evaluation for lead compounds, combinatorial libraries have become very important in the pharmaceutical, biotechnology and agricultural industries.[47]

When the cross-linked polystyrene resins are suspended in organic solvents, the solvents can penetrate into the resin, causing the beads to expand, and this phenomenon is called swelling. The solvents can bind to the polymer in a non-covalent manner. Because polystyrene is a hydrophobic material, swelling is generally strong in polar aprotic solvents, but poor in alkanes or protic solvents such as alcohols and water. Swelling of a cross-linked resin is equivalent to solvation of a linear polymer.[48] The cross-links act as anchors to prevent excessive motion of the polymer chains and prevent dissolution. As a result, solvent is taken up by the cross-linked resin and solvent molecules occupy the empty positions between polymer chains, causing an increase in volume. The capacity of swelling of a polymer resin is a prerequisite for any reaction to occur within a porous polymeric support. A cross-linked resin that does not swell when suspended in solvent provides little or no opportunity for reagents to interact with each other, thus precluding reaction.[49]

Solid-phase synthesis is a methodology whereby synthetic transformations are conducted with one of the reactant molecules (e.g. A in Scheme 1.26) attached to an

insoluble material referred to as the solid support. After each transformation, a simple filtration can separate the target product on the solid support and soluble byproducts or excess reagent. After a succession of transformations is carried out, the bond between the final product AB and the solid support has to be cleaved selectively under mild conditions without damaging the product. (Scheme 1.26).[50]

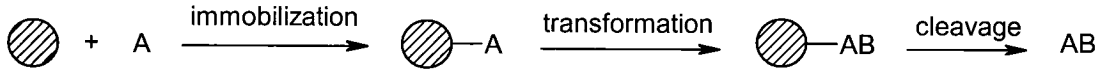

Scheme 1.26 A Schematic Presentation of Solid-Phase Synthesis

Besides this methodology, two other new techniques were established in solid-phase synthesis: scavenger resins and polymer-supported reagents.

Scavenger resins are functional group specific, reactive resins. The reaction of reagent A and reagent B is carried out in solution phase, with excess reagent B used to drive the reaction to completion (see Scheme 1.27).[50] Consequently, a scavenger resin, which is only reactive to reagent B, is added to the reaction mixture. After selective coupling of the resin to the excess reagent B, the insoluble material is removed by a simple filtration and nothing but the pure desired product AB is left in solution.

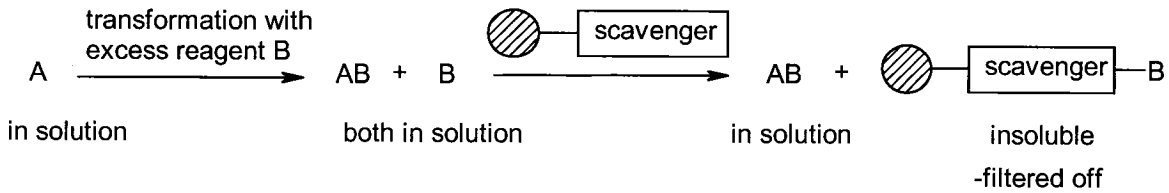

Scheme 1.27 Use of Scavenger Resins

Scavenger resins can be categorized into two main classes: electrophile and nucleophile scavengers. Examples of both electrophile scavenger[51] and nucleophile scavenger resins[51b, 52] are given in Table 1.1.

Table 1.1 Structures and Properties of Some Typical Scavenger Resins

Electrophile Scavengers	Nucleophile Scavengers
Aminomethylated polystyrene 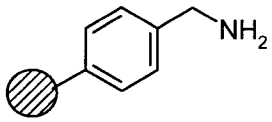 Scavenges acids, acid chlorides, anhydrides, aldehydes.	Activated ketone, polymer-bound 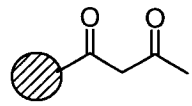 Scavenges primary amines. Also a highly efficient scavenger for hydrazines.
Ethylenediamine, polymer-bound 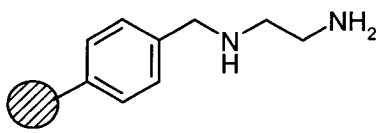 Scavenges aldehydes.	Sulfonyl chloride, polymer-bound 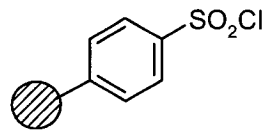 Scavenges many types of nucleophiles.
Mercaptomethyl, polymer-bound 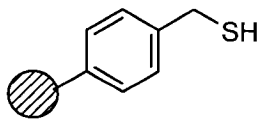 Scavenger for allyl and benzyl halides. Also used as a scavenger for some oxidants.	Isocyanate, polymer-bound 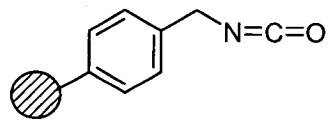 Scavenges amines, anilines, and hydrazines.
p-Toluenesulfonyl hydrazide, polymer-bound 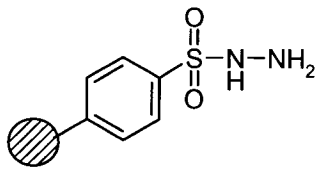 Scavenges aldehydes and ketones.	*p*-Toluenesulfonic acid, polymer-bound 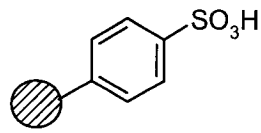 Scavenges nitrogen nucleophiles.

The other new technique established in solid-phase synthesis is the use of polymer-supported reagents. Instead of immobilizing the starting material A on the support, as

shown in Scheme 1.26, the starting material A in solution is treated with a reagent that is attached to a solid support (see Scheme 1.28).[50] Subsequently, a simple filtration removes any insoluble material and the pure desired product B is left in solution.

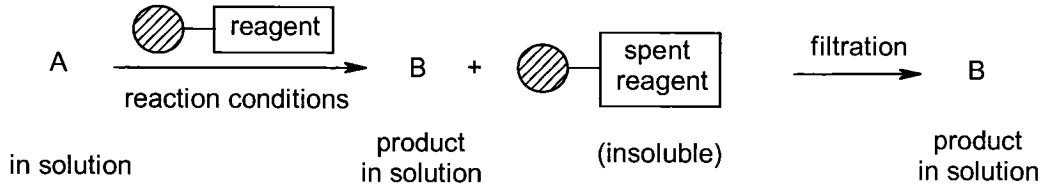

Scheme 1.28 The Principle of Polymer-Supported Reagents

To date, more and more polymer-supported reagents have become commercially available in multigram quantities and these reagents can be categorized into four classes:

- Polymer-supported bases, including polymer-bound DBU, DMAP, diethylamine, diisopropylamine, morpholine, ethylpiperidine, piperazine, etc.
- Polymer-supported oxidizing reagents, including polymer-bound chromic acid, morpholine-*N*-oxide, PCC, perruthenate, etc.
- Polymer-supported reducing reagents, including polymer-bound sodium borohydride, zinc borohydride, cyanoborohydride, etc.
- Polymer-supported coupling reagents, including polymer-bound *N*-Benzyl-*N'*-cyclohexylcarbodiimide, Grubbs' catalyst, phosphine ylides, palladium catalysts for Suzuki and Stille coupling, etc.

1.3.3 Preparation of the Resin for Solid Phase Synthesis

Almost all of the solid supports used in early solid-phase synthesis were variants on the polystyrene bead **61**, prepared by radical polymerization of styrene **(42)** in the presence of a controlled amount of divinylbenzene **(62)** as a crosslinking agent (see

Scheme 1.29). The degree of cross-linking affects not only the mechanical properties of the resin, but also the ability of the reactive sites to interact. If the degree of cross-linking exceeds 0.2%, these polymers are essentially insoluble in any solution and the capacity of polystyrene to swell generally decreases with excessive cross-linking.[53]

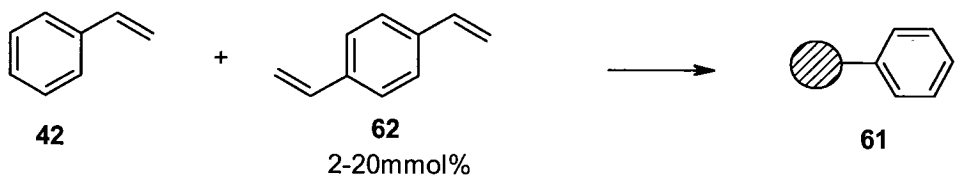

Scheme 1.29 Synthesis of Cross-Linked Polystyrene

Cross-linked polystyrene **(61)** can be functionalized in many ways. Many of these functionalized resins which are frequently used as solid supports and the polymer-supported reagents mentioned in section **1.3.2** are now commercially available (Fig. 1.3), and their preparation will be mentioned only briefly here. Treatment of **61** with chloromethyl methyl ether **(63)** in the presence of $SnCl_4$ affords Merrifield resin **(64)**. Lithiated polystyrene **(65)** is a versatile intermediate for the preparation of a variety of polystyrene derivatives. Lithiated polystyrene **(65)** can be prepared by either direct lithiation of the polystyrene **61**, which is the simplest and most convenient way, or by halogen-metal exchange of *para*-bromo polystyrene **66**, which can achieve better regioselectivity for the *para*- position over the *othro*- position.[54] Lithiated polystyrene **(65)** can also react with electrophiles, including carbon dioxide, dimethyl disulfide, chlorodiphenylphosphine and oxygen for the preparation of variously functionalized polystyrene (see Scheme 1.30).

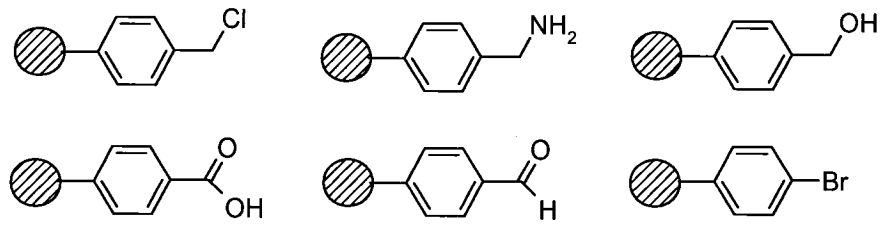

Fig. 1.3 Some Commercially Available Functionalized Cross-Linked Polystyrenes

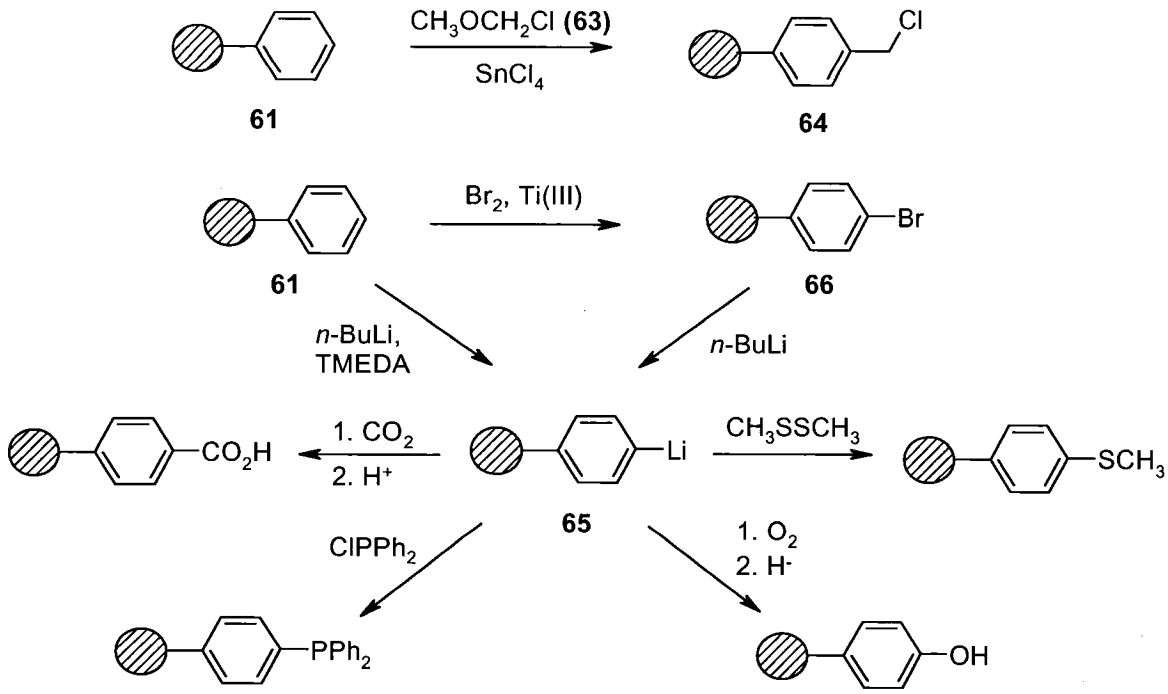

Scheme 1.30 Functionalization of Cross-Linked Polystyrene

1.3.4 The Advantages of Solid Phase Synthesis over Solution Phase Synthesis

Solid phase synthesis has several advantages over classical solution phase synthesis, as discussed below.[55]

First, the solid-phase synthesis can minimize solubility problems. In the solution-phase synthesis of peptides, their poor solubilities often cause problems. However, carrying out the peptide synthesis on a totally insoluble polymeric support can actually circumvent solubility problems. When constructing a peptide on a solid support, it is not necessary for the growing chain to be soluble any more. Any solvent which could effectively swell the resin and is compatible with the reagents can be used as the solvent.

Second, the solid-phase synthesis can simplify the reaction procedure and purification. Time-consuming purification and isolation steps are eliminated by the covalent binding of the substrate and product to the support. On solid phase, purification is simply achieved by washing the resin with a variety of solvents, thus dissolving and subsequently washing away any unbound impurities and byproducts without any extraction, evaporation, crystallization, or chromatography.

Third, the solid-phase synthesis can improve the reaction yield. The use of a large excess of one reagent is an excellent way to drive a bimolecular reaction to completion. As discussed at the beginning of section **1.3.2**, one of the disadvantages of solution phase synthesis is that the use of excess reagents requires their eventual removal, usually by either chromatography or crystallization. On solid support, where the product is still on the support and the excess reagents can simply be washed away or left behind, using two equivalents of one reagent is as easy as using one, providing the reagent is inexpensive or can be recycled. This can lead to dramatically increased yields for a given reaction. Site isolation, also referred to as pseudo-dilution, is one of the properties of solid supports to increase an intramolecular reaction yield. Because all the functional groups are immobilized on the polymeric framework and they are separated from each other, their ability to diffuse is dramatically restricted.[56] Thus, it has the potential to suppress intermolecular reactions in favour of intramolecular reactions.

Fourth, the solid-phase synthesis can simplify manipulation of small quantities. Besides the cost of the resin, for a given reaction sequence, the chemical costs will dramatically increase with the increase in the amount of material synthesized. For example, the monomeric precursors for the syntheses of oligonucleotides are quite expensive, and the amounts needed for bioassay are small (10-100 mg are usually more than enough). So, it would be advantageous to be capable of preparing mg quantities of the desired oligomer. However, dealing with low-mg quantities is a big challenge even for those with good manual dexterity. Attaching starting molecules to a solid support is an effective way for synthetically increasing the weight of the reagent being handled, allowing convenient manipulation up to the ultimate cleavage step.

Last, the solid-phase synthesis is suitable for the preparation of libraries of compounds. In principle, libraries of biologically active, or otherwise interesting compounds can be systematically assembled by conducting various combinations of reactions on solid-supported starting materials. For example, coupling reagent A' with resin-A yields a single product AA' after cleavage, whilst combinatorial synthesis with a range of systematically altered resins (resin-A to resin-C) with species A'-C', produces every possible product combination (Fig. 1.4).[57]

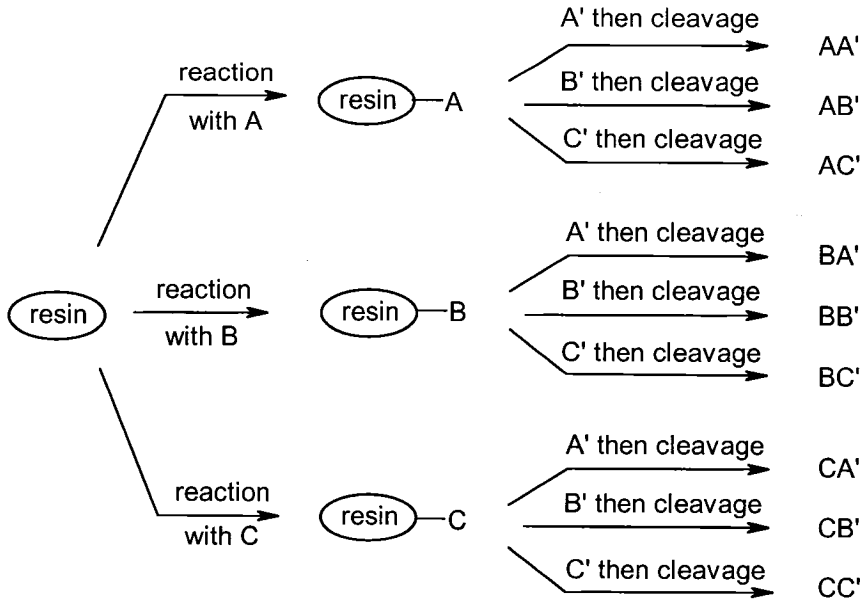

Fig. 1.4 A Combinatorial Library Constructed from Solid-Supported Starting Materials

1.3.5 Linkers for Solid Phase Synthesis

One of the requirements of solid phase chemistry is for a compatible linker to attach a starting molecule to the solid phase. At the end of the synthesis, this starting material is transformed to product by cleavage from the resin (Scheme 1.26). If we want the solid-phase synthesis to be more practical and easier to handle, several important factors need to be considered. The first and most important factor is the choice of a suitable linker and the mode of attachment and cleavage of products from the resin. Second is the efficiency in anchoring and cleavage from the resin, which relies on the correct choice of the linker group. The attachment point of the linker to the solid support, analogous to the use of protecting groups in any solution-phase synthesis, should be chemically stable to all of the reagents used during the synthesis. Yields for the loading and cleavage should be as quantitative as possible. Also, it should be possible to remove these groups under mild conditions without damaging the final products. New linkers are being discovered every year and more than 200 linkers have been developed over the past 15 years in order to allow diverse multistep organic syntheses to be performed with a wide variety of reagents and to allow the linkers to be cleaved in a more selective manner.[58]

1.3.5.1 Linker Types

In general, linkers can be classified into one of two types: (i) Integral linkers in which the linker is attached directly to the resin and part of the resin core forms part of the linker and (ii) Nonintegral (or grafted) linkers in which the linker is attached further from the resin core using a spacer (see Fig. 1.5).[58]

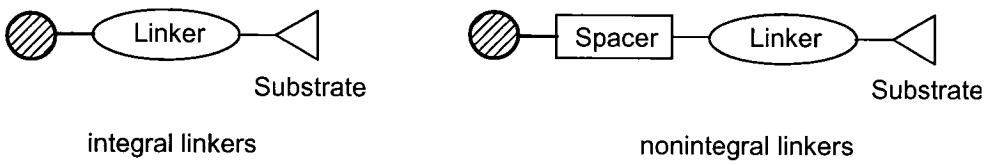

Fig. 1.5 Linker Types: Integral and Nonintegral Linkers

There are many examples of integral linkers (see Fig. 1.6), and they were widely used in the early days of solid-phase synthesis. A molecule with a reactive or potentially reactive functional group is coupled directly to the linker. This strategy is useful if the linker and the building block can be coupled efficiently, usually requiring yields greater than 90%. Thus, the *o*-nitro-(α-nitro)bromobenzyl linker **66** prepared by Pillai[59] is an example of an integral linker, which can be cleaved by photolysis. The benzhydrylamine (BHA) linker **67** is another example, which was prepared by a Friedel-Crafts acylation of polystyrene with benzoyl chloride, followed by amination.[60] The original well-known Merrifield resin **(64)** can also be considered as an integral linker, which can immobilize *N*-protected amino acids onto solid supports by esterification. The trityl linker **68** was developed by Leznoff by reaction of lithiated polystyrene **(65)** with benzophenone.[61] Cross-linked benzenesulfonyl chloride **69** was prepared from Dowex 50W ion-exchange resin (polystyrene-SO_3H).[62] In each of the examples in Fig. 1.6, the integral linker is shown in bold.

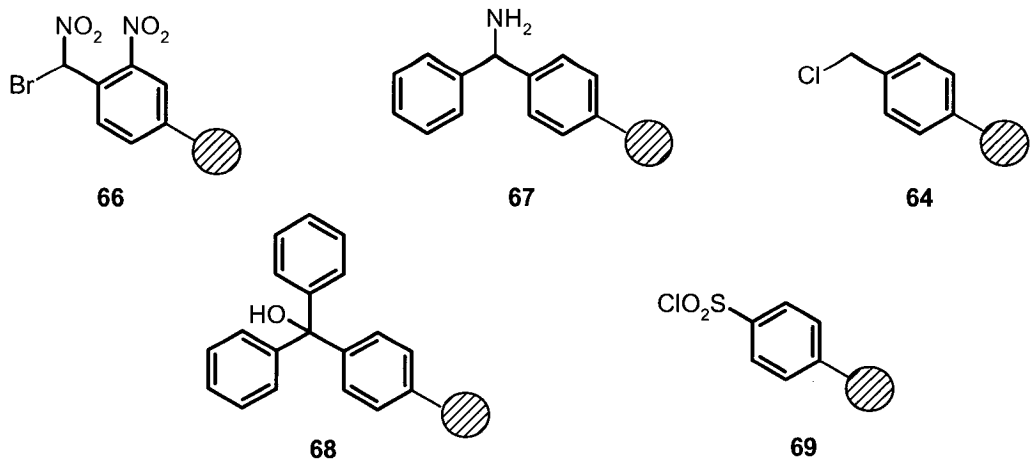

Fig. 1.6 Integral Type Linkers

The disadvantage of any integral linker is that it decreases the control over subsequent synthetic steps. Because the reaction is taking place directly on the resin, steric and electronic effects may influence the synthetic results, resulting in a low loading yield. The majority of linkers now used in solid-phase synthesis are the nonintegral type. Examples are shown in Fig. 1.7. In general, this nonintegral type linker is formed through one of three spacers: (1) Amides, (2) Ethers, and (3) Carbon-Carbon bonds. The nonintegral linker is again shown in bold in Fig. 1.7.

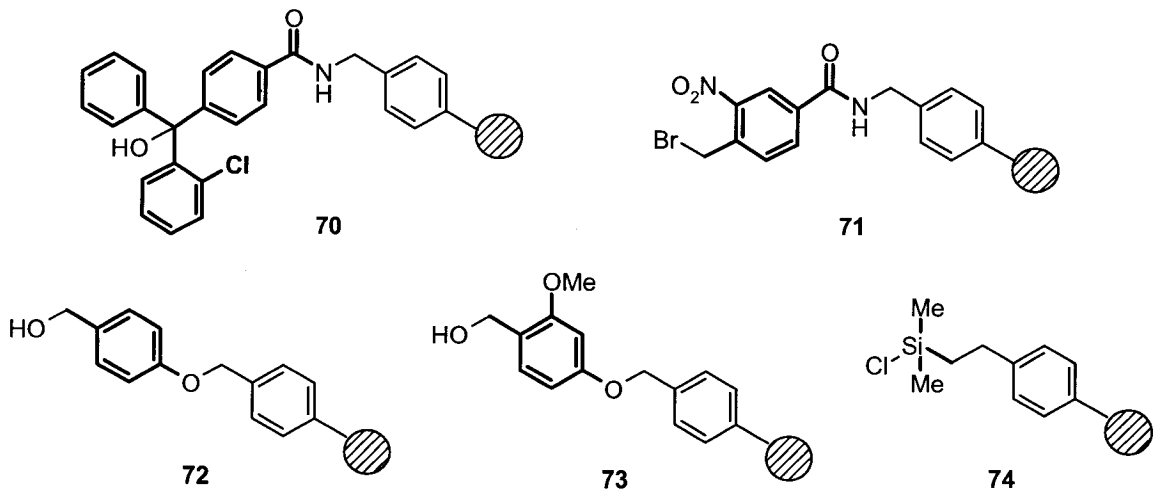

Fig. 1.7 Nonintegral Type Linkers

Thus, the 2-chlorotrityl linker **70** has been prepared as a nonintegral linker through an amide spacer.[63] The *o*-nitrobenzyl linker **71**[64] was prepared by coupling 3-nitro-4-bromomethylbenzoic acid to an aminomethylpolystyrene resin, which can be cleaved by photolysis under neutral conditions. The *p*-alkoxybenzyl alcohol linker **72**, also known as Wang resin, was initially prepared by reacting 4-hydroxybenzyl alcohol with Merrifield resin in the presence of sodium methoxide to create an ether spacer.[65] The Sasrin linker **73** was first synthesized by Mergler[66] and was immobilized onto the resin by etherification. The dimethylsilyl chloride linker **74** has been achieved by hydrosilylation of vinylpolystyrene[67] through a carbon-carbon spacer. The spacer acts as a connection of the resin core and the linker and the advantage of using a spacer lies in its ability to increase the mobility of the substrate, making it more 'solution-like' and solvent compatible. However, one of the drawbacks of the use of spacers is that it requires an additional synthetic step, usually resulting in a decrease of loading yield and sometimes the spacer is not stable toward subsequent reaction conditions.

These nonintegral linkers can either be built sequentially or can be built via a 'handle' approach. A linker which has been prepared in solution is defined as an unloaded linker (or handle).[68] The advantage of using a handle approach is that there is an additional step in solution, which can increase the loading yield and the purity of final products, especially in cases where the linker tends to decompose or can be formed only in moderate yields and purities. So, one must take into account that the use of spacers requires both an additional synthetic step, and that the spacer has to be as robust as the linker toward the reaction conditions performed on the bead.

1.3.5.2 Linker Families

Intense efforts have been focused on the development of linkers between starting materials and solid supports, and hundreds of linkers have been designed over the last decade. These linkers can be classified into several families according to the kind of functional group or substrate class they are able to selectively immobilize. The members of each linker family have certain reactivity patterns and can be cleaved under different conditions.

Benzyl-type linkers are the most common immobilizing groups for various kinds of functional groups, such as esters, amines, alcohols, and thiols (see Table 1.2).[68] For example, a benzyl ether linker, which is compatible with diverse reaction conditions, particularly under basic conditions, can be formed by O-alkylation or O-arylation of Merrifield or related resins. The benzyl ester linker is another very popular benzyl-type linker. Its acid lability and sensitivity toward nucleophiles, makes the cleavage facile.

Table 1.2 Structures of Some Benzyl Linkers Including Trityl Linkers

Generic name of the resin	Stucture
Merrifield resin (X = Cl) AM PS (X = NH_2) (aminomethyl polystyrene) Hydroxymethyl polystyrene (X = OH)	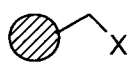
Wang resin (X = OH) Boba resin (X = NH_2)	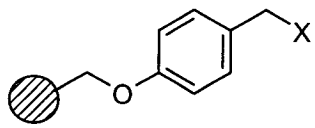
PAM resin (phenylacetamidomethyl)	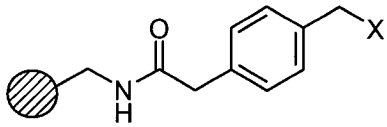
BHA resin (X = NH_2) (benzhydrylamine)	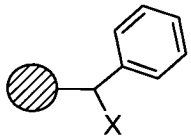
Rink acid (X = OH) Rink amide (X = NH_2) Rink chloride (X = Cl) Rink triflate (X = OTf)	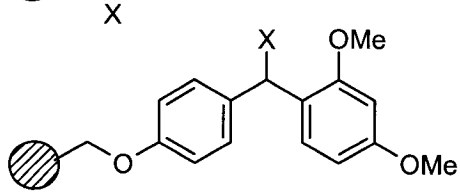
Trityl resin (X = Cl)	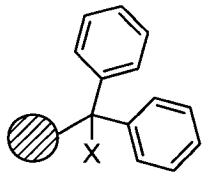
2-Chlorotrityl resin (X = Cl)	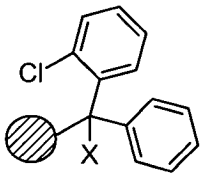

Besides the most popular benzyl-type linkers, esters, thioesters and amides have also been extensively studied for this purpose. In general, two different means can be used

for the attachment of substrates containing alcohols, thiols or amino groups, or acyl-type functionalities, respectively (Fig. 1.9).[68]

X = O, NR', N=N; Y = O, S, NR'

Fig. 1.8 Ester and Amide Linkers: General Structures

Ketals and thioketals are generally used as protecting groups for alcohols or ketones in solution phase synthesis. Hydroxyl linkers based on the tetrahydropyranyl (THP) protecting group have been developed by Thompson and Ellmann.[69a] Many types of alcohols can readily add to dihydropyran attached to the solid support and the resulting THP protecting group is stable to strong bases and organometallic reagents, but can be easily cleaved with aqueous TFA. Since ketals and acetals are the predominant protecting groups for carbonyl functionalities in solution phase, vicinal diols[69b] or dithiols[69c] on solid phase, as shown in Fig. 1.8, have also been used to immobilize ketones or aldehydes onto the resin.

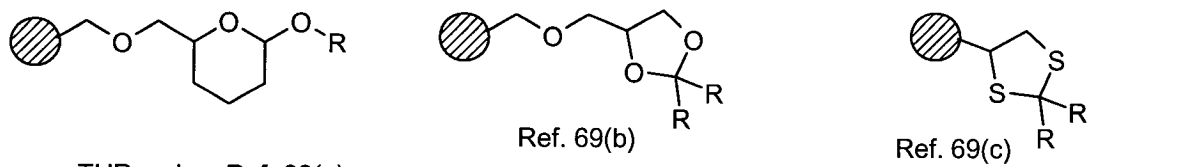

THP resin Ref. 69(a)
Most common linker for alcohols

Ref. 69(b)
Common linker for ketones and aldehydes

Ref. 69(c)
Linker for sterically hindered ketones

Fig. 1.9 Structures of Acetal/Ketal-Based Linkers

The stability of silyl linkers toward basic or organometallic reagents makes them suitable for solid phase synthesis involving such conditions. A variety of new silyl ether linkers (Fig. 1.10) have been developed for this purpose. The silicon-arene or the silicon-oxygen bond can be cleaved selectively under different conditions to elaborate arenes or alcohols, respectively. Boehm and Showalter have developed an efficient method for the

preparation of benzofurans by protodesilylation of the Si-Ar bond via a silyl ether linker (see Scheme 1.31).[70] After successive transformations, fluoride-induced desilylation of the resulting siloxane (TBAF in DMF at 65 °C) then affords benzofurans in good yield.

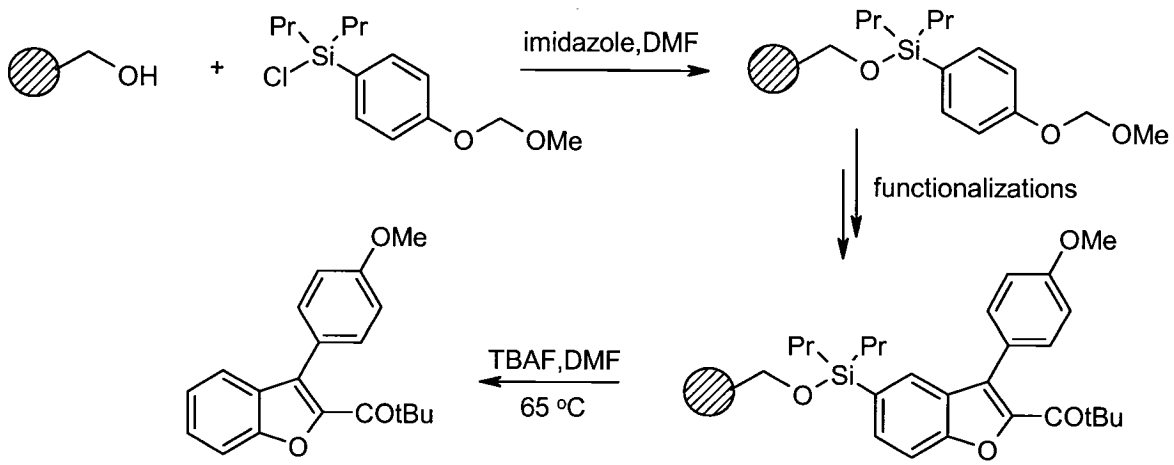

Scheme 1.31 the Silyl Linker for Benzofurans

Other linkers based on silyl groups are the silyl amide linker (SAL linker),[71] the silyl acid linker (SAC linker)[72] and the silyl ether linker. (Fig. 1.10).

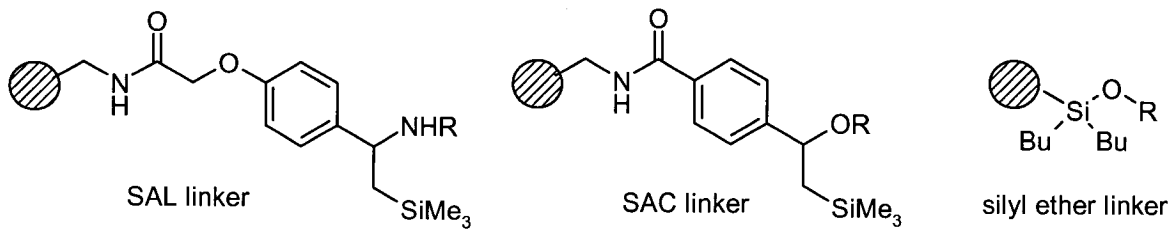

Fig. 1.10 Structures of Silyl Linkers

Since sulfur can esist in several oxidation states, various functional groups bearing sulfur atoms have been used as linkers, such as thioethers, sulfoxides, sulfones and sulfonates. Because of the weakness of the sulfur-carbon bond compared to the carbon-carbon bond, it can readily undergo homolytic cleavage to generate radicals under reductive conditions or photolytic conditions. Moreover, sulfonates and sulfonamides can

be cleaved by strong bases, whiles sulfones are subject to reductive desulfonylation. Since sulfides can be oxidized to the corresponding sulfoxides or sulfones under mild conditions, they have been used in the design of various safety-catch linkers (see section **1.3.7.1)** (Fig. 1.11).[68] A safety-catch linker was developed by Timar and Gallagher for the formation of libraries of amines based on the base-labile 2-(thiobenzyl)ethylcarbamates (see Scheme 1.32).[73] Attachment of acrylate carbamates to Merrifield SH resin was performed under conditions involving radicals. The cleavage was carried out with an oxidation with *m*CPBA, which facilitated elimination to form the retro-Michael substrate.

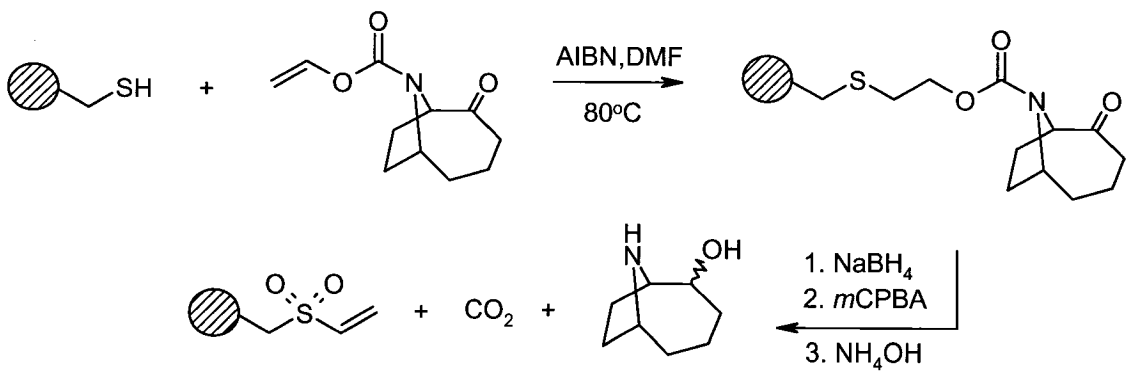

Scheme 1.32 the Sulfur Linker for Amines

Structures of some other sulfur-based linkers such as sulfonamides, thiol esters, aryl sulfonates, and aryloxymethyl sulfones are shown in Fig. 1.11.

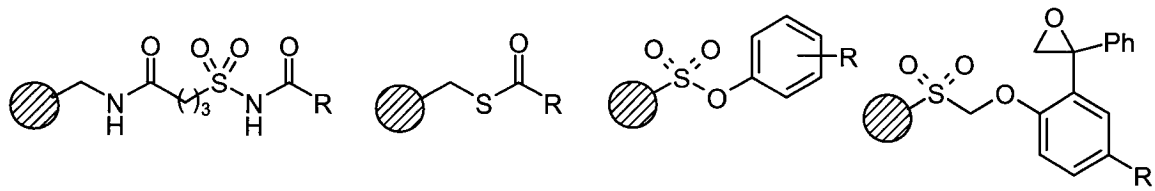

Fig. 1.11 Structures of Sulfur-Based Linkers

Because of the weakness of the selenium-carbon bond compared to the carbon-carbon bond, it can readily undergo homolytic cleavage to generate radicals. Moreover, the selenide can be gently oxidized to the conresponding selenoxide, followed by *syn*-

elimination to produce the corresponding alkene. So, the selenium-carbon bond offers additional possibilities for selenium-containing resins and their traceless cleavage (see section **1.3.7.3**), as illustrated by recent publications by Nicolaou *et al.*[74] and Ruhland *et al.*[75] One example is shown in Scheme 1.33.[74] The resin **75** was first alkylated to give selenide resin **76**. Then, the alkane **77** was obtained via traceless cleavage by means of a radical mechanism using tributyltin hydride in the presence of the radical initiator AIBN, while the alkene **78** can be obtained after a mild oxidation with hydrogen peroxide to the corresponding selenoxide, followed by *syn*-elimination.

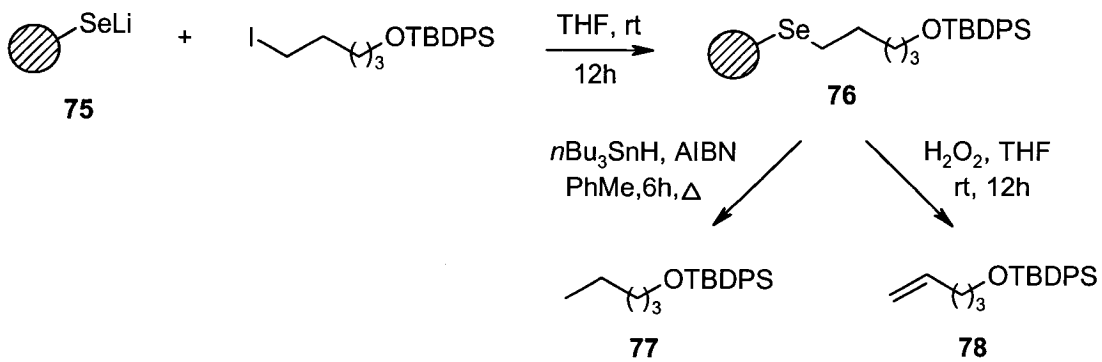

Scheme 1.33 the Selenium Linker for Alkanes and Alkenes

Boronate linkers have been used as precursors for Suzuki coupling and metal-assisted cleavage[76] (Fig. 1.12) (see section **1.3.6**), for the separation of *cis-trans* diol mixtures and for the protection of various diols. Boronate linkers can be formed by condensation of boronic acids with diols and this linker can be easily cleaved with silver salts or by simple hydrolysis.

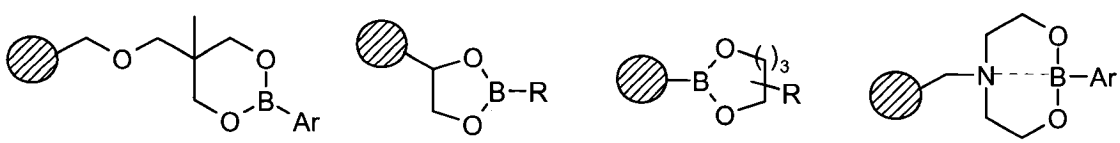

Fig. 1.12 Structure of Boronate Linkers

Stannane resins have also been employed in inter- as well as intramolecular Stille coupling reactions for cyclorelease cleavage (see section **1.3.7.2**). Nicolaou *et al.*[77] have demonstrated the use of this method for the total synthesis of (*S*)-zearalenone (see Scheme 1.34). The polymer-supported Weinreb amide **79** was converted to the alkenylstannane **80**. The loading of alkenylstannane **80** can be measured by tin elemental analysis (see section **1.3.8.2**). Finally, cyclorelease cleavage involved the use of palladium-catalyzed insertion and cross-coupling, leading to the macrocyclic (*S*)-zearalenone.

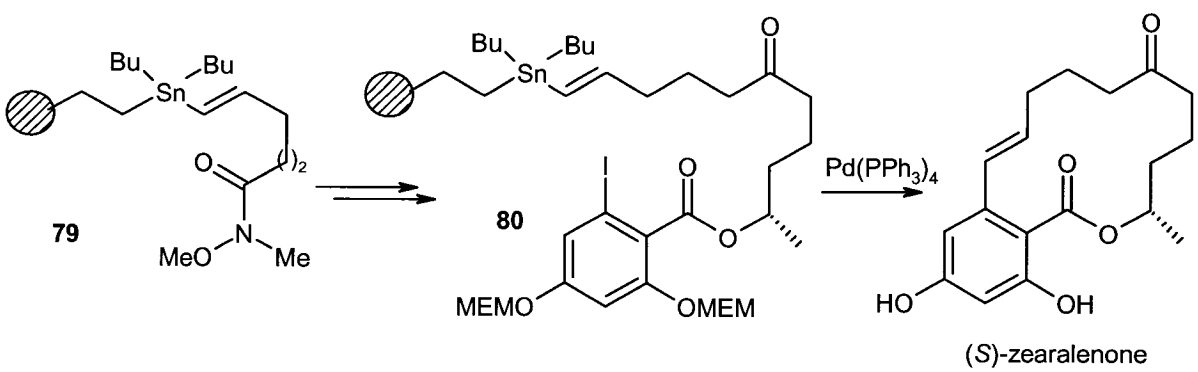

Scheme. 1.34 Stannane-based Linkers for Stille Coupling

1.3.6 Cleavage of the Linker in Organic Synthesis

In this section, various methods and reagents, including electrophiles, nucleophiles, light, oxidizing and reducing reagents that can also be used for the cleavage of linkers are presented.[58, 68]

Electrophilically and nucleophilically cleaved linkers are most commonly used. Electrophilic cleavage of linkers can be conducted with various kinds of electrophiles including Bronsted acids. In most cases, cleavage of linkers is conducted under acidic conditions and the most popular cleaving reagent is trifluroacetic acid in various solvents and concentrations. A variety of different compounds have been cleaved from the resin using TFA, including acids, amides, alcohols, amines, etc. Because the boiling point of TFA is only 72 °C, it can be readily removed by evaporation. Besides TFA, various other acids, such as triflic acid or anhydrous hydrogen fluoride have also been used for some of

the more stable linkers. Three types of commonly used nucleophilic cleavage are saponification, transesterification and aminolysis. Saponification to release peptide acids has been used since the introduction of solid-phase chemistry by Merrifield in 1963[44] and constitutes the classical preparation of peptide acids. Saponification of ester linkers has been used to regenerate alcohols or acids from polymer supports. Esters instead of acids can be released by transesterification of ester linkers by nucleophilic attack of an alkoxide. Displacement reactions involving amines (aminolysis) have generally been directed toward the preparation of amides from esters supported by means of alcohol-derivatized linkers.

Photolysis offers a milder method of cleavage which takes place under neutral conditions, offering new possibilities for the removal of acid- or base- labile moieties. The use of photocleavable linkers has been used in the generation of combinatorial libraries of organic molecules under mild conditions. The *o*-nitrobenzyl linker **71** in Fig.1.7 is a typical example that can be cleaved by photolysis under neutral conditions.

Metal-assisted solid-phase cleavage has also been extensively studied. Two approaches have been used in metal-assisted cleavage. Olefins can be activated by transition metal complexes, such as those of ruthenium and palladium, facilitating cyclorelease strategy (section **1.3.7.2**), which may involve ring-closing methathesis or Stille coupling. Carbon-heteroatom bonds can be activated or polarized by Lewis acids. Lewis acids have been used in solid phase synthesis to accelerate aminolysis and ester cleavage.[58]

Besides the use of electrophilic and nucleophilic conditions, cleavage under reductive or oxidative conditions has also been studied in solid-phase synthesis. For example, the selenium linker can be reductively cleaved by tributyltin hydride to form hydrocarbons (Scheme 1.33). Benzylic ether linkers can be cleaved by catalytic hydrogenolysis. The ester linker can be reduced with lithium borohydride to form alcohols. The sulfone group can be reductively removed to form alkanes. There are two different approaches toward oxidative cleavage. The first approach is to design a linker that is sensitive to oxidation, as in the case of ozonolysis of an alkene, or alternatively by oxidation of sulfur- or selenium-based linkers. The second approach involves oxidation of *p*-alkoxybenzyl ether groups using DDQ to generate alcohols.

1.3.7 Linker and Cleavage Strategies

Apart from the simple cleavages mentioned in section **1.3.6**, various more sophisticated cleavage strategies have been developed in recent years, such as safety-catch linkers, cyclorelease strategies, and traceless linkers.

1.3.7.1 Safety-Catch Linkers

A safety-catch linker is "cleaved by performing two different reactions instead of occurring in a single step, thus providing greater control over the timing of compound release."[56] Safety-catch linkers involve a functional group that is unreactive during the synthesis and has to be activated by chemical transformation immediately prior to cleavage. The oxidation of sulfides to sulfones[78] or the reduction of sulfones to sulfides[79] can be used for the construction of a safety-catch linker. One example is shown in Scheme 1.35. Marshall and Liener reported that sulfide ester **81** is stable to nucleophilic cleavage conditions, while the corresponding sulfone ester **82** can readily undergo nucleophilic cleavage upon mild oxidation of **81** with *m*CPBA.[78]

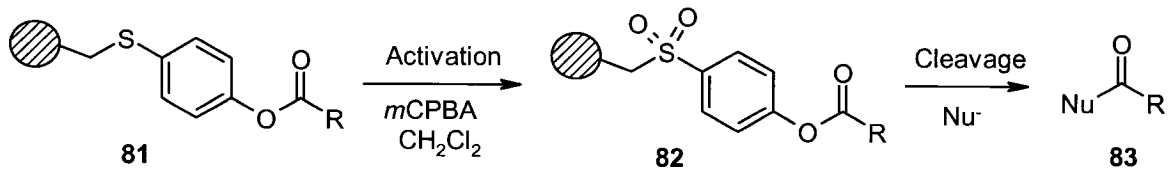

81 82 83

Scheme 1.35 Sulfide Safety-Catch Linker by Marshall and Liener

1.3.7.2 Cyclorelease Strategy and Cleavage-Cyclization

The cyclorelease strategy is typically used for the synthesis of cyclic structures on solid supports through an intramolecular cleavage reaction. Since an intramolecular reaction is often much faster than a comparable intermolecular reaction and only the

cyclized products can be detached from the bead, this strategy provides an additional purification step. Unconsumed starting material and byproducts that did not cyclize thus remain on the solid support.[56] In general, the starting material with a nucleophilic group Z at one end is anchored to the resin via a leaving group X. Then the internal nucleophile Z directly displaces the leaving group X, finishing an intramolecular cyclorelease-cleavage (see Scheme 1.36). The nucleophilic attack and cyclic cleavage take place at the same time. For example, an intramolecular Wittig cyclization of polymer-bound phosphonates was applied by Spivey and coworkers to the synthesis of 2-areneindoles (see Scheme 1.36).[80]

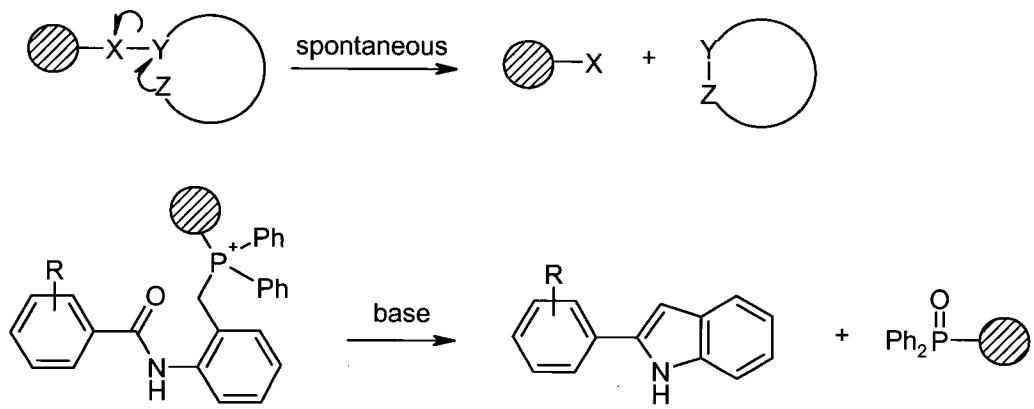

Scheme 1.36 General Scheme and One Example of Cyclorelease Cleavage

In a related approach, as shown in Scheme 1.37, the cleavage-cyclization strategy is based on the nucleophilic attack taking place after cleavage of the leaving group X. One example is shown in Scheme 1.37.[81] The enol ether was first cleaved from the solid support by treatment with aqueous TFA and an intramolecular cyclization resulted in the formation of benzofurans.

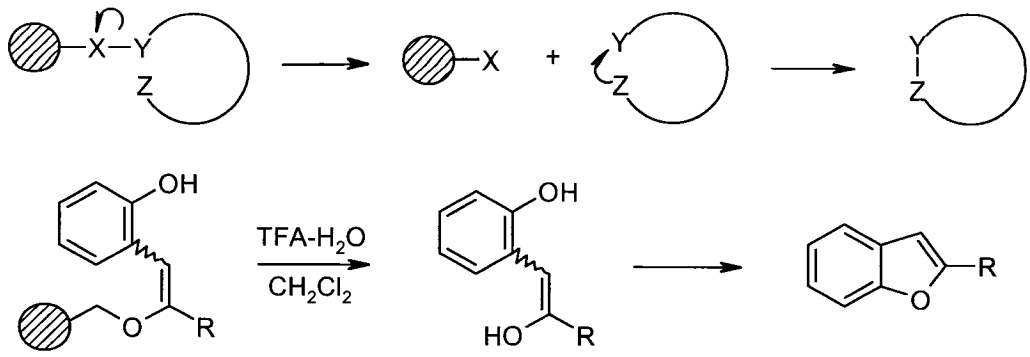

Scheme 1.37 General Scheme and One Example for Cleavage-Cyclization Cleavage

1.3.7.3 Traceless Linker

A traceless linker forms an unfunctionalized C-H bond after cleavage (Fig. 1.13).[56] A wide variety of heteroatom-carbon single bonds can be used as traceless linkers because most heteroatom-carbon bonds have lower energies than a carbon-carbon bond. The weak heteroatom-carbon bond can then be cleaved homolytically or heterolytically.

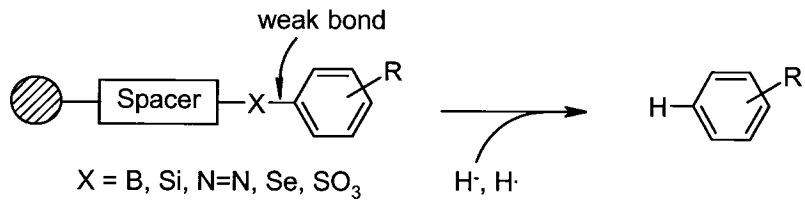

Fig. 1.13 General Scheme for Traceless Linkers

A few examples using traceless linkers are shown in Scheme 1.38. The first traceless linker was developed by Kamogawa and coworkers in 1983.[82] Starting from the commercially available polymer-supported sulfonylhydrazine **84**, formation of sulfonylhydrazone resin **85** was achieved by reaction with ketones or aldehydes. Alkanes **86** were obtained by a reductive traceless cleavage with sodium borohydride. As discussed in section **1.1.5**, a sulfone group can be removed reductively without affecting other existing functional groups. Sulfone groups are therefore suitable as traceless linkers for the

formation of alkanes in solid phase synthesis. In a second example, treatment of the β-keto-sulfone **87** with sodium amalgam resulted in the formation of the corresponding hydrocarbon side chain in high yield with the amide group untouched.[83] Electron-poor aryl sulfonates are also suitable traceless linkers for oxidative palladium insertion. Jin *et al.*[84] have employed phenol sulfonate resins **88**, bearing electron-withdrawing groups in the *para*-positions, in a palladium-catalyzed reductive traceless cleavage using formic acid. Arenes **89** were isolated in good yield.

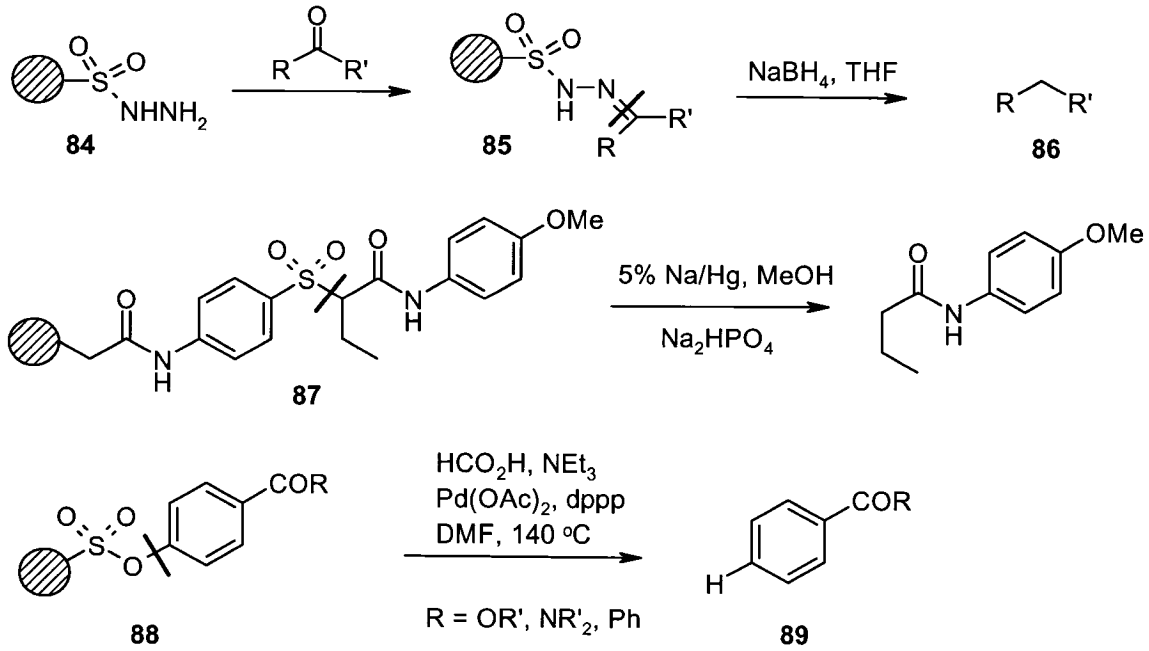

Scheme 1.38 Some Examples of Cleavage of Traceless Linkers

1.3.8 Reaction Monitoring

As in any synthesis protocol, solid phase techniques require monitoring of the reactions to optimize the yields of the target molecules while minimizing the generation of byproducts from side reactions. This can be done with off-bead methods, in which the polymer-bound products are first cleaved from the support with subsequent analysis of the

cleaved product, and on-bead methods, in which single or multiple beads are analyzed directly.

1.3.8.1 Off-Bead Methods

Off-bead methods involve cleavage of resin-bound materials and their characterization by methods utilized in classical organic chemistry. This is the most accurate way to monitor the result of a reaction on a solid-support. However, this method has some limitations.

First, resin beads cleaved after each step of a multi-step solid-phase synthesis are lost, and accurate gravimetric yield determination requires a significant amount of compound. This can lead to a significant reduction in the amount of the target compound prepared. Second, the cleavage reaction may take a long time, thus preventing rapid reaction monitoring and requiring parallel sets of quenching experiments at different reaction times. The reagents used to quench the reaction are also present in the cleavage solution and may require purification steps prior to the analytical determination. Finally, care must be taken to ensure that polymer-bound intermediates are not sensitive to the cleavage conditions to avoid possible misinterpretation of the reaction outcome.

1.3.8.2 On-Bead Methods

The use of fast, reliable, sensitive on-bead methods circumvents the drawbacks to off-bead analysis described above. Most involve modification of common analytical techniques. There are a range of classical analytical techniques which can give useful information on the progress of solid phase reactions, such as combustion elemental analysis, which is widely used in determination of yields of solid-phase synthesis reactions, because of its accuracy and reproducibility. Although this method is destructive, it only requires a small amount of resin (about 2 mg) for CHN analysis. It is also possible to analyze Cl, S, P, Br, I, and metals using this method.

Colour tests are another classical analytical technique used in solid-phase synthesis. Coloured reagents are used to monitor the disappearance of a functional group by

producing a colour change.[55] For example, this method is frequently used to detect the presence or absence of free polymer-supported amines. Reagents commonly used include ninhydrin **(90)**, bromophenol blue **(91)**, and picric acid **(92)** (Fig. 1.14) among others.

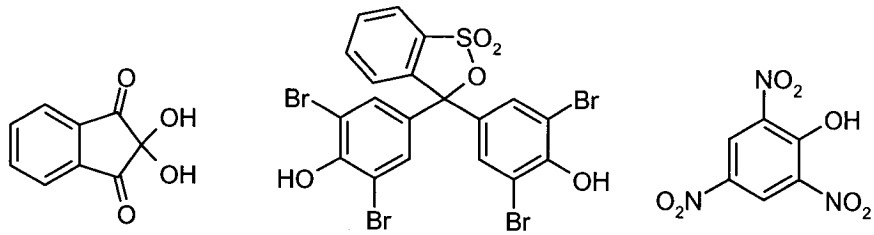

90 ninhydrin

91 bromophenol blue

92 picric acid

Fig. 1.14 Commonly Used Colorimetric Detection Reagents

The use of NMR spectroscopy to monitor relatively fast reactions in solution is limited by the time required to prepare the solution and to record a meaningful spectrum. The use of NMR methods in solid-phase synthesis is more sophisticated because of two factors. First, the spectra generally show significant line-broadening due to restricted molecular motion.[85] This may be partially overcome by swelling of the beads in a suitable deuterated solvent. Second, the heterogeneity of the resin slurry produces microenvironments with different magnetic susceptibilities that cannot be shimmed well in the same way as homogeneous samples where the magnetic susceptibility is uniform. This also leads to significant line-broadening, but can be overcome by recording the NMR spectrum in a solvent in which the resin swells properly (the so-called gel-phase NMR technique).[86] Long spacers can also be used because they increase the mobility of the substrate and reduce the line broadening. Ford and Balakrishnan[87] analyzed cross-linked polystyrene gels using ^{13}C NMR spectroscopy. They found that spectra of the least cross-linked polymers displayed the narrowest lines. This is consistent with the idea that cross-linking puts extra restrictions on the motion of the polymer backbone. The degree of swelling was also found to be important; a poorly solvated resin does not allow motion of the polymer backbone.

MAS-NMR spectroscopy is a relatively new technique to be applied to structure, purity, and yield determination for compounds synthesized on solid-phase. It derives from the observation that the dipolar coupling *D* depends on the orientation of the internuclear vector with the external magnetic field. So, spinning a heterogeneous NMR sample at the "magic angle" ($\theta = 54.736^{o}$) reduces the line-broadening of solid polymer samples.[88]

The use of infrared spectroscopy as a reaction monitoring tool has increased in the past few years and a number of techniques specific to solid-phase synthesis have been developed. Even so, there have been reports that describe the use of classical IR by thorough mixing of a few milligrams of ground-up resin beads in KBr pellets.[89] Most functionalized polystyrene-divinylbenzene supports give very good IR spectra.

Mass spectrometric analysis has recently been demonstrated as a useful analytical method for bead analysis by using matrix-assisted laser desorption/ ionization time-of-flight (MALDI-TOF) spectrometry after *in situ* cleavage of a small number of resin beads. Although this technique involves cleavage from the resin, the cleavage takes place directly on the MALDI plate and can be considered 'on-bead'. The extreme sensitivity (often only a single bead is needed) and the reliability of this method make it very attractive for the analysis of easily ionized compounds. However, the requirement of an expensive MALDI-TOF spectrometer and its limited utility for compounds with molecular weight < 600 are significant limitations to this technique.[90]

1.3.9 Loading and Yield Determination in Solid Phase Synthesis

The loading of a support with functional groups is usually expressed in mmol/g, which depends on the number of attachment sites in the polymer per unit weight. Commercially available functionalized polystyrenes generally have loadings of 0.5-1.5 mmol/g, which corresponds to about 20% derivatization of all available phenyl groups.[91] Determination of the purity and yield of reactions is an essential component for the development of any solid-phase synthesis process. In general, this may be done by both off-bead and on-bead methods (see section **1.3.8**).

1.3.10 Regeneration of the Resin

An attractive feature of many linkers is that they permit the original resin to be recycled after the target product is released, thus allowing for another synthetic cycle to begin on the same resin. Importantly, recyclable resins improve the cost effectiveness of large scale solid phase organic syntheses, whereby multigram quantities of product can be achieved by repeated syntheses. The success of such method is obviously dependant on the robustness of the resin to withstand continuous exposure to a wide range of reaction conditions. The development of new, more robust resins could therefore be significant in facilitating this strategy.[92]

The concept of regeneratable resins was first demonstrated with the so-called **REM** resin, which is used, for example, in the alkylation of secondary amines to tertiary amines. This support is synthesized from hydroxymethyl resin **93** by derivatization to acrylate ester **94** (Scheme 1.39), which, after Michael addition of a secondary amine, gives resin-bound tertiary amine **95**.[93] Quaternization of the tertiary amine with an alkyl halide to give ammonium salt **96** activates the linker for cleavage by a facile Hofmann elimination reaction. Then, DIPEA liberates the tertiary amine **97** at room temperature into solution and regenerates the acrylate resin **94**. Since the resin linker is **RE**generated after cleavage of the product and is functionalized via a **M**ichael addition, it was named **REM** resin.

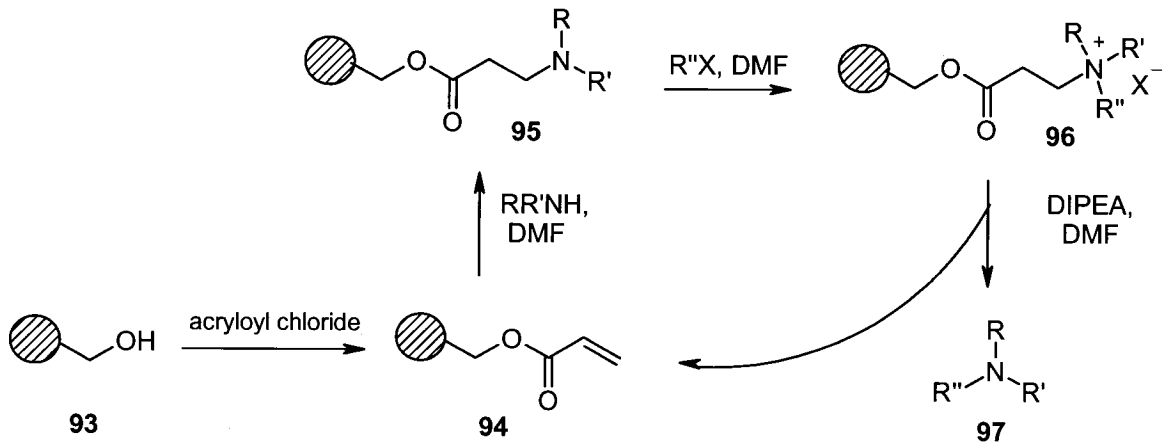

Scheme 1.39 Synthesis of Tertiary Amines on a **REM** resin.

The REM linker is stable to both mild acidic and basic conditions and the REM resins can be recycled and used successfully with no substantial loss of reactivity. FT-IR and ^{13}C gel phase NMR spectroscopy showed that the regenerated resin was identical to the original resin even after five synthesis cycles.[94] The purity of the products was also consistent by ^{1}H NMR spectroscopy. Recyclable resins also include Merrifield resin, 2-chlorotrityl resins, and hydroxymethylated resins, among others.

The ester linkage is however not compatible towards Grignard reagents, metal hydride reducing agents or transesterification conditions, which limits the scope of reactions that can be performed on solid phase. This problem has been addressed through the use of the more stable sulfone REM resins **98-101** (Fig. 1.15), which have been successfully used in the synthesis of tertiary amine libraries.[95] These sulfone REM resins provide enhanced chemical stability and compatibility to a wider range of chemical reagents and reaction conditions.

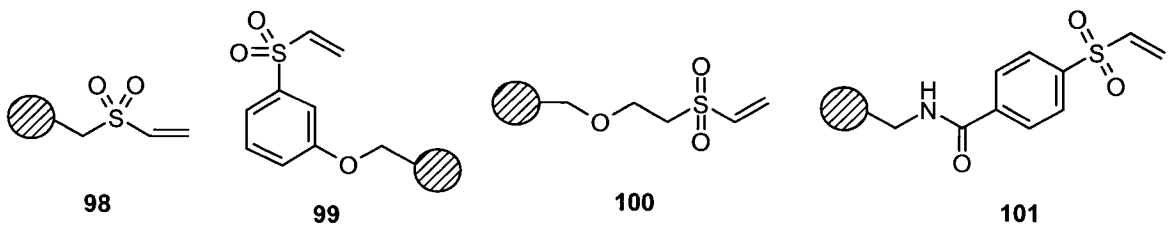

Fig. 1.15 Other **REM** Resins Used in the Synthesis of Tertiary Amines

1.3.11 Some Limitations of SPOS

Despite the success and advantages of solid-phase organic synthesis, there are also several limitations to this approach which are noteworthy. First, the reactions can be slow relative to their solution-phase counterparts and sometimes it is difficult to monitor the reaction progress. Although some techniques, such as FT-IR, gel-phase and MAS NMR, can significantly help to monitor and characterize the reaction process, these techniques still cannot provide the same quality of analysis as rapidly and conveniently as traditional solution-phase techniques (e.g. TLC, GC-MS, LC-MS, HPLC, NMR etc.). A second essential disadvantage of solid-phase synthesis is that additional steps are required to

attach and detach products from the polymers and sometimes the linker and/or spacer compatibility with the reagents used can be a problem or limitation. Third, the loading yield of the resin and its swelling property in some solvents can be poor.[42]

Even though solid-phase organic synthesis has some limitations, it is still widely believed that the advantages of SPOS so far outweigh its disadvantages. We can choose a suitably functionalized polymer support for the desired target, separating it from any impurities or excess reagents by filtration, and then detaching it from the resin in its pure form. Almost all of the standard reactions in organic solution-phase chemistry can be carried out in solid-phase using suitable supports, linkers, and protecting groups with all the advantages of SPOS. Among the reported organic reactions using solid supports are Diels-Alder reactions, 1,3-dipolar cycloadditions, Wittig and Wittig-Horner reactions, Michael additions, oxidations, reductions, Pd-catalyzed C-C bond formation, and many others.[96]

1.3.12 Sulfone-Functionalized Resins

Because Chapter three will deal specifically with acetylenic sulfone groups that are introduced onto polymer supports, some more detail about sulfone-functionalized resins will be presented in this section. To date, several β-benzoyloxyalkyl and γ-hydroxyalkyl sulfones anchored to solid supports have been employed in Julia–Lythgoe olefinations,[97] in the preparation of trisubstituted 2-pyridones,[98] and in the preparation of substituted benzofurans[99] and furans via sulfone elimination.[100] Supported vinyl sulfones have also been converted into libraries of tetrahydro-β-carbolines[101] or tertiary amines by Hofmann elimination,[95a, 102] and into peptides used as probes of cysteine proteases.[95c]

1.3.12.1 Polymer-Supported Vinyl Sulfone Resins

Polymer supported vinyl sulfones have been prepared by methods based on conventional solution-phase vinyl sulfones synthesis,[103] Usually, Merrifield resin **64** is treated with mercaptoethanol to give thioether alcohol **102**. Oxidation of the thioether gives sulfone alcohol **103** (see Scheme 1.40). This sulfone resin can be converted to either

the bromide or mesylate **104** (X = Br or OMs), and subsequent treatment with base affords supported vinyl sulfone **98**.[95a]

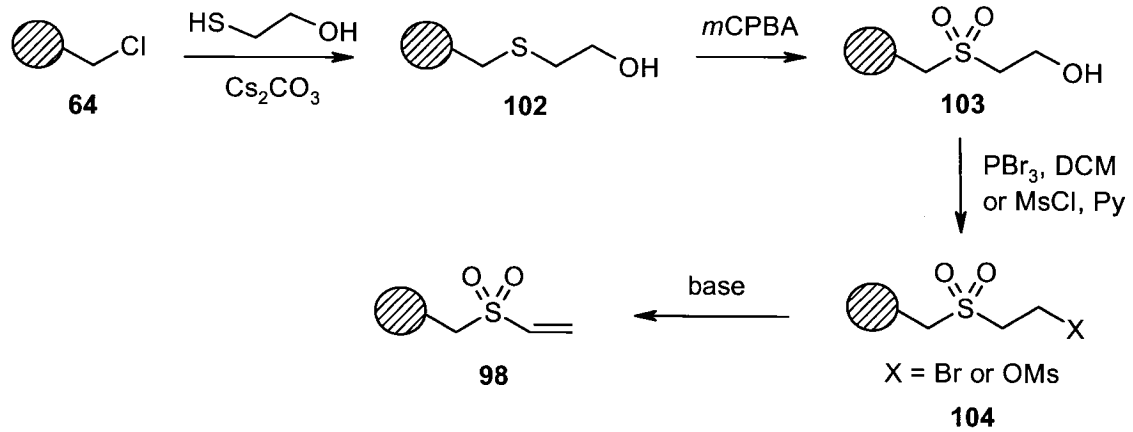

Scheme 1.40 Synthesis of Integral Type Vinyl Sulfone Resin

In another example (see Scheme 1.41), the phenolic alcohol **105** was attached directly to either Merrifield resin **(64)**[100] or 2-chloro-trityl resin **(70)**[104] to give the corresponding resin-bound arylsulfonylphosphonate **106**. Then aldehydes were reacted with the resin in a Wadsworth-Horner-Emmons condensation reaction, generating the *trans* isomer **107** as the predominant product. The supported vinyl sulfone resins **107** were then subjected to further transformations to produce more complex compounds.

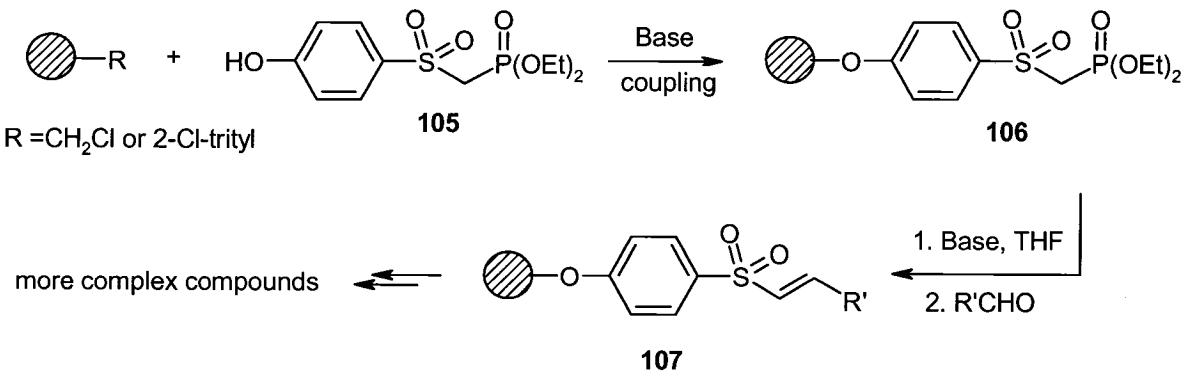

Scheme 1.41 Synthesis of Nonintegral Type Vinyl Sulfone Resins

1.3.12.2 Michael Addition to Vinyl Sulfone Resins and Cleavage

As mentioned in section **1.3.10**, vinyl sulfone resins such as **98** and **100**, can be made to undergo Michael additions with secondary amines, giving resin-bound tertiary amines. Quaternization of the tertiary amines with alkyl halides to give the corresponding ammonium salts activates the linker for cleavage by a facile Hofmann elimination reaction to generate amine libraries, such us **108**[95a] and **109**[95b] (see Scheme 1.42). These sulfone resins provide enhanced chemical stability and compatibility with a wide range of chemical reagents and reaction conditions relative to many of the acrylate resins.

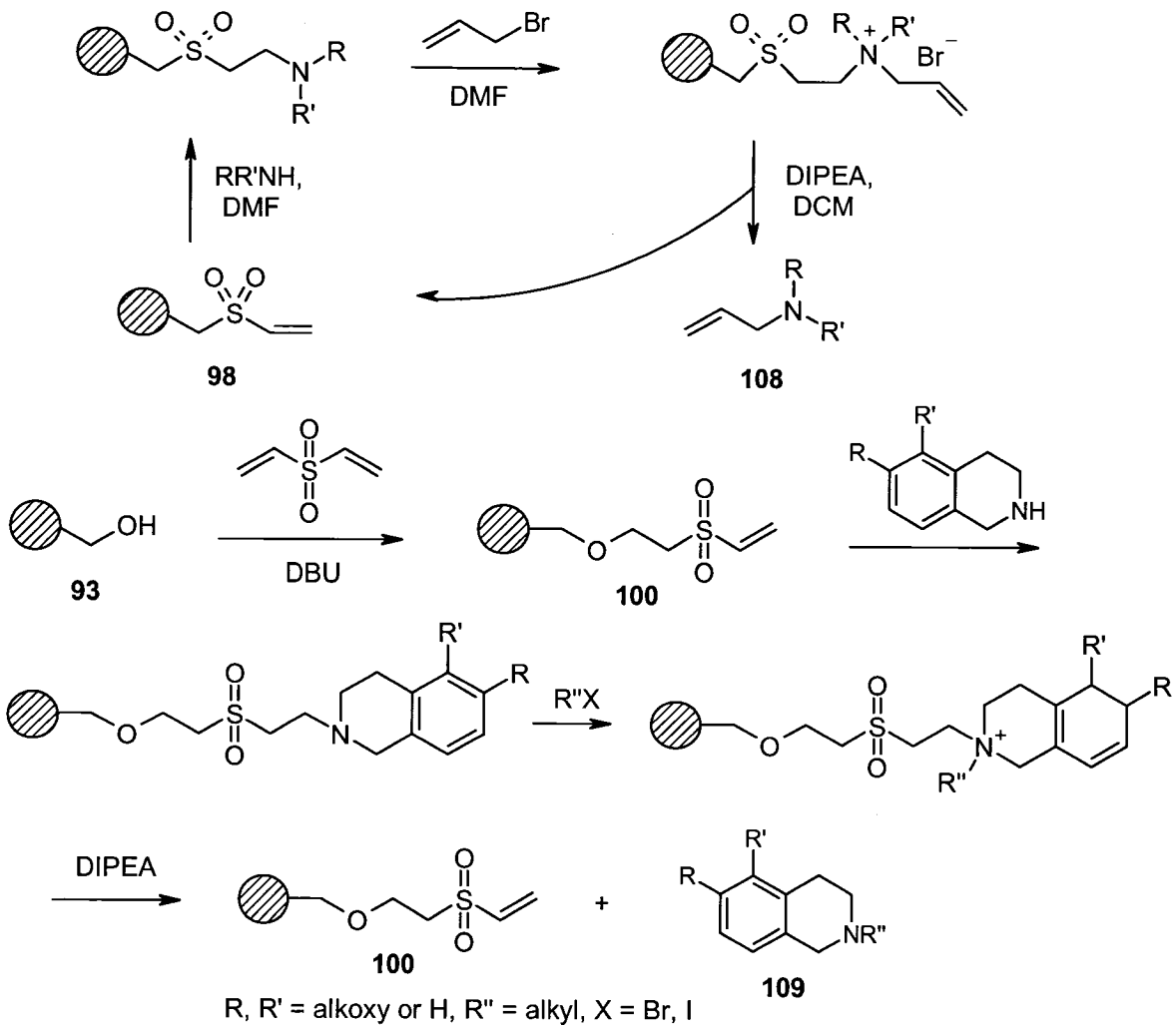

Scheme 1.42 Examples of Applications of Vinyl Sulfone Resins

To date, no acetylenic sulfones anchored to solid supports have been reported. In this thesis, the synthesis of the first polymer-supported acetylenic sulfones and their applications will be described in Chapter three.

1.4 Diels-Alder Cycloadditions and Further Transformations of Products from 1,3-Diphenylisobenzofuran (DPIBF)

During the course of our investigation of Diels-Alder cycloadditions on polymer-supported acetylenic sulfones, which will be described in Chapter three, we examined the use of 1,3-diphenylisobenzofuran (DPIBF) and came across some unexpected results that prompted us to look more closely at the solution phase process that corresponds to these results. Chapter four will describe the cycloaddition and further transformations of acetylenic sulfones and DPIBF. Therefore, it is appropriate to describe some basic chemistry involving Diels-Alder reactions and further transformations of DPIBF in the following sections.

1.4.1 Diels-Alder Reactions of 1,3-Diphenylisobenzofuran

1,3-Diphenylisobenzofuran (DPIBF **110**) is a highly reactive diene that can readily undergo Diels-Alder cycloadditions with a wide range of dienophiles as well as other types of cycloaddition reactions.[105] It has served as a powerful reagent for the preparation of various polyaromatic compounds, as well as for trapping unstable dienophiles. The aromatization of the benzene ring during cycloadditions is the driving force for such processes.

Earlier studies have shown that the Diels-Alder products obtained from DPIBF and various alkenes or acetylenes can undergo further reactions under pyrolytic conditions, or upon subsequent workup or treatment under acidic conditions. When an acetylene is employed as the dienophile, the resulting Diels-Alder product is an oxabenzonorbornadiene derivative **111** (see Scheme 1.43), which can undergo a variety of

further transformations. These cycloadducts have proven to be a valuable source of naphthalene and hydronaphthalene derivatives.

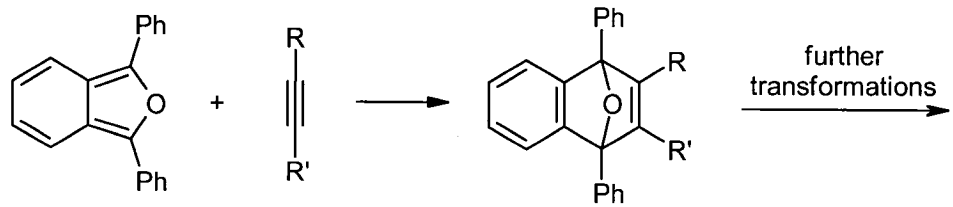

110 **111**

Scheme 1.43 Diels-Alder Reaction of DPIBF with Acetylenes

1.4.2 Further Transformations of Diels-Alder Adducts of DPIBF

1.4.2.1 Hydrogenation and Dehydration

When cyclooctyne **(112)** was employed as the dienophile with DPIBF, the Diels-Alder product was hydrogenated to give a mixture of *cis*- and *trans*-cyclooctane species (4:1) (Sheme 1.43).[106] The *cis* product readily dehydrated to give naphthalene derivative **114** under acidic condition in 84% yield. Similarly, the Diels-Alder product of cyclopentene **(115)** with DPIBF was treated with acid to give napthalene derivative **116** in only 10% yield (see Scheme 1.44).[107]

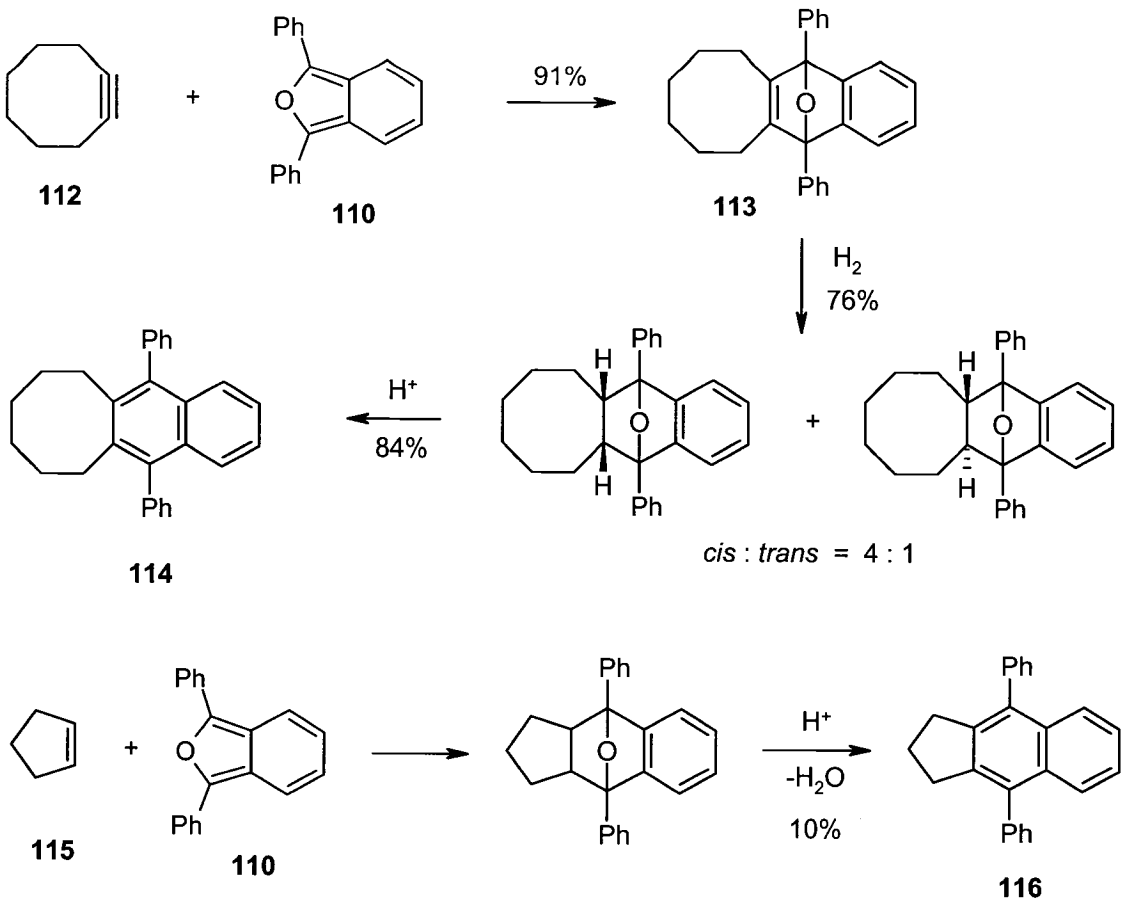

Scheme 1.44 Dehydration of the Cycloadducts

1.4.2.2 Deoxygenation

Diels-Alder adducts of DPIBF with alkyne dienophiles can extrude oxygen either by reductive aromatization or pyrolytic aromatization to produce naphthalene or other polycyclic aromatic derivatives.

Adducts of DPIBF with triply-bonded dienophiles (cycloalkynes, dimethyl acetylenedicarboxylate, benzyne, etc.) can be reduced to polycyclic arenes in variable yields by treatment with sodium borohydride in trifluoroacetic acid,[108] or zinc and acetic acid.[109] Two examples are shown in Scheme 1.45.

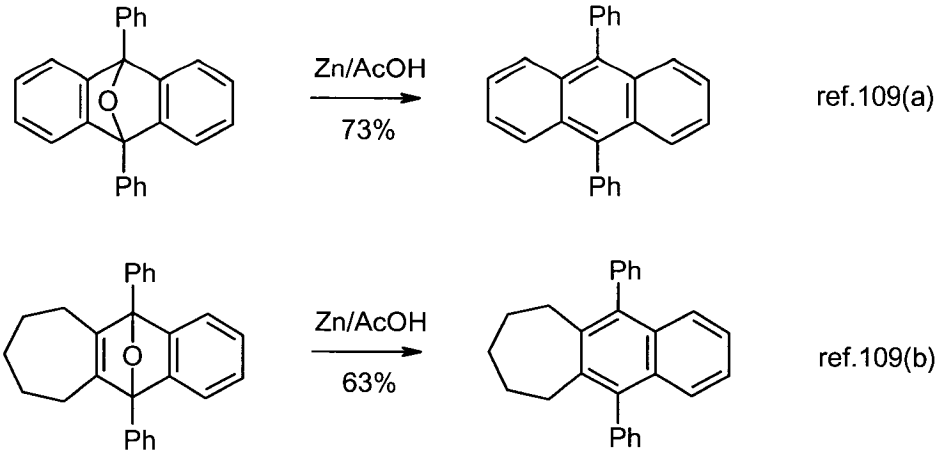

Scheme 1.45 Reductive Aromatization of the DPIBF Cycloadducts

Adducts of DPIBF with triply-bonded dienophiles can also formally extrude oxygen and produce polycyclic arenes in variable yields by heating the adducts at a relatively high temperature. Two examples are shown in Scheme 1.46.[110] While the mechanism of such processes is not known, it seems more reasonable to assume that the oxa-bridged cycloadduct oxidizes a second molecule to an unidentified product(s) than that it simply extrudes nascent oxygen.

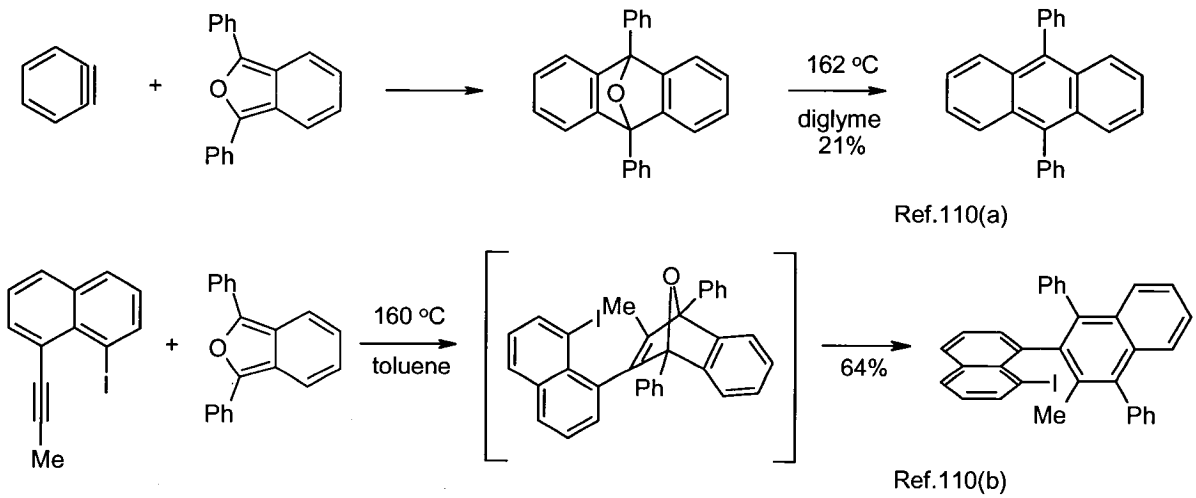

Scheme 1.46 Aromatization of the Cycloadducts under Pyrolytic Condition

These methods of bridge deoxygenation have expanded the scope of the cycloaddition to make it a convenient pathway to many polyaromatic hydrocarbons.

1.4.2.3 Rearrangements to Ketones

1.4.2.3.1 Rearrangements to Ketones under Acidic Conditions

Wittig and coworkers reported that cycloadducts **117**, derived from the reaction of DPIBF with cycloalkynes, isomerized to the corresponding ketones **120** under acidic conditions at room temperature.[106, 107, 111] It was proposed that the key step involves ring-opening to give carbocation **118**, followed by a pinacol type rearrangement involving a 1,2-phenyl shift (see Scheme 1.47).

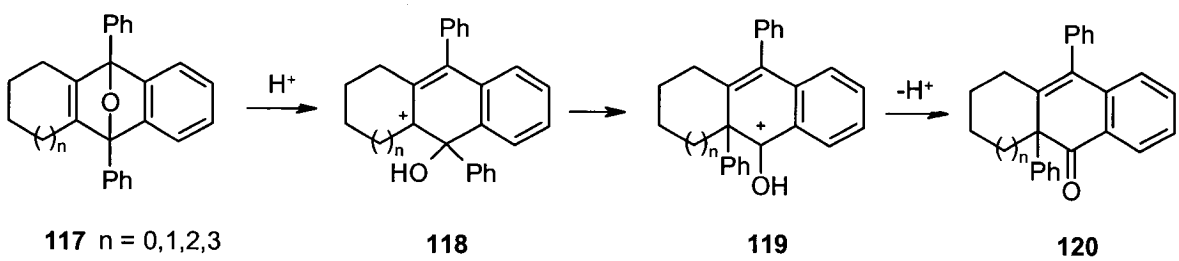

117 n = 0,1,2,3 **118** **119** **120**

Scheme1.47 Acid Catalyzed Rearrangement to Ketone

The similar trapping of the highly strained bicyclo[2.2.2]oct-2-yne **(121)** with DPIBF afforded a high yield (86%) of the [4+2] cycloadduct **122**. The latter rearranged readily to the ketone **123** upon chromatography over silica gel (see Scheme 1.48).[112] Due to the acidity of silica-gel and the similarity of ketone **123** to ketone **120**, this kind of rearrangement can also be classified as a rearrangement under acidic condition.

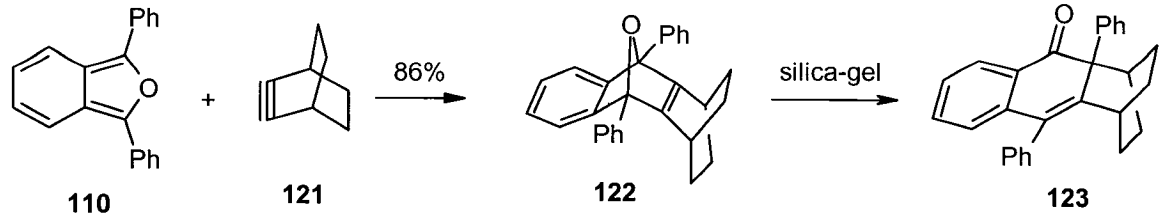

Scheme 1.48 Silica-Gel Promoted Rearrangement to Ketone **123**

According to Wittig's reports,[106, 109b] the cycloadducts derived from the reaction of DPIBF with cycloheptyne and cyclooctyne isomerized to ketones on heating in acetic acid (see Scheme 1.49). Unlike the ketone **120**, exocyclic ketones were obtained in this case.

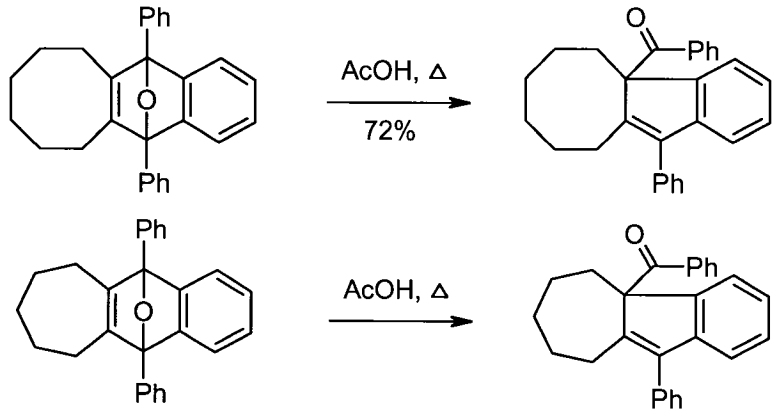

Scheme 1.49 Acid-Catalyzed Rearrangements of Cycloadducts to Exocyclic Ketones

1.4.2.3.2 Rearrangements to Ketones under Neutral Conditions

When cyclic iodonium triflate **124** was treated with a THF solution of TBAF in the presence of DPIBF in dichloromethane, the carbonyl-containing cycloadduct **125** was obtained in 43% yield in the absence of an acid catalyst. The reaction presumably involves the isomerization of the cycloadduct **126**, derived from the reaction of bicyclo[2.2.1]hept-2-en-5-yne **(127)** with DPIBF, to the corresponding exocyclic ketones (Scheme 1.50).[113]

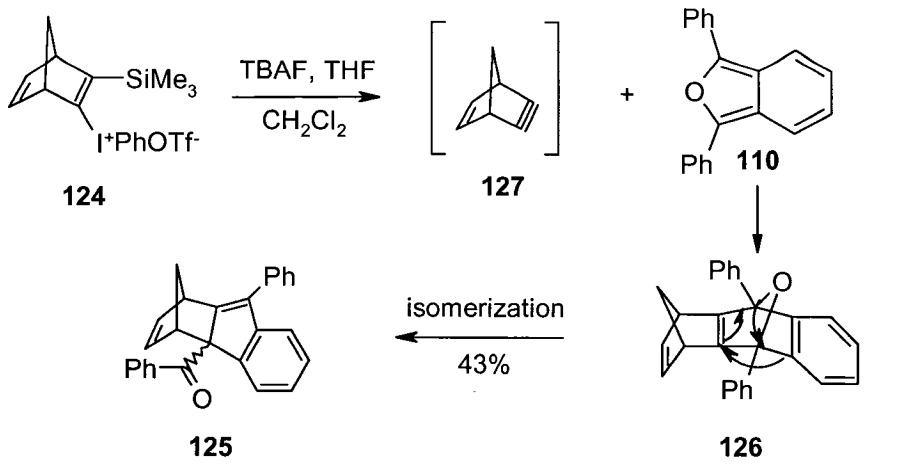

124 127 110 125 126

Scheme 1.50 Spontaneous Rearrangement to Ketone **125**

1.4.2.3.3 Rearrangement in the Presence of a Bridgehead Alkylthio Substituent

The Pummerer rearrangement[114] is a reaction in which a sulfoxide, such as **128**, when treated with an acid or an anhydride, is converted to an α-substituted sulfide such as **129**, which has a similar structure and properties to DPIBF.[115] As shown in Scheme 1.51, when keto sulfoxide **128** was heated to 120 °C with acetic anhydride in the presence of an appropriate acetylenic dienophile, the sulfoxide smoothly underwent a tandem Pummerer cyclization-Diels-Alder reaction to produce the corresponding cycloadduct **130** *in situ*. Furthermore, **130** was found to rearrange readily to tetralone derivative **131** in 38% isolated yield. It was proposed that the key step involves oxabicyclic ring opening, which is driven by electron donation from sulfur, followed by a pinacol rearrangement proceeding by way of a 1,2-phenyl shift.[116]

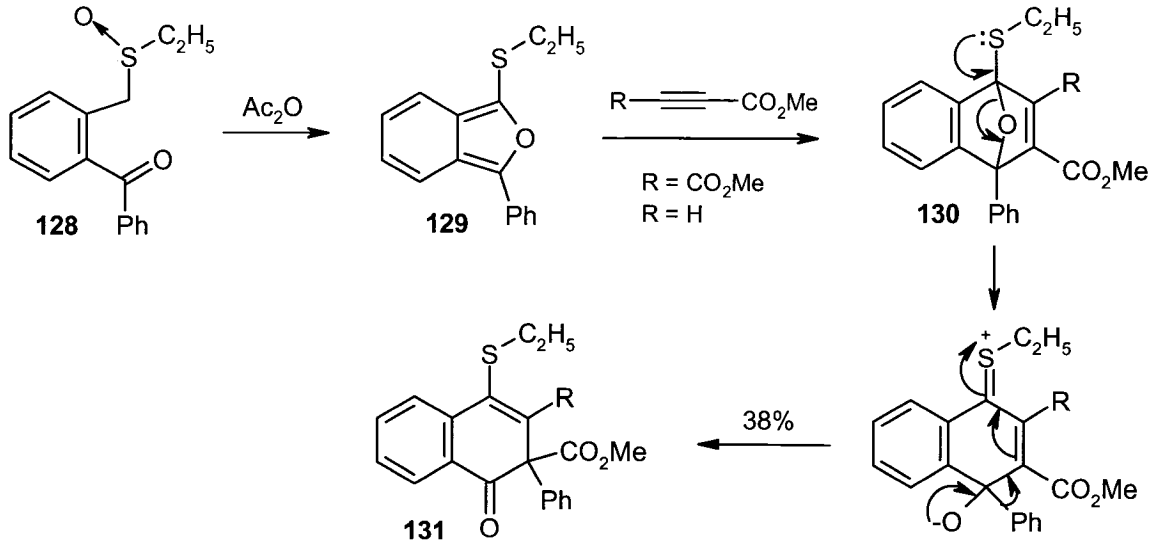

Scheme 1.51 Rearrangement to Ketones Assisted by a Bridgehead Alkylthio Substitutent

1.4.2.3.4 Via Free Radical Reactions

Elimination of **132** with methyllithium in ether solution yielded highly strained tricyclo[3.2.1.$0^{2,4}$]octa-2,6-diene **(133)**, which was trapped with DPIBF, affording exo-exo adduct **134** and endo-exo adduct **135** in the ratio of 1:2. The further isomerization of the endo-exo adduct **135** to the styrene derivative **136** was reported to proceed via the diradical **137**, as shown in Scheme 1.52.[117]

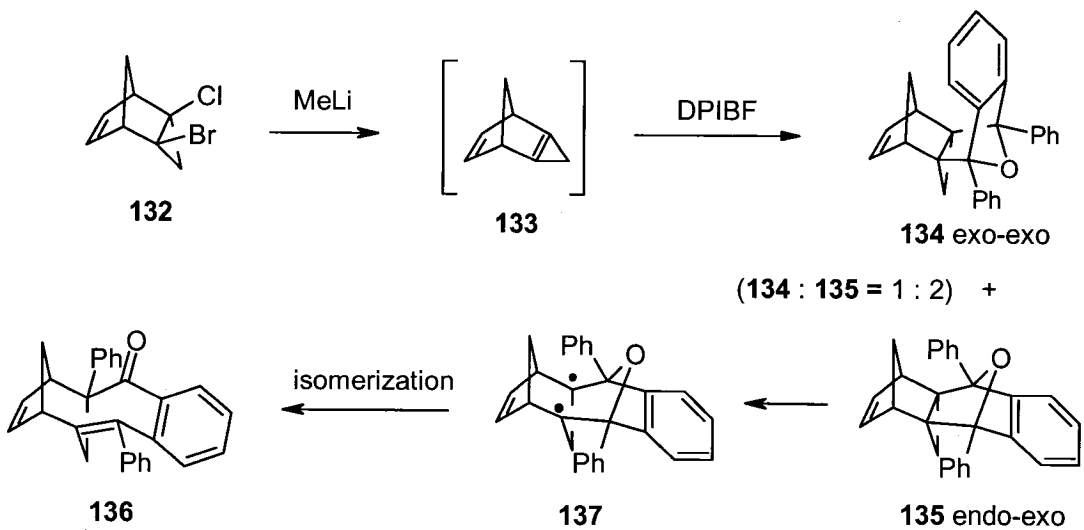

Scheme 1.52 Rearrangement to a Ketone via a Free Radical Reaction

1.4.3 Diels-Alder Reaction of 1,3-Diphenylisobenzofuran with Acetylenic Sulfones

Among the acetylenic dienophiles that have been investigated to date, three fluorinated acetylenic sulfones underwent Diels-Alder reactions with DPIBF, affording the corresponding stable, isolable cycloadducts, as shown in Scheme 1.53.[110b, 118]

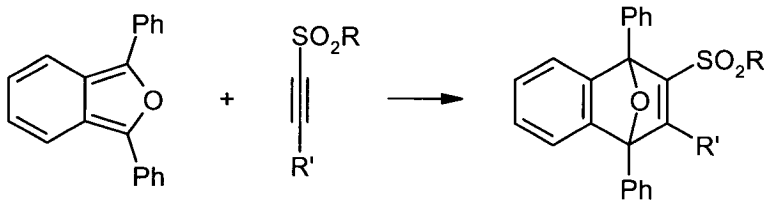

110 **138**

R = CF_3 R' = 1-(8-iodonaphthyl)
R = n-C_4F_9 R' = Ph or n-Pr

Scheme 1.53 Diels-Alder Reaction of DPIBF with Fluorinated Acetylenic Sulfones

Our ongoing interest in acetylenic sulfones prompted us to investigate the cycloadditions of two representative nonfluorinated derivatives (R = *p*-tolyl; R′ = Ph, *n*-Bu) with DPIBF. This work will be the subject of Chapter four.

In summary, the stabilities and further transformations of cycloadducts derived from the reaction of DPIBF with alkyne or cycloalkene dienophiles are highly variable and depend on their specific structures and the conditions. Whereas some such cycloadducts are stable and isolable in excellent yield, others readily undergo further rearrangement to ketones or deoxygenated arenes under acidic or pyrolytic conditions.

1.5 Enantioselective Synthesis of (-)-Julifloridine

Section 1.1.6 described some applications of the acetylenic sulfone-based cyclization methodology by our group to the synthesis of some natural products. It appeared that similar cyclization protocols might also be useful for preparing 2,6-disubstituted 3-piperidinol alkaloids. The total synthesis of one molecule of this family (-)-

julifloridine **(151)** will be described in Chapter five. A brief review of this family of alkaloids is presented in the following section.

1.5.1 Background of 2,6-Disubstituted Piperidinol Alkaloids

2,6-Disubstituted 3-piperidinols, such as *Cassia* and *Prosopis* alkaloids, are wide-spread in nature. They contain three stereogenic centers in the piperidine ring and several examples are shown in Fig. 1.16. This family of alkaloids has been the subject of several reviews. [119] Besides the interesting structural features, these compounds are also of pharmaceutical interest as they exhibit a broad spectrum of biological activities. *Cassia* is a major genus of the Leguminosae and is widely distributed throughout the world. The alkaloid cassine **(139)** from *Cassia excelsa* revealed antimicrobial activity against *Staphylococcus aureus*, *Bacillus subtilis* and *Candida albicans*.[120] (-)-Spectaline **(141)**, (-)-spectalinine **(142)**, (-)-carnavaline **(143)** and leptophyllin B **(145)** were isolated from *Cassia leptophylla* species. Of these, alkaloids **141**, **142** and **143** showed inhibitory activity on mutant yeast strains RS 322YK and RS 321N. Alkaloids **141** and **142** also showed cytotoxicity in the Vero monkey and Chinese hamster ovary cell cytotoxicity assays.[121]

Several related alkaloids such as azimic acid **(149)** and carpamic acid **(150)** also showed a wide range of biological activities, indicating effects on the brain and cardiovascular system.[119a]

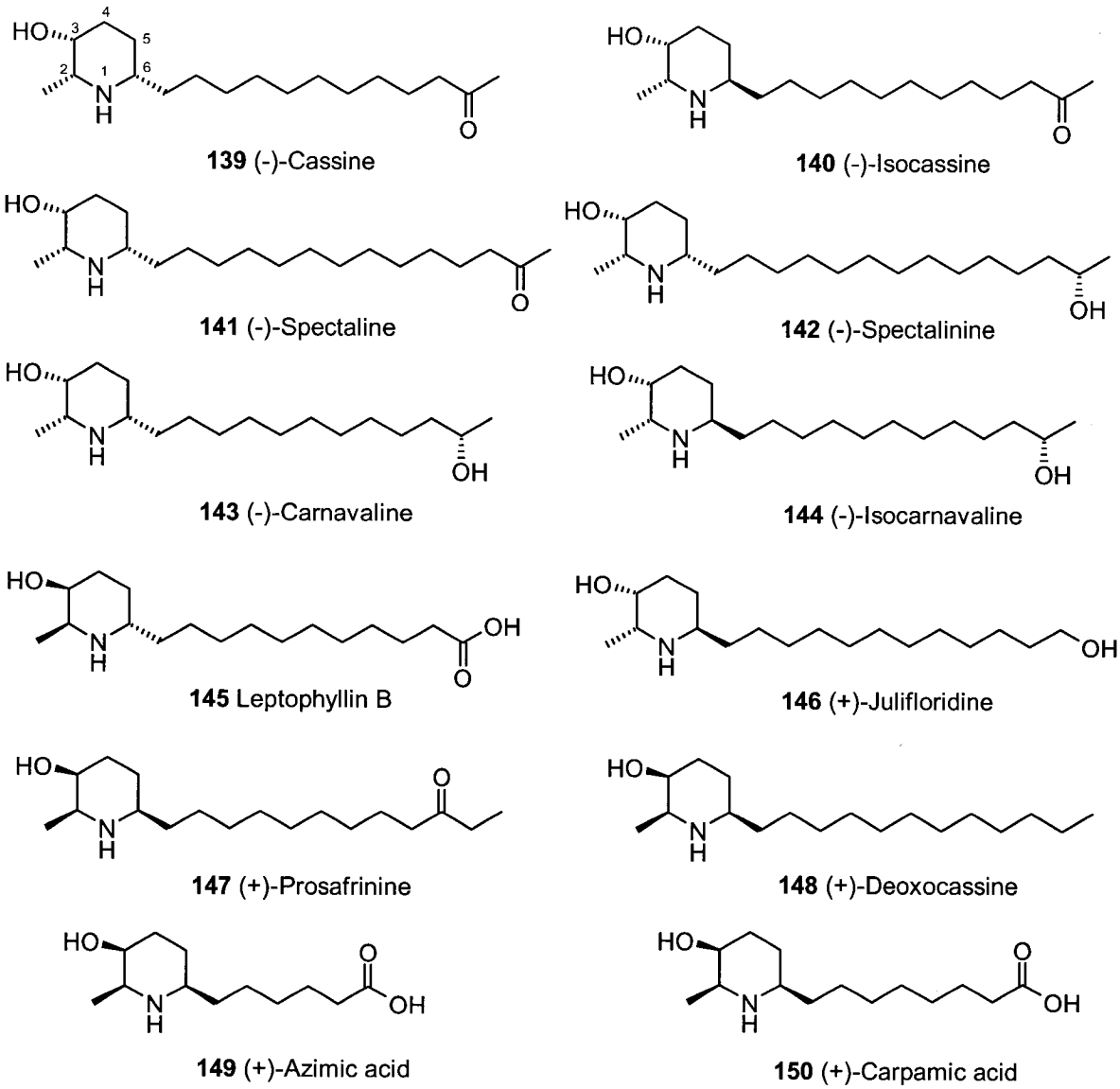

Fig. 1.16 Some Examples of 2,6-Disubstituted 3-Piperidinol Alkaloids

After the discovery and structure elucidation of a variety of 2,6-disubstituted 3-piperidinol alkaloids, much effort was directed towards efficient and stereoselective syntheses of this unique class of compounds. Looking at the above examples, it can be seen that both 2,6-*cis* and 2,6-*trans* substitution patterns exist, as well as either 3α or 3β configurations. As such, it would be useful to develop our acetylenic sulfone-based cyclization methodology so that either 2,6-*cis* or *trans* systems could be accessed to broaden the range of synthetic targets and increase the flexibility of the methodology.

The initial target chosen for this investigatation was julifloridine. The next sections will cover the isolation and biological activity of naturally-occurring (+)-julifloridine, previous syntheses of (+)-julifloridine, and our approach to its unnatural enantiomer, (-)-julifloridine **(151)** (see Fig. 1.17), as illustrated by its retrosynthesis from the cheap starting material *L*-alanine. Of course, in principle, the same steps could be used to make the natural (+)-**146** starting from the commercially available, but more expensive *D*-alanine. Secondly, since **151** has never been made and has not been discovered in nature, it would be interesting to see if displays any bioactivity.

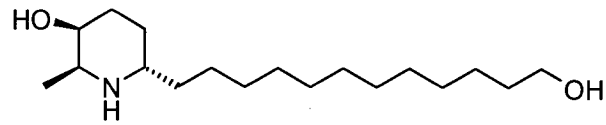

(-)-Julifloridine **(151)**

Fig. 1.17 Absolute Stereochemistry of (-)-Julifloridine

1.5.2 (+)-Julifloridine

1.5.2.1 Background

Many plants of the genus *Prosopis* (Leguminosae) are known to possess medicinal properties and are used in folk medicine as astringents, in rheumatism, and as remedies against scorpion stings and snake bites.[122] *Prosopis juliflora* DC (mesquite) is a shrub that grows abundantly as a weed in Sind and Punjab provinces of Pakistan. Siddiqui and Murthi[123] reported, as far back as 1948, that aqueous and alcoholic extracts of this plant show antibacterial activity. Merzabani and coworkers[124] have also reported the presence of cytotoxic principles in *Prosopis juliflora*. The antibacterial and antifungal activities of these plants were reported by Ahmad.[125] They have activity against 10 Gram positive and 6 Gram negative bacteria at levels similar to those of known antibiotics, such as penicillin and ampicillin.[126] Juliflorine **(152)** and julifloricine **(153)**, the main alkaloids of *Prosopis juliflora*, as well as the less abundant alkaloid julifloridine **(146)** were first isolated by Ahmad *et. al.*[127] The structures of **152** and **153** are shown in Fig. 1.19. The relative

configurations of the stereocenters of julifloridine were confirmed by the synthesis of its racemate.[128] The absolute stereochemistry of (+)-julifloridine was ascertained in 1983,[129] five years after its initial isolation, and was deduced to be 2R, 3R, 6R based on comparison with isocassine **(140)** (see Fig. 1.16).

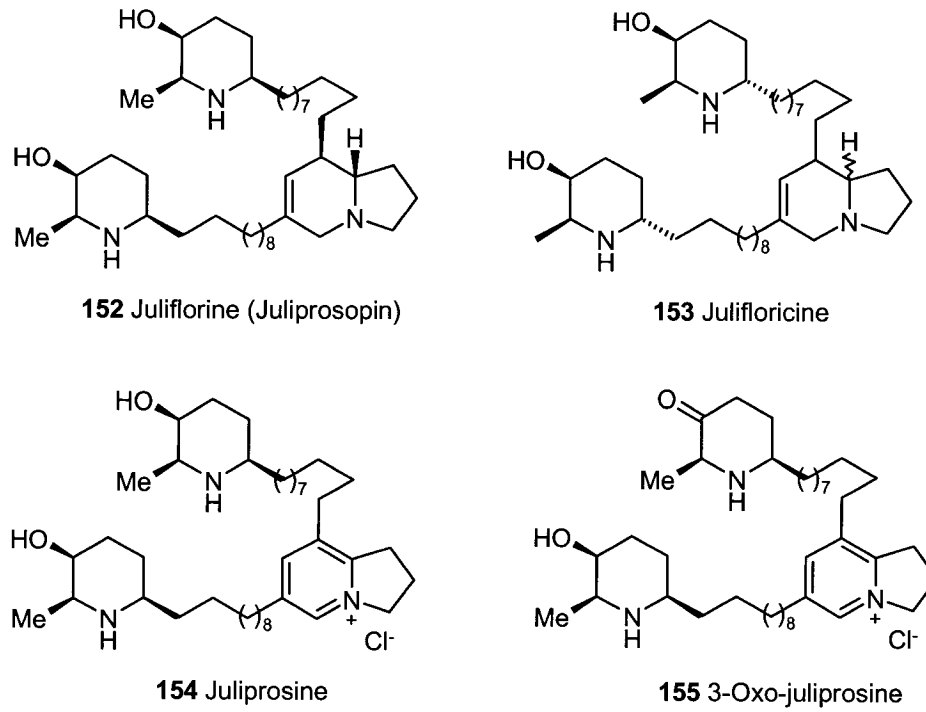

152 Juliflorine (Juliprosopin)

153 Julifloricine

154 Juliprosine

155 3-Oxo-juliprosine

Fig. 1.18 the Structures of Other Alkaloids Isolated from *Prosopis Juliflora*

Two new alkaloids, juliprosine **(154)** and 3-oxo-juliprosine **(155)**, were isolated from *prosopis juliflora* by Hesse and co-workers.[130] The structures of these alkaloids are shown in Fig. 1.18. Alkaloids **152, 154** and **155** showed growth inhibitory activity against both monocotyledonous and dicotyledonous plants.[131]

1.5.2.2 Previous Syntheses

(+)-Julifloridine has been used as a synthetic target in several instances and there exist one racemic and two enantioselective syntheses. Only the enantioselective syntheses will be summarized in sections **1.5.2.2.1** and **1.5.2.2.2**.

1.5.2.2.1 Naito's Synthesis

Naito's synthesis of (+)-julifloridine via adduct **160** is shown in Scheme 1.54.[132] The nitrone **157** was prepared by the condensation of *N*-benzylhydroxylamine and 13-benzoyloxytridecanal **(156)**, which is readily available from the corresponding alcohol by oxidation. Cycloaddition of nitrone **157** to the (+)-allyl alcohol **158** gave a 2.7 : 4.4 : 1 mixture of three adducts **159 - 161** in 57% combined yield. The structures of the adducts were deduced from comparison of their ^{1}H NMR spectra. The major adduct **160** has the correct stereochemistry for the synthesis of (+)-julifloridine **(146)**. Protection of the hydroxyl group in the adduct **160** with a MOM group and deprotection of the silyl group with TBAF gave the alcohol **163** in 59% yield. The chloromethanesulfonyloxy group[133] was introduced as a leaving group for the transformation of isoxazolidine **163** into **164**. Treatment of **163** with $ClCH_2SO_2Cl$ gave the bicyclic compound **164**, which was successively subjected to catalytic hydrogenolysis in the presence of Pearlman's catalyst to give the piperidinol **165** in 77% yield.

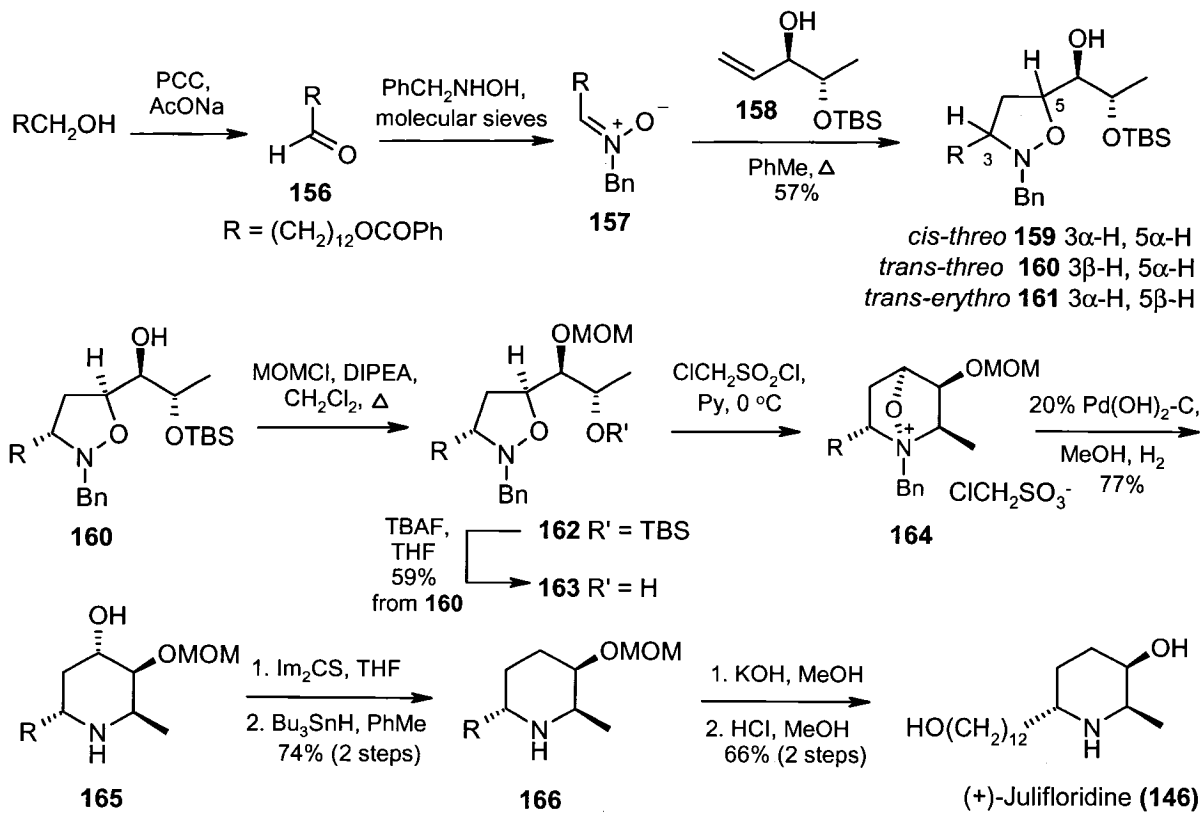

Scheme 1.54 Asymmetric Synthesis of **146** by Naito

Deoxygenation of the piperidinol **165** *via* Barton's ester[134] gave the piperidine **166** in 74% yield. Upon hydrolysis of the ester with potassium hydroxide-methanol solution and deprotection of the MOM group with methanolic hydrogen chloride, piperidinol **146** was obtained in 66% yield. This synthesis afforded (+)-julifloridine **(146)** in nine steps in an overall 6.9% yield from nitrone **157**.

1.5.2.2.2 Charette's Synthesis

Charette's synthesis of (+)-julifloridine was completed while our work was in progress and is shown in Scheme 1.55.[135] The synthesis was based on the ability to chemoselectively functionalize various positions of the chiral dihydropyridine **170**, obtained by diastereoselective nucleophilic 1,2-addition of Grignard reagent **168** to chiral pyridinium salt **169**, in turn generated from amide **167**.[136] Dihydropyridine **170** was then chemoselectively monohydrogenated, affording tetrahydropyridine **171**. The diastereoselective epoxidation of **171** with dimethyldioxirane (DMDO) generated epoxide **172**, that was opened with dimethyl zinc to afford 2,6 *trans*-disubstituted 3-piperidinol **173** in excellent yield. Simultaneous removal of the amidine chiral auxiliary group and benzyl ether cleavage, leading to **146**, was achieved upon treatment with lithium in ammonia. This synthesis afforded (+)-julifloridine in four steps in an overall 33% yield from pyridine. This synthesis is more concise than Naito's synthesis.

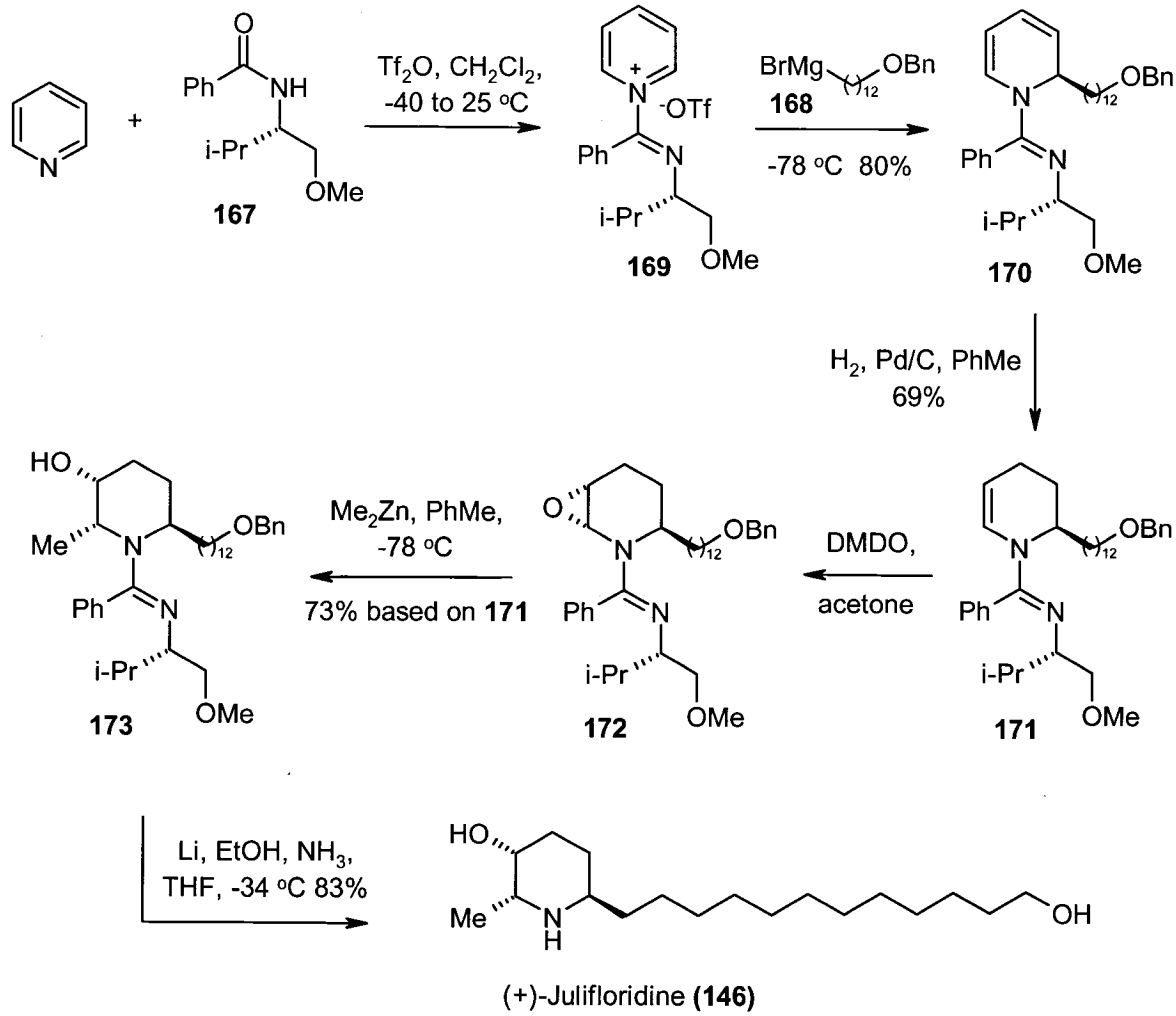

Scheme 1.55 Asymmetric Synthesis of **146** by Charette

1.5.2.3 Application of the Acetylenic Sulfone-Based Cyclization Methodology to a New Approach to 2,6-Disubstituted 3-Piperidinols

In earlier work from our laboratory, M. D. Hamilton showed that either 2,6-*cis* or *trans* disubstituted piperidines **174** and **175**, respectively, can be prepared from a common intermediate, enamine **176**,[137] as shown retrosynthetically in Scheme 1.56.

The common intermediate **176** was synthesized using the cyclization methodology described in section **1.1** from two starting materials: chloroamine **178** and acetylenic sulfone **179**. While this methodology was not developed further at the time, it points the

way to a stereodivergent approach to 2,6-*cis* or *trans* alkaloids which appeared worthy of further pursuit.

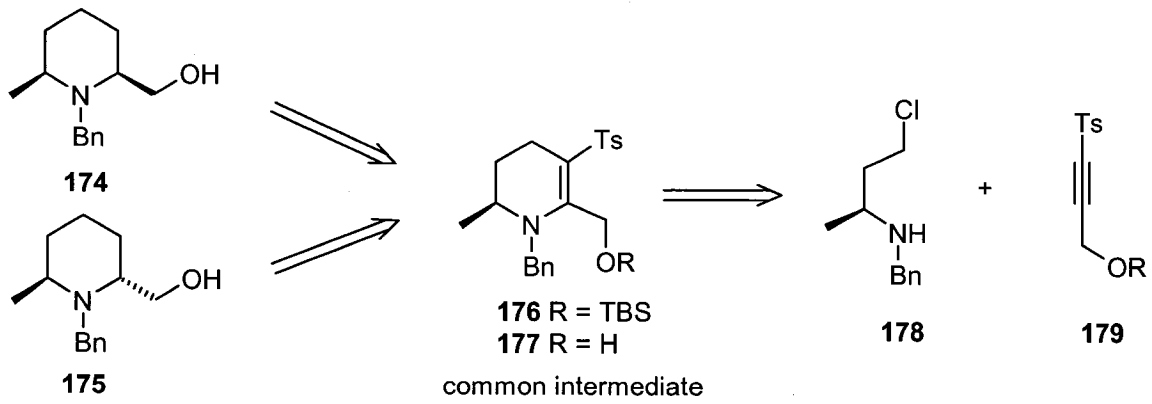

Scheme 1.56 Retrosynthesis of 2,6-Disubstituted Piperidines

More specifically, M. D. Hamilton studied the reduction of **176** and the free alcohol **177** (see Scheme 1.57) and the results are summarized in Table 1.3. The best selectivity for the reduction of **176** was a 2:1 ratio in favour of the *cis* isomer **180** using 9-BBN(CN) and trifluoroacetic acid, with a yield of 44%. The same selectivity was obtained using hydrogen and a palladium catalyst, but the yield was reduced to 30%. With sodium cyanoborohydride a yield of 64% was obtained, but no selectivity was observed. The *cis/trans* ratios of products were determined by desulfonylation, followed by deprotection of the silyl ethers **184** and **185** to the known amino alcohol **174** and its *trans* isomer **175**, respectively. A better stereoselectivity on the reduction of the free alcohol **177** was obtained using 9-BBN(CN) and trifluoroacetic acid, but the reduction favoured the *trans* piperidine **183** by a ratio of 4:1 with a yield of 30%. Sodium cyanoborohydride also favoured the *trans* isomer, with a ratio of 3:1 and a yield of 56%. Hydrogenation over palladium resulted in no reduction at 1 atm. The *cis/trans* ratios of products were also determined by conversion to the known amino alcohols **174** and **175**.

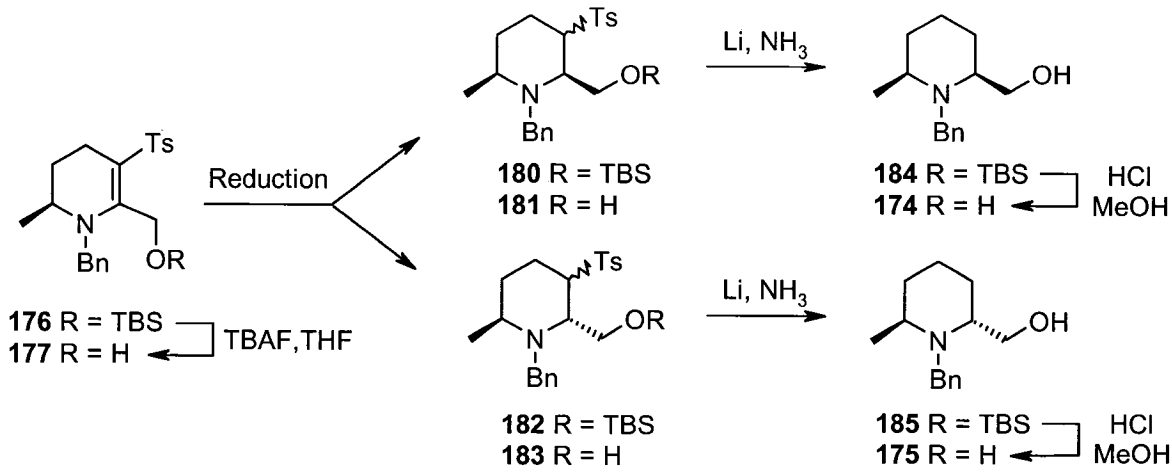

Scheme 1.57 Reduction of Enamine Sulfones **176** and **177**

Table 1.3 Results of Reduction of Enamine Sulfones **176** and **177**

Reduction Method	Yield of **180** and **182**	Ratio **(180:182)**	Yield of **181** and **183**	Ratio **(181:183)**
$NaBH_3CN$/TFA	64%	1:1	56%	1:3
9-BBN(CN)/TFA	44%	2:1	30%	1:4
H_2 (1atm), Pd/C	30%	2:1	0%	n/a

Further improvements in the stereoselective formation of **174** and/or **175** would then provide access to a large number of naturally-occurring 2,6-*cis* and/or 2,6-*trans* disubstituted piperidines.[119c] However, the 2,6- disubstituted 3-piperidinol system has not been explored by this method and the synthesis of (-)-julifloridine appeared to be a worthy extension of the earlier work by Hamilton. Ultimately, if this approach proved successful, its extension the natural (+)-enantiomer could be pursued, as well as to other members of the 2,6-*cis* and/or 2,6-*trans* 3-piperidinols.

Like the proposed retrosynthesis of 2,6-disubstituted piperidine alkaloids discussed above, my approach to the 3-piperidinol skeleton, shown retrosynthetically in Scheme 1.58, is focused on the utilization of enamine sulfone **189** as a building block to generate the 2,6-*trans*-piperidinol skeleton. The 2,6-*trans*-piperidinol should be available from **187**

by a Swern oxidation followed by Wittig reaction and hydrogenation/hydrogenolysis. The diastereoselective reduction of the desilylated derivative of enamine sulfone **189** using sodium cyanoborohydride, followed by reductive desulfonylation should afford the 2,6-*trans*-piperidine **187**. Similarly, it should be possible to achieve the synthesis of 2,6-*cis*-piperidinols by diastereoselective reduction of the enamine sulfone **189** by hydrogenation, followed by desilylation and desulfonylation. The common intermediate enamine sulfone **189** whould be prepared from the sequence of a conjugate addition followed by base-mediated cyclization of chloroamine **190** and acetylenic sulfone **191** via the general method described in section **1.1.6**. The results of the application of this approach to the synthesis of (-)-julifloridine will be described in Chapter five.

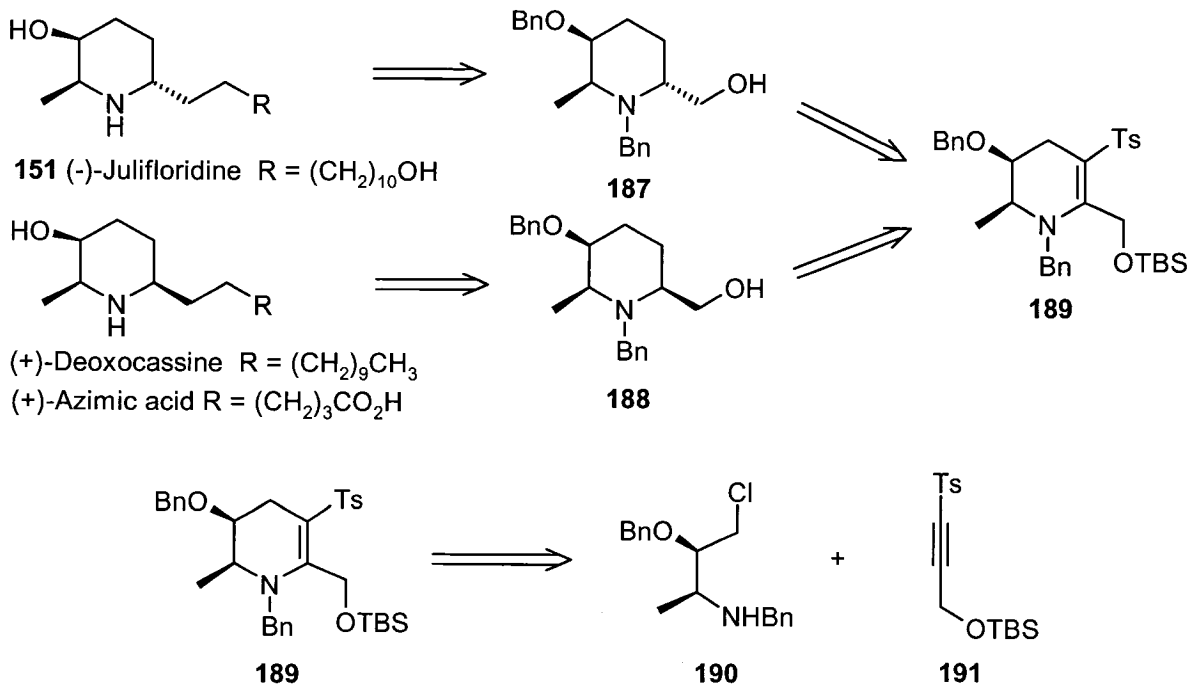

Scheme 1.58 Retrosynthesis of 2,6-Disubstituted 3-Piperidinol Alkaloids

1.6 Objectives

The objectives of this thesis can be separated into four areas. First is the investigation of vinyl sulfones as an extension to the cyclization methodology developed previously with acetylenic sulfones, and of certain stereospecific rearrangements that were

observed during these studies. Second, we intended to develop the first syntheses of polymer-supported acetylenic sulfones and to investigate their applications to the preparation of various cyclized products. Third, we wished to examine the mechanism of rearrangements of the Diels-Alder cycloadducts obtained from acetylenic sulfones and 1,3-diphenylisobenzofuran under various conditions. Last, we wished to explore the extension of the established conjugate addition-cyclization protocol of acetylenic sulfones to construct 2,6-disubstituted 3-piperidinol alkaloids. In particular, (-)-julifloridine was chosen as the target molecule to illustrate this methodology.

Chapter 2

Synthesis of Nitrogen Heterocycles Using Vinyl Sulfones

2.1 Background

As described in section 1.2, we wished to extend the current acetylenic sulfone-based cyclization methodology to include vinyl sulfones. We were interested in extending this methodology toward the preparation of saturated sulfone products directly without the reduction of the enamine double bond as is necessary when acetylenic sulfones are used. We were particularly interested in accessing pyrrolidine, piperidine, quinolizidine, and indolizidine structures. These targets are shown collectively in Fig. 2.1, with bold lines used to indicate the molecular fragment which would originate from the vinyl sulfones.

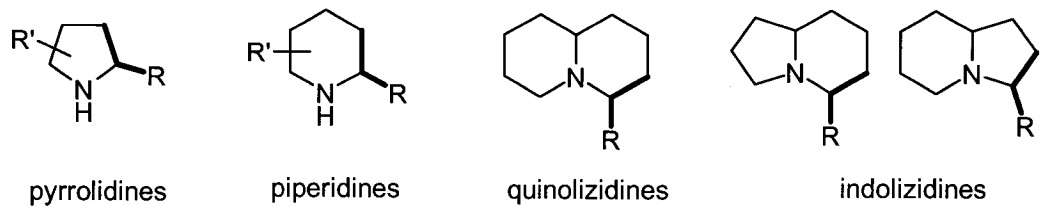

Fig. 2.1 Nitrogen Heterocycles That Might be Synthesized from Vinyl Sulfones

Scheme 2.1 illustrates retrosynthetically how the conjugate addition / cyclization / desulfonylation approach outlined in section 1.1 for the synthesis of nitrogen heterocycles might be adapted to the use of vinyl sulfones for the synthesis of structures shown in Fig. 2.1. This approach requires the conjugate addition of an amino alcohol to a vinyl sulfone, which is considerably less reactive than the corresponding acetylenic sulfone.

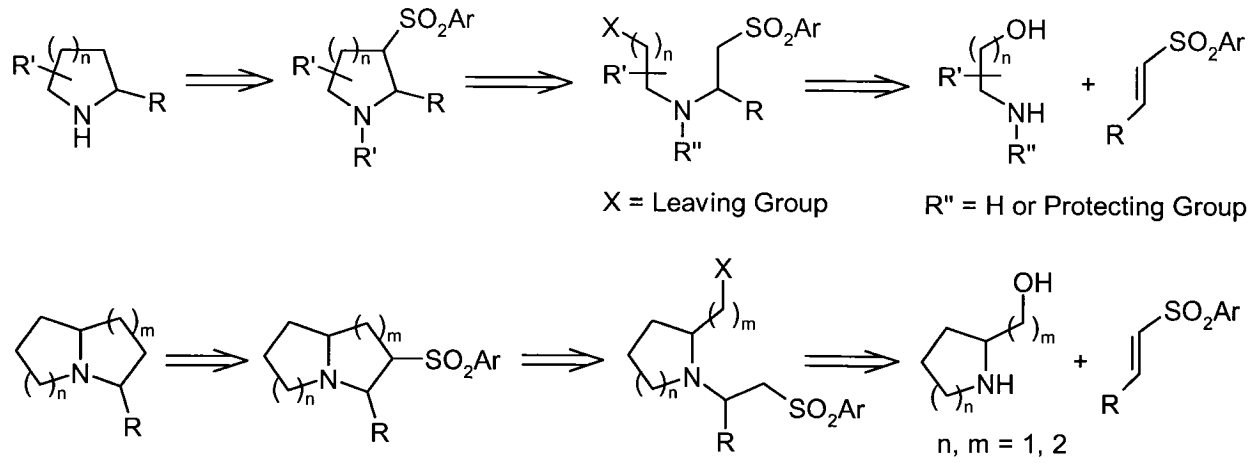

Scheme 2.1 Retrosynthesis of Nitrogen Heterocycles Using Vinyl Sulfones

We were concerned that the first step might not proceed without harsh reaction conditions and also that the steric bulk of the R substituent might adversely affect the reaction. The utilization of amines as nucleophiles in conjugate addition reactions with vinyl sulfones was explored thoroughly in the 1960's by Stirling.[5a, 34, 40] Stirling's reports showed that additions of amines to *p*-tolyl vinyl sulfone are not reversible under the conditions used, and that the products, therefore, result from a kinetic rather than thermodynamic process. Stirling and coworkers suggested a concerted process involving two equivalents of amine where the function of the second molecule (or of an alcohol solvent) is in the catalysis of a proton transfer step (see Fig. 2.2).[34]

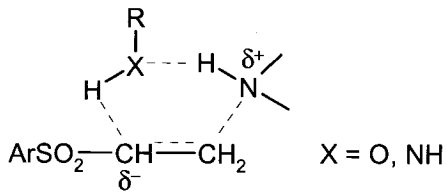

Fig. 2.2 Transition State for Amine Addition Proposed by Stirling

Three aspects affecting the rate constants measured by Stirling for these reactions are noteworthy. First, steric effects play an important role in the determination of reactivity. For example, piperidine is 7000 times as reactive as its 2,6-dimethyl derivative,

and chain-branching in acyclic amines similarly lowers reactivity, although the effect is less pronounced. Secondly, provided that the steric requirements of amines are the same, large differences in basicity have relatively little effect on reactivity. In solution, the inductive effect of *N*-alkyl substituents was overwhelmed by steric effects. Thirdly, solvation effects also play an important role in determination of reactivity. If the solvent is ethanol, the primary amines are notably less reactive than the secondary amines. It seems probable that a primary amine in ethanol forms hydrogen bonds through both of its *N*-hydrogen atoms, while only one such atom is available in secondary amines. The reactivity of the primary amine is thus depressed by its relatively greater bulk together with the need to shed solvent molecules in the transition state. The reverse reactivity order was observed when the reactions took place in *t*-butanol. The effect of solvent upon the reactivities of two primary-secondary amine pairs is shown in Table 2.1.[34]

Table 2.1 Solvent Effects on Rates of Addition of Amines to *p*-Tolyl Vinyl Sulfone at 25 °C (k in $M^{-1}\cdot s^{-1}$)

Amine	10^3k_{EtOH}	$10^3k_{t\text{-}BuOH}$
Bu^nNH_2	8.0 ± 0.1	14.4 ± 0.2
n-$C_6H_{13}NH_2$	10.6 ± 0.4	15.8 ± 0.5
$Bu^n{}_2NH$	12.5 ± 0.1	0.59 ± 0.01
Et_2NH	23.3 ± 0.2	1.31 ± 0.02

Stirling also studied the rates of addition of piperidine to a series of methyl-substituted *p*-tolyl vinyl sulfones, as indicated in Fig. 2.3. Reaction rates of additions of piperidine to sulfones **192-194** at 25 °C in ethanol were measured to be 5850 × 10^{-4}, 7 × 10^{-4}, and 0.9× 10^{-4} $M^{-1}\cdot s^{-1}$, respectively. Piperidine did not react at all with sulfone **195**.[5a]

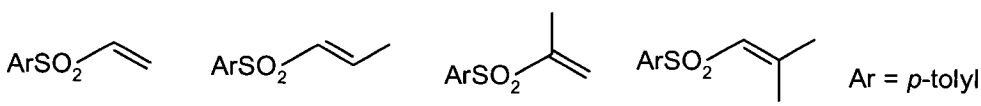

192 **193** **194** **195**

Reaction rate: 5850×10^{-4} $M^{-1}\cdot s^{-1}$ 7×10^{-4} $M^{-1}\cdot s^{-1}$ 0.9×10^{-4} $M^{-1}\cdot s^{-1}$

Fig. 2.3 Substituted *p*-Tolyl Vinyl Sulfones Studied by Stirling

The effect of substitution in decreasing the reactivity of the double bond is clear. At least three factors may be responsible: (1) an increase in non-bonded interactions between the nucleophile and the olefin, (2) additional stabilization of the olefin in the ground state by hyperconjugative interaction with the methyl groups, and (3) destabilization, by electron donation from the methyl group, of the carbanionic centre developed in the transition state.[5a]

The reaction rates show that the combination of factors more effectively retards addition to the α-methyl isomer **194** compared to the β-methyl isomer **193** and indicate that the carbanion-destabilizing effect of an α-methyl group has a greater influence on rates of addition than the combination of the adverse steric and olefin stabilization effects of a β-methyl group.

A further search of the chemical literature[138] revealed similar examples of the conjugate additions of functionalized amines to vinyl sulfones. The relevant examples that were found either involved more nucleophilic amines or less bulky substituents in the β position of the vinyl sulfone compared to the examples of Stirling.

2.2 The Synthesis of Nitrogen Heterocycles Using Vinyl Sulfones

2.2.1 Additions of Amino Alcohols to Phenyl Vinyl Sulfone and Subsequent *N*-Benzylation

We began our investigations by attempting to react phenyl vinyl sulfone **(27)** with amino alcohols **196-202** indicated in Fig. 2.4. The amino alcohols **196-198** were readily obtained from *L*-alanine, *L*-phenylalanine and *L*-valine, respectively,[139] while sulfone **27** was obtained as outlined by Brace.[140] 3-Aminopropanol **(199)**, (-)-ephedrine **(200)**, as well as compounds **201-202** are all commercially available.

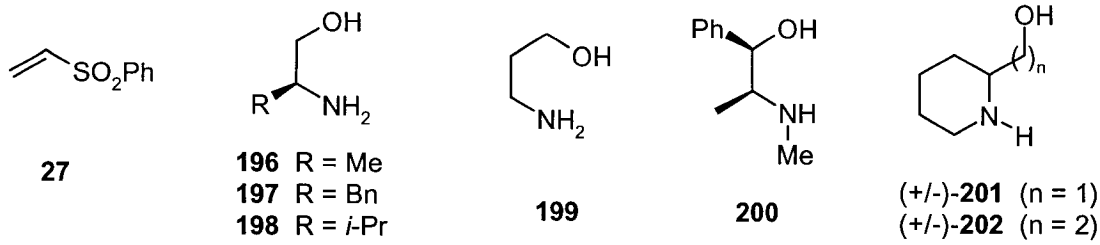

Fig. 2.4 Structures of Amino Alcohols for Reaction with **27**

Typically, the reactions failed at room temperature but proceeded at reflux in a variety of solvents to afford adducts **203-209** (see Scheme 2.2). The conjugate addition reactions between **196-202** and **27** in isopropanol or xylenes were thus successful in producing the desired products in almost quantative yield, except in the case of **198**, where a slightly lower yield was obtained. These examples show that both primary and secondary amines can be employed in this process.

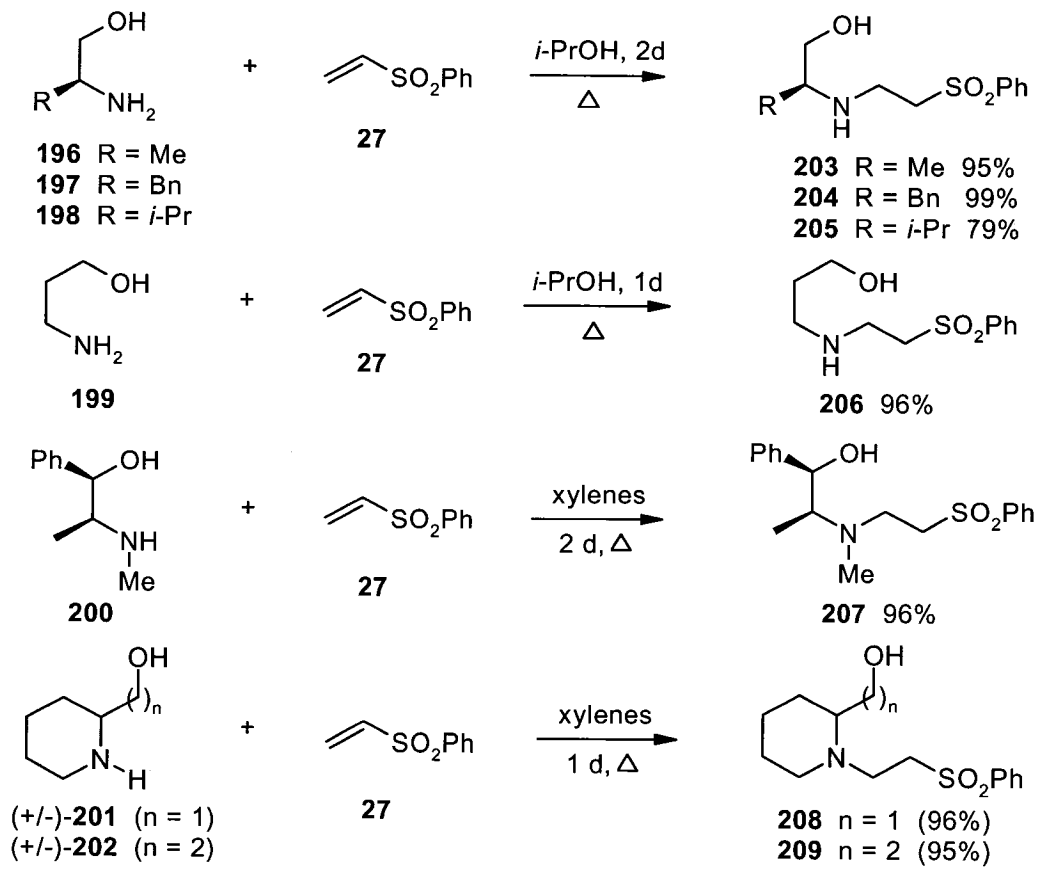

Scheme 2.2 Conjugate Additions of Amino Alcohols to Sulfone **27**

In order to permit easier handling in subsequent steps, products **203-206** were *N*-benzylated to give amines **210-213** as shown in Scheme 2.3. The conjugate addition adducts, benzyl bromide (1.2 equiv.), and DIPEA (1.5 equiv.) were refluxed for 4 h in anhydrous acetonitrile to provide the *N*-benzylated products in high yield.

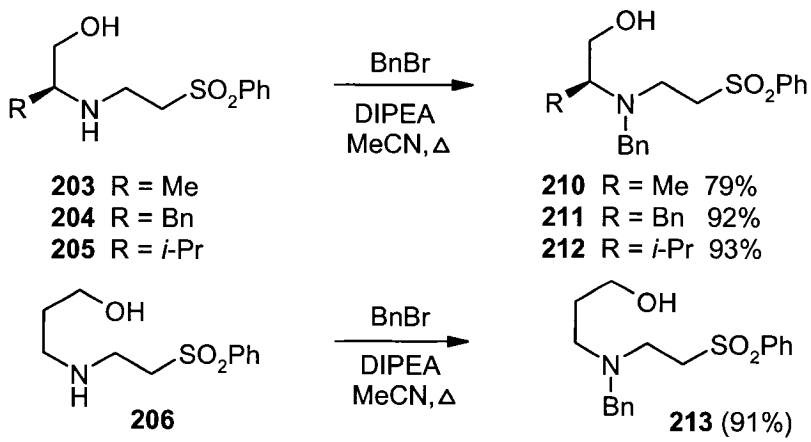

Scheme 2.3 *N*-Benzylation of Products **203-206**

Alternatively, amino alcohols **196-199** were first *N*-benzylated using sodium borohydride and benzaldehyde to afford the corresponding products **214-217**, which were then employed in the initial conjugate addition step. This resulted in a more sluggish reaction, leading to diminished yields of the corresponding adducts **210-213** (see Scheme 2.4).

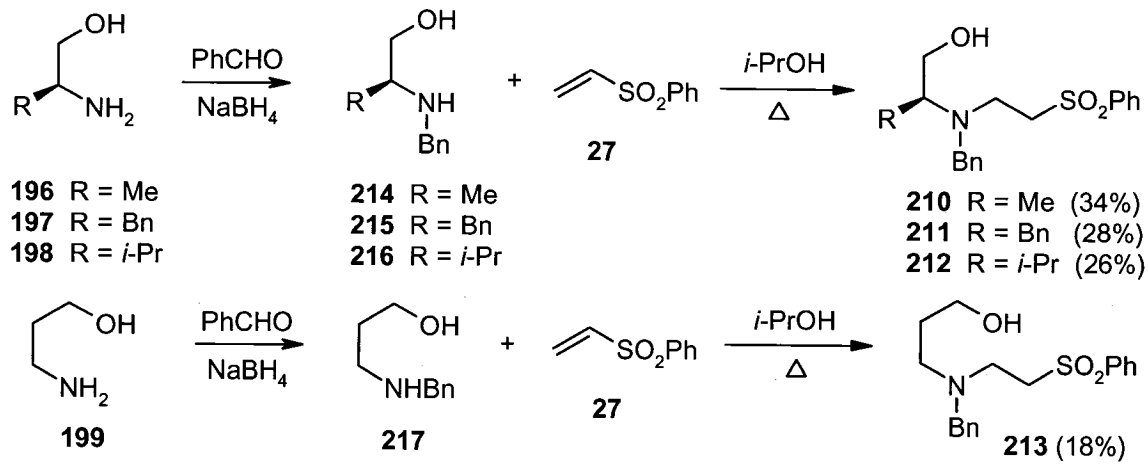

Scheme 2.4 Additions of *N*-Benzylated Amino Alcohols to Sulfone **27**

2.2.2 Chlorination or Tosylation of Adducts and Subsequent Cyclization

Products **210-212** were treated with thionyl chloride, followed by workup with aqueous potassium hydroxide solution. Interestingly, we observed that a facile rearrangement occurred during this process, leading to the stereospecific formation of the chloroamines **218** and **219**. Cyclization of the latter compounds with LDA then afforded the pyrrolidine derivatives **220-222** (see Scheme 2.5). The chlorination product of amino alcohol **211** was not isolated and it was subjected to intramolecular alkylation after removal of the excess thionyl chloride without basic workup.

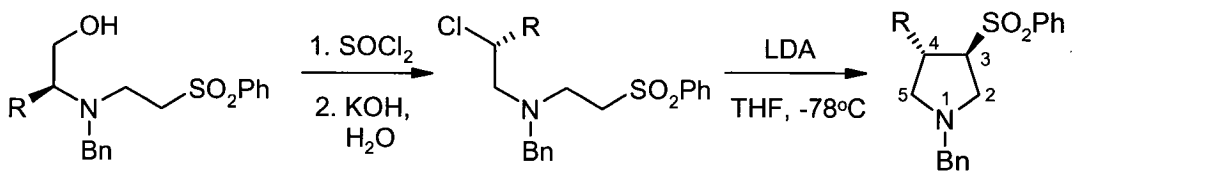

210 R = Me
211 R = Bn
212 R = *i*-Pr

218 94%

219 95%

220 80%
221 79% (overall from **211**)
222 90%

Scheme 2.5 Chlorination and Subsequent Cyclization of Adducts **210-212**

Assignment of the structure of the chloroamine product **218** obtained after the chlorination step was based on NMR evidence, including the observation of relatively downfield ^{1}H and DEPT-135-NMR signals of its **C**HRCl group (Fig. 2.5). The ^{1}H NMR spectrum of **218** showed two doublets of doublets at δ 2.75 ppm and at δ 2.60 ppm that couple with each other and with one other neighboring H at δ 3.92 ppm. As such, the former protons were initially assigned to an AB pattern that corresponds to the H_a and H_b in either **218** or **223**, as shown in Fig. 2.6. As well, the multiple at δ 3.92 ppm was attributed to H_c in either **218** or **223**.

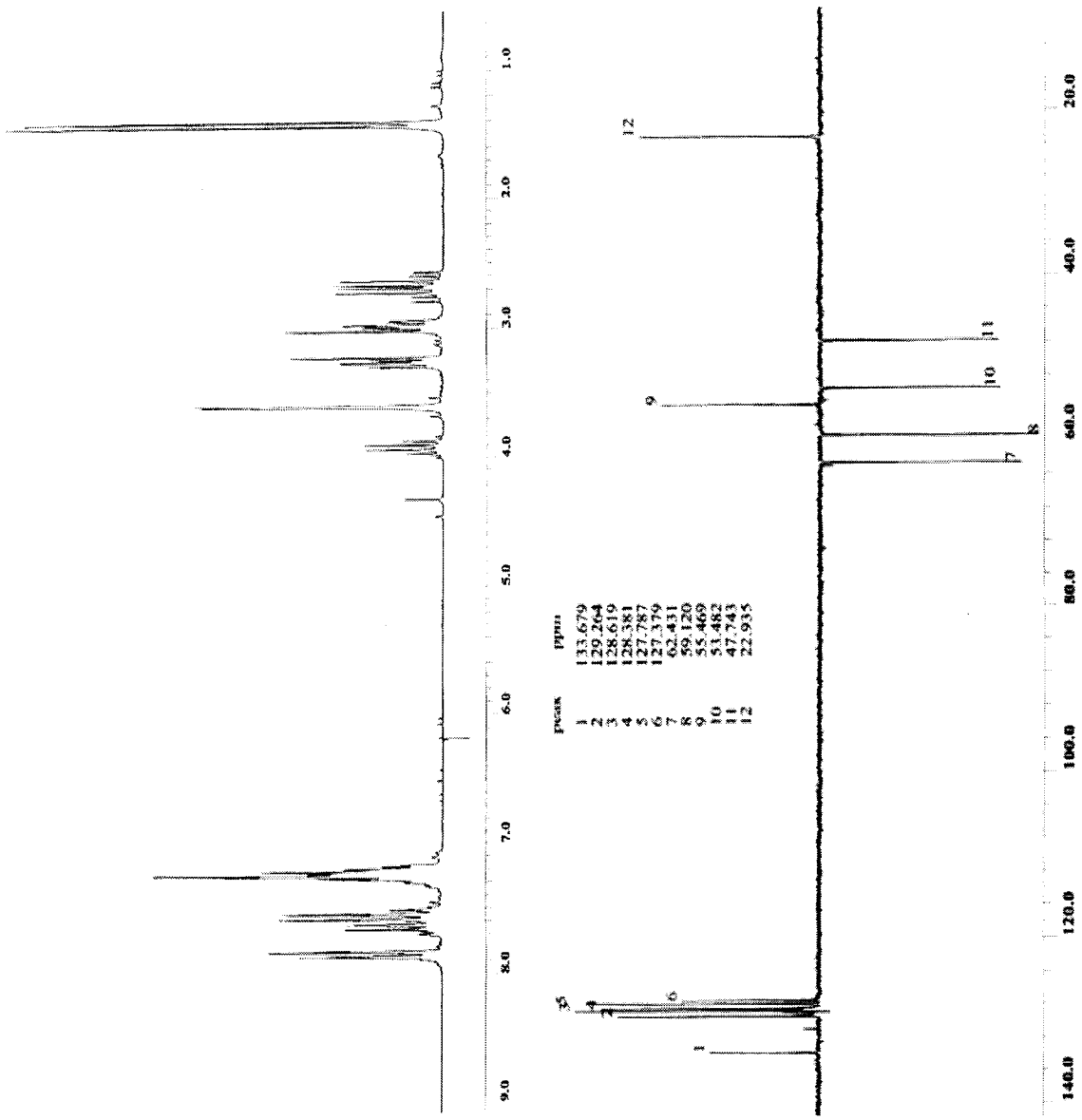

Fig. 2.5 ^{1}H and DEPT-135-NMR Spectra of Chloramine **218**

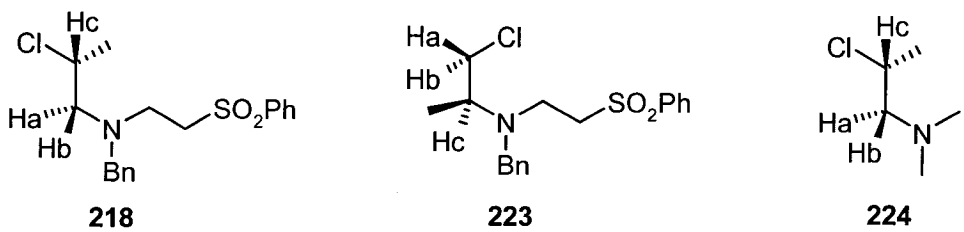

Fig. 2.6 Structures of Chloroamines

The ^{1}H NMR spectrum of $Me_2NCH_2CH(Me)Cl$ **(224)** is reported to show a chemical shift of H_c at δ 4.0 ppm, while the AB pattern of H_a and H_b is found around δ 2.5 ppm, which is in reasonably close agreement to the observed spectrum of the chlorination product obtained from **210**.[141] Furthermore, the DEPT-135 spectrum of the chlorination product shows the CH_c signal at δ 55.5 ppm, and that of CH_aH_b at δ 47.7 ppm. In the case of **224**, CH_c is more deshielded than CH_aH_b. Thus, based on the above spectroscopic evidence, the structure of the chlorination product was assigned to be **218** rather than **223**. This was later confirmed by its further conversion to **220** (vide infra).

As illustrated in Scheme 2.5, cyclization of adduct **218** was carried out with LDA in THF at -78 °C and afforded **220** in high yield. All ^{1}H and ^{13}C NMR signals of the cyclized product **220** were assigned by DEPT, COSY, and HMQC experiments. The *trans* orientation of the methyl and benzenesulfonyl substituents in **220** was confirmed by an NOE experiment. Irradiation of the CH_3CH signal at δ 1.03 ppm enhanced the $CHSO_2$ signal at δ 3.3 ppm by 3%, while irradiation of the latter signal enhanced that of the CH_3 group by 9%. This confirmed that the methyl group and α-sulfonyl proton were vicinal and *cis* oriented. Further evidence for the configuration at the 4-position of the pyrrolidine ring was confirmed by reductive desulfonylation to the known compound **265**[142] (see section **2.2.6**). Similar rearrangements were observed with **211** and **212**, which produced pyrrolidine **221** and **222**, respectively. Again, the ^{1}H and ^{13}C NMR signals indicated that a similar rearrangement had occurred as in the case of **210**.

The tosylate group can also be employed as a good leaving group; therefore tosylation and subsequent cyclization were applied to adduct **213**. Using standard techniques, the tosylate was synthesized and isolated as a white solid in high yield. Unfortunately, several attempts to cyclize the tosylate with LDA in THF at -78 °C, or even at room temperature, afforded unreacted starting material and complex mixtures of unidentified products (see Scheme 2.6).

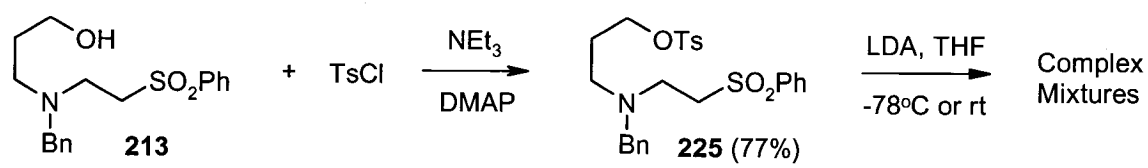

Scheme 2.6 Tosylation and Attempted Cyclization of Adduct **213**

Treatment of **207** with thionyl chloride (2 equiv.) in chloroform under reflux for 3 h and then concentration in vacuo to remove excess thionyl chloride provided the corresponding chloroamine hydrochloride salt, which was used in the next step without basic workup. The residue was dissolved in THF and was treated with three equivalents of LDA at -78 °C to afford smooth conversion, via intramolecular alkyation, to the cyclized products **226** and **227** (see Scheme 2.7).

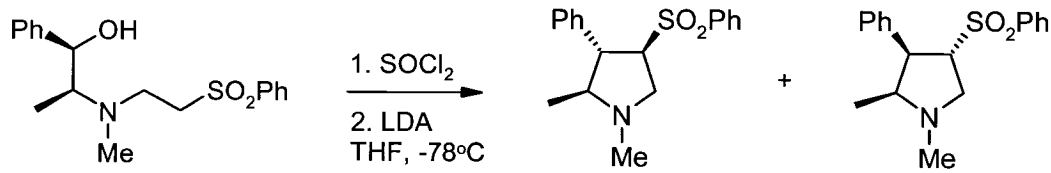

207 **226** (40%) **227** (29%)

Scheme 2.7 Chlorination and Subsequent Cyclization of Adduct **207**

Interestingly, **226** and **227** were diastereomers obtained in the ratio of about 4:3, and neither had undergone rearrangement of the *C*-methyl group as had previously been observed for compounds **210-212**. However, epimerization at the phenyl-substituted carbon atom had clearly occurred during the cyclization of **207** to **226** and **227**. The structure of the major product **226** was confirmed by X-ray crystallography. Details of the crystal structure of **226** are given in Appendix I and the ORTEP (Oak Ridge Thermal Ellipsoid Plot) diagram is shown in Fig. 2.7. The structure of **227** was based on NMR evidence. The *trans* orientation of the phenyl and benzenesulfonyl substituents in **227** was suggested by an NOE experiment. Irradiation of PhCH only slightly enhanced SO_2CH by 1%, while irradiation of the latter signal gave no enhancement of PhCH. In addition, the *cis* relationship of phenyl group and methyl group in **227** was confirmed by reductive desulfonylation with sodium amalgam, affording the known compound (*R*)-*N*-benzyl-2-methyl-3-phenylpyrrolidine **(267)**[143] (see section **2.2.6**).

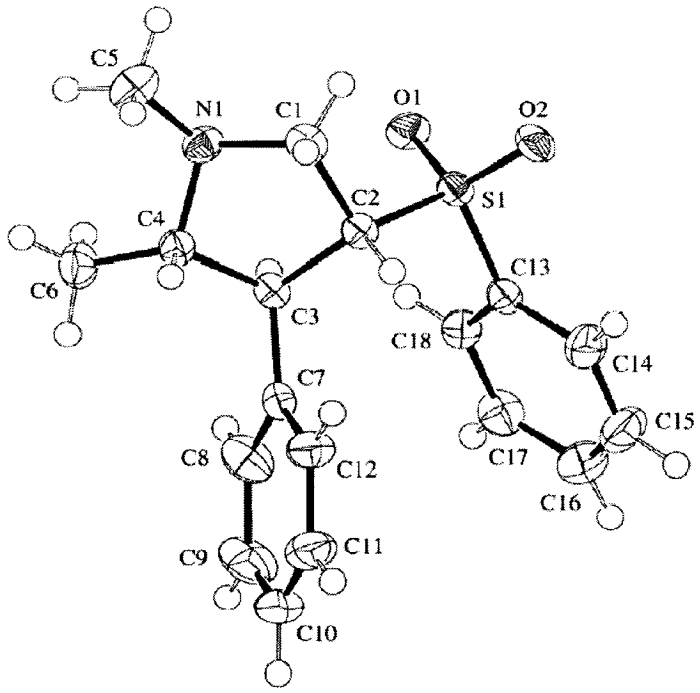

Fig. 2.7 ORTEP Diagram of **226**

The similar chlorination and subsequent cyclization of adducts **208** and **209** afforded the corresponding indolizidine **230** and quinolizidine **231**, respectively. Product **230** was obtained as a 54:46 mixture of separable diastereomers, while **231** was obtained as a single diastereomer. Unambiguous assignment of respective stereochemistry was not possible for **230** and **231**. Compound **231** has been reported previously with unspecified stereochemistry.[144]

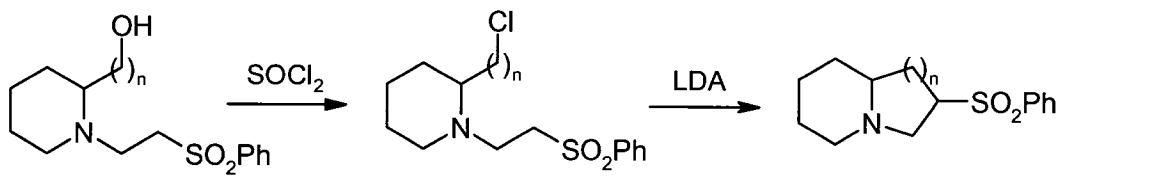

208 n = 1
209 n = 2

228 n = 1 (87%)
229 n = 2

(+/-)-**230** n = 1 84% (mixture of two diastereomers)
(+/-)-**231** n = 2 74% (based on **209**; single diastereomer)

Scheme 2.8 Chlorination and Subsequent Cyclization of Adducts **208-209**

2.2.3 Rationale for the Rearrangements of 210-212

The rearrangements leading to **220-222** can be rationalized by invoking the formation of aziridinium ion intermediates **232** during the chlorination of **210-212** with thionyl chloride (Scheme 2.9). The neighbouring group effects of nitrogen mustards and related species are well-known to involve such intermediates. [145] Although many nucleophiles typically open aziridinium ions at the less substituted carbon atom, we envisaged that the regiochemistry of ring-opening of aziridinium species is determined by a combination of steric and electronic factors. The steric bias could be overcome by the electron-donating effect of the R substituent group of **232**, which would sufficiently stabilize cationic character at the tertiary center to facilitate preferential nucleophilic opening at that site. Furthermore, there is precedent for preferential reaction at the more substituted carbon atom of aziridinium species **234** with inversion of configuration by unhindered nucleophiles such as chloride ion to afford **224** (Scheme 2.9).[146]

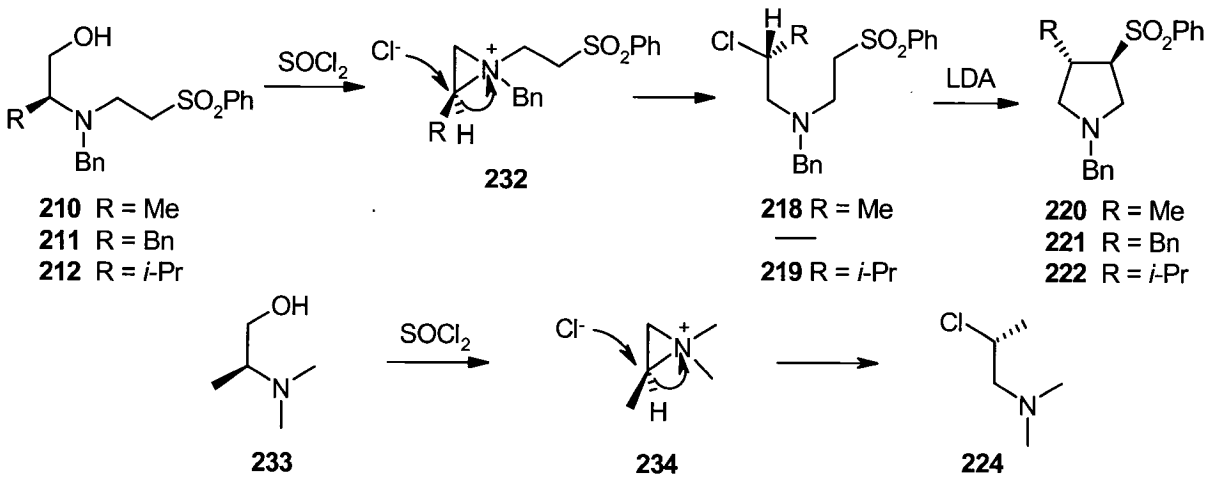

Scheme 2.9 A Plausible Mechanism for Rearrangements Leading to **220-222**

In our case, attack by chloride ion at the tertiary carbon atom of **232** with inversion of configuration afforded the rearranged products **218-219**, and ultimately **220-222**, respectively, after a second inversion during intramolecular alkylation of the corresponding sulfone-stabilized anion. This accounts for the observed stereochemistry during the overall cyclization of **210-212** to **220-222**, respectively.

2.2.4 Rationale for the Absence of Rearrangement in 207-209

The absence of rearranged products from the (-)-ephedrine adduct **207**, along with the observed epimerization of the phenyl-substituted carbon atom, suggests the formation of carbocation **235** rather than aziridinium ion **236** during the chlorination step (Scheme 2.10). The epimerization is the expected result of attack by chloride ion upon either face of the carbocation **235**. This is in contrast to the reactions of the mesylates of other ephedrine and pseudo-ephedrine derivatives, which react via aziridinium ions.[147]

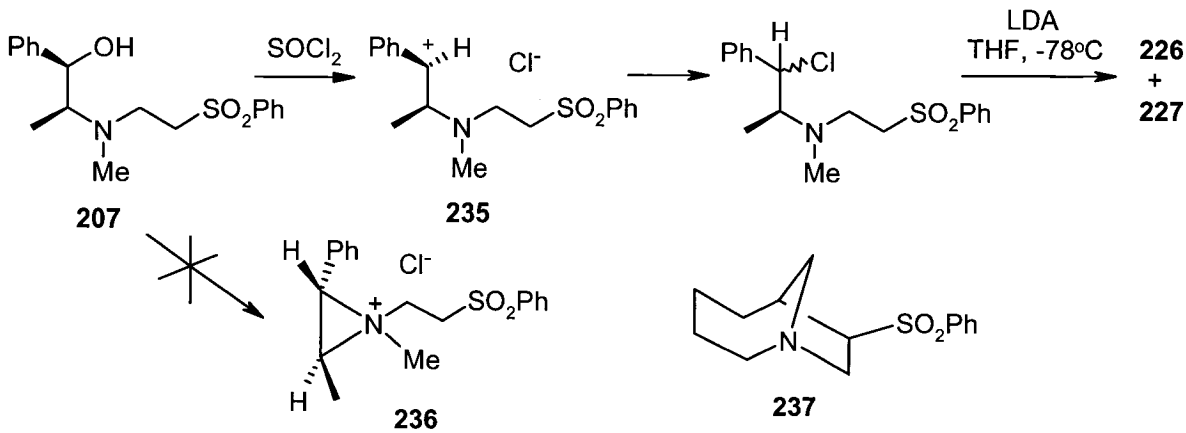

Scheme 2.10 Rationale for the Absence of Rearrangement in **207**

Similarly, the formation of **230** (Scheme 2.8) instead of the rearranged product **237** (Scheme 2.10) from **208**, indicates either that aziridinium ion formation does not occur during the chlorination of **208**, or that chloride ion attack occurs at the less substituted aziridinium carbon atom, in contrast to the outcome with **232**. There is precedent for the ring-opening of an aziridinium ion fused to a five[148] or six-membered[149] ring occurring at the less substituted site with chloride ion and other nucleophiles.

2.2.5 Additions of Amino Alcohols to Vinyl Sulfone 238 and Subsequent *N*-Benzylation, Chlorination or Tosylation and Cyclization

2.2.5.1 Reactions of Acyclic Amines with Vinyl Sulfone 238

The same sequence of conjugate addition, *N*-benzylation, chlorination and cyclization with LDA was applied to amino alcohols **196** and **197** with vinyl sulfone **238** (Scheme 2.11). Due to greater steric hindrance associated with β-substituted vinyl sulfones, the rate of addition of **196** and **197** to sulfone **238** was expected to be dramatically lower than that to sulfone **27**. However, the direct addition of **196** to **238** proved to be facile and proceeded in isopropanol to afford 50% of **239** upon refluxing for 1 day. When refluxed in xylenes, the reaction of **196** and **197** with **238** was largely complete in one day and proceeded cleanly to form **239** and **240** in 91% and 87% isolated yield, respectively.

The previous sequence of *N*-benzylation, chlorination and cyclization with LDA was then applied to **239** and **240**. The rearrangement of the R substitutent was again observed. The structures of the two main cyclized products **243** and **244** (in the case of **241**) were confirmed by X-ray crystallography (Fig. 2.8 and Fig. 2.9, respectively), which clearly indicated that rearrangement of the methyl group of **241** that was originally present in **196** had occurred. The structure of the major cyclized product **245** (in the case of **242**) was also confirmed by X-ray crystallography and the ORTEP diagram is shown in Fig. 2.10. Details of the crystal structures of **243**, **244**, and **245** are given in Appendix II, III, and IV, respectively. Cyclized product **246** was more complex, because it is a mixture of unseparatable epimers at the sulfone position. Since **242** is a 1:1 mixture of two epimers and the yield of (2*S*)-**245** is 50%, this suggests that **246** is a mixture of epimers at C-3, each with the *R* configuration at the 2-position of the pyrrolidine ring.

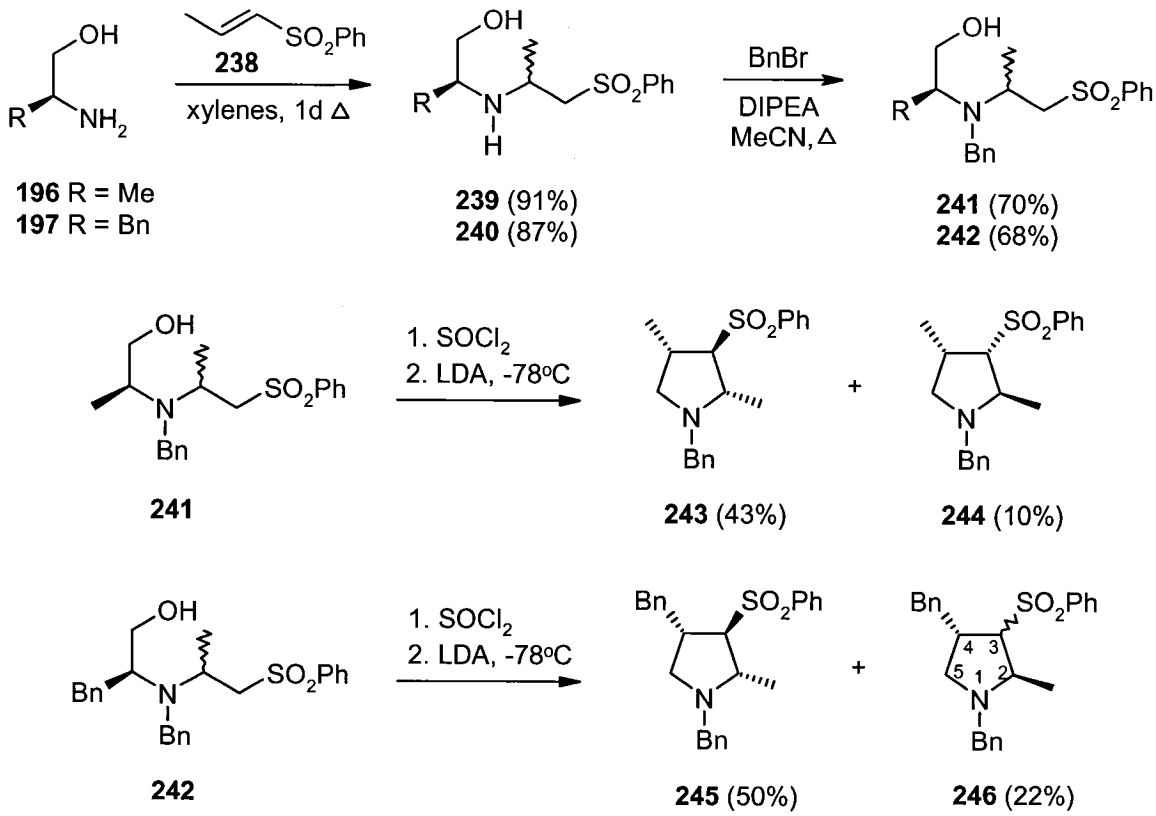

Scheme 2.11 Conjugate Additions of **196** and **197** to **238**, followed by *N*-Benzylation, Chlorination and Cyclization

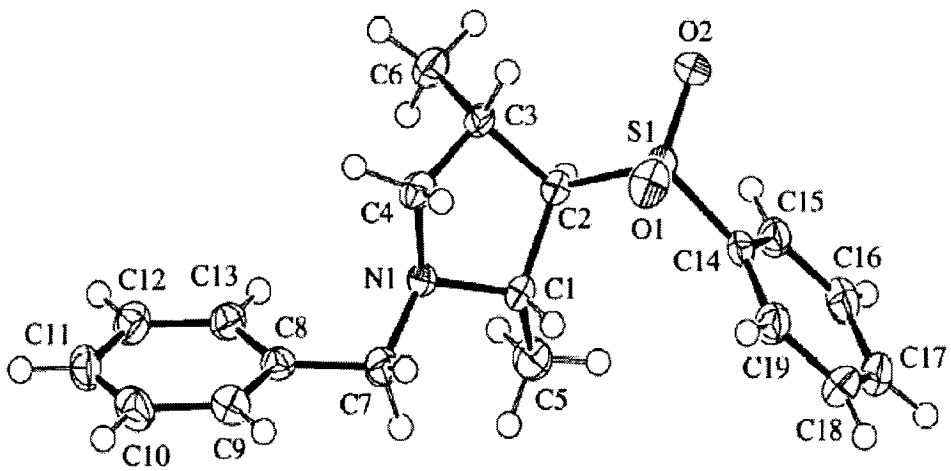

Fig. 2.8 ORTEP Diagram of **243**

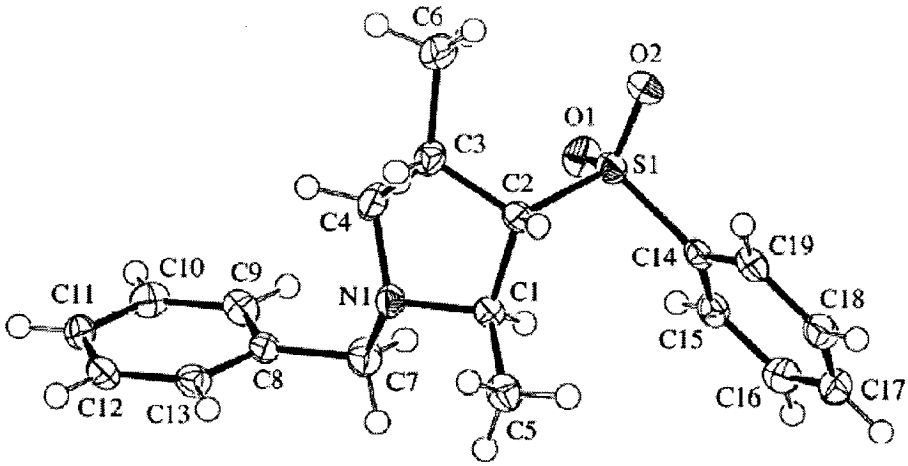

Fig. 2.9 ORTEP Diagram of **244**

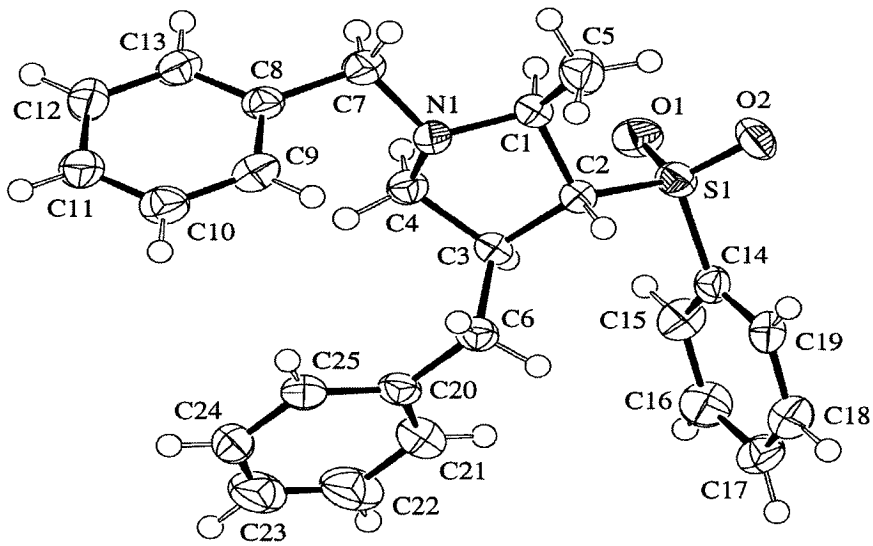

Fig. 2.10 ORTEP Diagrams of **245**

Amino alcohol **199** was also reacted with **238**, followed by *N*-benzylation, tosylation, and cyclization. Unlike tosylate **225**, cyclization of tosylate **249** with LDA in THF at -78 °C afforded 43% of the cyclized product **250** and 43% of unreacted starting material (see Scheme 2.12). The *trans* orientation of the methyl and benzenesulfonyl substituents in **250** was confirmed by an NOE experiment. Irradiation of the $\mathbf{CH_3CH}$

signal at δ 1.28 ppm enhanced the **CH**SO_2 signal at δ 3.00 ppm by 4%, while irradiation of the latter signal enhanced that of the **CH**$_3$CH group by 5%. Furthermore, there was no NOE between the **CH**CH_3 and **CH**SO_2 signals. This suggests that the methyl group and α-sulfonyl proton are vicinal and *cis* oriented.

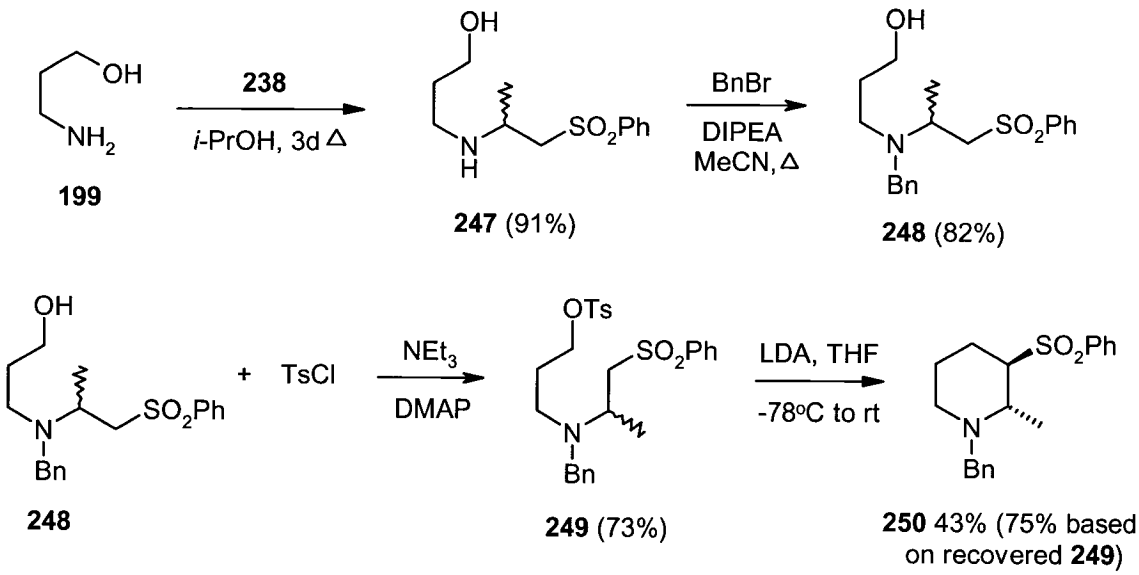

Scheme 2.12 Conjugate Addition of **199** to **238**, followed by *N*-Benzylation, Tosylation, and Cyclization

The conjugate addition of (-)-ephedrine **(200)** to **238** was also attempted, but gave very poor yields even after prolonged reaction times, presumably reflecting the greater steric hindrance associated with a secondary amino group and a β-substituted vinyl sulfone.

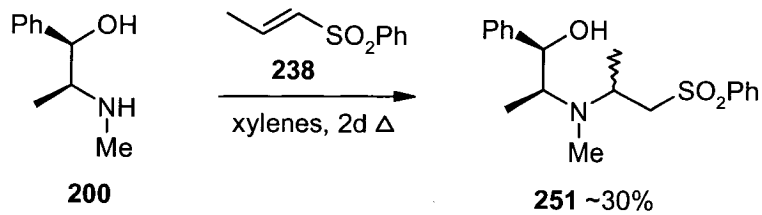

Scheme 2.13 Conjugate Addition of **238** with (-)-ephedrine

2.2.5.2 Reactions of Cyclic Amines with Vinyl Sulfone 238

Finally, we attempted the same sequence of reactions (chlorination, cyclization) of cyclic amines **201** and **202**, with sulfone **238**. To our surprise, **202** provided the unexpected product **257** as a single epimer. The ^{1}H NMR spectrum of **257** showed a singlet for the methyl peak, indicating that it is most probably attached to a quaternary carbon (Fig. 2.11). Also, in the ^{13}C NMR spectrum (Fig. 2.11), there is a quaternary carbon signal at δ 62.7 ppm, which implies that this downfield carbon is attached to both the sulfone moiety and the methyl group (see Scheme 2.14). The structure of **257** was later unequivocally determined by X-ray crystallography (Fig. 2.12), clearly displaying that the methyl group had migrated from the β- to the α-position of the sulfone moiety (see Scheme 2.14). Details of the crystal structure of **257** are given in Appendix V. A similar rearrangement was observed with **201**, which produced a mixture of separable epimers of **256**. Again, the ^{1}H NMR methyl signal was observed as a singlet in each epimer, indicating that a similar rearrangement had occurred as in the case of **202**.

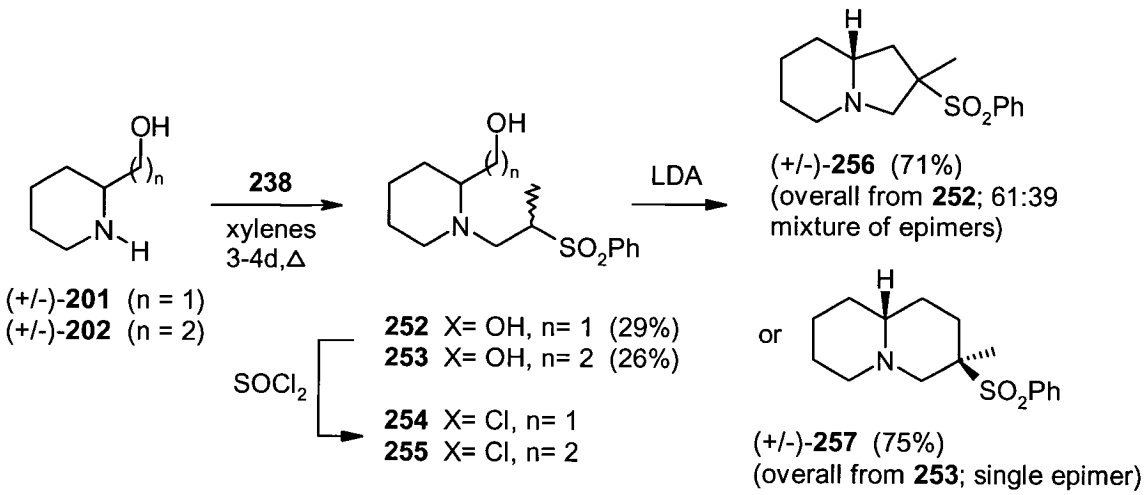

Scheme 2.14 Conjugate Addition of **201** and **202** to **238**, followed by Chlorination, and Cyclization

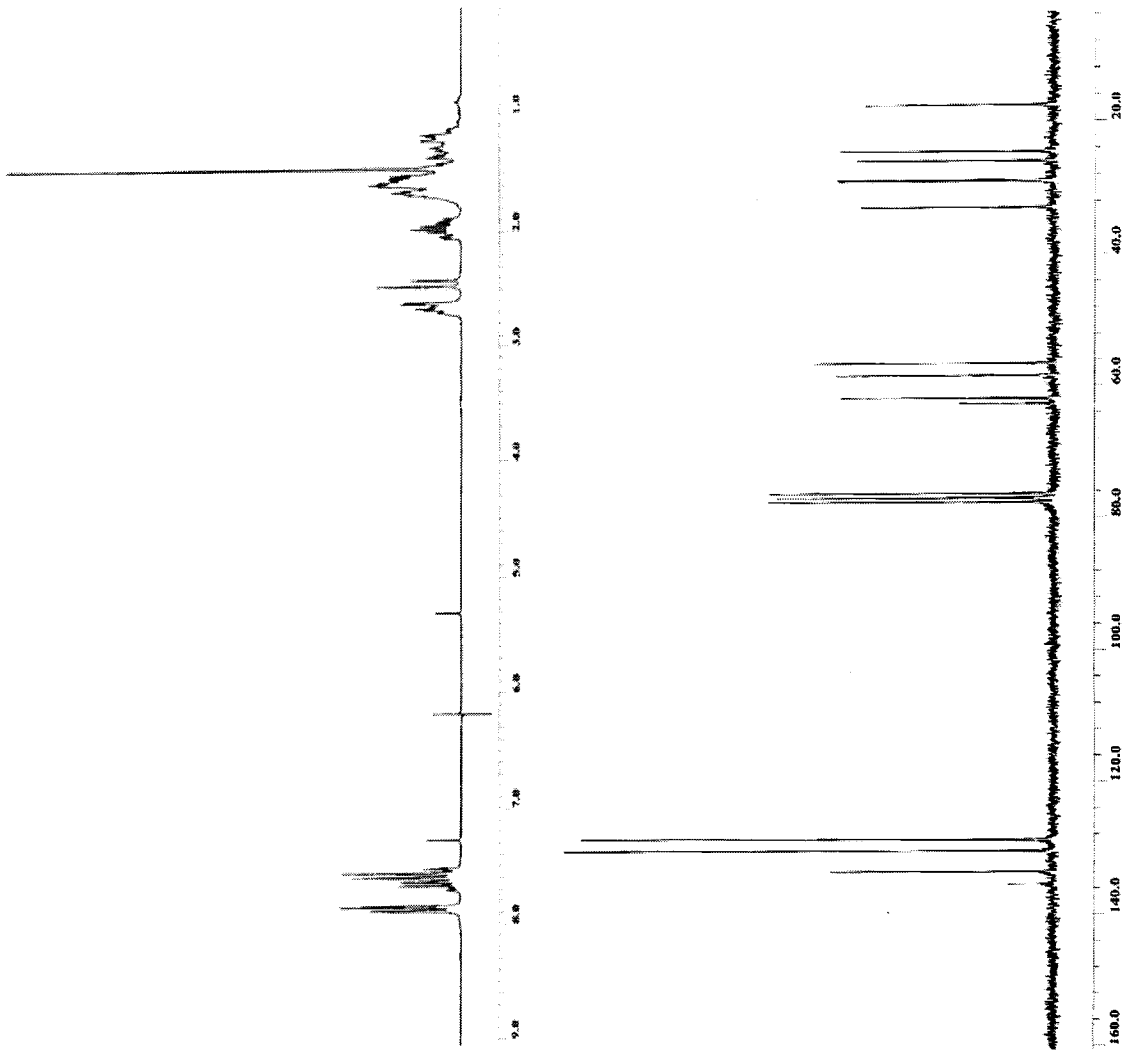

Fig. 2.11 ^{1}H and ^{13}C NMR Spectra of **257**

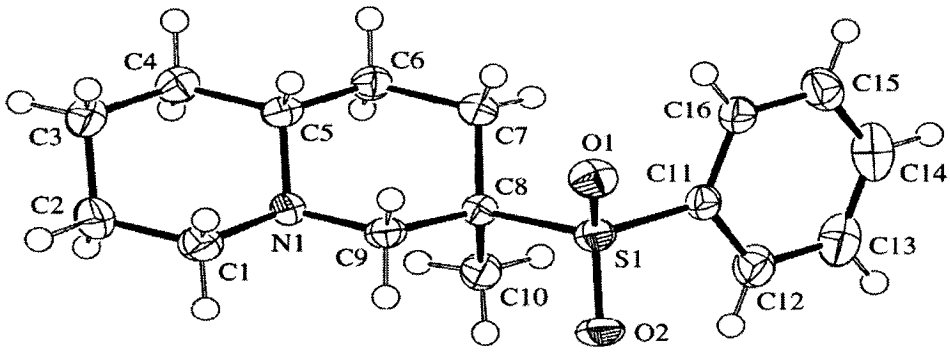

Fig. 2.12 ORTEP Diagram of **257**

In the case of both **201** and **202**, the initial conjugate addition step was sluggish and afforded poor yields (29% and 26%, respectively) of the corresponding adducts **252** and **253**, even after refluxing in xylenes for three and four days, respectively. This was presumably due to the greater steric hindrance associated with the β-substituted vinyl sulfone. A syringe pump was used to inject a xylenes solution of **201** into a refluxing xylenes solution of **238** over 14 h in an attempt to increase the yield, but no increased yield was observed, suggesting that other side reactions proceed faster than the desired conjugate addition under these conditions.

2.2.5.3 Rationale for the Rearrangement of the Methyl Group

In order to rationalize how the puzzling methyl migration occurred, further analysis of the crude mixture obtained upon reaction of **201** with **238** was performed. It revealed the presence of small amounts of the isomeric sulfones **258** and **259**, as well as some other unidentifiable byproducts. We therefore postulate that, under the relatively high temperature and prolonged reaction conditions required for the reaction, a small amount of vinyl sulfone **238**, or the corresponding initial conjugate addition product, first undergoes elimination of benzenesulfinate anion **(260)**. The latter could then add to **238** to afford the bis-sulfone intermediate **261**. Further elimination of sulfinate anion would then afford either the isomerized vinyl sulfone **258**, or regenerate **238**, or form the unactivated allylic sulfone **259** more slowly.[150] Therefore, in this scenario, the anion **260** catalyzes the conversion of **238** to **258** and **259** by a sequence of addition-elimination reactions proceeding via the bis-sulfone **261** (Scheme 2.15). Although the unactivated allyl sulfone **259** cannot undergo conjugate addition reactions, we postulate that the isomerized vinyl sulfone **258** reacts preferentially with the amino alcohols **201** or **202** to give the observed products **252** or **253**, ultimately leading to **256** or **257**, respectively.

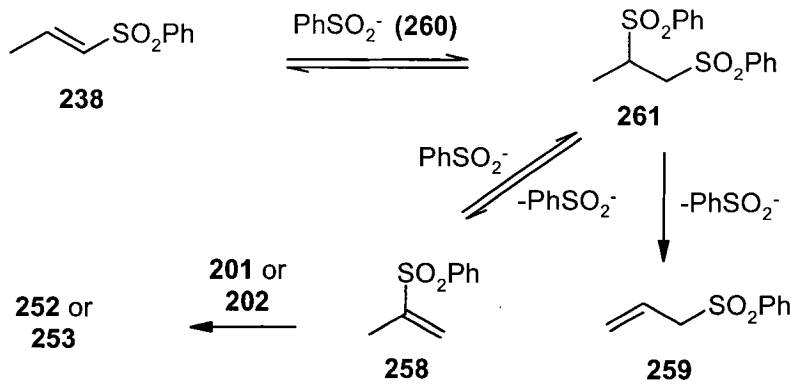

Scheme 2.15 A Postulated Mechanism for the Formation of Adducts **252** and **253**

2.2.5.4 Control Experiments to Test the Postulated Mechanism

Several control experiments were performed to test the mechanism proposed in section **2.2.5.3**. First, treatment of sulfone **238** with either a catalytic amount (e.g. 0.1 equivalent) or a stoichiometric amount of sodium benzenesulfinate **(262)** in the absence of amino alcohol **201**, under the same conditions as used for the conjugate additions, resulted in the formation of **258** and **259** (Scheme 2.16). Thus, the ^{1}H NMR spectrum of the crude mixture showed that the ratio of **238**, **258**, and **259** was about 3.75: 1: 1.75 with either 0.1 or 1.0 equivalent of **262** after refluxing in xylenes for 3 days. Treatment of an authentic sample of **258**, prepared by a literature method,[151] under the same heating conditions with either 0.1 or 1.0 equivalent of **262** also resulted in a mixture of **258**, **238**, and **259** in a ratio about 95:3:2 (Scheme 2.16). These experiments confirm that isomerization of **238** to **258** is feasible under these conditions and support the proposed addition-elimination steps shown in Scheme 2.15. If the reaction time is long enough, treatment of **238** or **258**, under the same heating conditions in the presence of **262**, should give the same ratio of **238**, **258**, and **259**.

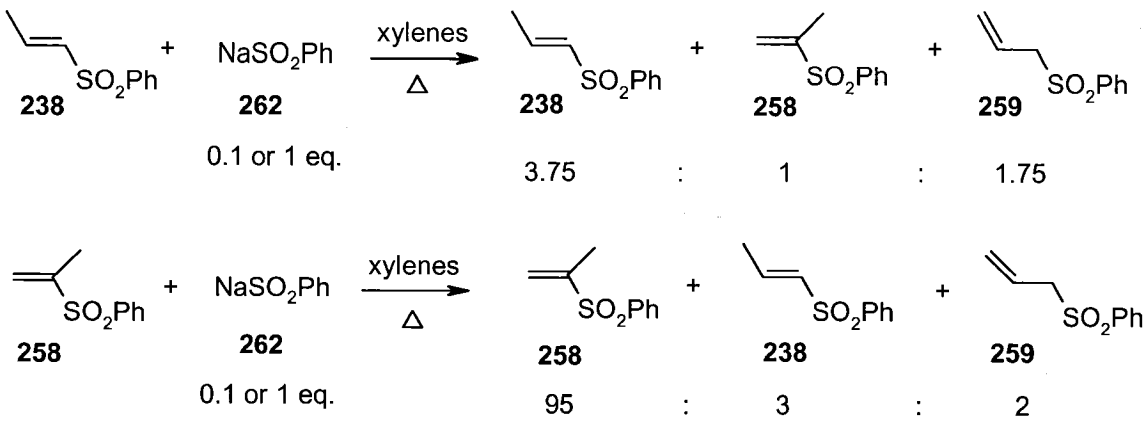

Scheme 2.16 Isomerization of Sulfones **238** and **258**

Stirling's study showed that the rate of addition of piperidine to sulfone **193** is about 8 times faster as that to **194** at 25 °C (see Section **2.1**, Fig. 2.3).[5a] However, in our case, these relative rates may be reversed with substituted piperidines such as **201** and **202** at high temperature because of the additional steric interaction between the piperidine substituent and the β-methyl group of **238**.

In a separate experiment, the reaction of **201** with authentic sulfone **258** was performed under the same reaction conditions. This resulted in the formation of the same product **252** in comparable yield, as well as sulfones **258**, **238** and **259** (see Scheme 2.17). These results are also consistent with the formation of **258**, and its further reaction with **201**, when **238** is employed as the initial sulfone.

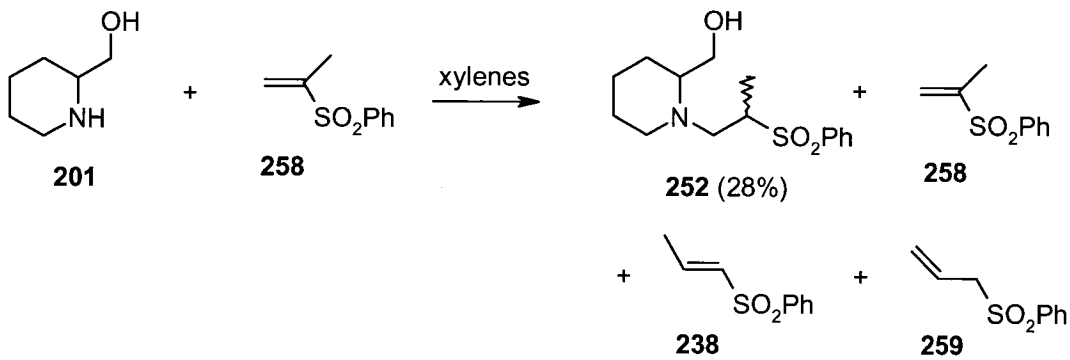

Scheme 2.17 Conjugate Addition of **201** to Authentic Sulfone **258**

Finally, a crossover experiment was conducted in which **201** and **238** were allowed to react in the presence of sodium *p*-toluenesulfinate **(263)**. This resulted in a mixture of adduct **252** and its *p*-toluenesulfonyl analogue **264** (see Scheme 2.18). These results are all consistent with the mechanism in Scheme 2.15.

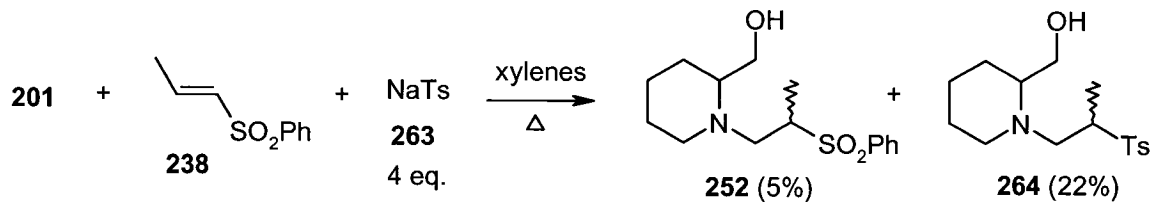

Scheme 2.18 Crossover Experiment

The failure to observe a similar rearrangement during the reaction of **196** or **197** with **238** in Scheme 2.11 is attributed to the fact that **196** and **197** are primary amines that undergo far more facile conjugate additions to **238** as compared to the more hindered secondary amines **201** and **202** shown in Scheme 2.14. The amines **201** and **202** failed to add to **238** at an appreciable rate, thus providing the opportunity for the competing isomerization of **238** to the more reactive isomer **258** (and the inert allylic isomer **259**) and allowing conjugate addition to occur to **258**.

2.2.6 Reductive Desulfonation of Cyclized Products

As discussed in section **1.1**, the sulfone group can be removed at the end of a synthetic sequence by a reductive desulfonation.

Treatment of **220** with 5% sodium amalgam[152] afforded the known compound **265**[142] (see Scheme 2.19). A comparison of the specific rotation of desulfonylated product **265** $\{[\alpha]_D^{22} = -13.5$ ($c = 0.21$, $CHCl_3$)$\}$ to that reported for **265** $\{[\alpha]_D^{25} = -10.5$ ($c = 3.25$, EtOH)$\}$[142b] provided further evidence for the structure of **220**. Moreover, reductive desulfonylation of **226** and **227** under similar conditions furnished the known compounds *trans*- and *cis*-*N*,2-dimethyl-3-phenylpyrrolidine **(266)** and **(267)**, respectively[143] (see Scheme 2.19).

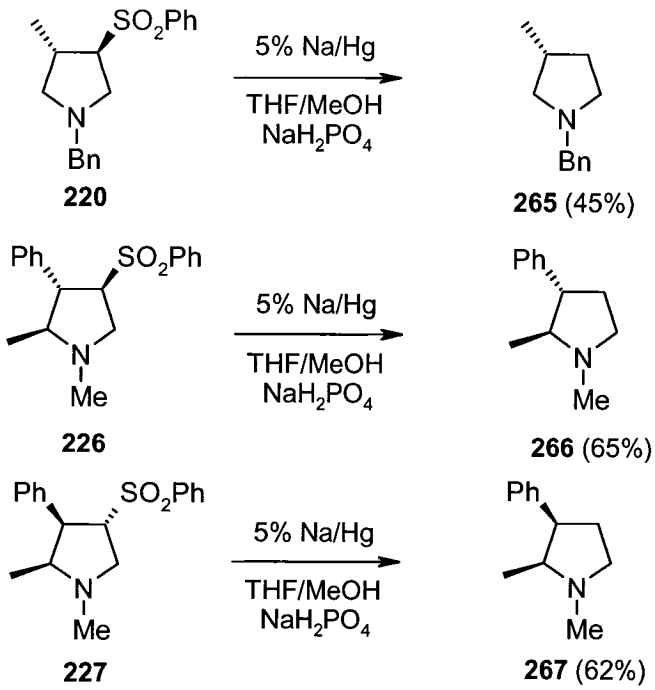

Scheme 2.19 Reductive Desulfonation of Some Pyrrolidine Products

2.3 Conclusions

In conclusion, the conjugate additions of amino alcohols derived from α-amino acids to vinyl sulfones, followed by *N*-benzylation, chlorination and intramolecular alkylation, provide a convenient route to substituted pyrrolidines. The process is accompanied by the stereospecific rearrangement of substituents from the α-position of the original amine moiety to the β-position of the pyrrolidine product. The rearranged structures were proved unequivocally by spectroscopic and X-ray methods, as well as by desulfonylation. While 2-substituted pyrrolidines are generally accessible from commercially available amino acids, [153] it is generally more difficult to prepare 3-substituted analogues. The present methodology thus provides convenient access to the latter. A second type of rearrangement was discovered with piperidine-based amino alcohols **201** and **202** and the β-substituted vinyl sulfone **238**, resulting in the apparent migration of the β-substituent to the α-position of the sulfone moiety. However, further investigation revealed that this takes place via a novel overall process involving isomerization of the original vinyl sulfone, followed by conjugate addition of the amine.

Chapter 3

Cyclizations and Cycloadditions of Acetylenic Sulfones on Solid Supports

The use of acetylenic sulfones on solid supports for synthetic applications had not yet been reported. In this chapter, the synthesis of the first polymer-supported acetylenic sulfones and their applications will be described, particularly their synthetic utility as precursors of nitrogen heterocycles.

3.1 Acetylenic Sulfones on Solid Supports

The use of acetylenic sulfones in the solution phase has been extensively studied, and there exist numerous methods for the synthesis of these compounds.[1d] One of these methods, developed in our group, involves a straightforward, convenient process, based on the additions of selenosulfonates to alkynes by Back *et al.*[3] We have now extended this methodology to the solid phase.

Our first approach to attaching an acetylenic sulfone to a polymer support is shown in Scheme 3.1. The commercially available sulfonhydrazide resin **84** was converted into the selenosulfonate resin **269** by oxidation with benzeneseleninic acid **(268)**. The selenosulfonation of 1-hexyne (chosen as a representative acetylene) was successfully carried out by heating a mixture of **269** and the acetylene with a radical initiator (AIBN) in benzene. This reaction proceeds by a chain mechanism initiated by homolytic cleavage of the Se-S bond as shown earlier in Scheme 1.2. The sulfonyl radical adds to the acetylene, resulting in a vinyl radical which can react with a second molecule of selenosulfonate to give **270**. Since both the selenosulfonate and the intermediate vinyl radical are immobilized on the support, the chain-transfer step is inefficient. However, the addition of diphenyl diselenide to the reaction mixture circumvents this problem and improves the efficacy of the reaction (see Scheme 3.1). The resulting adduct **270** is formed regio- and stereoselectively (*anti* addition) and affords the desired acetylenic sulfone **271** upon oxidation and selenoxide *syn*-elimination. Evidence for its formation stems from a strong IR absorption at 2193 cm^{-1}, which is typical of an acetylenic sulfone. The loading was determined gravimetrically to be 0.90 mmol/g, based on the expected weight gain from the

starting sulfonhydrazide resin **84**.

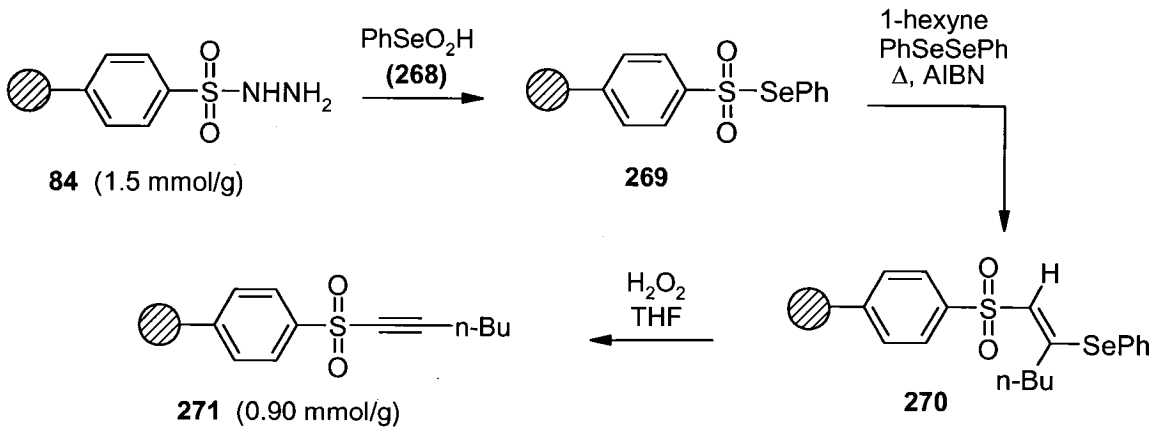

Scheme 3.1 Conversion of a Sulfonhydrazide to an Acetylenic Sulfone on a Solid Support

Selenosulfonates attached to a polystyrene support via their selenium atoms have also been reported.[154] Huang and Qian examined the selenosulfonation of acetylenes with resin **272** using AIBN as a catalyst (see Scheme 3.2). The resin **272**, the acetylenes and a catalytic amount of AIBN were refluxed in benzene for 20 h. The reaction mixture was filtered and washed. The resins **273** were converted to acetylenic sulfones **1** and resin **274** upon treatment with hydrogen peroxide in THF. The crude acetylenic sulfones **1** showed good purity (>95%) by ^{1}H NMR spectroscopy and did not require further purification. Resin **272** can be regenerated by reacting resin **274** with *p*-toluenesulfonhydrazide (**275**) by the general method developed earlier in our laboratory,[4] and can be reused. It should be noted, however, that this procedure affords free acetylenic sulfones, as opposed to ones anchored to the solid support, as needed for the present investigation.

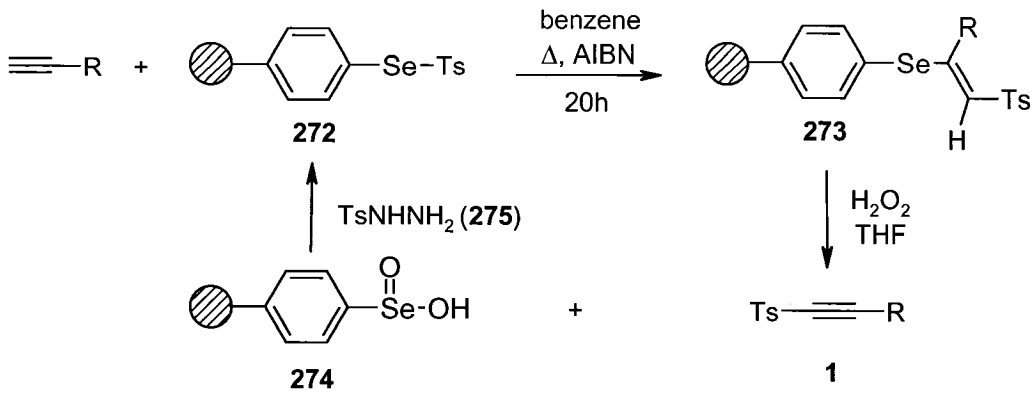

Scheme 3.2 Synthesis of Acetylenic Sulfones using a Selenosulfonate Resin

The use of resin **271** in conjugate addition reactions with two representative chloroamines **276**[155] and **277**[156] is shown in Scheme 3.3. Evidence for the success of the first reaction is based on the disappearance of the IR peak of the acetylenic sulfone at 2193 cm^{-1} in the product **278**. Further characterization of product **278** by solid-state MAS-NMR spectroscopy (see section **1.3.8.2.3**) showed a signal in the ^{13}C NMR spectrum at δ 66 ppm, which is characteristic of an aryl methoxy group. These results are consistent with the expected conjugate addition, followed by cyclization, but more thorough characterization of the products following cleavage from the solid support was required.

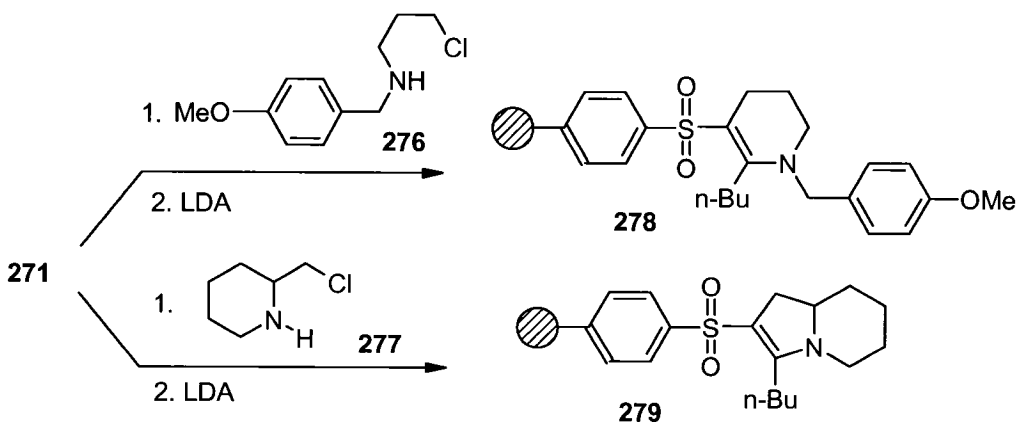

Scheme 3.3 Conjugate Addition and Subsequent Cyclization of Chloroamines with **271**

Unfortunately, several attempts to cleave resin **278** by reduction of the enamine

double bond, followed by reductive desulfonylation (e.g. with Na/Hg) resulted in low yields of relatively impure product **280**. A possible alternative way was therefore explored, using a linker between the acetylenic sulfone and the polymer support, which could be easily cleaved at any stage to see whether the reaction had proceeded as desired.

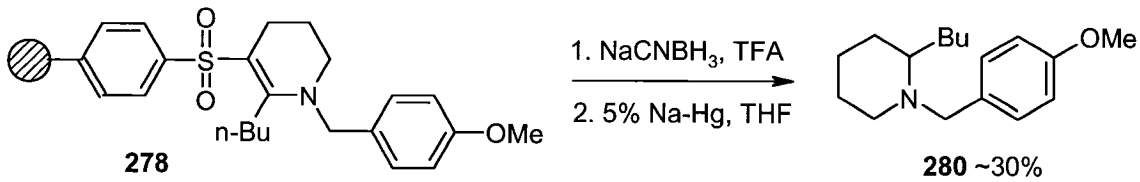

278 **280** ~30%

Scheme 3.4 Attempt to Cleave Resin **278**

3.2 Use of Linkers to Attach Acetylenic Sulfones to a Solid Support

Since cleavage of the products from their supports is essential for the objective of preparing diverse nitrogen heterocycles, as well as for their characterization, attention was now turned to the investigation of the use of linkers to attach the acetylenic sulfones to the solid supports (see section **1.3.5.2**). Several different strategies can be used to install a linker between an acetylenic sulfone and the support. One is to prepare an appropriately functionalized acetylenic sulfone **282** first, then later attaching it to the support **281** via a suitable linker X-Y. Alternatively, **281** could be linked similarly to a functionalized precusor **(283)** of an acetylenic sulfone, such as a sulfonyl chloride or sulfonhydrazide, via a linker X-Y, followed by conversion to the acetylenic sulfone at the end (see Scheme 3.5). Attempts to install different linkers between acetylenic sulfones and various polymer supports using either of these two strategies will be discussed in the following sections.

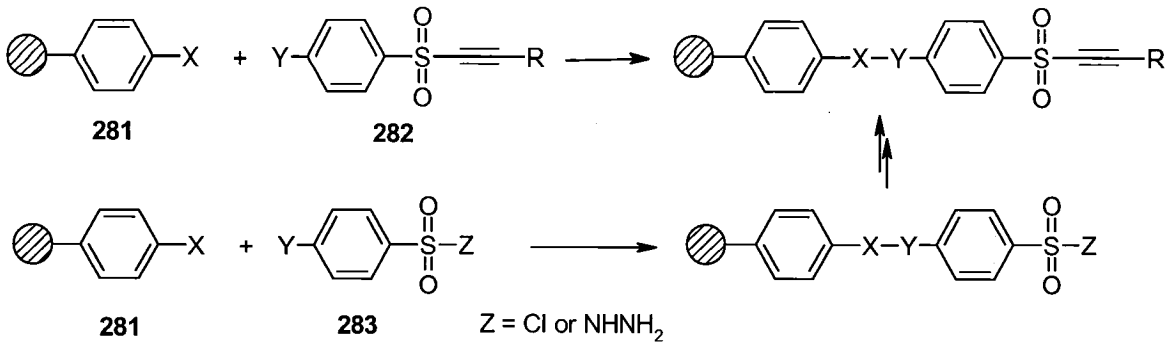

Scheme 3.5 General Synthesis of Acetylenic Sulfones on Solid Supports by Use of a Linker

3.2.1 Attempt at Coupling via a Benzylic Ether Linker

A benzylic ether can be used as a linker in solid phase synthesis, which can be cleaved by hydrogenolysis or acid hydrolysis. One possible route to ether-linked acetylenic sulfones is shown in Scheme 3.6. The Merrifield resin **64** was linked with the phenolic dianion of sulfonate **284** to afford **285**, followed by conversion to the corresponding arenesulfonyl chloride **286** by a literature procedure.[157] Attempts were made to carry out the direct sulfonation of various acetylides with **286**, with the hope of obtaining the desired products **287**. Furthermore, this method would permit the installation of a variety of acetylenic units (i.e. different R groups) on to the same key intermediate **286**. To date, this approach has not been successful because it appears that the product **287** competes with **286** for the acetylide nucleophile, as it is capable of undergoing facile conjugate additions. However, we considered that it may be possible to overcome this problem through a direct coupling of **286** with acetylenes under Sonogashira conditions.

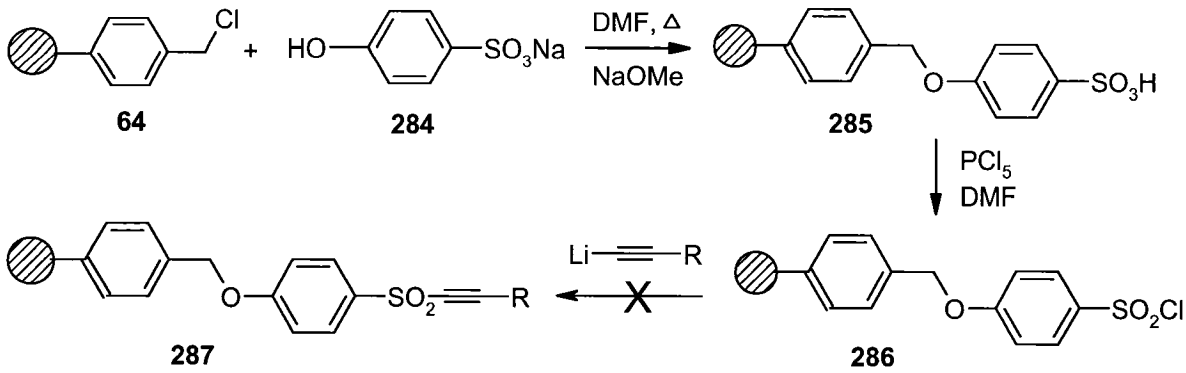

Scheme 3.6 Attempt to Attach Acetylenic Sulfones to a Resin using a Benzyl Ether Linker

Since the Sonogashira coupling of acetylenes and sulfonyl halides had not been previously reported in the literature, conditions for this coupling reaction were first investigated in solution phase. When phenylacetylene and tosyl chloride **(288)** were reacted under standard Sonogashira conditions,[158] diacetylene **289**[159] was the sole product isolated quantitatively from the reaction mixture, implying that **288** is not reactive enough to compete with the formation of the homocoupled product **289** through an Eglinton reaction (see Scheme 3.7). The reaction was attempted with the more reactive tosyl iodide **(290)**,[160] but again diacetylene **289** was isolated as the sole product.

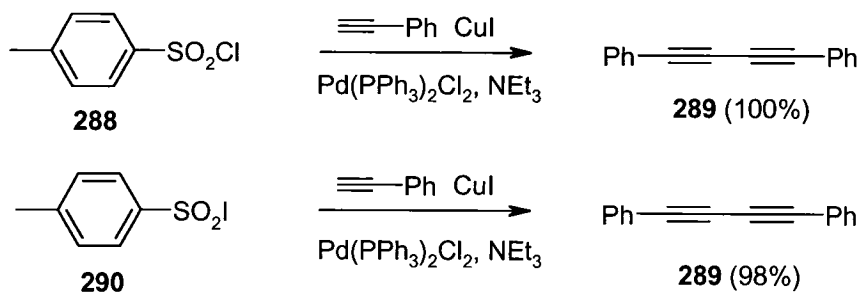

Scheme 3.7 Attempt to Synthesize Acetylenic Sulfones under Sonogashira Conditions

The failure to couple an acetylene to a sulfonyl halide by direct means prompted us to explore other approaches. The sulfonyl chloride **286** was reacted with hydrazine and the resulting sulfonhydrazide **291** was oxidized to the corresponding selenosulfonate,

followed by selenosulfonation of 1-hexyne and selenoxide-elimination to afford acetylenic sulfone **292** (Scheme 3.8). Unfortunately, the IR absorption of the acetylenic sulfone at 2194 cm^{-1} was relatively weak, probably due to the low loading of **286** made from **64**.

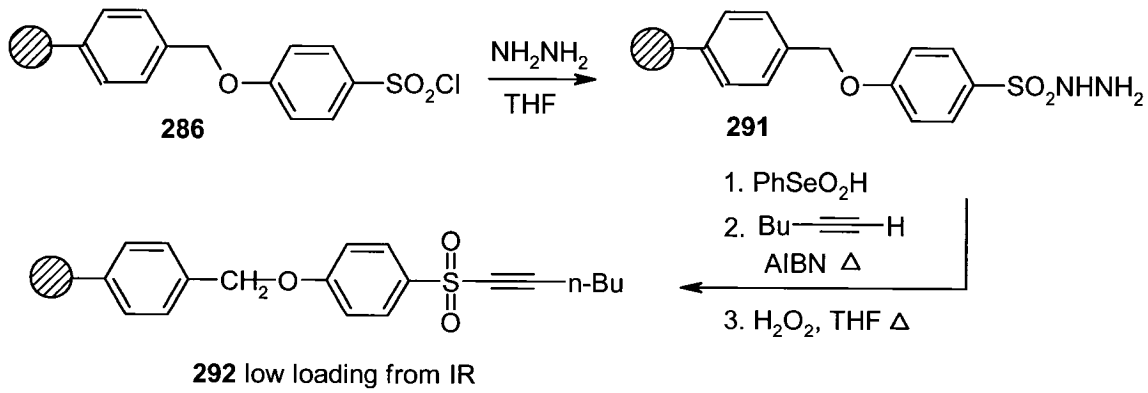

Scheme 3.8 Synthesis of Resin **292** using a Benzylic Ether Linker

3.2.2 Attempt at Coupling via a Sulfonamide Linker

The low loading of **292**, containing a benzylic ether linker, prompted us to investigate an alternative route involving the use of a sulfonamide linker to connect the sulfonyl chloride resin **69** (see Fig. 1.6) to an aniline-functionalized acetylenic sulfone **297**. Thus, the selenosulfonation of 1-hexyne with **294**[4], which was in turn prepared from the commercially available sulfonyl chloride **293**, afforded adduct **295** (Scheme 3.9). The acetylenic sulfone **296** was obtained in excellent yield after selenoxide elimination. The nitro group was then reduced using sodium dithionite [161] to give a mixture of the corresponding acetylenic sulfone **297** and β-keto sulfone **298**, which is formed by the addition of water to **297**. Reduction of **296** using tin in aqueous alcoholic hydrochloric acid[162] gave exclusively the β-keto sulfone **298**.

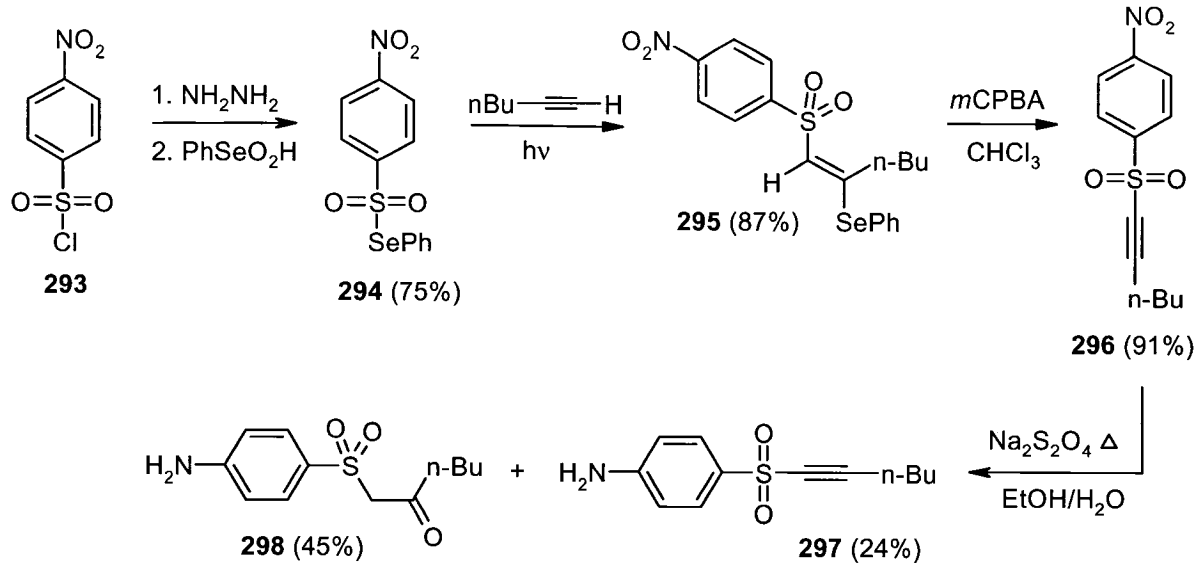

Scheme 3.9 Synthesis of Aniline **297**

Due to the moisture-sensitive nature of acetylenic sulfone **297**, the nitro group was then reduced to the corresponding amine at the vinyl sulfone **295** stage prior to selenoxide elimination. Thus the aniline **299** was obtained in good yield and was attached to sulfonyl chloride resin **69**, followed by oxidation and selenoxide elimination (see Scheme 3.10). Unfortunately, the IR absorption of acetylenic sulfone **300** at 2200 cm^{-1} was relatively weak, suggesting a low coupling efficiency of **299** and **69**, and consequently low loading of **300**.

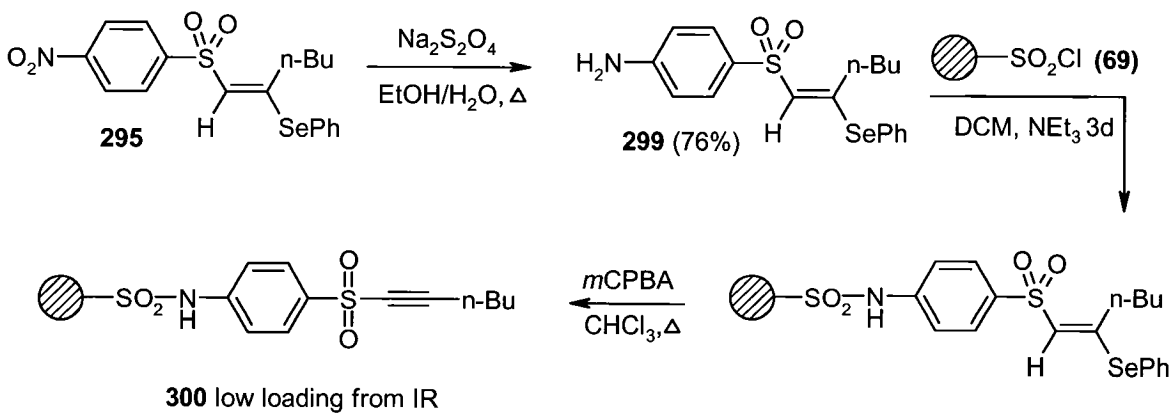

Scheme 3.10 Attempt to Install a Sulfonamide Linker

3.2.3 Acetylenic Sulfone Resins with an Ester Linker

The low loading of **300**, containing a sulfonamide linker, prompted us to investigate an alternative route involving the use of an ester linker. As discussed in section **1.3.5.2.3**, two different connections can be used for ester-linked acetylenic sulfones (see Scheme 3.11). Resin **301** belongs to the first type, which can be obtained by coupling of Merrifield resin **64** or Wang resin **302** with benzoic acid species **303**. On the other hand, resin **304** belongs to the second type, which can be obtained by coupling of polymer supported benzoic acid **305** with benzyl bromide species **306**.

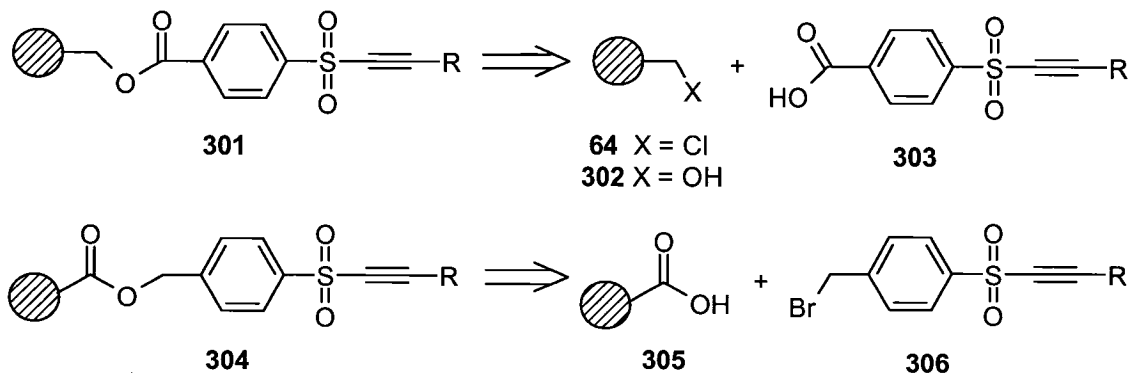

Scheme 3.11 Two Different Ester-Based Linkers

3.2.3.1 Resin 301 from Benzoic Acid Species 303

It was reasoned that the benzoic acid species **303** could be synthesized by the typical selenosulfonation approach. Unfortunately, sulfonhydrazide **308** proved very difficult to purify by either crystallization or flash chromatography (Scheme 3.12). This resulted in a low yield and low purity of the selenosulfonate **309**, thereby obviating the usual selenosulfonation approach.

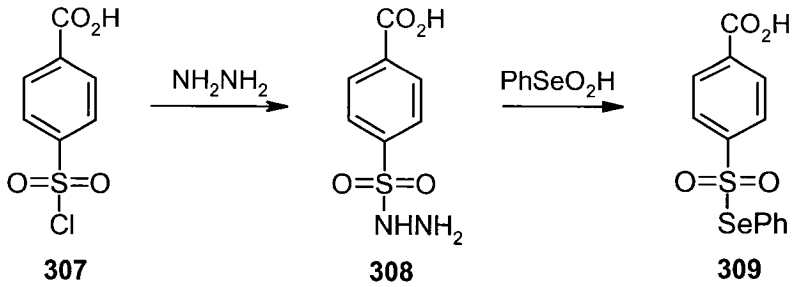

307 **308** **309**

Scheme 3.12 Attempt to Prepare Selenosulfonate **309**

Since difficulties were encountered in the above attempt to prepare the benzoic acid species **303**, an investigation into an alternative method was carried out by oxidation of the corresponding sulfide. This synthesis began with the conversion of thiosalicylic acid **(310)** to the acetylenic sulfone **313**, as shown in Scheme 3.13 by a literature procedure.[163] Attempts to alkylate **310** directly with propargyl bromide selectively at the thiol gave the corresponding sulfide in poor yield and so an extra step which involved forming the ester **311** was required. Since the acetylenic sulfide **312** is thermodynamically more stable than its propargylic isomer,[5a, 6b, 6c] the alkylation of thiolester **311** with propargyl bromide was simply followed by potassium hydroxide-catalyzed isomerization. The ester group was saponified at the same time. The resulting potassium benzoate derivative was acidified to afford **312**, followed by subsequent oxidation with hydrogen peroxide in refluxing acetic acid to give acetylenic sulfone **313** in good yield. Similarly, starting from commercially available 4-mercaptobenzoic acid **(314)**, acetylenic sulfone **316** was also made in moderate yield.

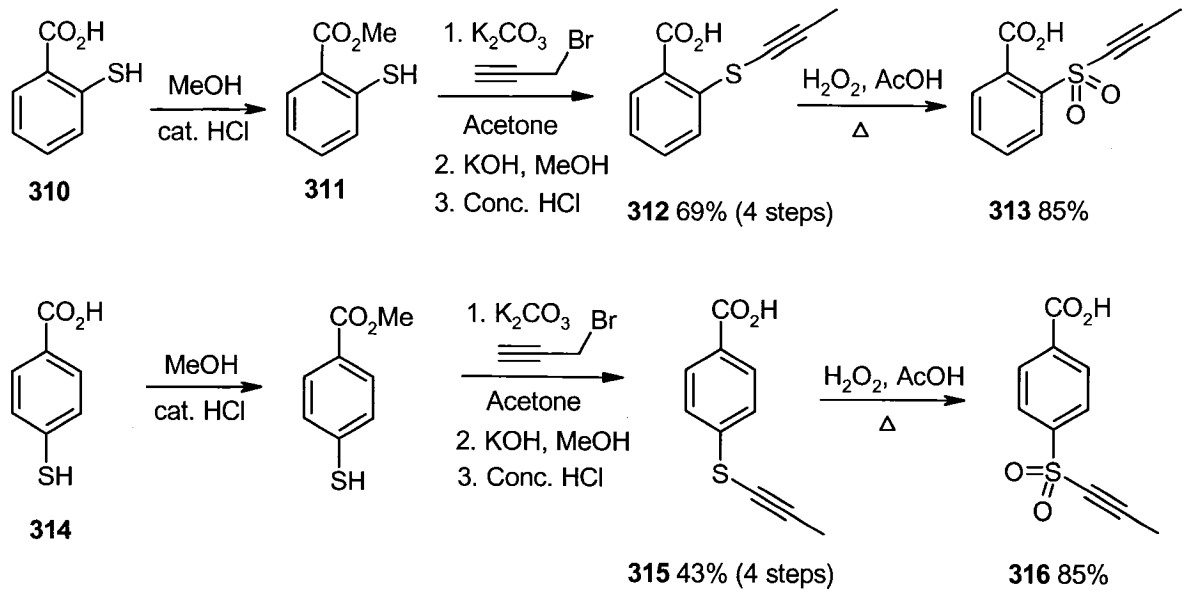

Scheme 3.13 Preparation of Acetylenic Sulfones **313** and **316**

The carboxylic acid moiety of **316** was then attached to Merrifield resin **(64)** at 90 °C in DMF[164] in the presence of cesium carbonate and a catalytic amount of potassium iodide. Unfortunately, the deactivated propargylic sulfone isomer **317** was the predominant product. In contrast to acetylenic sulfide **315**, the acetylenic sulfone **318** is less thermodynamically stable than the corresponding propargylic isomer **317** under basic conditions[16, 165] (see Scheme 3.14). Thus, isomerization occurred to afford **317** rather than desired **318**. The ester linker could be easily cleaved with sodium methoxide in methanol to afford **319** by transesterification, which was isolated and identified unambiguously.

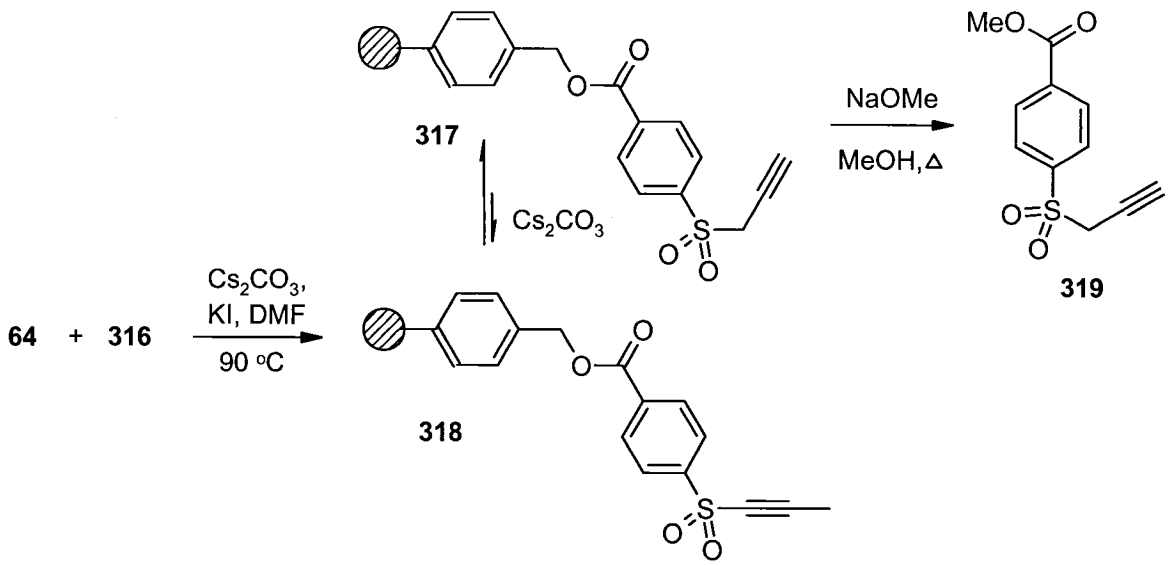

Scheme 3.14 Isomerization between Polymer-Supported Acetylenic Sulfone **318** and Propargylic Sulfone **317**

This result indicated the coupling step is possible in this particular case, and there exist several options to improve this method. First, under base-catalyzed conditions, such as in the presence of an amine or cesium carbonate, the propargylic sulfone is thermodynamically more stable than its acetylenic isomer, while the corresponding acetylenic sulfide is thermodynamically more stable than its propargylic isomer. The carboxylic acid moiety of **315** was therefore attached to the Merrifield resin **(64)** under basic conditions as previously described to afford the stable, polymer-bound acetylenic sulfide **320**, which was subsequently oxidized to the corresponding polymer-bound acetylenic sulfone **318** without isomerization of the latter (see Scheme 3.15). The loading of **318** was determined gravimetrically to be 0.87 mmol/g, based on the weight gained from the Merrifield resin. Second, to avoid the isomerization of **316** under basic conditions, Wang resin **(302)** rather than Merrifield resin **(64)** was employed in an esterification with **316** under less basic conditions (see Scheme 3.15). The loading of **318** by the latter method was also determined gravimetrically to be 0.84 mmol/g.

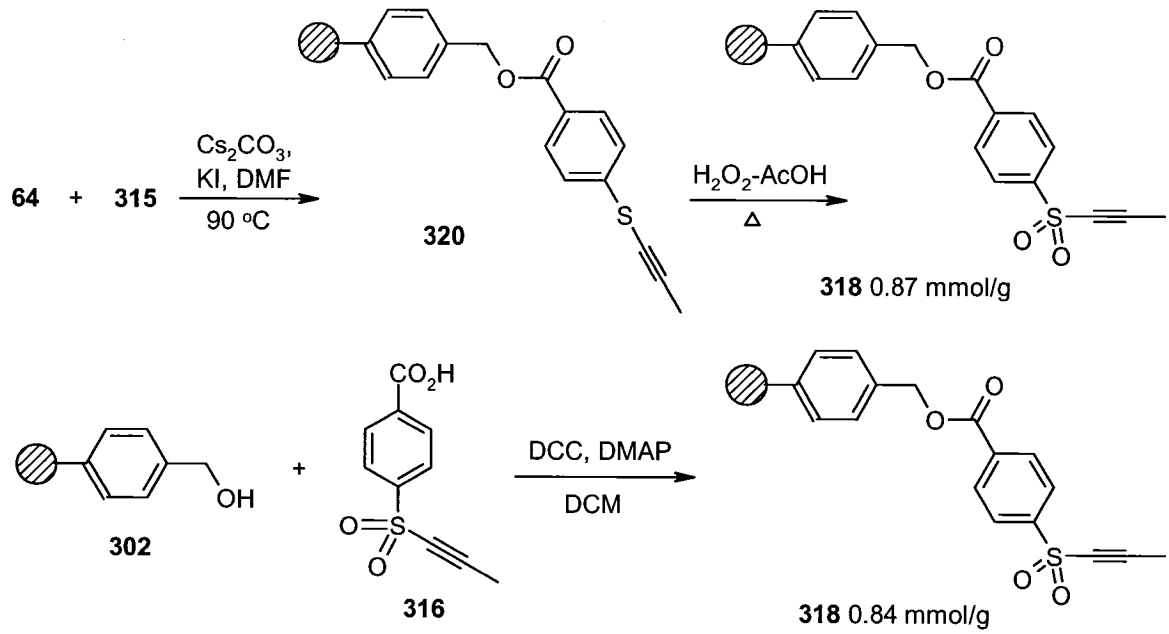

Scheme 3.15 Two Different Routes to the Polymer-Bound Acetylenic Sulfone **318**

Considering the relatively low price of Merrifield resin **(64)** compared with Wang resin **(302)**, the method of making **318** from **64** is more cost-effective. Similarly, the polymer-bound acetylenic sulfone **321** was obtained in the same way with a 0.83 mmol/g loading (see Scheme 3.16).

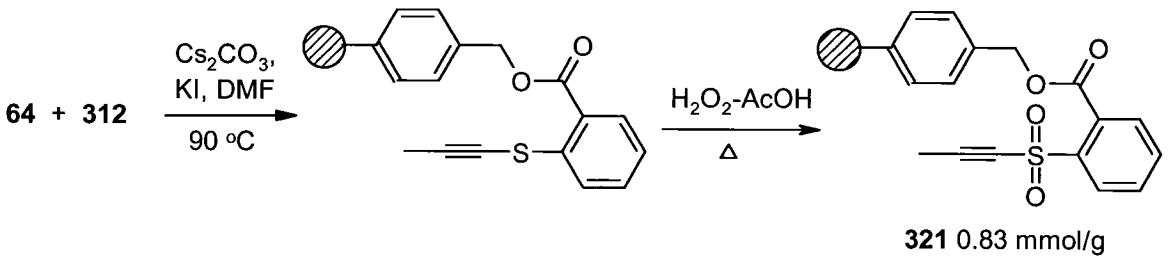

Scheme 3.16 Route to the Polymer-Bound Acetylenic Sulfone **321**

3.2.3.2 Resin 304 from Polymer-Supported Benzoic Acid 305

As described in the previous section, the acetylenic sulfones **318** and **321** were successfully attached to a solid phase via the first type of ester linker shown in the

generalized Scheme 3.11 (i.e. by coupling benzoic acid species **303** with resin **64** or **302**). This section will describe the synthesis of polymer-supported acetylenic sulfones **304** via the second type of ester linker shown in Scheme 3.11 (i.e. by coupling benzyl bromides **306** with resin **305**).

Thus, the selenosulfonation of three representative acetylenes with **324**, which was in turn prepared from sulfonyl chloride **322**[166] via sulfonhydrazide **323**, afforded adducts **325-327**. As described in the previous section, under basic conditions, the propargylic sulfone is thermodynamically more stable than its acetylenic isomer. We therefore decided to couple selenovinyl sulfones **325-327** with resin **328** prior to the oxidation-elimination step because the coupling step requires basic conditions. So, esterification[167] of polymer-supported benzoic acid **328**, which was prepared from Merrifield resin by the method of Beebe and coworkers,[168] with **325-327**, followed by selenoxide *syn*-elimination, produced the desired products **304a-304c**, respectively. Desilylation of **304c** with methanolic aqueous potassium carbonate solution[169] afforded the corresponding terminal acetylene **304d** (Scheme 3.17).

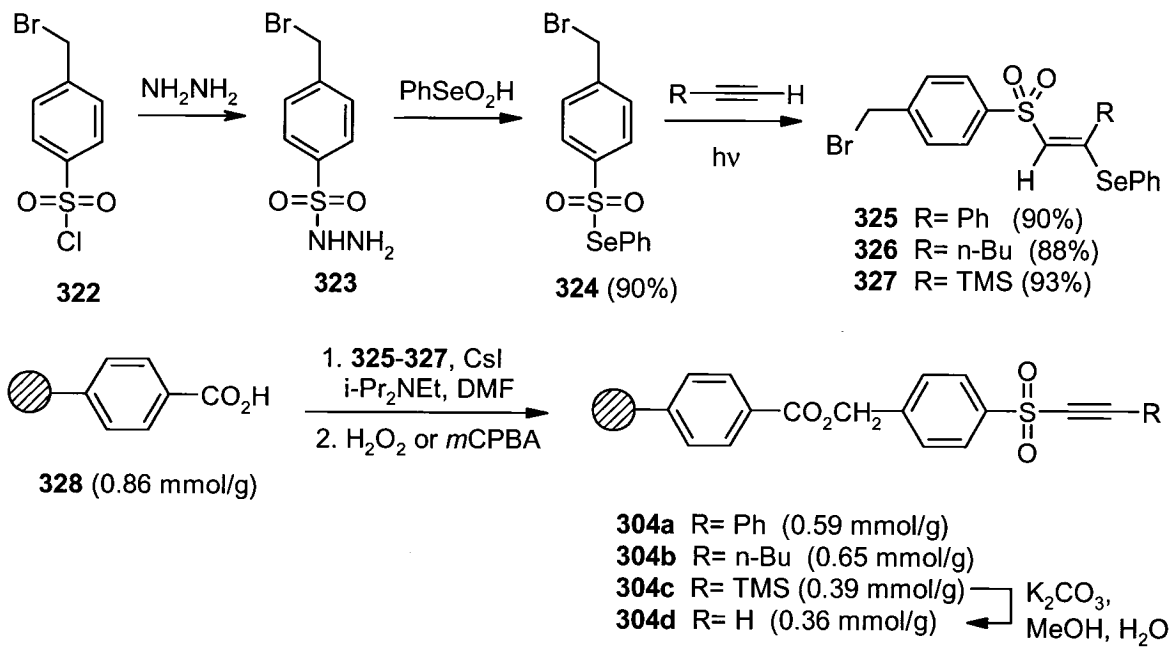

Scheme 3.17 Preparation of Acetylenic Sulfones on Solid Supports Using an Ester Linker

The loading of **328** was determined gravimetrically by conversion into the

corresponding cesium carboxylate.[168] The loading of **304a** and **304d** was determined by hydrolysis of the ester linkers with 5% aqueous lithium hydroxide in THF solution and isolation of the hydrolyzed products **329** and **330**, respectively. The loading of **304b** and **304c** was determined gravimetrically. When the resin **304a** was treated with lithium hydroxide, **329** was obtained in high purity. The loading of **304a** was calculated to be 0.59 mmol/g based on the weight of isolated **329**, assuming that **329** was obtained quantitatively. When the resin **304d** was treated with lithium hydroxide, the methyl ketone **330** was similarly obtained in high purity and was presumably formed by cleavage of the corresponding β-keto sulfone (see Scheme 3.18). The loading of **304d** was calculated to be 0.36 mmol/g based on the weight of isolated **330**. However, when the resin **304b** was treated with lithium hydroxide, **331** was obtained in low yield and low purity due to the addition of water to the activated acetylene to produce the corresponding β-keto sulfone **332**. Thus the loading of **304b** and **304c** were determined gravimetrically to be 0.65 mmol/g and 0.39 mmol/g, respectively, by determining the weight gained from the starting benzoic acid resin **328**.

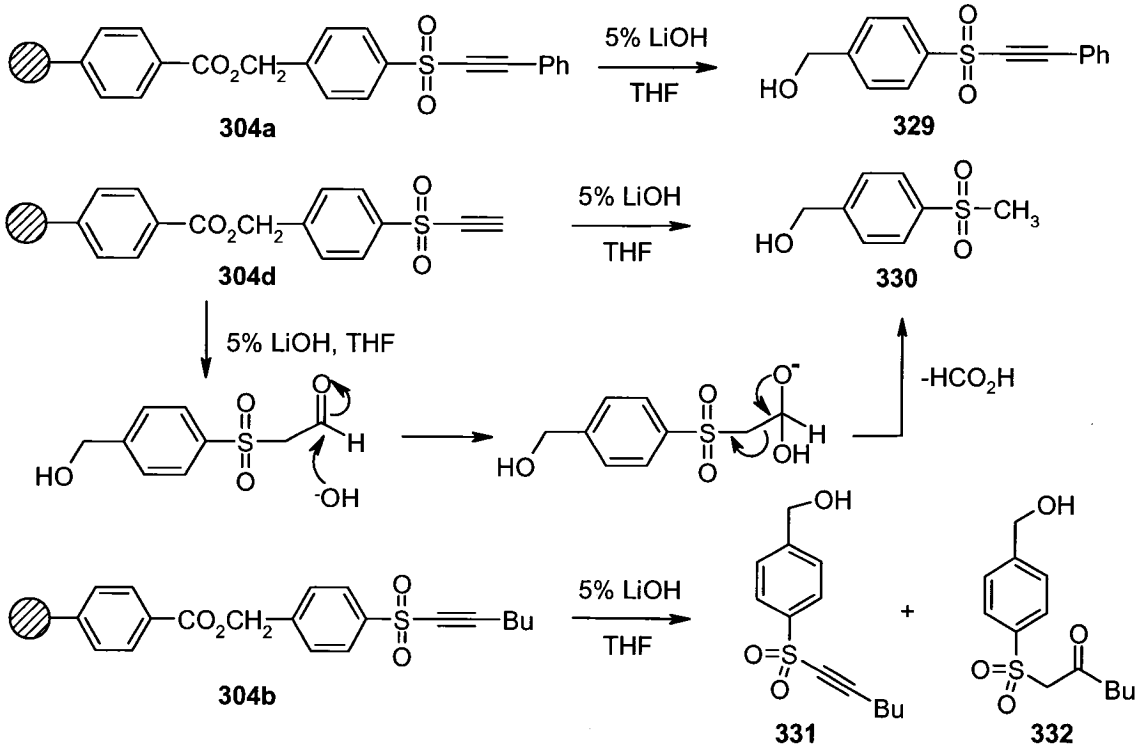

Scheme 3.18 Determination of Loading of Acetylenic Sulfones on Solid Supports

A final approach to ester-linked acetylenic sulfones involved the introduction of the selenosulfonate moiety to the resin via the sulfonhydrazide **333** by coupling **328** and **323**, as shown in Scheme 3.19, followed by oxidation with benzeneseleninic acid **(268)**, addition to the appropriate acetylene and selenoxide elimination. Resin **333** contains nitrogen, making elemental analysis for this element a useful method to determine the loading, which proved to be 0.67 mmol/g. This method produced comparable loading of the acetylenic sulfones as the method described in Scheme 3.17. However it has the advantage that a single polymer-supported selenosulfonate can be used to generate a series of polymer-supported acetylenic sulfones, making it more attractive for the eventual production of libraries of cyclization products when used in conjunction with subsequent transformations (vide infra).

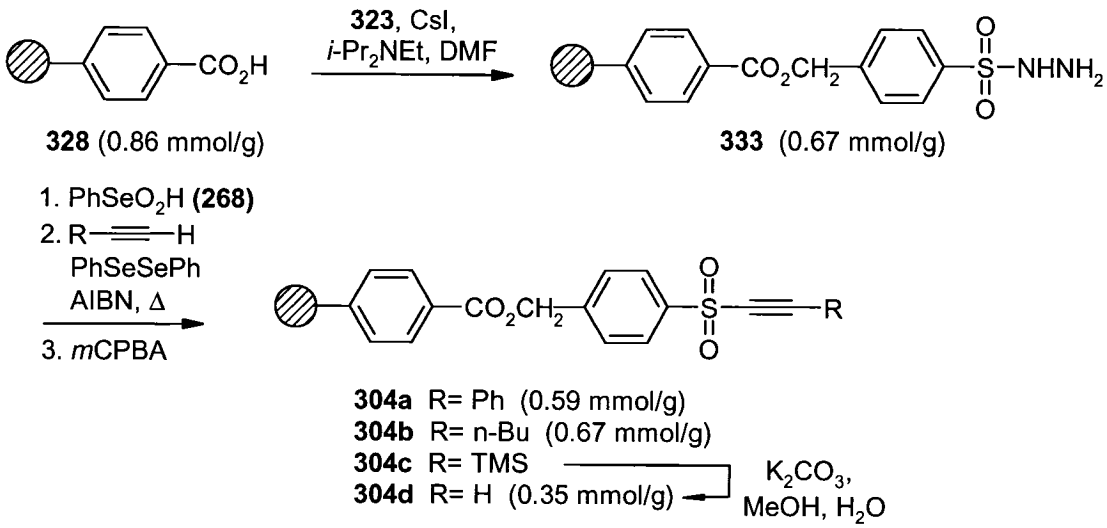

Scheme 3.19 Alternative Preparation of Ester-Linked Acetylenic Sulfones from Sulfonhydrazide **333**

3.3 Further Transformations of Solid-Supported Acetylenic Sulfones

It will be recalled from section 1.1.1 that the β–position of a typical acetylenic sulfone is electrophilic, allowing it to react with nucleophiles via conjugate addition reactions. In addition, acetylenic sulfones are good dienophiles and dipolarophiles due to their low-lying LUMOs. Thus, resins **318**, **321**, and **304** were subjected to a variety of illustrative cyclization and cycloaddition reactions with chloroamines **276**[155] and **334**,[156] cyclopentadiene **(335)**, nitrile *N*-oxide **336**[170], and diazomethane **(337)** (Fig. 3.1) in order to establish their ability to participate in further transformations. The results with solid-supported acetylenic sulfones **318** and **321** are summarized in Table 3.1.

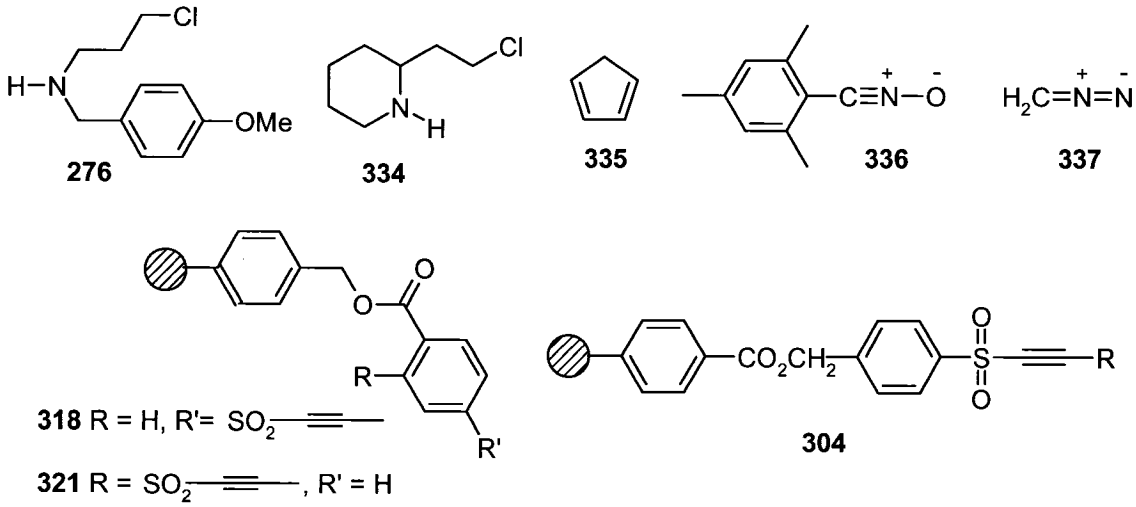

Fig. 3.1 Reagents Used to React with Solid-Supported Acetylenic Sulfones

The conjugate addition reactions of chloroamines **276** and **334** with acetylenic sulfone **318** proceeded smoothly in refluxing THF, as shown in Table 3.1. Evidence for the success of these conjugate addition reactions is based on the disappearance of the IR peak at 2193 cm^{-1} in the adduct. However, the base-mediated intramolecular alkylation followed by cleavage from the resin via transesterification with sodium methoxide in methanol/THF solution afforded only complex mixtures. In contrast to the conjugate addition reaction of **318**, the reaction of chloroamine **276** with **321** afforded the compound **338** in refluxing benzene, as shown in Table 3.1. Compound **338** was produced as only

one geometrical isomer by the intramolecular acylation of the α-position of the sulfone moiety in the initial adduct by the electrophilic ester group. Its structure was identified unambiguously by its NMR and mass spectra, but its geometry is not known and is showen as (*E*) arbitrarily.

The Diels-Alder cycloaddition is arguably the most synthetically versatile method for the preparation of six-membered rings.[171] The acetylenic sulfones **318** and **321** served as the dienophile in the solid-phase Diels-Alder reaction with cyclopentadiene **(335)**. The diene in benzene was heated at 90 °C in a sealed V-vial with the solid-supported acetylenic sulfones **318** or **321** for one day, and the corresponding polymer-bound cycloadducts were treated with methanolic sodium methoxide solution to afford exocyclic allyl sulfones **339** and **340**, respectively, as mixtures of two epimers (exo : endo = 7:1 and 6:1, respectively), arising from the epimerization of the corresponding sulfone moieties under basic conditions[172] (Table 3.1).

The dipolar cycloaddition with nitrile *N*-oxide **336** was also successful, affording cycloadducts **341** and **342**, respectively, after similar cleavage from the support. Products **341** and **342** were obtained as single regioisomers. The purity of the products in Table 3.1 was typically measured after simply filtering the polymer and evaporating the solvent from the filtrate after partitioning between water and an organic solvent to remove the sodium hydroxide. The crude cleaved products were subjected to NMR analysis and shown to be of at least 95% purity (see Table 3.1). The yield was calculated based on the crude material obtained.

Table 3.1 Cyclizations and Cycloadditions of Resins **318** and **321**

Reagents	Reaction Conditions	Cleaved Products (yield)[a]
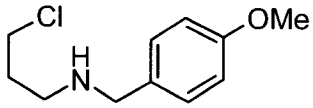 **276**	1. **318**, THF, 2dΔ 2. LDA, THF	Complex Mixtures
	321 benzene, 2dΔ	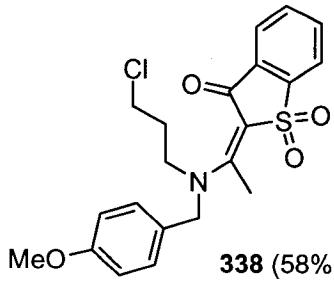 **338** (58%)
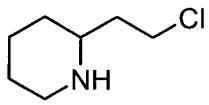 **334**	1. **318**, THF, 2dΔ 2. LDA, THF	Complex Mixtures
 **335**	**318** benzene, 1d Δ NaOMe THF, MeOH	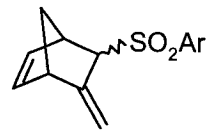 **339** (66%) epimer ratio 7:1
	321 benzene, 1d Δ NaOMe THF, MeOH	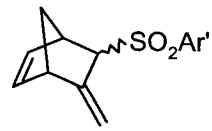 **340** (56%) epimer ratio 6:1
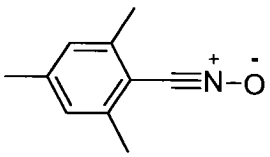 **336**	**318** ether, rt, 2d NaOMe THF, MeOH	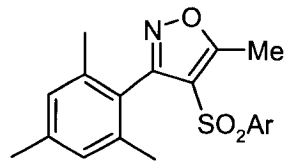 **341** (71%)
	321 ether, rt, 2d NaOMe THF, MeOH	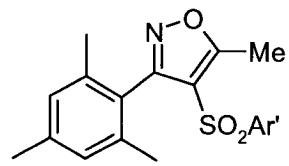 **342** (68%)

Ar = 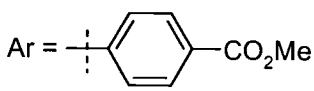

Ar' = 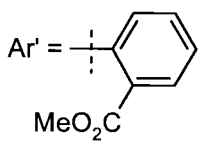

[a] Purity of crude products was >95%

Resins **304a**, **304b**, and **304d** were also subjected to a variety of cylization and cycloaddition reactions in order to determine their suitability for further transformations. The results of these reactions are summarized in Table 3.2.

The conjugate addition of **276** and **334** to **304a**, **304b**, and **304d**, followed by base-mediated (e.g. LDA) intramolecular alkylation and cleavage from the resin via ester hydrolysis with 5% lithium hydroxide in THF solution afforded the corresponding **343** and **344**, respectively. The ester linkage, however, was not fully compatible with the basic conditions of the intramolecular alkylation with LDA at -78 °C for one hour, and a small amount of cleaved products **343** and **344** were formed during the LDA reaction. However, 5% lithium hydroxide was added to make the cleavage go to completion. Suspensions of **304a**, **304b**, or **304d** with cyclopentadiene **(335)** in benzene, were heated at 90 °C in a sealed V-vial for one day, and the corresponding polymer-bound cycloadducts were treated with 5% lithium hydroxide in THF solution to afford the corresponding cycloadducts **345** in moderate to excellent yield (Table 3.2). The dipolar cycloadditions with nitrile *N*-oxide **336** and diazomethane **(337)** were also successful, affording the corresponding cycloadducts **346** and mixtures of **347** and **348**, respectively, in moderate to good yield after similar cleavage from the support.

Products **346** were obtained as single regioisomers, and their structures were later confirmed by reductive desulfonylation with sodium amalgam to afford **352** (vide infra). Product **348a** from **304a** with diazomethane was obtained as a single regioisomer, consisting of two tautomers formed in a ratio of ca. 1.2:1. Products **347b** and **348b** from **304b** with diazomethane were obtained as a mixture of two regioisomers in a ratio of ca. 1:3. Regioisomer **348b** consisted of two tautomers formed in a ratio of ca. 2:1. The structures of **347** and **348** were based on NMR evidence. The regiochemical assignments were tentatively based on NOE experiments. In the case of **347**, irradiation of the N**Me** protons strongly enhanced the signals from the protons in the R substituents, while irradiation of the N=C**H** proton gave only slight enhancement of the signals from protons in the R substituents. In the case of **348**, irradiation of the N=C**H** proton stongly enhanced the signals from the protons in the R substituents, while irradiation of the N**Me** protons gave only slight enhancement of the signals from protons in the R substituents.

Table 3.2 Cyclizations and Cycloadditions of Resins **304a**, **304b**, and **304d**

Reagents	Reaction Conditions	Cleaved Products (yield)
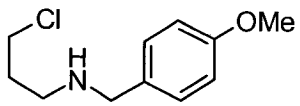 **276**	benzene, 2d Δ → **304**; 1) LDA,THF 2) 5% LiOH	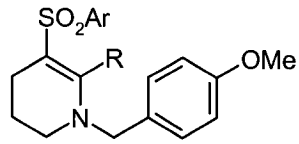 **343a** R = Ph (64%)[b] **343b** R = Bu (57%)[a] **343d** R = H (51%)[c]
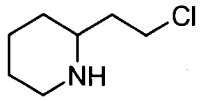 **334**	THF, 2d Δ → **304**; 1) LDA,THF 2) 5% LiOH	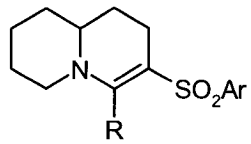 **344a** R = Ph (64%)[b] **344b** R = Bu (69%)[a] **344d** R = H (48%)[c]
 **335**	benzene, 1d Δ → **304**; LiOH,THF	 **345a** R = Ph (90%)[b] **345b** R = Bu (52%)[b] **345d** R = H (78%)[b]
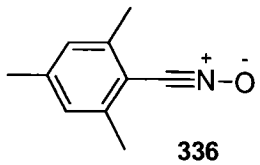 **336**	ether, rt, 2d → **304**; LiOH,THF	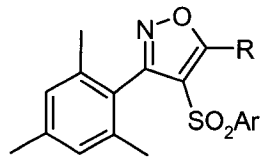 **346a** R = Ph (69%)[b] **346b** R = Bu (48%)[b] **346d** R = H (78%)[b]
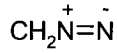 **337**	ether, rt, 40h → **304**; LiOH,THF	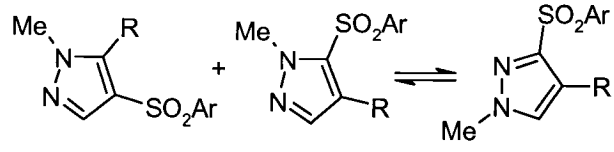 **347** + **348** **a** R = Ph (56%)[c] **348a** only **b** R = Bu (58%)[c] **347b**:**348b** = 1:3

Ar = 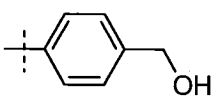

[a]Purity >90%
[b]Purity >95%
[c]Purity >95% after flash chromatography

The purities of isolated crude products were typically greater than 90% and in many cases better than 95% (NMR analysis), without any further purification (see Table 3.2). Only in the cases of **343d**, **344d**, **347** and **348** was it necessary to further purify the products by flash chromatography. In these cases, the yields were based on chromatographed material.

In all of the preceding examples, cleavage from the resin by transesterification or hydrolysis resulted in the sulfone group remaining incorporated in the released products. While this may be desired in some cases, other situations may require a desulfonylated product. An alternative cleavage protocol was therefore developed in which reduction with sodium cyanoborohydride (in the case of products from **276** and **334**), followed by reductive cleavage from the support with 5% sodium amalgam afforded the corresponding desulfonylated products **349**, **280** and known compound **350**.[173] To suppress cleavage of the ester linkage during the cyclization reaction after the conjugate addition of **276** and **334** to resin **304**, a bulkier base, LHMDS, was used and the reaction time was reduced to 30 min.

Similarly, reductive desulfonylation of the cyclopentadiene adduct afforded the known compound **351**,[174] while that of the nitrile *N*-oxide cycloadduct was accompanied by N-O cleavage to provide **352** as a single regioisomer. All the crude products except **352** were obtained in moderate to excellent yield and in purities greater than 90%. Only in the case of **352**, was it necessary to use flash chromatography to effect further purification.

Table 3.3 Cyclization and Cycloadditions of Resins **304a**, **304b** Followed by Reductive Desulfonylation

Reagents	Reaction Conditions	Cleaved Products (yield)
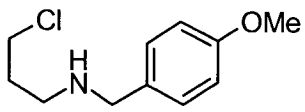 **276**	1. **304a** or **304b** THF, 2d, Δ; 2. LHMDS, THF; 3. $NaCNBH_3$, TFA; 4. 5% Na-Hg, THF	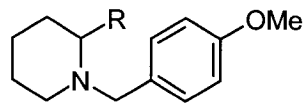 **349a** R=Ph (67%)[a] **280** R=Bu (46%)[a]
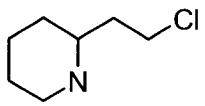 **334**	1. **304a**, THF, 2d Δ; 2. LHMDS, THF; 3. $NaCNBH_3$, TFA; 4. 5% Na-Hg, THF	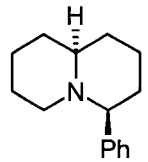 **350** 67%[a]
 **335**	**304a** benzene, 1d Δ; 5% Na-Hg, THF	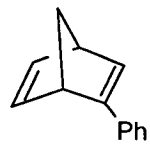 **351** 100%[b]
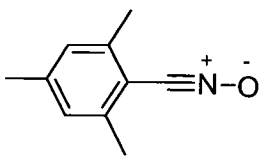 **346**	**304a** ether, rt, 2d; 5% Na-Hg, THF	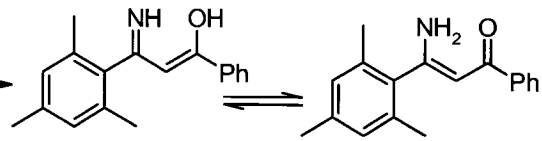 **352** 34%[c]

[a]Purity >90%
[b]Purity >95%
[c]Purity >95% after flash chromatography

3.4 Regeneration of the Resin 328

As discussed in section **1.3.10**, some solid supports can be regenerated upon substrate release, thus allowing for another synthetic cycle to be carried out with the same resin. This recycling process can improve the cost effectiveness of large scale solid phase organic syntheses, particularly when starting resins are expensive.

The solid-supported benzoic acid **328** can be recycled after cleavage of the product by ester hydrolysis. For example, after resin **304a** was subjected to a Diels-Alder reaction with cyclopentadiene **(335)**, the final product **345a** was cleaved and the lithium carboxylate resin was acidified to regenerate the benzoic acid resin **328** (see Scheme 3.20). This recycled resin **328** was subjected to another synthetic cycle to afford the

cleaved product **345a**, via acetylenic sulfone resin **304a**. The yield and purity (NMR analysis) of the cleaved product **345a** was comparable with that of the product obtained from the original resin **328**.

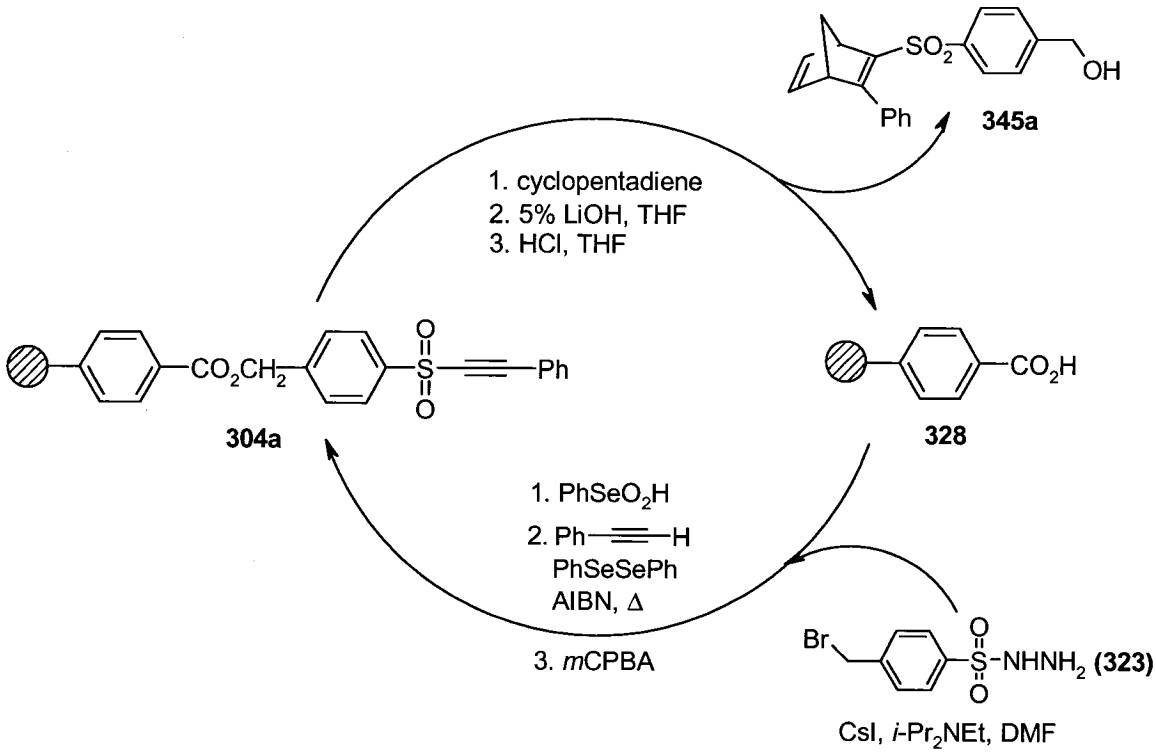

Scheme 3.20 Regeneration of Benzoic Acid Resin **328**

3.5 Conclusions

In comparing the different approaches that were tried, the method using the ester linker appears to be the most generally successful and should be useful in the future for the preparation of libraries of compounds. The methodology shown in Tables 3.1-3.3 has successfully demonstrated that these ester-linked acetylenic sulfones **318**, **321**, and especially **304** can undergo a variety of useful cyclization or cycloaddition reactions. The resulting products can be isolated by cleavage from the resin via ester hydrolysis (in the case of **304**) or via transesterification (in the cases of **318** and **321**) or reduction with sodium amalgam (in the cases of **304a** and **304b**) to afford the corresponding sulfone-functionalized or desulfonylated products, respectively.

Chapter 4

Rearrangements of the Diels-Alder Cycloadducts Obtained from Acetylenic Sulfones and 1,3-Diphenylisobenzofuran (DPIBF)

During the investigation of solid-supported acetylenic sulfones, an attempt was made to employ DPIBF as the diene. Unfortunately, it proved difficult to obtain clean products. This prompted us to examine the reaction more carefully, not only on the polymer support, but also in solution. Upon closer scrutiny of these reactions and the products they were generating, we realized that they were not proceeding according to simple Diels-Alder cycloaddition chemistry, but were undergoing a variety of further transformations. Since these were unexpected, they appeared to be worth studying in more detail. The investigation of these unexpected reactions utilized the cycloadducts of two representative acetylenic sulfones **1a** (R = *n*-Bu) and **1b** (R = Ph) with DPIBF and will be discussed in the following sections.

4.1 Diels-Alder Reaction of DPIBF and Acetylenic Sulfones

Like the fluorinated acetylenic sulfones in Scheme 1.53, the Diels-Alder cycloaddition of **110** with acetylenic sulfones **1a** and **1b** proceeded smoothly upon heating in toluene to afford the expected products **353** and **354** in high yield, respectively (see Scheme 4.1). The structure of the *n*-butyl substituted cycloadduct **353** was confirmed by X-ray crystallography. Details of the crystal structure are given in Appendix VI and the ORTEP diagram is shown in Fig. 4.1. The structure of cycloadduct **354** was confirmed by NMR spectroscopy due to the similarity of **354** and **353**.

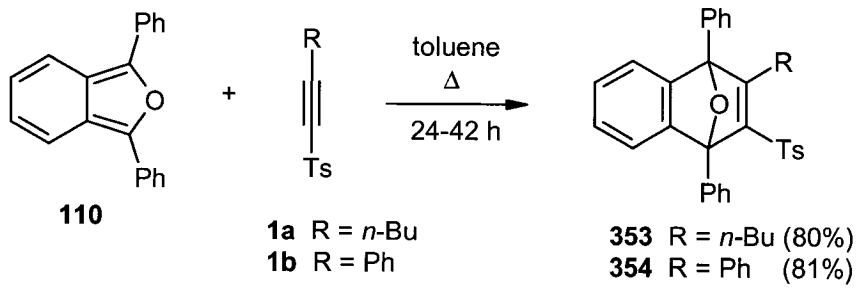

Scheme 4.1 Diels-Alder Reaction of **110** with Acetylenic Sulfones

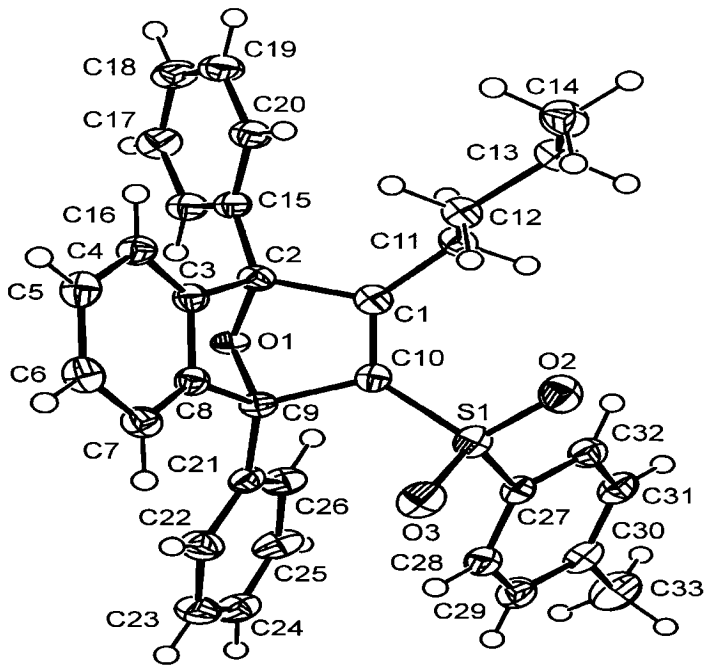

Fig. 4.1 ORTEP Diagram of Cycloadduct **353**

The cycloadducts **353** and **354** were then subjected to further transformations under pyrolytic, acid-catalyzed and photolytic conditions, under which they readily rearranged to some unusual and unexpected products.

4.2 Further Transformations under Pyrolytic Conditions

When the butyl-substituted cycloadduct **353** was heated for 60 h in xylenes at 152 °C, it afforded the rearranged ketone **355** and the alkenyl naphthalene **356** in almost equal amounts. Similar treatment of the cycloadduct **354** produced **357** (analogous to **355**) along with the transposed ketone **358** in the ratio of ca. 1:2. The results are summarized in Scheme 4.2. The structures of **355**, **357** and **358** were confirmed by X-ray crystallography. Details of the crystal structures are given in Appendix VII, VIII and IX, respectively, and their ORTEP diagrams are shown in Fig. 4.2, Fig. 4.3, and Fig. 4.4, respectively. The structure of alkenyl naphthalene **356** was deduced from NMR and mass spectrometric data.

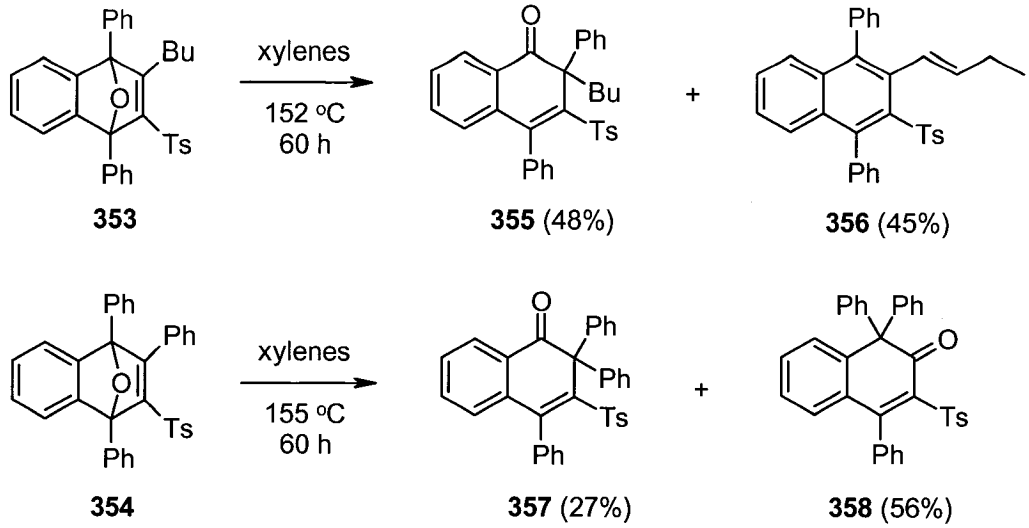

Scheme 4.2 Rearrangement under Pyrolytic Conditions

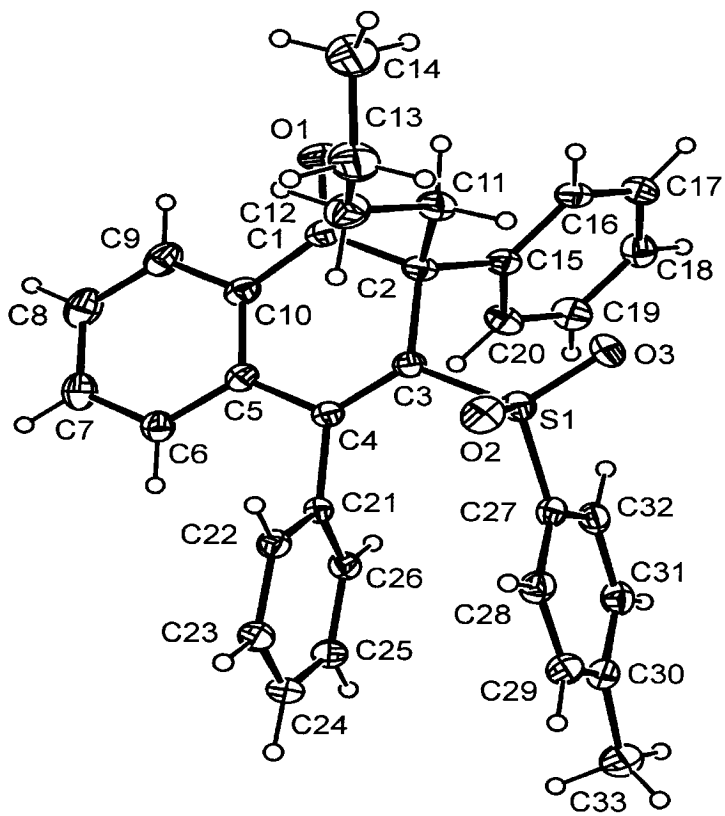

Fig. 4.2 ORTEP Diagram of Rearranged Ketone **355**

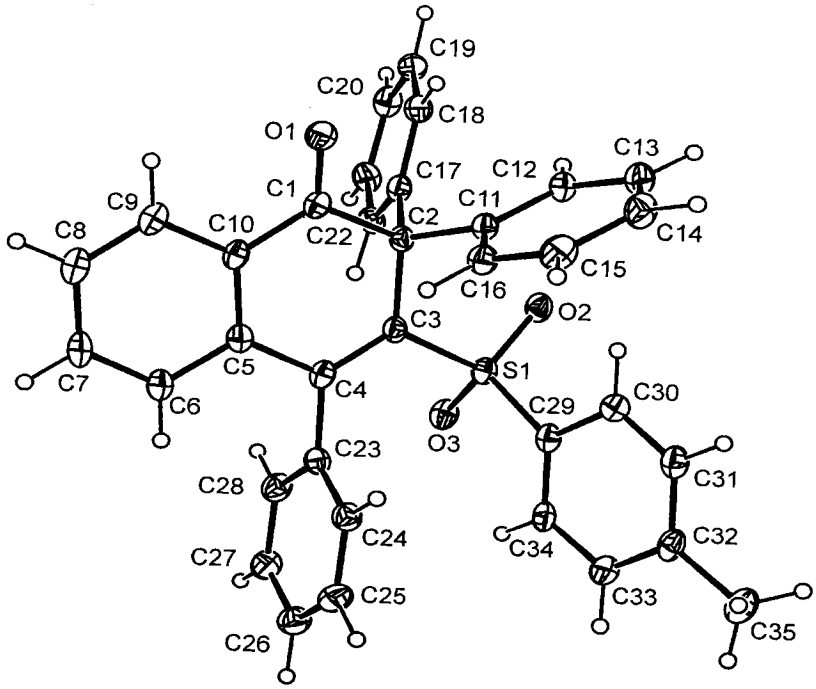

Fig. 4.3 ORTEP Diagram of Rearranged Ketone **357**

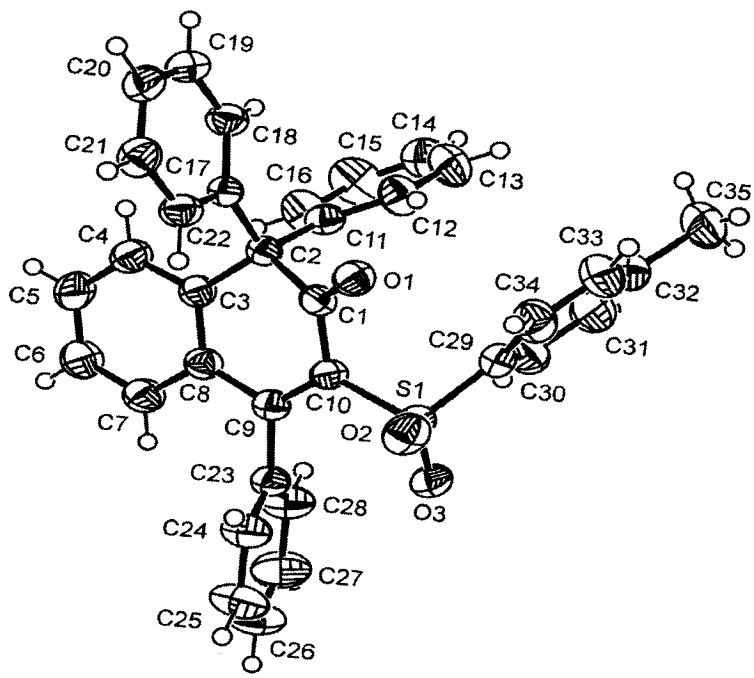

Fig. 4.4 ORTEP Diagram of Rearranged Transposed Ketone **358**

4.3 Further Transformations under Acidic Conditions

When cycloadducts **353** and **354** were treated with hydrochloric acid in acetic acid solution at room temperature, **355** was the exclusive product from **353**, while **354** afforded a mixture of **357** and **358** similar to that obtained earlier under neutral pyrolytic conditions. The results are summarized in Scheme 4.3.

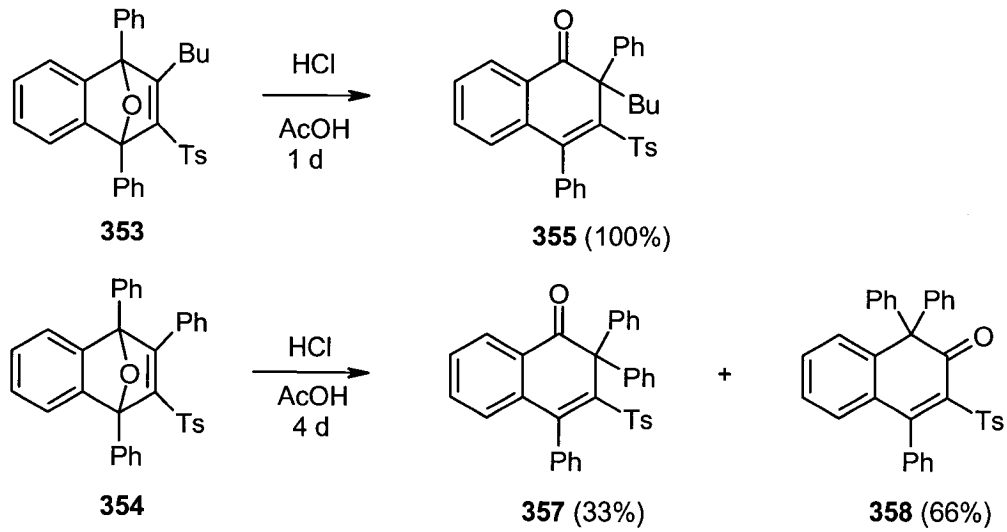

Scheme 4.3 Rearrangement under Acidic Conditions

4.4 Rationale for the Rearrangements under Pyrolytic and Acidic Conditions

As indicated in Schemes 4.2 and 4.3, very similar results were obtained under both thermal and acid-catalyzed conditions, with the exception that **356** was only produced in the thermal case.

A plausible mechanism for the rearrangement of **353** to **355** and **354** to **357** and **358** under acid-catalyzed conditions is shown in Scheme 4.4. First, the bridging oxygen atom could be protonated and one C-O bond could be cleaved selectively to form carbocations **359** and **360**. A 1,2-shift of the phenyl substituent via the phenonium ions **361** and **362** would lead to the observed ketones **355** and **357**, respectively. There are earlier reports of the formation of similar ketones from O-bridged systems in the early work of Wittig and coworkers,[106, 107, 111] as shown in Scheme 1.47. The formation of **358**

from **354** under similar conditions is more noteworthy since it requires the formal 1,2-transposition of the bridging oxygen atom with that of the phenyl group. This can be rationalized by invoking epoxide intermediates **363** and **364**, which can either regenerate **359** and **360** or produce the rearranged carbocations **365** and **366**, respectively. 1,2-Phenyl migration in **366** leads to the observed isomeric ketone **358**. The formation of the transposed ketone **358** that takes place in the phenyl series but is absent in the butyl series can be attributed to the more facile migration of the phenyl group in cation **366** compared to that of an *n*-butyl group in cation **365**.[175]

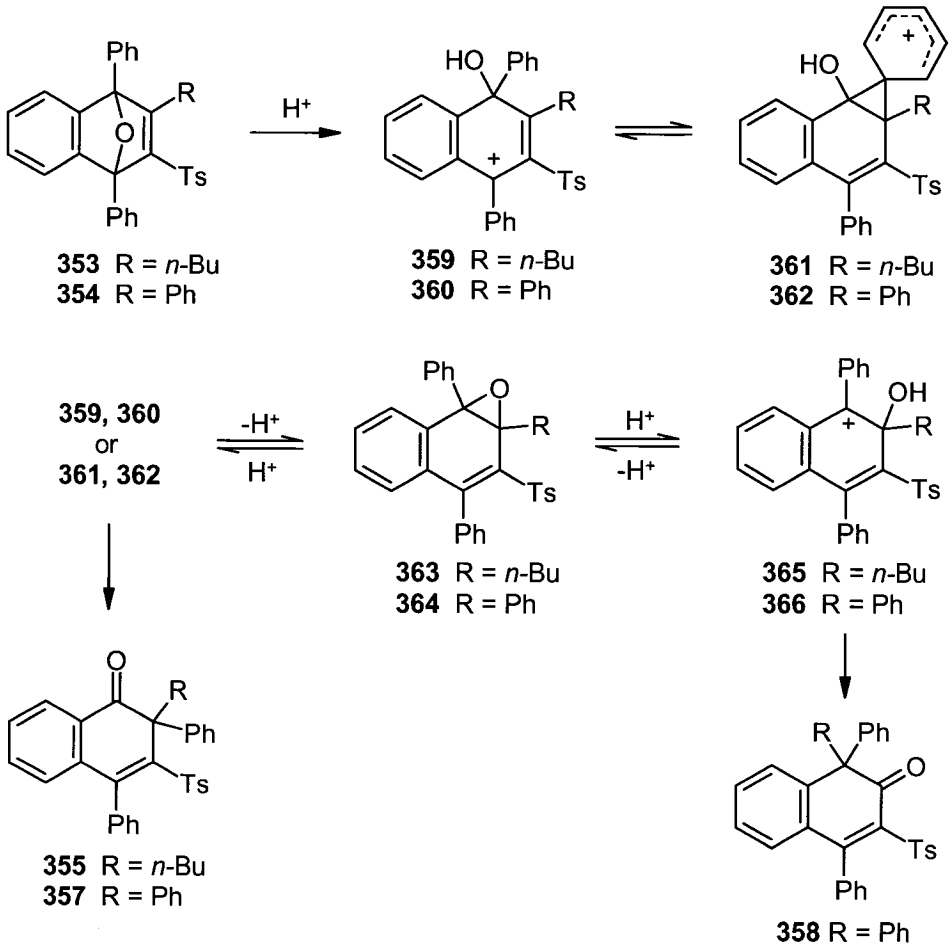

Scheme 4.4 A Plausible Mechanism for the Rearrangement under Acid-Catalyzed Conditions

Although the epoxides **363** and **364** could not be isolated, their intermediacy in

Scheme 4.4 is supported by a control experiment. The alkenyl naphthalene **356** that had been obtained from **353** in Scheme 4.2 was first hydrogenated to form **367**, which was then treated with *m*CPBA to produce the same rearranged ketone **355** as was obtained from **353** in Scheme 4.4. Since the formation of epoxide intermediates is known to occur when naphthalenes and related polycyclic aromatic systems are oxidized with peracids,[176] it is reasonable to postulate similar epoxide intermediates **363** and **364** in Scheme 4.4.

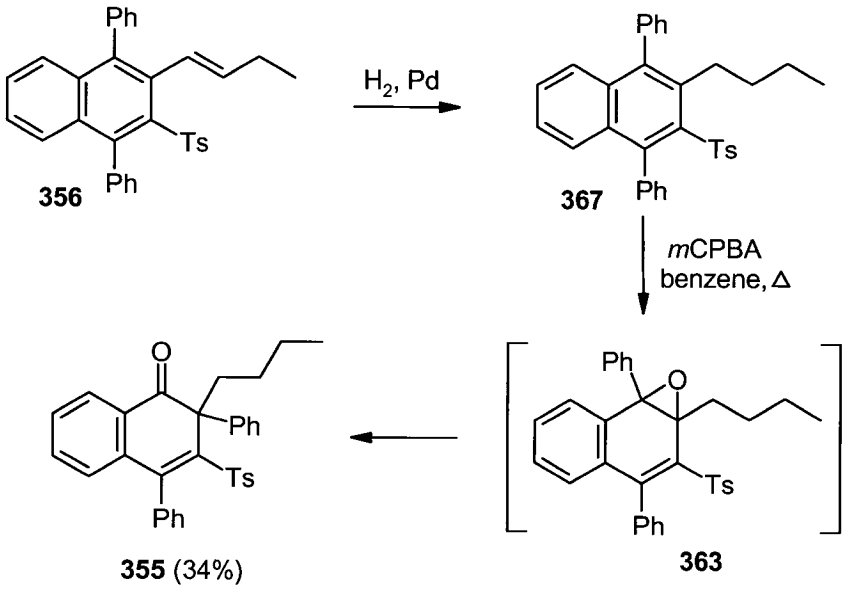

Scheme 4.5 Control Experiment to Test the Intermediacy of Epoxide **363**

So, under acid-catalyzed conditions, **353** and **354** first formed carbocations **359** and **360**, which rearranged to produce ketones **355**, **357** and **358**. The formation of **355** and **357** can be envisaged to take place directly from their carbocation precursors, or through the reversible formation of epoxides **363** and **364**. The rearranged ketone **358** is assumed to arise via the corresponding epoxide **364**. However, there also exists the possibility that after protonation of the bridging oxygen, the upper C-O bond could be cleaved to give cations **368** and **369**, which would be expected to lead to the regioisomeric products **374** and **375**, via a similar pathway (see Scheme 4.6). The absence of any noticeable amounts of **374** and **375** is noteworthy. At first glance, cations **359** and **360** appear to be relatively stable compared with their regioisomeric species **368** and **369** due

to the cross-conjugation of the delocalized cation with the sulfone moiety in the former compared to the linear conjugatation in the latter. That is, one might expect that in **368** and **369**, the electron-withdrawing sulfone group would destabilize the respective cations more than in **359** and **360**. Molecular modeling using the SPARTAN platform (Wavefunction, Inc.) was performed by subjecting each structure to a MMFF conformation search and PM3 geometry optimization, followed by a 3-21G* ab initio single point energy calculation. The results of these calculations are shown in Scheme 4.6. They indicate that **368** and **369** are actually more stable than **359** and **360** by 4.26 and 10.83 kcal/mol, respectively. Similarly, the isomeric phenonium ions **370** and **371** proved to be more stable than **361** and **362** by 15.76 and 9.16 kcal/mol, respectively. This can be attributed to hydrogen bonding between the hydroxyl hydrogen atom and a sulfone oxygen in each of **368-371** (interatomic OH---O=S(O) distances were calculated to be 1.791 and 1.788 Å for **368** and **369**, and 1.760 and 1.738 Å for **370** and **371**, respectively). On the other hand, epoxides **363** and **364** were calculated to be more stable than their regioisomers **372** and **373** by 9.17 and 4.83 kcal/mol, respectively. Similarly, the observed final products **355** and **357** were more stable than their hypothetical counterparts **374** and **375** by 5.54 and 0.62 kcal/mol, respectively. All these computational results suggest that there are two possibilities: one is that a freely equilibrating mixture of regioisomeric cation intermediates is present and the Curtin-Hammett Principle[177] applies. Alternatively, there also exists the possibility that the rearrangements of **353** to **355** and **354** to **357** and **358** are more concerted than what is shown in Scheme 4.4. In any case, it must be kept in mind that Scheme 4.6 depicts the results from relatively low-level calculations that must be regarded as tentative.

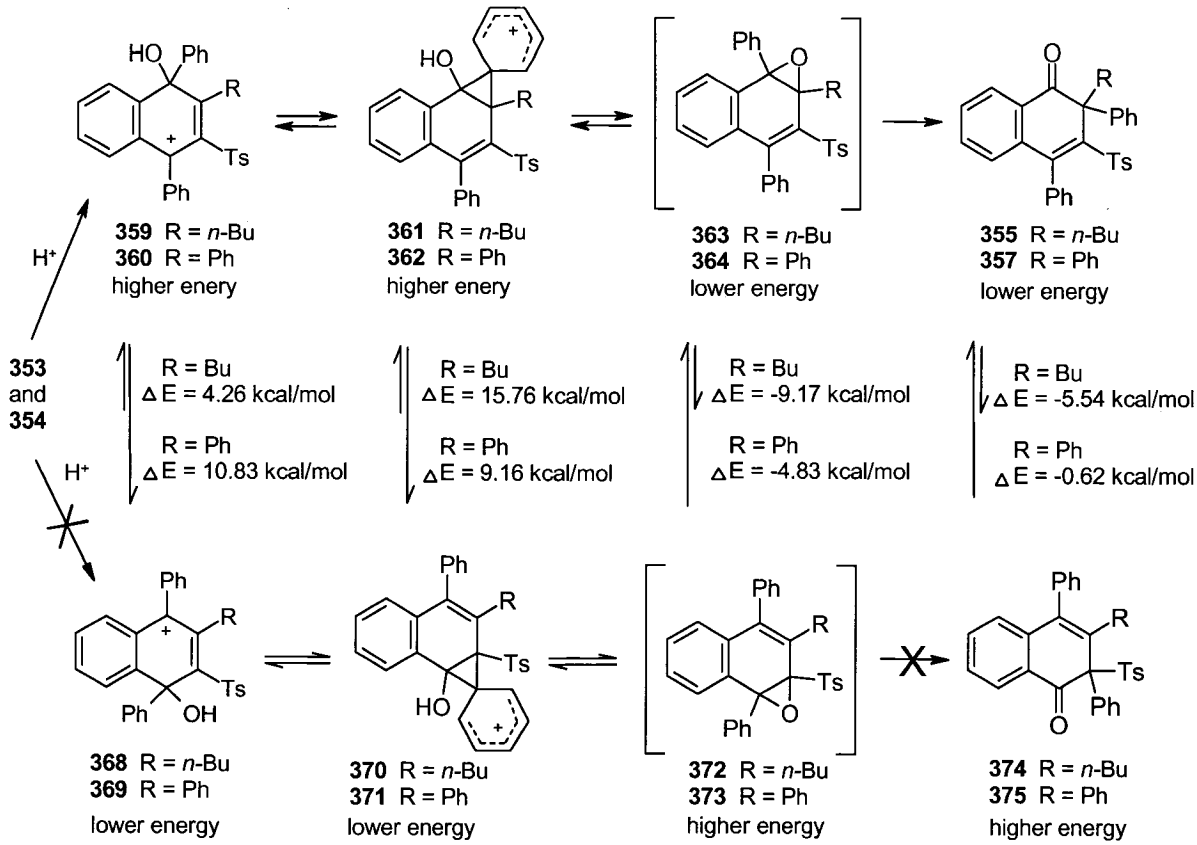

Scheme 4.6 Calculation of Energies of Possible Intermediates

It is likely that a very similar mechanism to that described under acid-catalyzed conditions is taking place under pyrolytic conditions, because similar results were obtained under both conditions. The C-O bond can be selectively cleaved to form either dipolar or diradical intermediates in the pyrolytic reaction. In order to test the existence of radical intermediates, a control experiment with the radical inhibitor 2,6-di-*tert*-butyl-4-cresol (butylated hydroxytoluene, BHT) was conducted. Inclusion of either 0.2 or 2.0 mol of BHT did not suppress the formation of the above products. This control experiment suggests that **353** and **354** undergo heterolytic C-O bond cleavage to produce dipolar, rather than diradical intermediates in the pyrolytic reaction. The proposed mechanism is shown in Scheme 4.7.

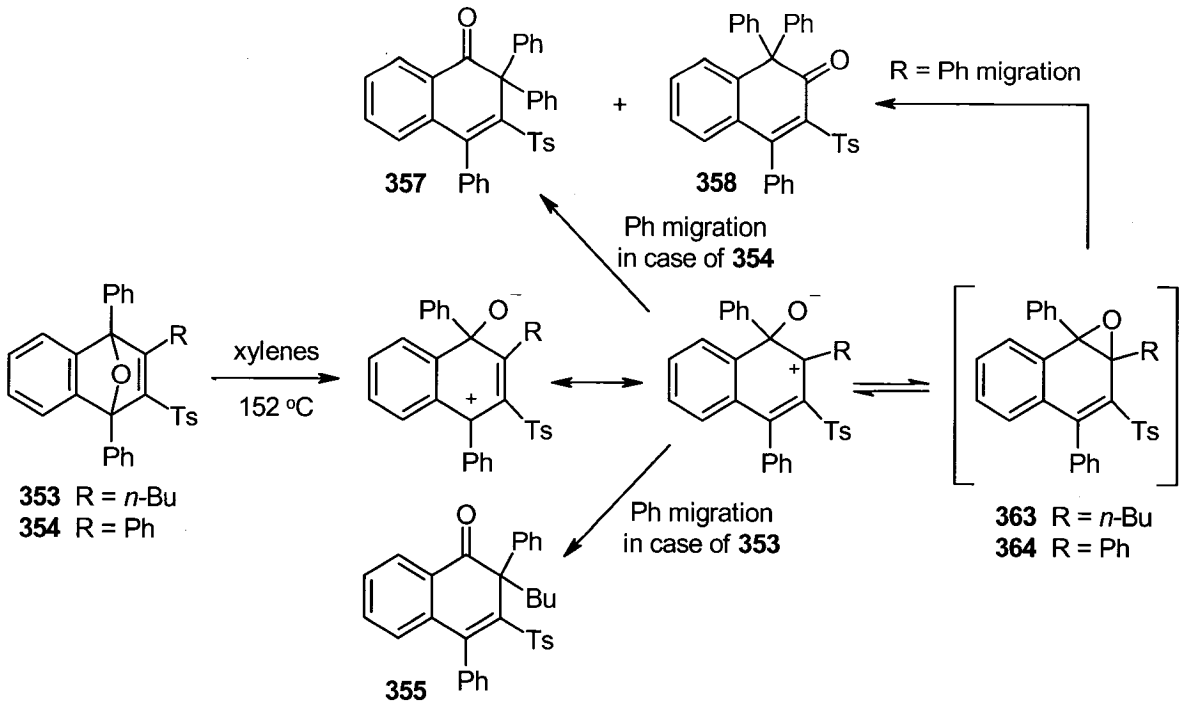

Scheme 4.7 Proposed Mechanism for the Rearrangement under Pyrolytic Conditions

The formation of the remaining product **356** in the *n*-butyl series can be rationalized by the ring-opening of the oxygen bridge in **353** to generate **376**, followed by elimination of water and aromatization (Scheme 4.8).

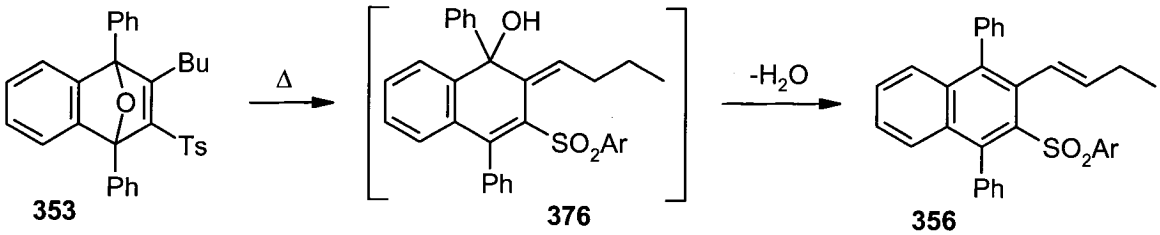

Scheme 4.8 Formation of Dehydration Product **356** from **353**

4.5 Further Transformations of 353 and 354 under Photochemical Conditions

The unexpected results that were observed under acid-catalyzed and pyrolytic conditions led us to investigate the photochemistry of these cycloadducts (see Scheme 4.9). Photolysis of the cycloadducts **353** and **354** in dichloromethane at 300 nm produced

ketone **355** as the only isolable product in the *n*-butyl series, while the corresponding analogue **357** was absent in the phenyl series. Surprisingly, in the case of the phenyl series, two completely different products were obtained. The benzoxepin **377** and the indenyl phenyl ketone **378** were formed as the major and minor product, respectively. The structure of **377** was established unequivocally by X-ray crystallography, while that of **378** was deduced from spectroscopic data. Details of the crystal structure of **377** are given in Appendix X and the ORTEP diagram is shown in Fig. 4.5.

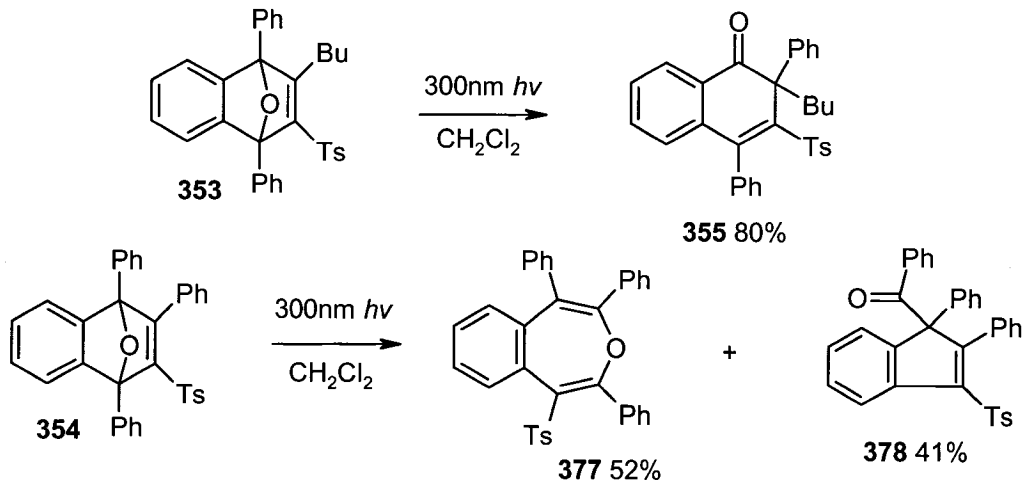

Scheme 4.9 Rearrangement under Photochemical Conditions

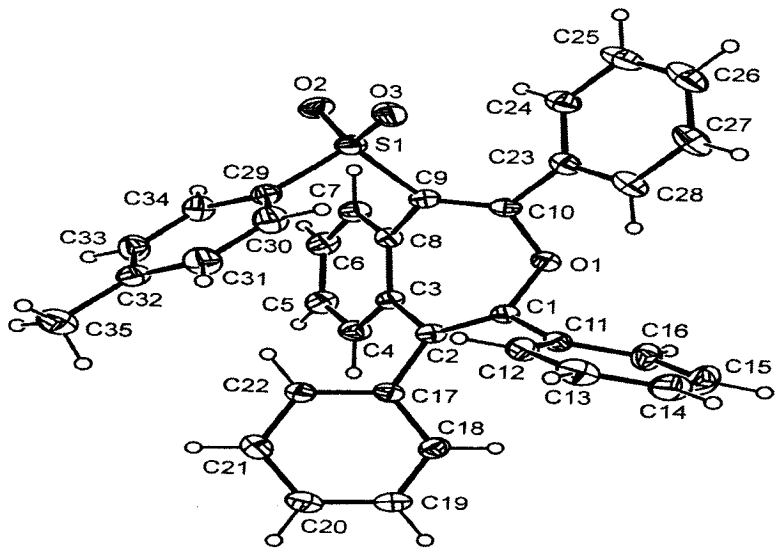

Fig. 4.5 ORTEP Diagram of Benzoxepin **377**

Both ^{13}C and ^{1}H NMR spectra, as well as COSY, HMQC and HMBC spectra were used to deduce the structure of **378**. We can identify certain signals from their chemical shifts with reasonable certainty. The ^{13}C spectrum shows a nonaromatic quaternary carbon signal at δ 79.5 ppm, which was assigned to the only nonaromatic quaternary carbon atom in the indene skeleton of **378**. Protons at the *ortho*-position and *meta*-position of the the *p*-toluenesulfonyl group were assigned to signals at δ 7.59 ppm and δ 7.18 ppm, respectively, which were distinguishable from all other aromatic protons. Confirmation of these assignments was made by COSY and HMQC experiments. The HMBC spectrum, which shows two and three bond correlations between protons and carbons, was used to further confirm the structure of **378**. The quaternary carbon signal at δ 79.5 ppm correlates with two (integration) aromatic hydrogens at δ 6.65 ppm, assigned to the *ortho* positions of the phenyl ring attached to it. However, in the case of the regioisomer of **378**, the quaternary carbon at δ 79.5 ppm should only correlate with a single proton in the indenyl moiety and not with the *ortho* hydrogens of a phenyl substituent at δ 6.65 ppm with an integration of two. Furthermore, the ^{13}C spectrum shows a quaternary carbon signal at δ 160.3 ppm, which can be assigned to the β-carbon atom of vinyl sulfone moiety in **378**. This signal correlates with two (intergration) *ortho* hydrogens of a phenyl substituent at δ 6.37 ppm. Neither the alkene carbons of the regioisomer (an allyl sulfone moiety), nor the *ipso* carbon atom of the phenacyl substituent would be expected at such low field. Thus, only the structure of **378** fits the HMBC correlations. The data is summarized in Tables 4.1 and 4.2, and Fig. 4.6.

Table 4.1 COSY and COSY (Long Range) Analysis for **378**[a]

Signal (ppm), multiplicity, integration	Correlated to: Signal (ppm), multiplicity[a]
8.39, d, 1H	7.56, m; 7.40, m(LR)
7.59, d, 2H	7.18, d
7.56, m, 1H	8.39, d; 7.40, m
7.42, m, 1H	7.36, d
7.40, m, 1H	7.56, m; 7.34, m
7.36, d, 2H	7.14, d

7.34, m, 1H	7.40, m
7.26, d, 1H	7.11, d; 6.65, dd (LR)
7.23, d, 1H	7.05, dd; 6.37, dd (LR)
7.18, d, 2H	7.59, d; 2.38, s (LR)
7.14, d, 2H	7.42, m; 7.36, d
7.11, d, 2H	7.26, d; 6.65, dd
7.05, dd, 2H	7.23, d; 6.37; dd
6.65, dd, 2H	7.11, d; 7.26, d (LR)
6.37, dd, 2H	7.05, dd; 7.23, d (LR)
2.38, s, 3H	7.18, d (LR)

(a) Due to the symmetrical nature of a COSY and COSY (long range) spectrum, some of the redundant correlations have been omitted.

Table 4.2 HMQC and HMBC Correlations for **378**[a]

Carbon signal (ppm)	Correlations in HMQC spectrum: proton signal (ppm)	Correlations in HMBC spectrum: proton signal (ppm)
195.9, C	--	7.36
160.3, C	--	6.37
144.1, C	--	7.59, 2.38
143.3, C	--	8.39, 7.34
140.6, C	--	--
140.0, C	--	--
137.9, C	--	--
137.3, C	--	--
136.3, C	--	--
132.4, CH	7.42	--
132.2, C	--	7.05
129.7, CH	6.37	--
129.3, CH	7.18	--
129.1, CH	7.34	--
129.0, CH	6.65	--
128.6, CH	7.36	--
128.2, CH	7.56	--
128.1, CH	7.14	--
127.9, CH	--	--
127.8, CH	--	--
127.7, CH	7.11	--
127.4, CH	7.59	--

126.6, CH	7.05	--
125.6, CH	7.40	--
123.9, CH	8.39	--
79.5, C	--	6.65
21.4, CH3	2.38	--

(a) Due to the proximity or overlap of several signals, some correlations could not be determined with certainty.

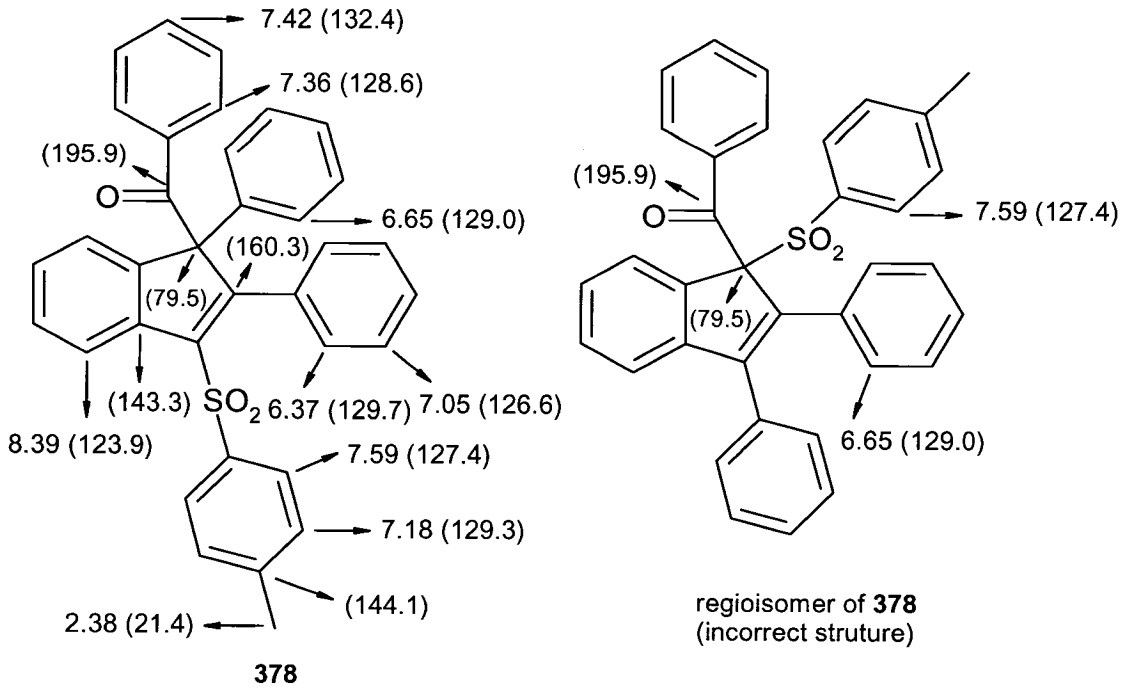

Fig. 4.6 NMR Assignments for **378**, based in part on HMBC and HMQC experiments (δ of ^{1}H signals are given first, followed by ^{13}C signals in parentheses)

The photolysis of the butyl derivative **353** afforded the same ketone **355** that had been previously observed as the sole or major product under acid-catalyzed or pyrolytic conditions, respectively. In contrast to the pyrolytic conversion of **353** to **355**, the photochemical formation of **355** was suppressed by the inclusion of BHT, suggesting that, under these conditions, the photochemical process does proceed via a radical pathway, possibly involving diradical species derived from the homolytic cleavage of a bridging C-O bond. However, in the phenyl series, **354** produced no significant amounts of either ketone **357** or **358**. Instead, the benzoxepin **377** and exocyclic ketone **378** were obtained.

The mechanism of the transformation of **354** to **377** and **378** will be discussed in the following sections.

4.6 Transformations of Oxanorbornadienes under Photochemical Conditions

Previous studies of oxanorbornadienes upon irradiation with filtered UV light at low temperatures have shown that 7-oxanorbornadiene **379** undergoes rapid and quantitative [2π + 2π] cycloaddition to form 3-oxaquadricyclane **(380)**.[178] On exclusion of acid, e. g. by heating in benzene, the highly strained tetracyclic **380** undergoes thermal rearrangement to give the more stable oxepin **381**. Experimental evidence, as well as MO computations by Haselbach and Martin,[179] favours a two-step mechanism. This 3σ → 3π isomerization of **380** is believed to go through a 1,3-dipolar cycloreversion via a carbonyl ylide intermediate **382** (see Scheme 4.10). The intermediacy of the carbonyl ylide **382** was demonstrated by trapping the 1,3 dipolar species with dipolarophiles, such as dimethyl acetylenedicarboxylate (DMAD)[180] (see Scheme 4.10). During the reaction of **380** with DMAD, it was confirmed that the addition does not take place until the temperature range of the thermolysis to the oxepin has been reached. The reaction in excess DMAD afforded approximately equal amounts of the tricyclic compound **383** and oxepin **381**.

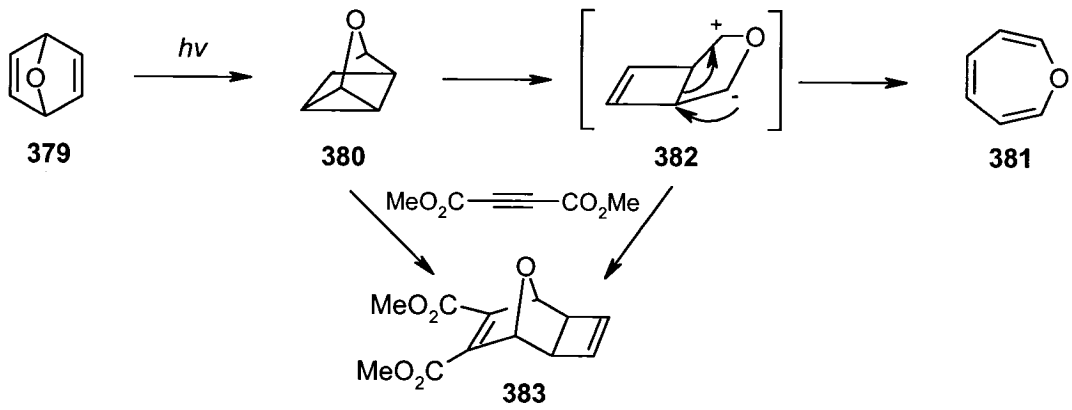

Scheme 4.10 Formation of **381** from **379** via Carbonyl Ylide **382**

Using Schleyer's value of 101 kcal/mol for the ring strain of quadricyclane and the value of 38 kcal/mol for the strain remaining in the carbonyl ylide,[181] Huisgen[182] has

estimated a release of 63 kcal/mol of strain energy for the isomerization of 3-oxaquadricyclane **380** to carbonyl ylide **382**, which makes the reversal unfavourable.

Based on the mechanism discussed above, a similar process for our case is shown in Scheme 4.11. It is therefore possible to rationalize the conversion of **354** to **377** if one assumes the photochemical isomerization of the former to the corresponding oxaquadricyclane **384**, followed by thermal conversion to **377** via ylide **385**. The isomeric structure **386** was not formed, probably because of higher strain in the tricyclic ring system of carbonyl ylide intermediate **387**, and in the product **386**.

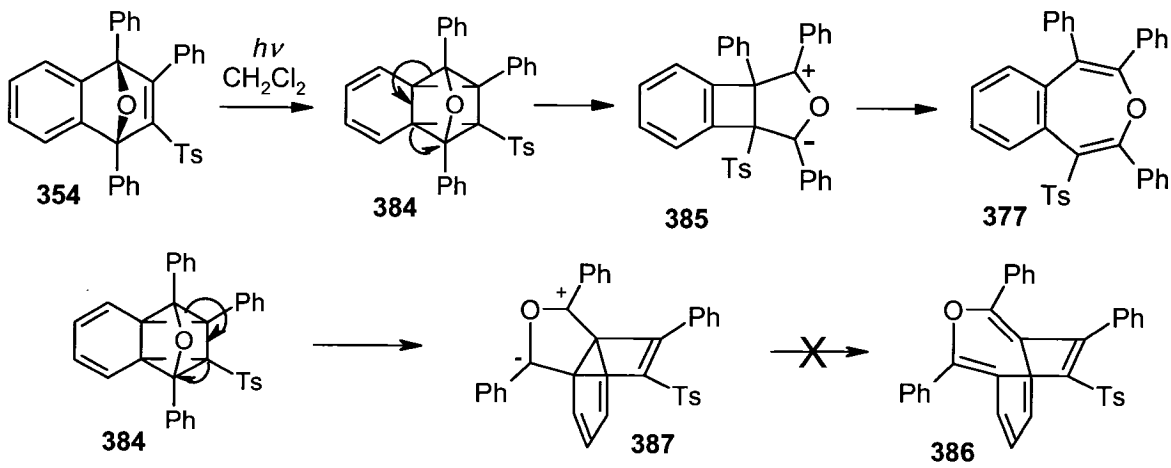

Scheme 4.11 A Plausible Mechanism Leading to Benzoxepin **377**

Now it remains to rationalize the formation of the other observed product **378**, shown in Scheme 4.9.

4.7 Further Transformation of Benzoxepin 377 to Exocyclic Ketone 378

In the previous section, a plausible mechanism regarding the rearrangement of **354** to **377** through oxaquadricyclane **384**, and carbonyl ylide **385** was proposed, but the mechanism by which exocyclic ketone **378** forms still needs to be addressed. Another control experiment revealed that photolysis of pure benzoxepin **377** under similar conditions to those used in its original formation (Scheme 4.9) resulted in its conversion to ketone **378**, whereas this transformation failed in the dark (see Scheme 4.12). This

indicates that **378** is produced from the further photoisomerization of the benzoxepin **377** rather than via an independent pathway from **354**, or via a thermal process from **377**.

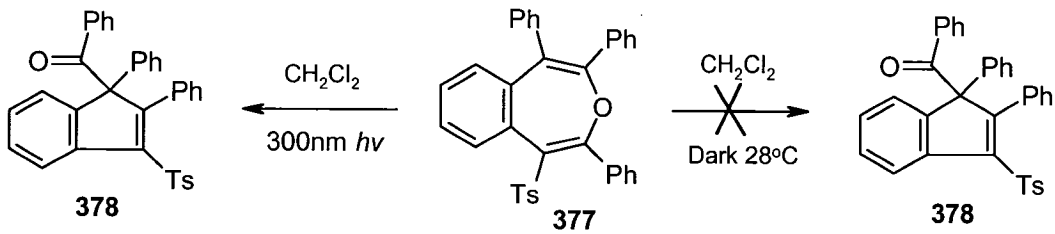

Scheme 4.12 Control Experiments to Test Conversion of **377** to **378**

Several possible pathways for the transformation of **377** to **378** have at least partial precedent in the literature and will be discussed in detail in the following sections.

4.7.1 Diradical Mechanism

A diradical mechanism was suggested as a possible pathway for the related photoisomerization of 4,5-dihydrooxepin **(388)** to 2-cyclopentenecarbaldehyde **(389)** via homolytic cleavage of a C-O bond, followed by recombination, as shown in Scheme 4.13.[183]

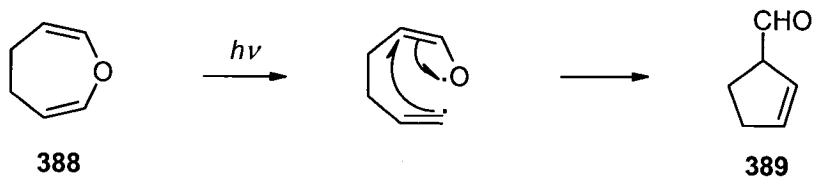

Scheme 4.13 Proposed Radical Recombination to Form **389**

In our case, the analogous mechanism for the isomerization of **377** to **378** is shown in Scheme 4.14. One of the C-O bonds is cleaved homolytically to form the diradical **390**, which recombines to afford the exocyclic ketone **378**.

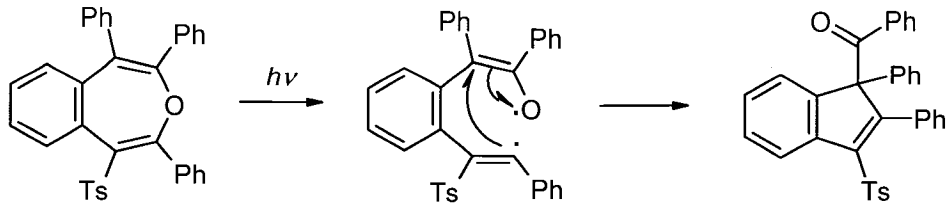

377 390 378

Scheme 4.14 Isomerization via Diradical Intermediate **390**

The photoisomerization of **377** to **378** was repeated under the same conditions as those used in its formation (Scheme 4.12) in the presence of the radical inhibitor BHT, but no significant change was observed in reaction rate or nature of the products of the reaction. This control experiment suggests that, under these conditions, the photochemical process does not proceed via a diradical pathway.

4.7.2 Arene Oxide Mechanism

The interconversions of arene oxides with the corresponding oxepins have been extensively studied in aromatic hydrocarbon systems.[184] In benzene oxide **(391)**, the two π bonds and the C-C σ bond undergo a facile thermal disrotatory electrocyclic reaction to give a 6π-oxepin system (see Scheme 4.15). In the case of **391**, the enthalpy difference between itself and the valence tautomer **381** is only 1.7 kcal/mol (see Scheme 4.15).[185] At room temperature, the rate of exchange is so fast that the NMR spectrum shows the average of the chemical shifts due to protons represented by both structures **391** and **381**.

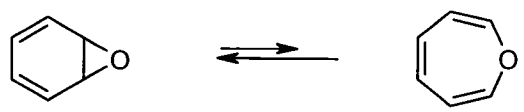

391 381

Scheme 4.15 Valence Tautomerism of Benzene Oxide and Oxepin

In our case, the analogous process would require **377** to tautomerize to benzene oxide **392**, which could then undergo further rearrangement to **378**, possibly via diradicals **393** and **394** (Scheme 4.16), or similarly by means of dipolar intermediates.

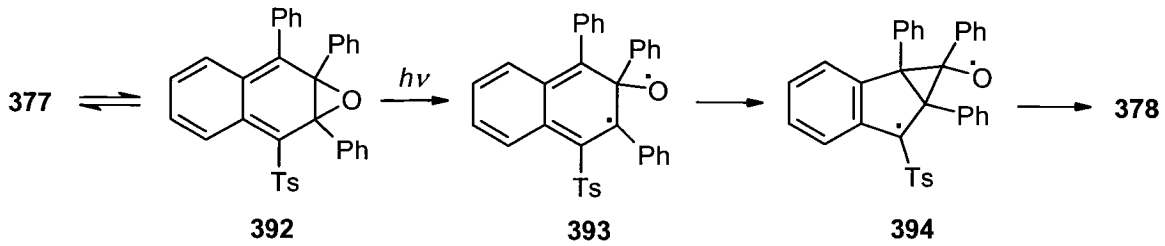

392 **393** **394**

Scheme 4.16 Mechanism for Isomerization of **377** to **378** via Benzene Oxide **392**

Furthermore, certain other oxepins do not undergo this valence tautomerism. Thus in some instances, the oxepin tautomer better represents the actual structure and reactivity of a compound, whereas in other cases the arene oxide form alone describes the structure and reactivity. All four arene oxides derived from naphthalene have been prepared and their structures are well defined. None of them shows valence tautomerism. They exist exclusively either in the oxepin or arene oxide forms (see Scheme 4.17). In the cases of **396**, **397**, and **398**,[186] the resonance energy of the benzene moiety (~39 kcal/mol) shifts the equilibrium irretrievably towards the oxepin in the cases of **396** and **397**, and in the case of **398** the arene oxide is favoured. Tautomerism, which ordinarily is manifested with systems having small energy differences, is therefore not possible. However, in the case of the 9,10-oxide **395**, this limitation does not exist, but even so, the compound exists only in the oxepin form **395**,[185] probably because of a very high strain associated with the oxirane ring in the epoxide form.

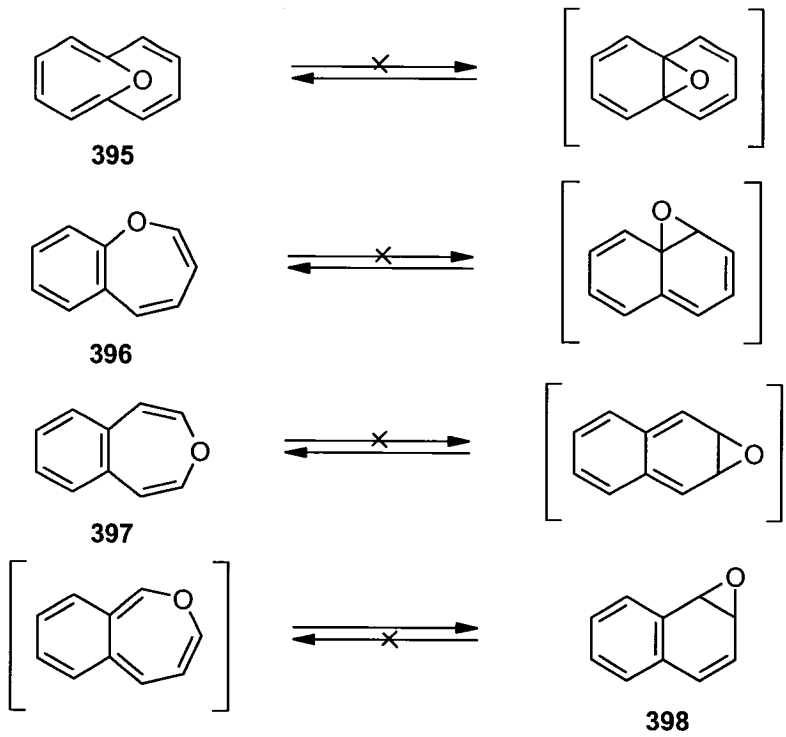

Scheme 4.17 Absence of Valence Tautomerism of Arene Oxides Derived from Naphthalene

By analogy, it might be expected that there is no thermal interconversion between benzoxepin **377** and arene oxide **392** and the compound will only exist in the oxepin form due to the resonance energy of the benzene moiety (Scheme 4.18).

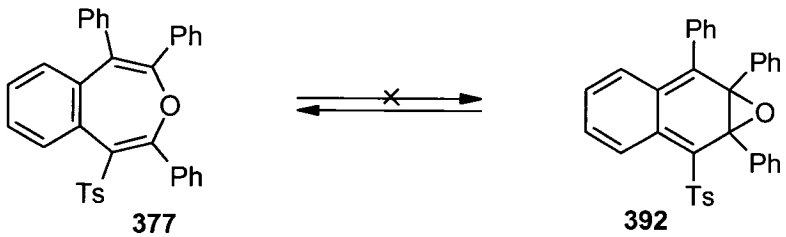

Scheme 4.18 No Valence Tautomerism of Benzoxepin **377**

Moreover, the photochemical 6π electron electrocyclic reaction required to convert **377** to arene oxide **392** in Scheme 4.16 would require a conrotatory ring-closure under

photochemical conditions that would lead to a highly strained *trans*-epoxide. Therefore, we conclude that the photochemical rearrangement of **377** to **378** does not proceed via an arene oxide pathway involving the intermediate **392**.

4.7.3 Zwitterion Mechanism

Zwitterionic intermediate **399** has been proposed in the photochemical transformation of 6,6-diphenylbicyclo[3.1.0]hex-3-en-2-one to 2,3- and 3,4-disubstituted phenols **400** and **401**, respectively (Scheme 4.19).[187] Zwitterions have also been proposed in the somewhat related photochemical rearrangements of cyclohexadienones and bicyclo[3.1.0]hex-3-en-2-ones.[188a-c] However, this mechanism has aroused debate and is not universally accepted. [188d]

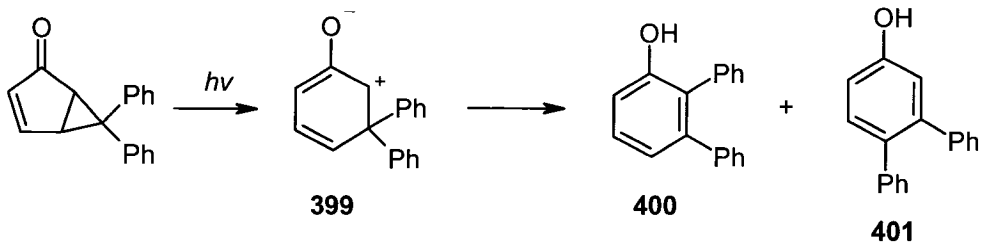

Scheme 4.19 Proposed Zwitterion **399** by Zimmerman

A similar mechanism may be envisaged to transform **377** to **378** via the zwitterionic intermediate **402** (Scheme 4.20). Since radical intermediates are not required in the transformation of **377** to **378**, this proposed mechanism cannot be ruled out at this time.

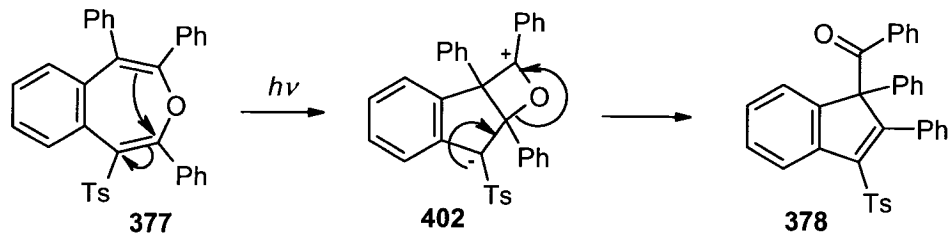

Scheme 4.20 Proposed Mechanism via Zwitterions **402**

4.7.4 Proposed Dihydrofuran-Cyclobutene Mechanism

A fourth possibility that was considered is based on earlier work by Tochtermann *et al.*,[189] who reported that the photolysis of certain 3,6-alkanooxepins **403** and **404** produced the corresponding cyclopentadienecarbaldehydes **405** and **406**, respectively, in moderate yields, via a series of fused-ring dihydrofuran-cyclobutenes **407**, and cyclopropanecarbaldehydes **408** (see Scheme 4.21). Evidence for this pathway was based on the NMR detection of the intermediates **407** and **408**. More evidence for the formation of dihydrofuran intermediates in such processes was reported by Paquette and coworkers[190] during the irradiation of the simple oxepin **381** (see Scheme 4.22). The structure of **411** was proved by the formation of 2-oxabicyclo[3.2.0]heptane **(412)** upon hydrogenation. Formally, one can imagine that the transformations in Scheme 4.21 included a photochemical 4π electron electrocyclic disrotatory ring-closure, followed by a [1,3]sigmatropic rearrangement and a 4π electron electrocyclic cycloreversion under photochemical conditions to the cyclopentadienecarbaldehyde **409**. A transannular hydrogen shift,[191] followed by radical recombination, would afford the products **405** and **406**. A similar mechanism in our case would proceed via intermediates **413** and **414**, and is shown in Scheme 4.23. The transformation takes place by means of a disrotatory 4π electron electrocyclic ring closure of **377**, which leads to the less strained *cis*-fused dihydrofuran-cyclobutene **413**. The subsequent [1,3]sigmatropic rearrangement of **413** to **414** would be expected to proceed with retention of configuration under photochemical conditions to again afford a *cis*-fused cyclopropane moiety. Finally, a photochemical disrotatory 4π electron electrocyclic cycloreversion of **414** would lead to **378**, finishing the transformation.

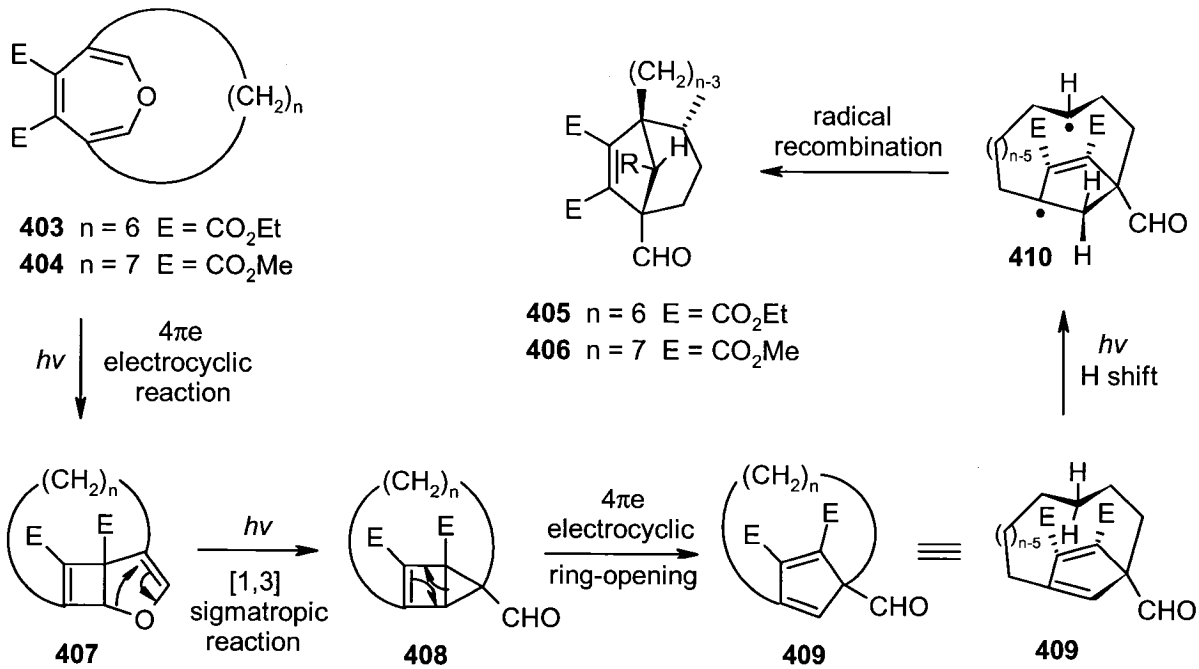

Scheme 4.21 Transformation of Bicyclic Compounds to Tricyclic Aldehydes

Scheme 4.22 Ring-Closure of Oxepin **381** under Photochemical Condition

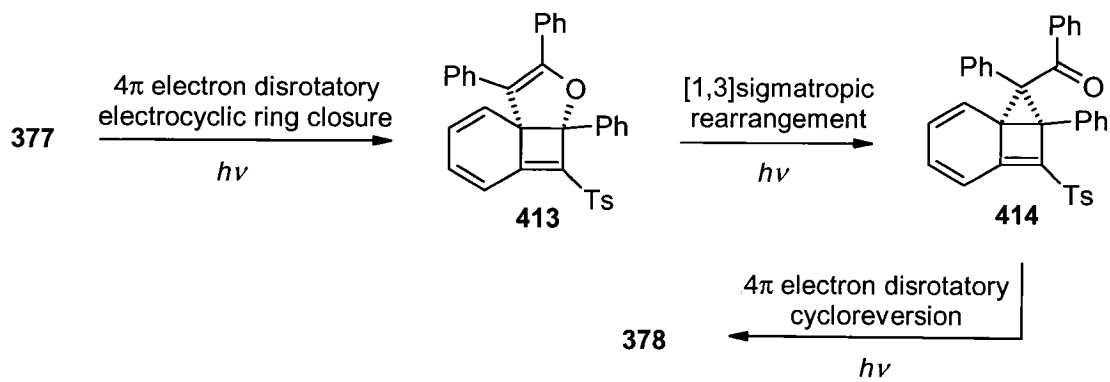

Scheme 4.23 A Plausible Mechanism for the Formation of Exocyclic Ketone **378**

It will also be recalled from section 4.7.1, that the addition of the radical inhibitor BHT did not suppress the photochemical transformation, which is consistent with the dihydrofuran-cyclobutene mechanism where radical intermediates are not required. Based on the above considerations and on precedents with analogous systems reported by Tochtermann[189] and Paquette,[190] we tentatively favour the dihydrofuran-cyclobutene mechanism shown in Scheme 4.23.

4.8 Conclusions

In conclusion, the cycloaddition of 1,3-diphenylisobenzofuran **(110)** with acetylenic sulfones **1a** and **1b** afforded the expected Diels-Alder cycloadducts **353** and **354**. The further transformations of **353** and **354** under acid-catalyzed and pyrolytic conditions resulted in the regioselective formation of rearranged ketones **355**, **357** and **358**, as well as the dehydration product **356** from the pyrolysis of **353**. The remarkable formation of transposed ketone **358** from **354** was rationalized by invoking an epoxide intermediate that provides a pathway for the transposition of the oxygen functionality. Although **353** produced the same ketone **355** under photochemical conditions as under acid-catalyzed and pyrolytic conditions, different products **377** and **378** were observed from **354** on irradiation. Thus, benzoxepin **377** was the initial product via a postulated intramolecular [2+2] cycloaddition leading to an oxaquadricyclane intermediate, followed by photoisomerization via a carbonyl ylide. The exocyclic ketone **378** was produced by further irradiation of **377**, rather than via an independent pathway from **354**. The transformation of **377** to **378** is consistent with a mechanism involving successive pericyclic reactions: an electrocyclic ring-closure, a [1,3]sigamatropic rearrangement and an electrocyclic ring-opening. These processes further illustrate the rich and diverse behaviour of **110** and its Diels-Alder cycloadducts.

Chapter 5

Enantioselective Synthesis of (-)-Julifloridine (151)

5.1 Retrosynthesis – Initial Construction of the Piperidine Ring

A retrosynthetic analysis of the target alkaloid (-)-julifloridine **(151)** suggested that it could be obtained from a hydrogenation of **415** or **416** to remove the benzyl protecting groups and reduce the isolated double bond. The olefin **415** or **416** would be produced by a Wittig reaction of the corresponding aldehyde, in turn obtained by oxidation of the 2,6-*trans*-piperidine alcohol **187** or **417**. The stereoselective reduction of the enamine double bond in key intermediate **189** would afford **187** or **417**. The stage at which the sulfone moiety would be reductively cleaved is flexible. The desired enamine sulfone **189** would be obtained by employing the sequence of conjugate addition of chloroamine **190** to acetylenic sulfone **191**, followed by base-mediated cyclization of the resultant product. Chloroamine **190** is expected to be readily available from *L*-alanine, an inexpensive chiral starting material. The required acetylenic sulfone **191** is available from a procedure developed in our laboratory by M. D. Hamilton.[137] This involved the usual selenosulfonation methodology, using propargyl alcohol as the starting material.

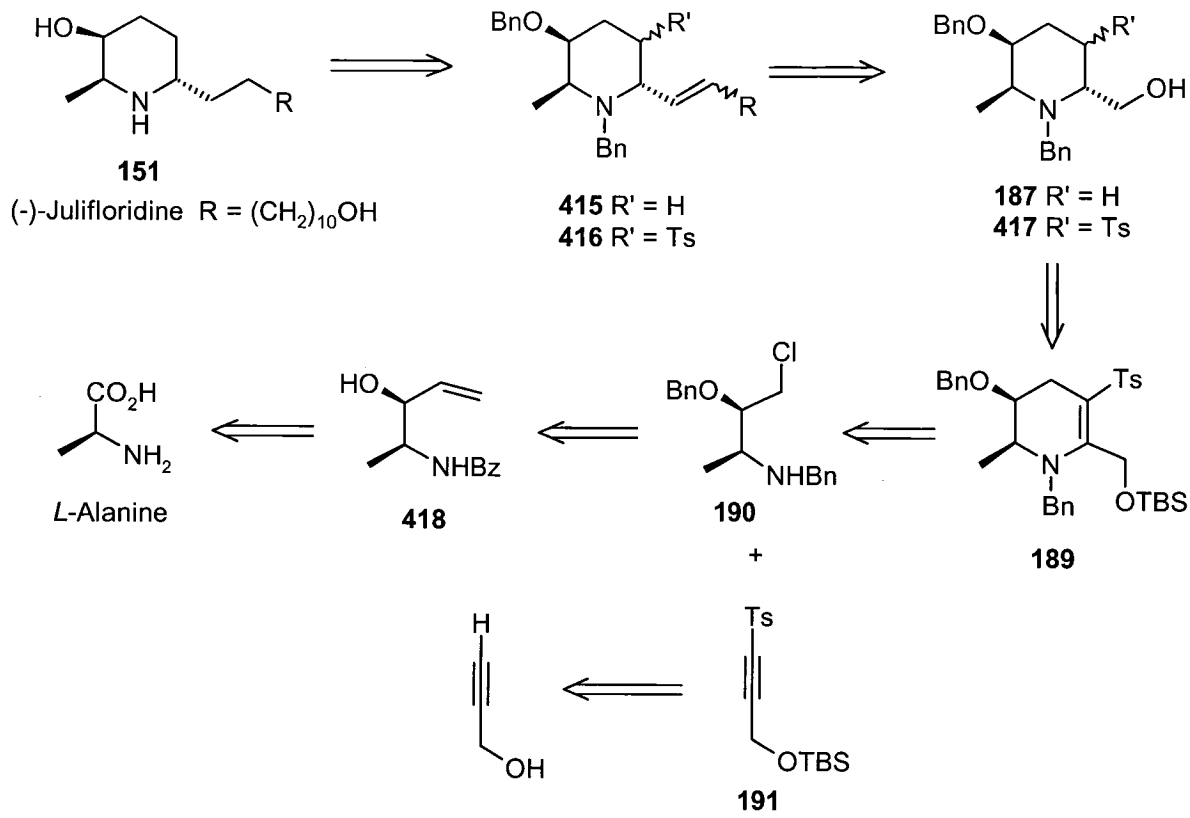

Scheme 5.1 Retrosynthetic Analysis of (-)-Julifloridine **(151)**

5.2 Route to (-)-Julifloridine (151) Starting with *L*-Alanine

The final part of the thesis will deal with the application of the conjugate addition-cyclization methodology using acetylenic sulfones that has been developed in our laboratory to the synthesis of **151**, which is the enantiomer of natural product **146**.

5.2.1 Preparation of Chloroamine 190

As shown in Scheme 5.2, chloroamine **190** was obtained in seven steps from *L*-alanine. Thus, esterification of the carboxylic acid using thionyl chloride in methanol, followed by protection of the amino functionality with a benzoyl group gave the amino ester **419**.

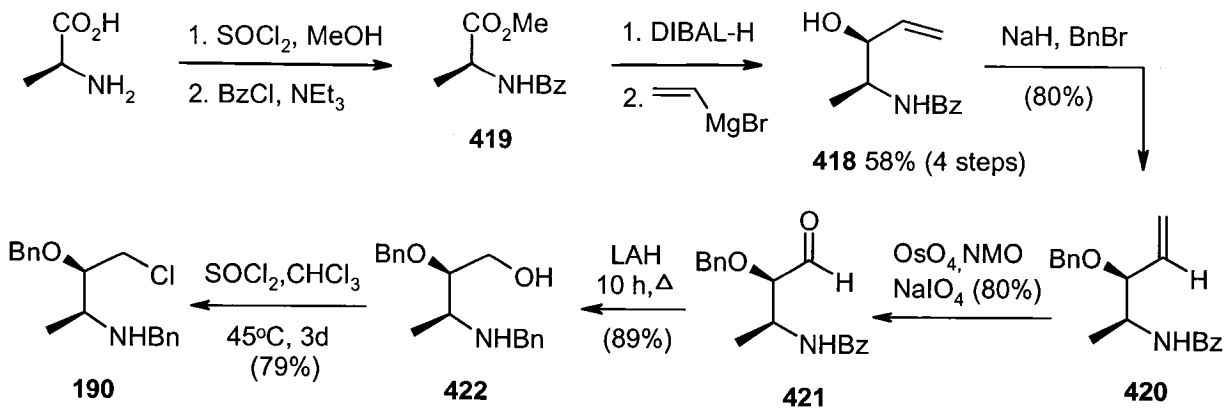

Scheme 5.2 Synthesis of Chloroamine **190**

Yamamoto and coworkers reported the transformation of *N-t*-Boc-alanine methyl ester to amino alcohols **423** and **424** in a single pot involving the sequential addition of DIBAL-H and vinylmagnesium chloride.[192] This procedure provided the resulting allyl alcohol as a 15:1 mixture of *syn/anti* diastereomers in 60% combined yield. The *syn*-diastereoselectivity of the reaction of the aldehyde with the vinylmagnesium halide is dependent on the presence of the NH group and was explained by the chelation-controlled Cram cyclic model **A** (M = MgX) [193] shown in Scheme 5.3. Thus, attack by vinylmagnesium chloride occurs from the less hindered side of the transition state **A** to give the *syn* vinyl alcohol as the major product.

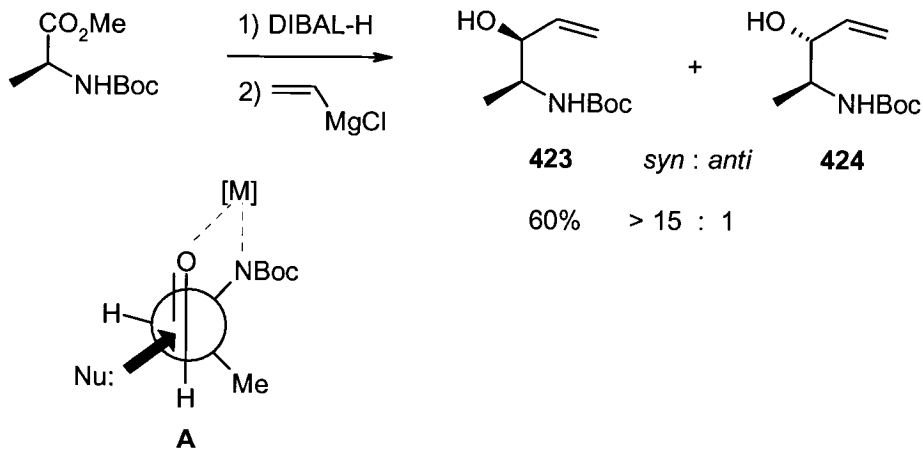

Scheme 5.3 One-Pot Preparation of the *Syn* Allyl Alcohol **423**

A slightly modified procedure of that reported by Yamamoto,[192] employing vinyl magnesium bromide instead of vinyl magnesium chloride, was used in our case. The reaction was allowed to stir at -20 °C for two days, providing a 48:1 mixture of *syn/anti* diastereomers in 66% combined yield. After recrystallization, the 2,3-*syn* allyl alcohol **418** was obtained as a single diastereomer from *L*-alanine in 58% yield in 4 steps. The *syn* relationship of the hydroxyl group and methyl group in **418** was confirmed by the synthesis of enamine sulfone **429**, whose structure was unequivocally determined by X-ray crystallography (vide infra).

The hydroxyl group was then protected as its benzyl ether and oxidative cleavage of the double bond by OsO_4 and $NaIO_4$ gave the corresponding aldehyde (Scheme 5.2). Subsequent treatment with lithium aluminum hydride reduced both the aldehyde and the benzoyl group to give *N*-benzyl amino alcohol **422**. Chlorination of **422** was accomplished using thionyl chloride in chloroform at 48 °C for three days. Temperatures higher than 55 °C resulted in decomposition of the chloroamine. The product **190** was isolated as the free base after basic work up in an overall yield of 26% from *L*-alanine. The chloroamine can be stored in the refrigerator for several months without decomposition.

5.2.2 Preparation of Acetylenic Sulfone 191

Acetylenic sulfone **191**[137] was synthesized using the procedure shown in Scheme 5.4. The vinyl selenide **425** was obtained by the general method previously reported by Back and coworkers.[3e] It was then oxidized to the selenoxide and subsequently underwent selenoxide elimination to afford the desired acetylenic sulfone **191.**

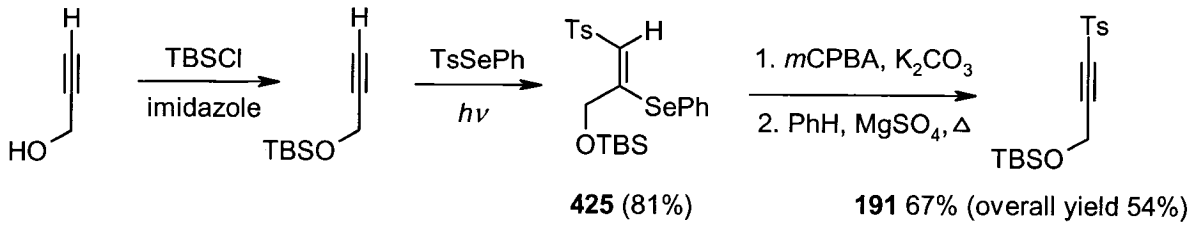

425 (81%) **191** 67% (overall yield 54%)

Scheme 5.4 Synthesis of Acetylenic Sulfone **191**

5.2.3 Preparation of Enamine Sulfone 189

The conjugate addition of chloroamine **190** to acetylenic sulfone **191** was carried out in methanol at room temperature over 20 h to afford crude vinyl sulfone **426** as a light yellow oil, which crystallized from ethyl acetate-hexanes as a fine white powder in 79% yield. Cyclization to the enamine sulfone **189** was achieved by treating a solution of vinyl sulfone **426** in THF with two equivalent of LDA at -78 °C (see Scheme 5.5). The successful cyclization was confirmed by the disappearance of the vinyl proton in the ^{1}H-NMR spectrum of **426**, along with the presence of the predicted molecular ion (*m/z* 591) for the product **189**. The results of the cyclization are summarized in Table 5.1.

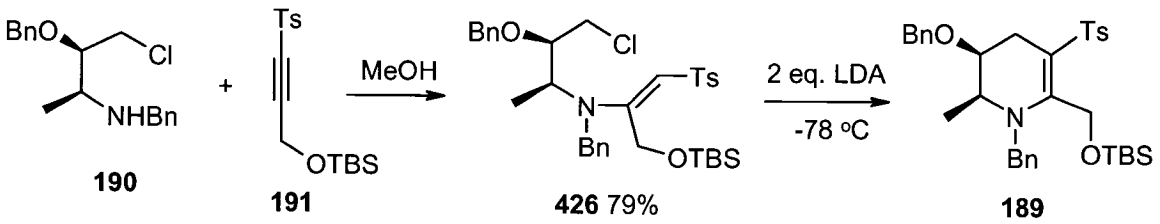

Scheme 5.5 Cyclization of Chloroamine and Acetylenic Sulfone

Table 5.1 Yields of Cyclization with Different Reaction Times

Reaction Time	Isolated Yield
4 min	91%
30 min	67%
90 min	25%

From Table 5.1, the highest yield of cyclization of enamine sulfone **426** was achieved by treating with LDA at -78 °C for 4 min, followed by immediate quenching with neutral alumina. If the reaction time was extended, the yield of cyclization product dropped dramatically, probably due to decomposition of the enamine sulfone under the strongly basic conditions.

5.2.4 Reduction of Enamine Sulfone 189

It was desirable to find conditions that would result in a stereoselective reduction of enamine sulfone **189** to afford either the corresponding 2,6-*trans* **(427)** or 2,6-*cis* **(428)** disubstituted piperidine as the major or sole product as both **427** and **428** could serve as potential precursors to respective families of alkaloids (see section **1.5.1**). In particular, piperidine **427** was required as an intermediate in the synthesis of (-)-julifloridine (see Scheme 5.6). The best selectivity obtained was with either sodium cyanoborohydride or sodium triacetoxyborohydride in the presence of trifluoroacetic acid, which gave predominantly the 2,6-*trans* isomer **427** in excellent yield, with a ca. 10:1 ratio of sulfone epimers. No reduced product was obtained by hydrogenation using palladium on charcoal at 1 atm.

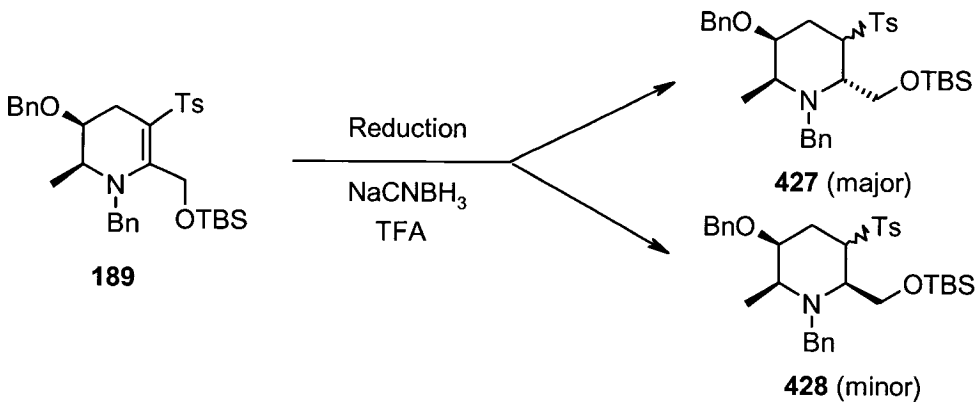

Scheme 5.6 Reduction of Enamine Sulfone **189**

5.2.5 Reduction of Deprotected Enamine Sulfone 429

In order to determine whether the reduction of the free alcohol would proceed with better stereoselectivity, the TBS group of compound **189** was removed using tetrabutylammonium fluoride (TBAF). Column chromatography of the reaction mixture led to the isolation of **429** as a pure stereoisomer (see Scheme 5.7). A crystal structure was obtained for **429** and was shown to contain the expected 5,6-*cis* configuration. Furthermore, if one assumes that retention of configuration at C-6 from the original *L*-

alanine precursor occurred, then the absolute configuration of the stereocenters of **429** must be 5*S*, 6*S*. Details of the crystal structure of enamine sulfone **429** are given in Appendix XI and the ORTEP diagram is shown in Fig. 5.1. Compound **429** was then reduced under the same conditions as compound **189** (see Scheme 5.7).

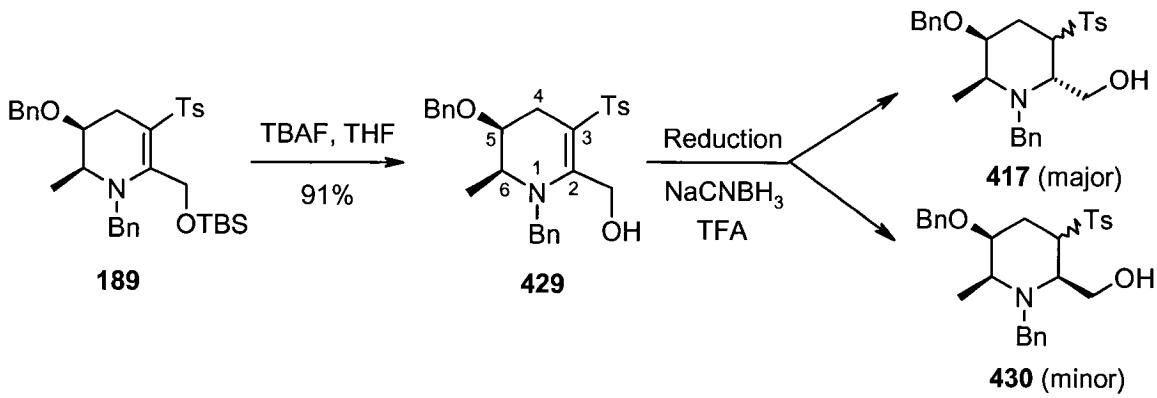

Scheme 5.7 Reduction of Deprotected Enamine Sulfone **429**

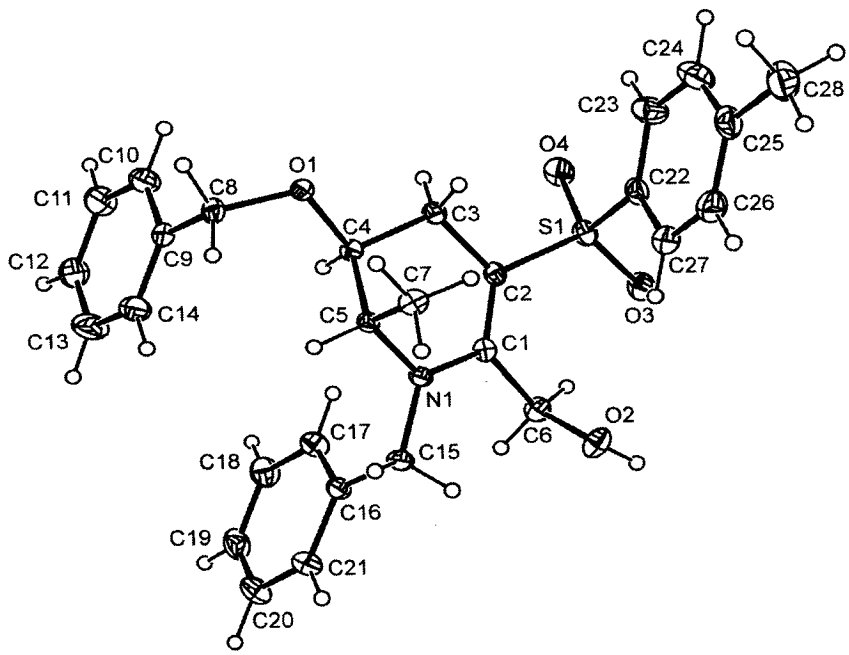

Fig 5.1 ORTEP Diagram of Enamine Sulfone **429**

The stereoselectivity obtained using sodium triacetoxyborohydride in the presence of trifluoroacetic acid favoured the 2,6-*trans* isomers **431** and **432**, obtained in 82% yield, with a *trans*:*cis* ratio of 19:1. An even higher stereoselectivity of 43:1 in favour of the 2,6-*trans* isomers (formed as a mixture of sulfone epimers **431** and **432**) was obtained using sodium cyanoborohydride in the presence of trifluoroacetic acid. The major product **432** was isolated as a single diastereoisomer in 84% yield, while the minor products **430** and **431** were isolated as a 1:1 mixture in 4% yield (see Scheme 5.8). The structure of the major product **432** was confirmed by NMR spectroscopy. All ^{1}H and ^{13}C NMR signals of product **432** were assigned by COSY, DEPT and HMQC spectra. The *trans* orientation of the methyl and CH_2OH substituents was confirmed by the eventual transformation of **432** to (-)-julifloridine **(151)** (vide infra). The *cis* orientation of the Ts and BnO substituents in **432** was confirmed by an NOE experiment. Irradiation of the C**Ha**Hb signal at δ 2.02 ppm enhanced the BnOC**H** signal at δ 3.58 ppm by 6%, and also enhanced the C**H**Ts signal at δ 3.80 ppm by 3%, while irradiation of the BnOC**H** signal enhanced that of the C**Ha**Hb group by 4%. Since Ha and Hb produced distict signals, and since one of these protons (Ha) produced enhancements of both the BnO**CH** and C**H**Ts signals, it can be concluded that the *p*-toluenesulfonyl group and the benzyl ether group are *cis* oriented in **432**.

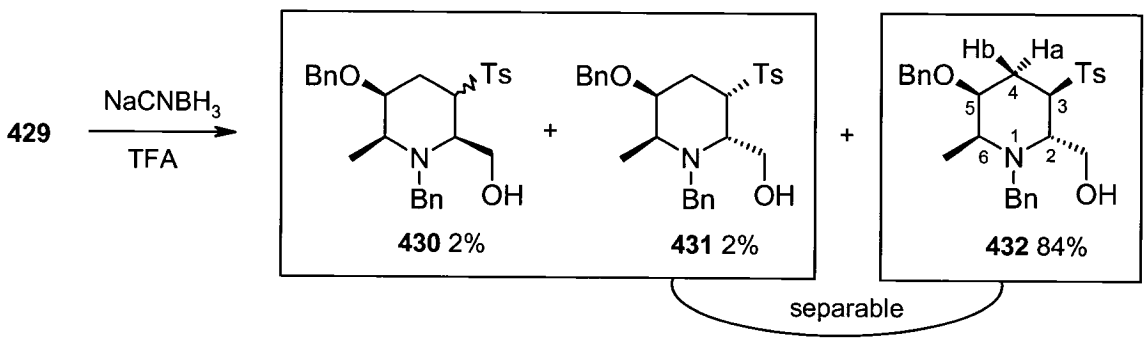

Scheme 5.8 Reduction of **429** Using $NaCNBH_3$

In addition, the 2,6-*cis*/*trans* ratio of the minor products **430** and **431** were determined by reductive desulfonylation to an inseparable 1:1 mixture of **187** and **188**, as will be discussed further in section **5.2.7**.

5.2.6 Rationale for Observed Stereochemistry

The selectivity observed for the hydride reduction of enamine sulfones **189** and **429** can be partially explained by stereoelectronic effects. Stevens[194] proposed that four transition states leading to products **434** are possible for the addition of nucleophiles (hydride in the present case) to iminium ions **433** derived from piperidine derivatives under acidic conditions.

Stevens proposed that of the four possible transition states, two comprised kinetically disfavoured boat-like conformations leading to **434b** and **434c**. Of the two remaining transition states, the one leading to **434a** suffers from an unfavourable 1,3-diaxial interaction between the ring substituent R and the incoming nucleophile. This leaves the favoured transition state that produces **434d**, which results in the *cis* relationship of the two ring substituents R and R'.

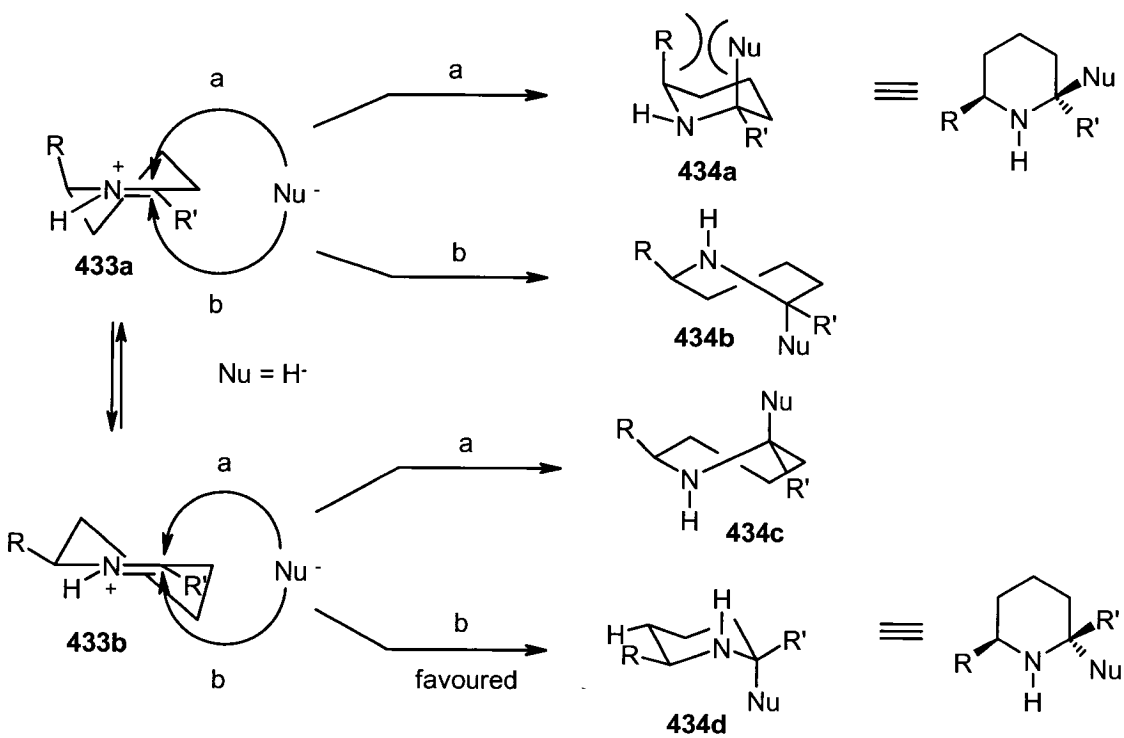

Scheme 5.9 Stevens' Stereoelectronic Analysis of the Addition of Nucleophiles to Iminium Ions **433**

Some previous studies of the reduction of iminium species similar to **433** by Toyooka and coworkers[195] showed that $A^{(1,2)}$ strain[196] also played an important role in the stereochemical outcome of the products. For example, conformer **435a** is favoured relative to **435b** because of $A^{(1,2)}$ strain between the *N*-benzyl and the methyl group in **435b**, so the hydride reacts from the preferred β-axial direction, leading to a chair-like transition state to give 2,6-*trans*-piperidine **436** (see Scheme 5.10).

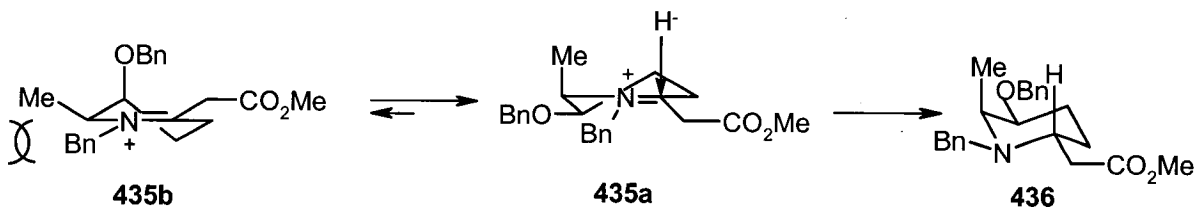

Scheme 5.10 Stereoselectivity of Reduction to **436**

Scheme 5.11 analyzes the reduction of iminium ion **437** using Stevens' and Toyooka's stereoelectronic arguments. The pathways that require a boat-like transition state, leading to **438b**, **438c**, **438e**, and **438h**, are disfavoured in our system as well. However, due to the presence of the *N*-benzyl group, the system also suffers from $A^{(1,2)}$ strain between the benzyl group and the methyl group in transition states **437b** and **437c**. It can be seen that the benzyl ether group stands in the axial position in both conformations **437b** and **437c**. However, epimerization between **437b** and **437c** via the corresponding enamine **189** also permits the sulfone group to reside in the equatorial position in **437b**, where it avoids the strong 1,3-diaxial interaction with the benzyl ether group in **437b**, but where it suffers $A^{(1,2)}$ strain between the sulfone group and the hydroxymethyl or silyloxymethyl group. In diastereomer **437c**, the axial sulfone group avoids $A^{(1,2)}$ strain with the hydroxymethyl or silyloxymethyl group, but suffers a 1,3-diaxial interaction with the benzyl ether group. Both **437b** and **437c** are unstable relative to their ring-flipped conformations **437a** and **437d**, respectively. In **437a**, the benzyl ether is in the equatorial position and the methyl group is shown in the axial position, thereby avoiding $A^{(1,2)}$ strain with the *N*-benzyl group. There is no 1,3-diaxial interaction between the equatorial benzyl ether substituent and the sulfone group, and the sulfone group is in

the axial position, thus avoiding $A^{(1,2)}$ strain between the sulfone group and the hydroxymethyl or silyloxymethyl groups. However, in **437d**, the benzyl ether is in the equatorial position and the methyl group is shown in the axial position, thus avoiding $A^{(1,2)}$ strain with the *N*-benzyl group. There is no 1,3-diaxial interaction between the equatorial benzyl ether substituent and the sulfone group, and the sulfone group is in the equatorial position, although there is $A^{(1,2)}$ strain between the sulfone group and the hydroxymethyl or silyloxymethyl groups.

Based on these analyses, only the pathways that require a chair-like transition state and proceed through conformations **437a** or **437d** look reasonable. It is hard to assess whether the axial sulfone group, which avoids $A^{(1,2)}$ strain in **437a** or the equatorial sulfone group that creates $A^{(1,2)}$ strain in **437d** is preferred. However, the major product observed was **438g**. In summary, the hydride approaches from the preferred β-axial side of the preferred conformation **437d**, leading to a chair-like transition state to give 2,6-*trans*-piperidine **438g**. Stevens' stereoelectronic explanation is consistent with our high stereoselectivity (2,6-*trans*:*cis* = 43:1).

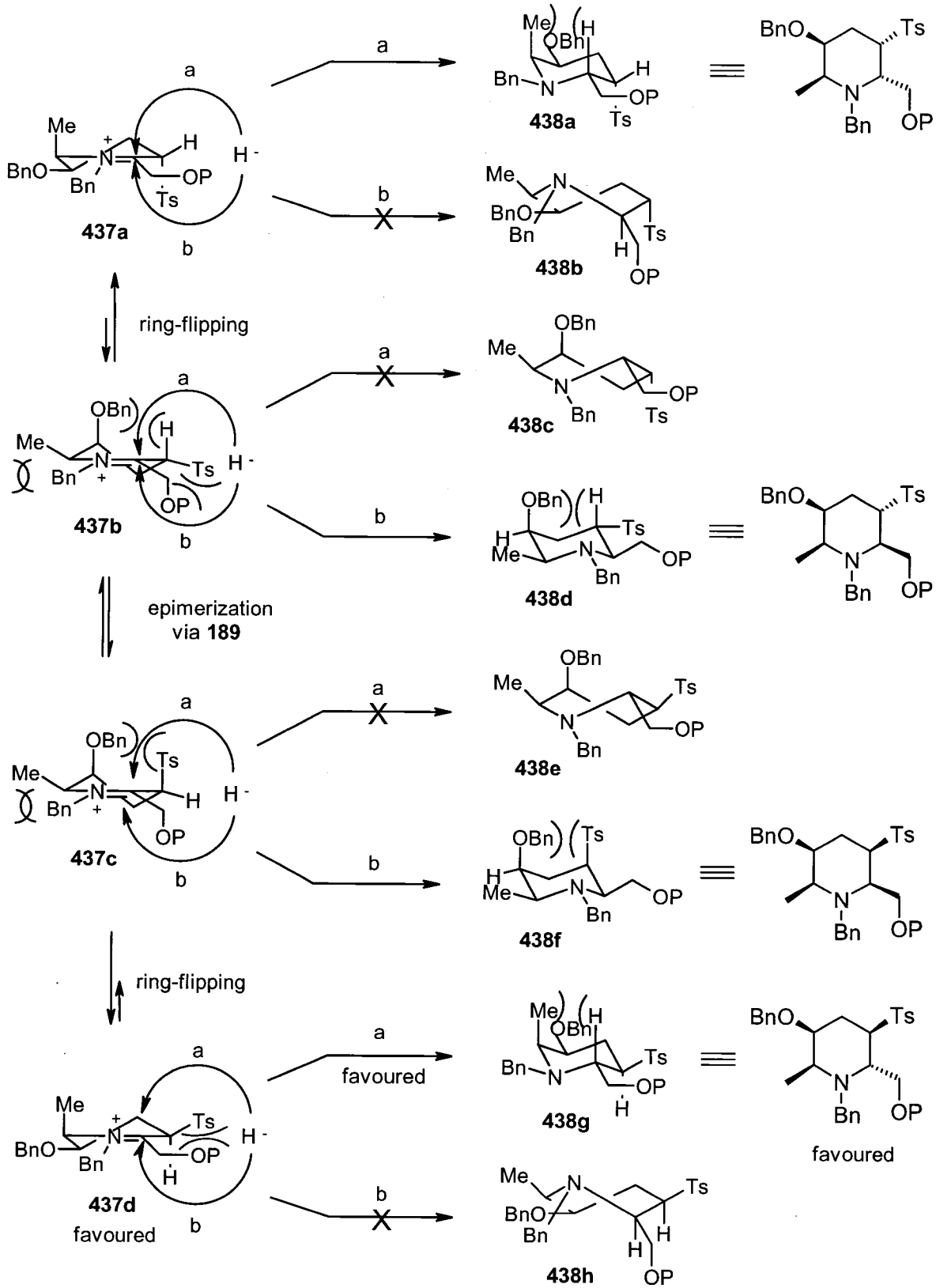

Scheme 5.11 Stereoselectivity of Reduction of **437** (P = H or TBS)

5.2.7 Desulfonylation of 430-432

The major reduced product **432** was treated with sodium amalgam in refluxing THF, as shown in Scheme 5.12, and the resulting reductive desulfonylation took place cleanly to afford the 2,6-*trans*-piperdidine **187** in 84% yield, with the two benzyl groups remaining intact. In addition, desulfonylation of the minor products **430** and **431** from the reduction of **429** afforded an inseparable mixture of 2,6 *cis* and *trans* products **187** and **188** in a 1:1 ratio. The formation of the same product **187** from desulfonylation of the mixture of **430** and **431** as was obtained from the major isomer **432** confirms that one of the products in the mixture (i.e. **431**) possesses the 2,6-*trans* configuration.

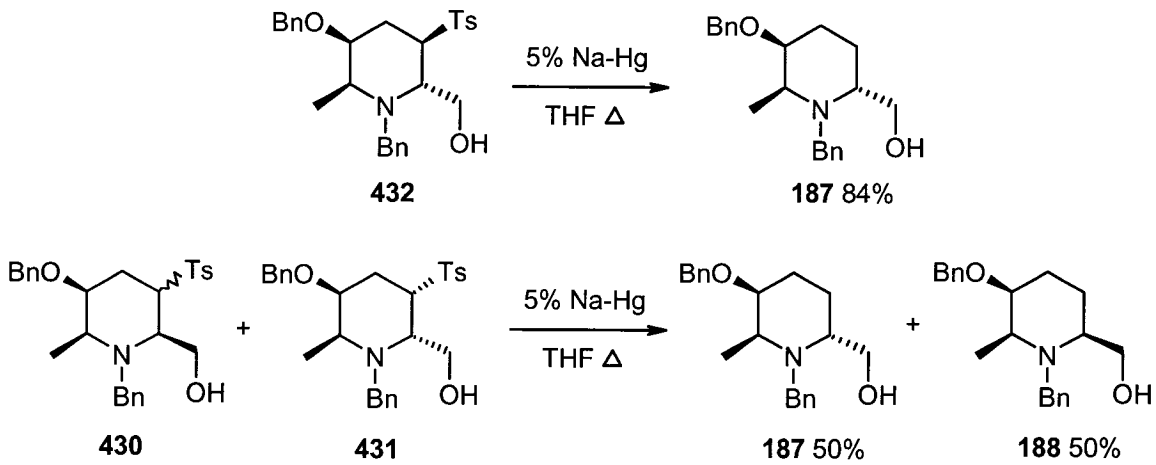

Scheme 5.12 Desulfonylation of **430-432**

5.2.8 Acid-Catalyzed Desulfonylation of 429

An even more convenient route to 2,6-*trans*-piperidine **187** was discovered serendipitously during the routine running of a ^{1}H NMR spectrum of the desilylated product **429** in $CDCl_3$. Within 5 minutes, peaks indicative of a new methyl group, as well as a new vinyl proton and an aldehyde proton began to appear. These new peaks continued to increase with time and after 10 hours, the reaction appeared to be complete (see Fig 5.2). After purification, the structure of the new product was confirmed to be the desulfonylated aldehyde **439** (Scheme 5.13).

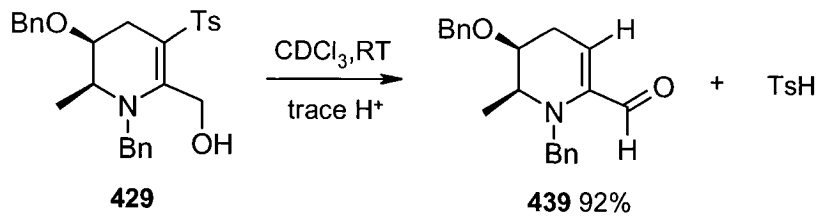

Scheme 5.13 Acid-Catalyzed Desulfonylation of **429**

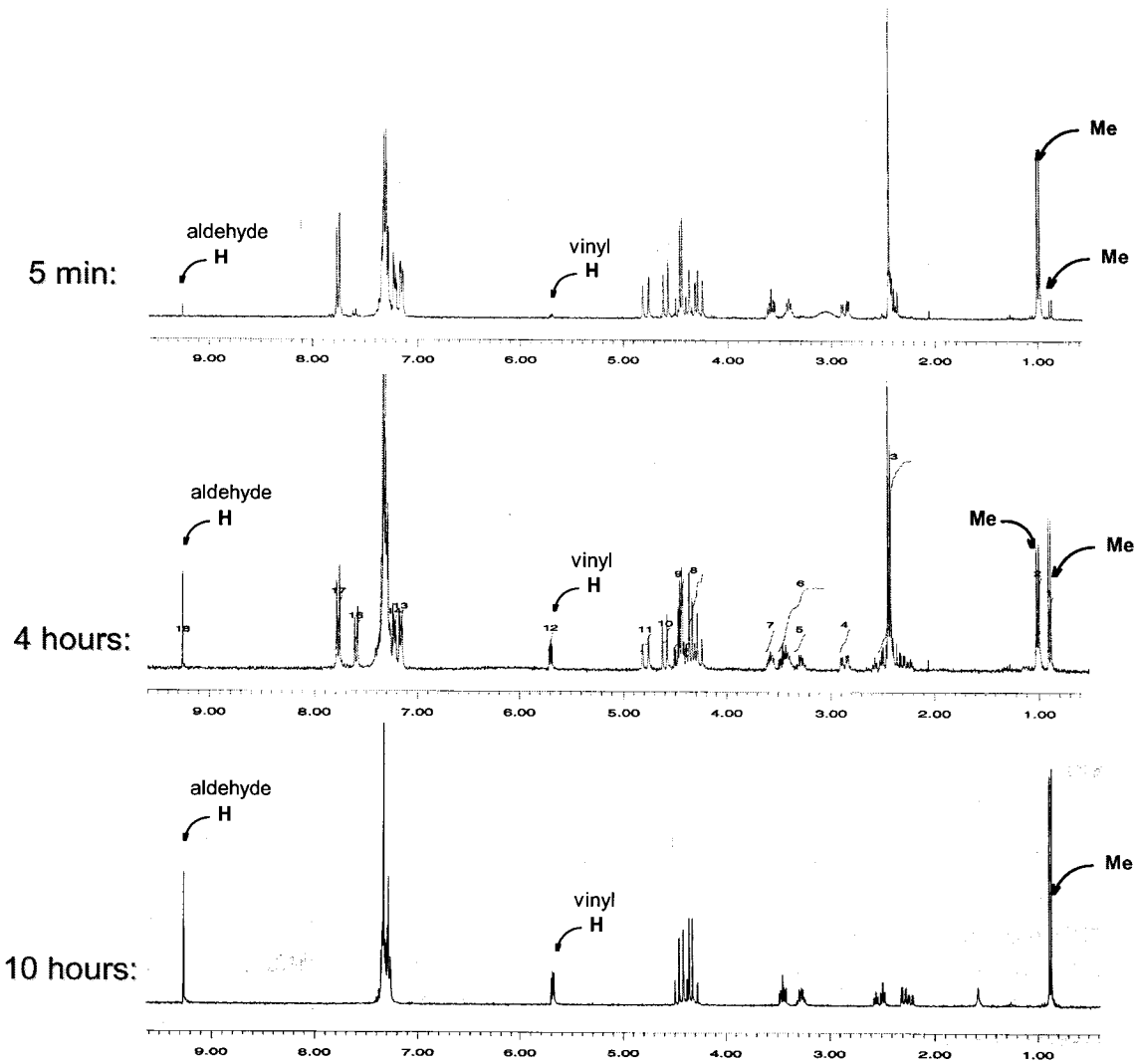

Fig. 5.2 ^{1}H-NMR Spectra of Enamine Sulfone **429** in $CDCl_3$ over 10 h

As deuterated chloroform may contain trace amounts of hydrochloric acid, it is likely that an acid-catalyzed reaction occurred, as shown in Scheme 5.14. We propose that

in the presence of catalytic amounts of acid, the enamine sulfone isomerized to enol **441** via the iminium salt **440**. The enol **441** can then tautomerize to the corresponding aldehyde **442**, from which elimination of *p*-toluenesulfinic acid occurs readily at room temperature to generate the α,β unsaturated aldehyde **439**.

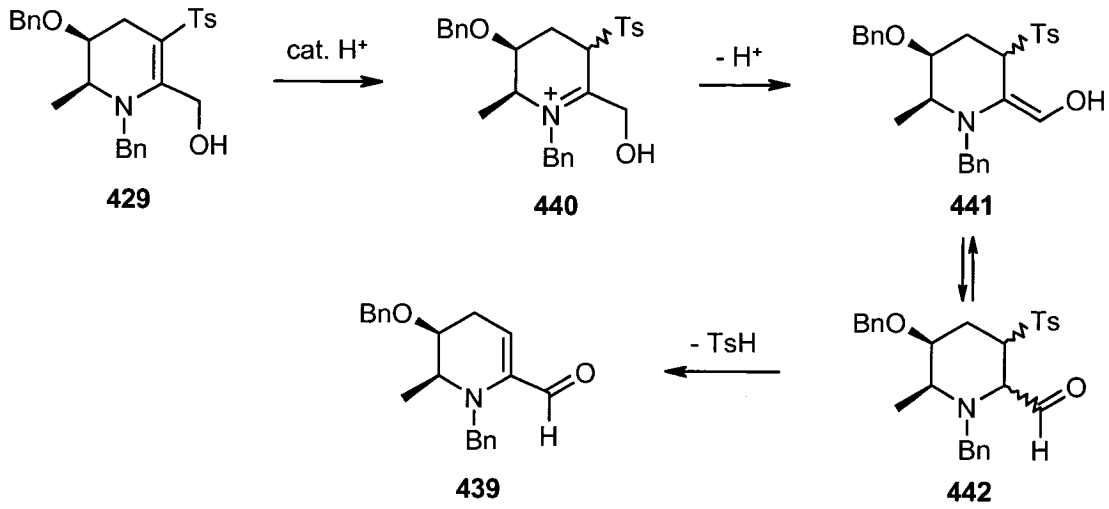

Scheme 5.14 Proposed Mechanism for the Acid-Catalyzed Desulfonylation of **429**

5.2.9 Elimination and Reduction of Enamine 189

It is also well known that the TBS group can be removed under strongly acidic conditions, such as in trifuoroacetic acid, or concentrated hydrochloric acid. Thus, a concise one-pot synthesis of aldehyde **439** from **189** (see Scheme 5.15) became possible. The crude cyclized product **189** was treated with a mixture of chloroform and methanol containing concentrated hydrochloric acid or trifuoroacetic acid for one day to afford enamine aldehyde **439** in 82% yield after purification. The results of several methods for the reduction of **439** to the saturated alcohol **187** are shown in Table 5.2. The most stereoselective procedure, favouring the 2,6-*trans* isomer, was obtained with sodium cyanoborohydride in the presence of concentrated hydrochloric acid.

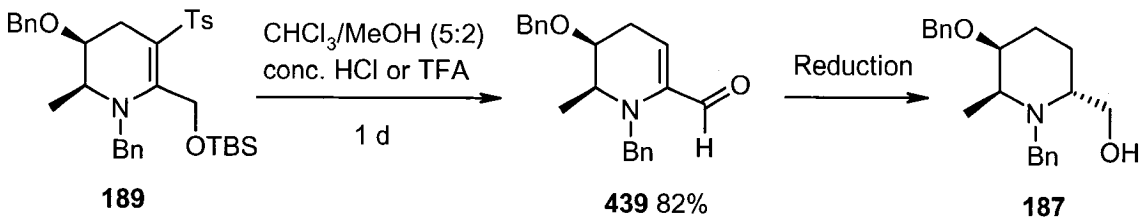

Scheme 5.15 A Convenient Procedure for Preparation of 2,6-*trans*-Piperidine **187**

Table 5.2 Reduction of Enamine Sulfone **439**[a]

Reduction Method	Isolated Yield	Ratio (2,6-*trans*:*cis*)
$NaBH_3CN$/TFA, rt	65%	4:1
$NaBH_3CN$/HCl, rt	75%	4:1
$NaBH_3CN$/HCl, -10 °C	75%	>99:1

(*a*) The ratio of 2,6-*trans*:*cis* was measured by ^1H NMR.

5.2.10 Rationale for the Observed Stereochemistry

Scheme 5.15 illustrates the reduction of aldehyde **439**, again invoking Stevens' stereoelectronic argument. Although the structure of iminium ion **443**, generated from **439** under acidic conditions, is similar to Stevens' iminium ion **433**, the reduction led to a different seterochemical outcome. As previously discussed, $A^{(1,2)}$ strain can also play an important role in directing the stereoselectivity. Thus, **443b** should be the favoured conformation because it avoids the axial benzyl ether moiety and $A^{(1,2)}$ strain between the *N*-benzyl group and the methyl group (see Scheme 5.16). The hydride reacts from the preferred β-axial side (path a towards **443b**), leading to a chairlike transition state to give 2,6-*trans*-piperidine **444c** at -10 °C as a single diastereoisomer in 75% yield. However, when the reaction was carried out at room temperature, a mixture of *trans* and *cis* products (ca. 4:1) was obtained, suggesting that the reduction of the enamine was under kinetic control at low temperature, but that at least some equilibration between **443a** and **443b** was occurring at room temperature.

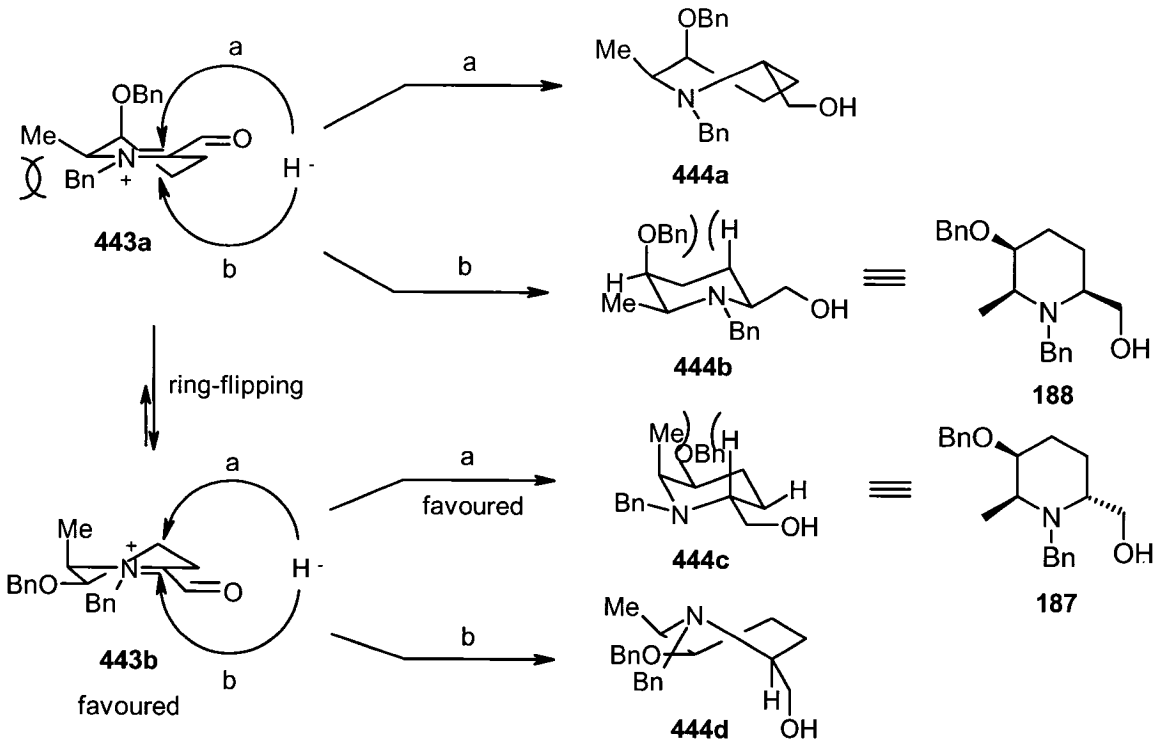

Scheme 5.16 Stereoselectivity of Reduction of **443**

5.2.11 Synthesis of (-)-Julifloridine (151)

A Swern oxidation[197] was performed on **187** to give the corresponding aldehyde **445**, which was confirmed by the appearance of a ^{1}H NMR doublet at δ 10.0 ppm (Scheme 5.17). Chain extension of the aldehyde by Wittig reaction using Wittig reagent **446**[198] gave olefin **415** as a 9:1 mixture of *cis/trans* geometrical isomers in 69% overall yield (based on **187**).

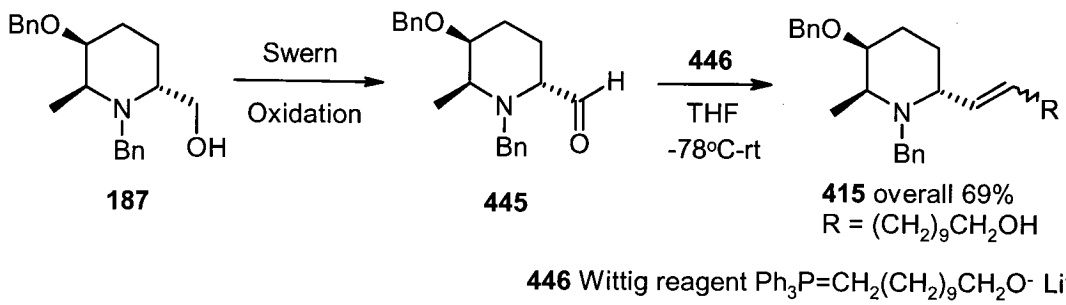

Scheme 5.17 Swern Oxidation and Chain Extension of **187**

Finally, hydrogenation of **415** over palladium hydroxide in ethyl acetate successfully reduced the isolated double bond, and cleavage of the benzyl protecting groups was achieved under Birch conditions to provide (-)-julifloridine in 62% overall yield (Scheme 5.18). The ^{1}H and ^{13}C NMR spectra (Figures 5.3 and 5.4), as well as the melting point of **151** (81-83.5 °C), were identical with those reported in the literature[135]. The ^{13} C NMR spectrum for compound (-)-julifloridine **(151)** suffers from extensive quadrupolar boadending of signals. Thus, the signals corresponding to C-2, C-5 and C-6 are very small and broad. The signal corresponding to C-7 is missing entirely. However, the DEPT135 spectrum (Fig. 5.5) showed all the carbons which were missing in the broad-band ^{13}C NMR spectrum. A comparison of the specific rotation of **151** $\{[\alpha]_D^{22} = -8.2$ (*c* 0.47, MeOH)} to that of (+)-julifloridine $\{[\alpha]_D^{20} = +7.3$ (*c* 0.23, MeOH),[135] $[\alpha]^{25}_D = +18$ (*c* 0.84, MeOH)[132]} provided further evidence that we had formed the unnatural enantiomer of julifloridine. Due to the difference in the optical rotation measured by Naito *et al.*[132] and Charette and Lemire[135], Charette and Lemire synthesized the Mosher ester derivative of (+)-julifloridine at the secondary alcohol position and found their synthetic (+)-julifloridine was 98.6% e.e. pure.[135] Our measured specific rotation is much closer to the value that was obtained by Charette and Lemire, thus confirming the high optical purity of our sample.

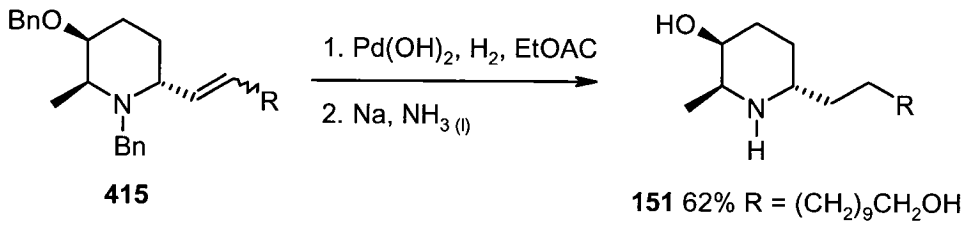

415

151 62% R = $(CH_2)_9CH_2OH$

Scheme 5.18 Hydrogenation and Birch Reduction to **151**

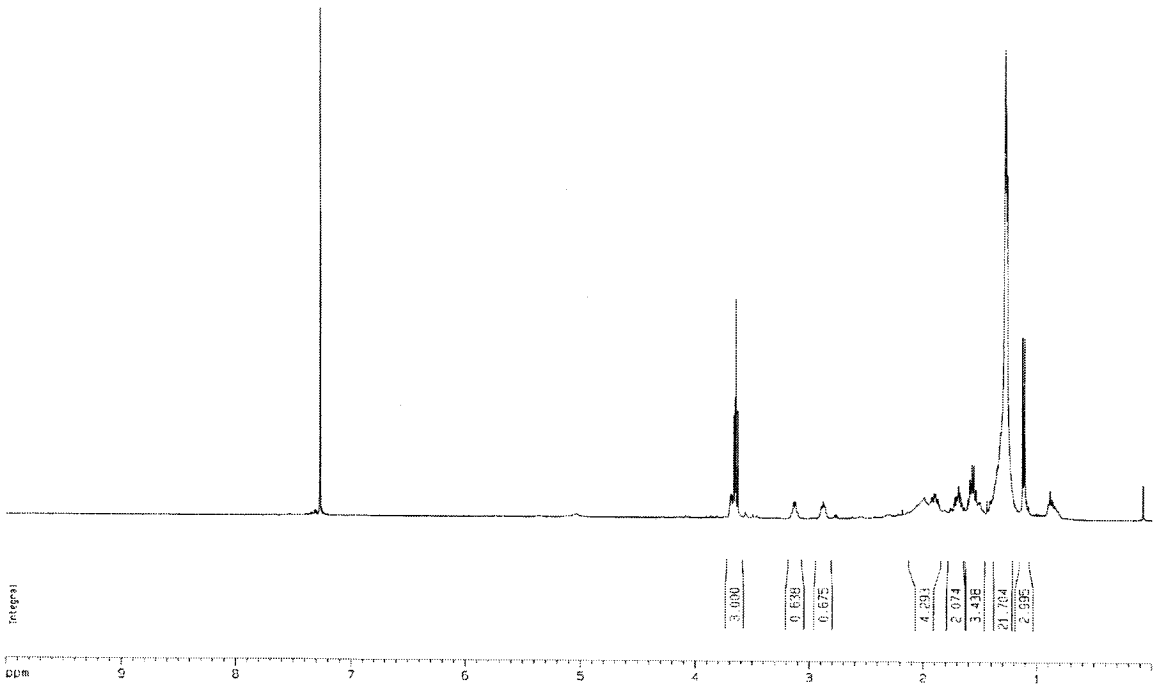

Fig. 5.3 ^{1}H NMR Spectrum of (-)-Julifloridine

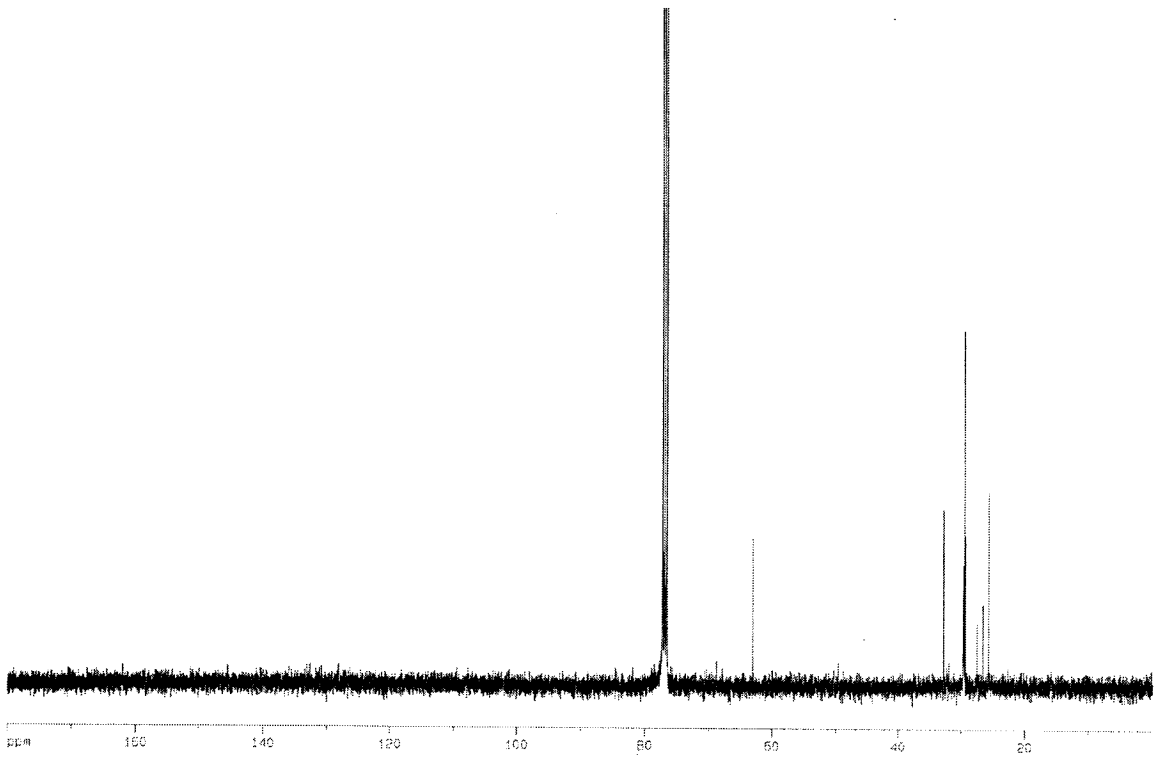

Fig. 5.4 ^{13}C NMR Spectrum of (-)-Julifloridine

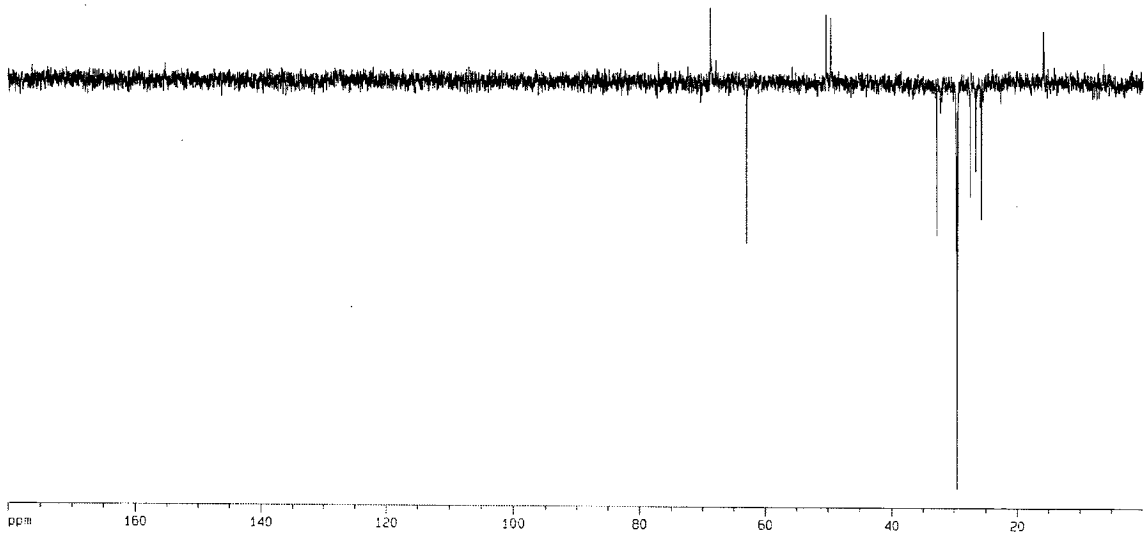

Fig. 5.5 DEPT135 NMR Spectrum of (-)-Julifloridine

A variety of solvents was explored for the hydrogenation, including methanol, ethanol, and methanolic hydrochloric acid. Unfortunately, these experiments did not result in the isolation of any of the desired product and produced complex mixtures of unidentifiable products. When the hydrogenation was carried out at 1 atm of hydrogen in ethyl acetate for 26 h with palladium hydroxide as the catalyst, the hydrogenated product and unreacted starting material were isolated in a ca. 3.5:1 ratio in a 52% combined yield. This reaction was still plagued by decomposition. A cleaner product was obtained when the reaction time was decreased and the pressure of hydrogen and temperature were increased. Thus, under 400 psi of hydrogen for 10 h at 45 °C catalyzed by palladium hydroxide, the desired hydrogenated product was isolated together with partially debenzylated products (ca. 6:1) in almost quantative yield. This mixture was subjected to the Birch reduction to give the final alkaloid (-)-julifloridine in 62% overall yield from alkene **415**.

5.3 Conclusions

The synthesis of (-)-julifloridine **(151)** is summarized in Scheme 5.19. As illustrated therein, our synthesis successfully afforded (-)-julifloridine **(151)** in seven steps in an overall 20% yield from chloroamine **190** and acetylenic sulfone **191** via **432**. Key steps included a conjugate addition, followed by sulfone-mediated intramolecular cyclization step, the reductive desulfonylation of **432**, and a Swern oxidation followed by a Wittig reaction to extend the side chain. In terms of numbers of steps, our synthesis lies between Naito's[132] and Charette's[135] (see Scheme 5.20). Although our synthesis is not as concise as Charette's, our methodology has the potential to access either 2,6-*cis* or *trans* disubstituted piperidinols. In addition, this is the first synthesis of the unnatural (-)-isomer. Finally, it shoud be pointed out that our route afforded (-)-**151** because the chloroamine **190** was prepared from *L*-alanine. However, the natural (+)-enantiomer **146** should be equally available via the same route, starting with *D*-alanine.

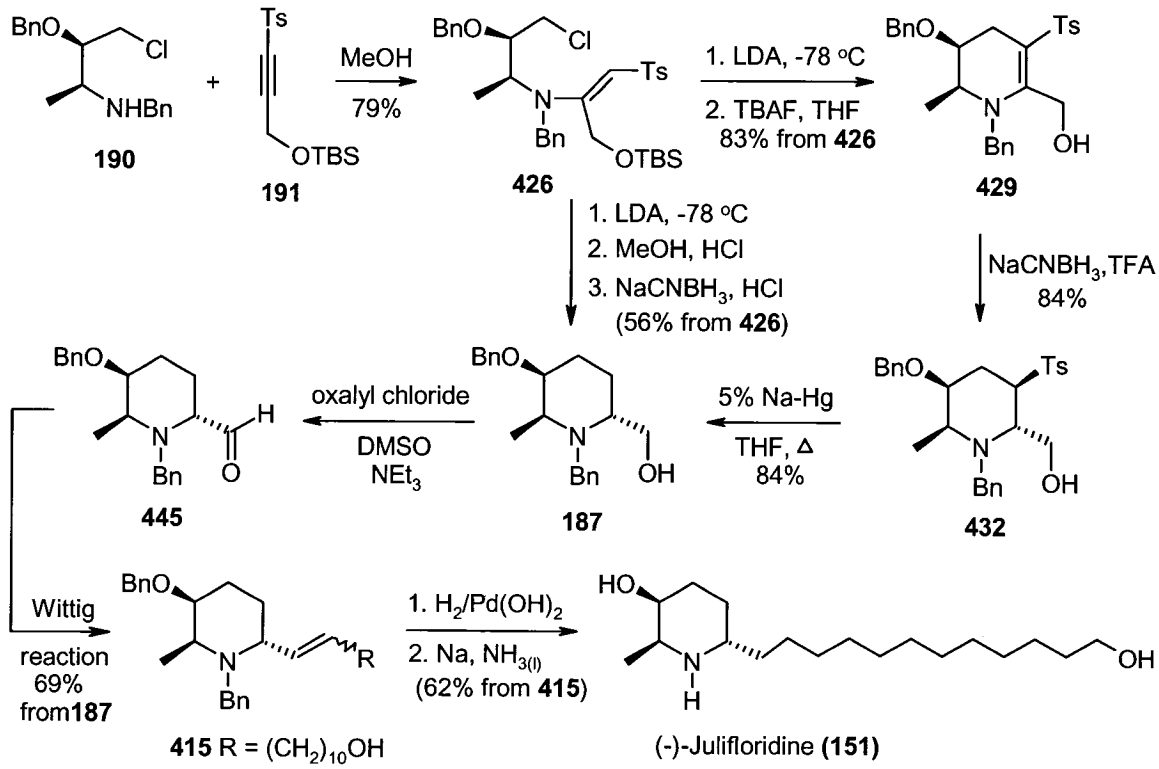

Scheme 5.19 Enatioselective Synthesis of (-)-Julifloridine **(151)**

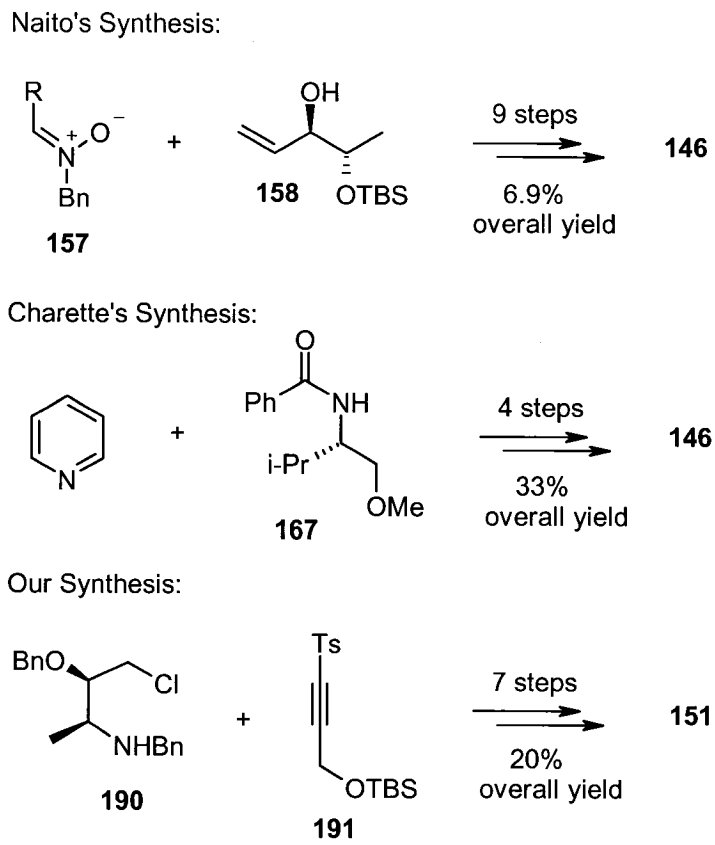

Scheme 5.20 A Comparison of the Three Enantioselective Syntheses of Julifloridine

Chapter 6

Overall Conclusions and Future Work

The investigation of novel aspects of the chemistry of acetylenic sulfones is the basis of this thesis. The cyclization methodology based on these useful compounds and developed in our group has shown a wide range of applicability in the synthesis of nitrogen heterocycles. An extension of this methodology to vinyl sulfones was attempted with the objective of obtaining saturated sulfone products directly without the need for reducing the double bond in the cyclization products of acetylenic sulfones. Two types of rearrangements were discovered and their mechanisms were elucidated. The use of vinyl sulfones and α-substituted amino alcohols **196-198** provided a convenient route to β-substituted pyrrolidines via a stereospecific rearrangement. This is noteworthy because α-substituted pyrrolidines are relatively easy to prepare, whereas β-substituted analogues are less readily accessible.

We also developed the first method for making the polymer-supported acetylenic sulfones, using an ester as a linker. We have demonstrated that we can perform a variety of reactions, such as conjugate additions followed by sulfone-mediated intramolecular cyclizations, Diels-Alder reactions and 1,3-dipolar cycloadditions, on the polymer support. Eventually, it should be possible to use polymer-supported acetylenic sulfones to generate libraries of products based on these and related reactions.

As previously discussed in section **3.1.5** the use of an ester linker can create complications when using basic conditions for required transformations. A further extension of this work could investigate the use of other types of linkers. For example, it might be advantageous to use a benzyl sulfide as the linker, which is stable to base and can be easily cleaved by nickel boride[199] (see Scheme 6.1).

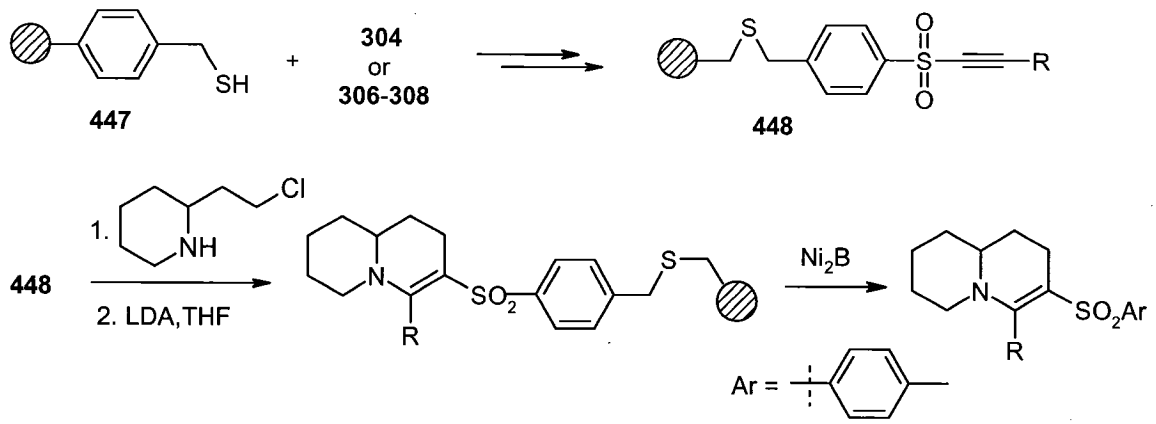

Scheme 6.1 Using Benzyl Sulfide as a Linker

The Diels-Alder adducts **353** and **354**, obtained from DPIBF and acetylenic sulfones underwent various types of rearrangements under pyrolytic, acid-catalyzed and photochemical conditions to provide a series of unexpected ketones and an oxepin. These processes further illustrate the rich and diverse behaviour of DPIBF **(110)** and its Diels-Alder cycloadducts **353** and **354**.

Finally, the synthesis of (-)-julifloridine **(151)** was accomplished using a variation of our acetylenic sulfone-based cyclization methodology. The product was made in seven steps in an overall 20% yield with high stereoselectivity from chloroamine **190** and acetylenic sulfone **191**. This method comprised the first synthesis of the unnatural enantiomer of julifloridine and it should be equally applicable to the natural enantiomer. Alternative reduction methods for the enamine aldehyde **439** should be studied in order to extend the method to 2,6-*cis* disubstituted 3-piperidinol **188**, which would serve as a key intermediate for the synthesis of 2,6-*cis* disubstituted piperidine alkaloids such as those illustrated in Figure 1.17. Previously in our group, M. D. Hamilton demonstrated that the reduction of silyl ether **176** and the free alcohol **177** (see Scheme 1.57) using 9-BBN(CN) in the presence of trifluoroacetic acid afforded mostly the corresponding 2,6-*cis* isomers. Thus, it is possible that further investigation of other reducing agents such as 9-BBN(CN) could lead to complementary protocols to the one described in Chapter 5, permitting new synthetic approaches to both 2,6-*cis* and 2,6-*trans* disubstituted products.

Chapter 7

Experimental Section

7.1 General Comments

All reagents, unless otherwise noted, were obtained from commercial sources and were used without further purification. Anhydrous THF was obtained by distillation from lithium aluminum hydride. n-Butyllithium was titrated using *N*-benzylbenzamide as both titrant and indicator. Unsaturated sulfones **27**,[20] **258**,[151] as well as *Se*-phenyl *p*-tolueneselenosulfonate **(5)**,[4] *Se*-phenyl *p*-nitrobenzeneselenosulfonate **(294)**,[4] sulfonyl iodide **290**,[160] *N*-oxide **336**[170] and chloroamine **276**,[155] were prepared by literature procedures. Amino alcohols **196-198**[139] were likewise prepared by known methods. Chromatography refers to flash chromatography on silica-gel (230-400 mesh). Proton and ^{13}C NMR were recorded on a Bruker ACE 200, a Bruker AC 300 or a Bruker DRX 400 spectrometer, using deuteriochloroform as the solvent, and chloroform as the internal standard (δ 7.27 and 77.0 for ^{1}H and ^{13}C NMR spectra, respectively), unless otherwise stated. Assignments of primary, secondary, tertiary, and quaternary carbons, where indicated, were based on DEPT-135 and DEPT-90 analysis. Melting points were measured using an A. H. Thomas hot-stage apparatus and are uncorrected. IR spectra were recorded on a Nicolet 5DX instrument. Low and high resolution mass spectra were obtained on a VG 7070 or a Kratos MS80 mass spectrometer by Ms. Q. Wu, Ms. D. Fox and Ms. R. Smith. All mass spectra were obtained by electron ionization at 70 eV with direct probe sample introduction unless otherwise indicated. Elemental analyses were obtained by Ms. O. Blagojevic or Ms. R. Smith, using a Control Equipment Corporation 440 Elemental Analyzer or a Perkin Elmer Series II 2400 CHNS/O Analyzer. TLC analyses were performed on aluminum sheets coated with Merck silica gel 60 F-254. Photolyses were carried out in a Rayonet RMR-500 reactor equipped with six 300 nm lamps. Optical rotation measurements were obtained on an Autopol IV polarimeter at 589 nm, with concentration given in units of g / 100 mL. X-ray crystal structures were solved by Dr. M. Parvez at the University of Calgary, and the results are provided in Appendixes. The data in these appendixes is reproduced directly from his reports. High pressure reactions were

carried out in a 50 mL Parr microreactor, model 4592. The numbering of positions in structures described in this Chapter is for convenience in assigning spectroscopic signals and does not follow IUPAC nomenclature.

7.2 Experiments Pertaining to Chapter 2

7.2.1 (*S*)-2-[2-(Benzenesulfonyl)ethylamino]propan-1-ol (203)

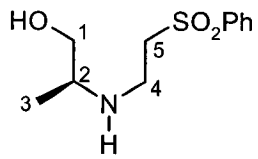

203

A solution of (*S*)-2-amino-1-propanol (**196**, 846 mg, 11.3 mmol) and sulfone **27** (1.895 g, 11.3 mmol) was refluxed for 2 d in 40 mL of isopropanol and concentrated *in vacuo*. The residue was chromatographed (hexane-ethyl acetate-methanol, 4:1:0.5) to afford 2.604 g (95%) of **203** as a colourless oil, which solidified upon standing, mp 47.5-49.5 °C; IR (film) 3305, 1303, 1148 cm^{-1}; ^1H NMR (200 MHz) δ 7.82-7.93 (m, 2 H), 7.66-7.47 (m, 3 H), 3.49 (dd, J = 10.8 Hz, 3.9 Hz, 1 H, H-1), 3.30-3.16 (m, 3 H), 3.15-2.99 (m, 1 H), 2.97-2.83 (m, 1 H), 2.77-2.61 (m, 1 H), 2.59-2.29 (br, s, 2 H, OH and NH) 0.95 (d, J = 6.5 Hz, 3 H, H-3); ^{13}C NMR (50 MHz) δ 139.1 (C), 133.7 (CH), 129.2 (CH), 127.7 (CH), 65.4 (CH_2, C-1), 56.2 (CH_2, C-5), 54.2 (CH, C-2), 40.3 (CH_2, C-4), 16.7 (CH_3, C-3); MS (*m/z*, %) 212 (10.5), 141 (33), 125 (27), 77 (51), 70 (100); HRMS calcd for $C_{10}H_{14}NO_2S$ (M^+-CH_2OH): 212.0745. Found: 212.0748.

7.2.2 (*S*)-2-[2-(Benzenesulfonyl)ethylamino]-3-phenylpropan-1-ol (204)

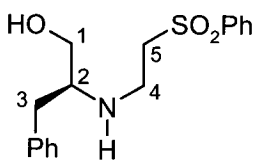

204

The same procedure was followed as for compound **203**, starting with 814 mg (5.39 mmol) of amino alcohol **197**, to give 1.705 g (99%) of **204** as a yellow oil: IR (film) 3514, 3324, 1445, 1301, 1139, 1082 cm^{-1}; ^1H NMR (200 MHz) δ 7.95-7.73 (m, 2 H), 7.71-7.46 (m, 3 H), 7.39-7.10 (m, 5 H), 3.57 (dd, J = 10.8, 3.6 Hz, 1 H, H-1), 3.38-3.13 (m, 3 H), 3.10-2.88 (m, 2 H), 2.88-2.76 (m, 1 H), 2.70 (crude d, J = 7.4 Hz, 2 H, H-3), 2.29 (br, s, 2 H, OH and NH); ^{13}C NMR (50 MHz) δ 138.8 (C), 138.1 (C), 133.5 (CH), 129.0 (CH), 128.8 (CH), 128.2 (CH), 127.5 (CH), 126.1 (CH), 62.4 (CH_2, C-1), 60.2 (CH, C-2), 56.0 (CH_2, C-3), 40.5 (CH_2), 37.7 (CH_2); MS (*m/z*, %) 288 (6), 228 (17), 146 (94), 118 (92) 91 (100); HRMS calcd for $C_{16}H_{18}NO_2S$ (M^+-CH_2OH): 288.1058. Found: 288.1039.

7.2.3 (*S*)-2-[2-(Benzenesulfonyl)ethylamino]-3-methylbutan-1-ol (205)

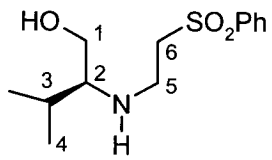

205

The same procedure was followed as for compound **203**, starting with 966 mg (9.37 mmol) of amino alcohol **198**, to afford 1.999 g (79%) of **205** as a yellow oil: IR (film) 3535, 1483, 1312, 1152, 1088 cm^{-1}; ^1H NMR (200 MHz) δ 8.02-7.83 (m, 2 H), 7.74-7.48 (m, 3 H), 3.56 (dd, J = 10.8, 4.1 Hz, 1 H, H-1), 3.35-3.10 (m, 4 H), 3.03-2.87 (m, 1 H), 2.33 (dt, J = 6.8, 4.1 Hz, 1 H), 2.47-1.85 (br, s, 2 H, OH and NH), 1.75 (m, 1 H, H-3), 0.94 (d, J = 6.8 Hz, 3 H), 0.88 (d, J = 6.8 Hz, 3 H); ^{13}C NMR (50 MHz) δ 138.5 (C), 133.1 (CH), 128.6 (CH), 127.1 (CH), 63.7 (CH, C-2), 60.3 (CH_2, C-1), 55.6 (CH_2), 40.5 (CH_2), 28.1 (CH, C-3), 18.4 (CH_3), 17.8 (CH_3); MS (*m/z*, %) 271 (M^+, 0.3), 240 (17), 141 (28), 98 (100), 86 (97); HRMS calcd for $C_{12}H_{18}NO_2S$ (M^+-CH_2OH): 240.1058. Found: 240.1057.

7.2.4 3-[2-(Benzenesulfonyl)ethylamino]propan-1-ol (206)

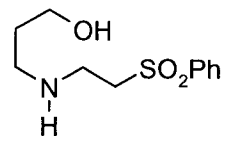

206

The same procedure was followed as for compound **203** starting with 1.002 g (13.34 mmol) of amino alcohol **199** to afford 3.096 g (96%) of **206** as a colourless oil: IR (film) 3308, 2929, 1308, 1148 cm^{-1}; ^1H NMR (200 MHz) δ 7.95-7.86 (m, 2 H), 7.73-7.51 (m, 3 H), 4.04 (br, s, 2 H, NH and OH), 3.73 (t, J = 5.5 Hz, 2 H), 3.32 (t, J = 6.4 Hz, 2 H), 3.07 (t, J = 6.5 Hz, 2 H), 2.83 (t, J = 6.0 Hz, 2 H), 1.70 (quintet, J = 5.7 Hz, 2 H); ^{13}C NMR (50 MHz) δ 139.0 (C), 133.9 (CH), 129.4 (CH), 127.8 (CH), 62.9 (CH_2), 55.2 (CH_2), 48.6 (CH_2), 42.7 (CH_2), 30.5 (CH_2); MS (*m/z*, %) 243 (M^++1, 2.83), 212 (23), 198 (18), 141 (27), 82 (31), 57 (100); HRMS calcd for $C_9H_{12}NO_2S$ (M^+-C_2H_4OH): 198.0589. Found: 198.0572.

7.2.5 (*1S,2S*)-*N*-Methyl-2-[2-(benzenesulfonyl)ethylamino]-1-phenylpropan-1-ol (207)

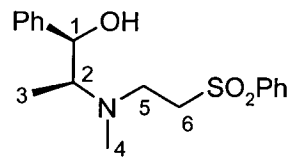

207

(-)-Ephedrine (**200**, 1.652 g, 10.0 mmol) and 1.680 g (10.0 mmol) of sulfone **27** were refluxed in 35 mL of xylenes for 2 d. The mixture was evaporated *in vacuo* and chromatography (50% ethyl acetate-hexanes) afforded 3.2093 g (96%) of **207** as a yellow oil: IR (film) 3513, 1449, 1304, 1144 cm^{-1}; ^1H NMR (200 MHz) δ 7.96-7.83 (m, 2 H), 7.71-7.50 (m 3 H), 7.37-7.15 (m, 5 H), 4.70 (d, J = 4.3 Hz, 1 H, H-1), 3.25-3.15 (m, 3 H), 3.00-2.89 (m, 2 H), 2.71 (qd, J = 6.8, 4.4 Hz, 1 H, H-2), 2.18 (s, 3 H, H-4), 0.85 (d, J = 6.8

Hz, 3 H, H-3); ^{13}C NMR (50 MHz) δ 142.1 (C), 139.4 (C), 133.6 (CH), 129.2 (CH), 127.9 (CH), 127.7 (CH), 126.9 (CH), 125.9 (CH), 73.6 (CH, C-1), 63.7 (CH, C-2), 53.9 (CH_2), 47.9 (CH_2), 38.7 (CH_3, C-4), 9.6 (CH_3, C-3); MS (*m/z*, %) 333 (M^+, 0.2), 316 (1), 226 (30), 84, (100), 42 (99); HRMS calcd for $C_{18}H_{22}NO_2S$ (M^+-OH): 316.1371. Found: 316.1362.

7.2.6 [1-(2-Benzenesulfonyl)ethylpiperidin-2-yl]-methanol (208)

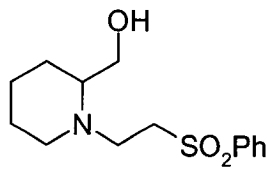

208

A solution of (2-piperidine)methanol (**201**, 1.540 g, 13.39 mmol) and sulfone **27** (2.249 g, 13.39 mmol) in 35 mL of xylenes was refluxed for 1 d and concentrated *in vacuo* gave crude **208**. Chromatography of the crude product (hexane:ethyl acetate:methanol = 4:1:0.5) gave 3.650 g (96%) of **208** as a light yellow oil: IR (film) 3510, 1442, 1302, 1145, 1082 cm^{-1}; ^1H NMR (200 MHz) δ 7.96-7.78 (m, 2 H), 7.69-7.42 (m, 3 H), 3.62 (dd, J = 11.5, 3.9 Hz 1 H, C**H**$_2$O), 3.42 (dd, J = 11.5, 4.4 Hz, 1 H, C**H**$_2$O), 3.35-3.07 (m, 3 H), 3.00-2.77 (m, 1 H), 2.76-2.62 (m, 2 H), 2.33-2.01 (m, 2 H), 1.66-1.10 (m, 6 H); ^{13}C NMR (50 MHz) δ 139.4 (C), 133.3 (CH), 128.9 (CH), 127.5 (CH), 62.6 (CH2), 60.5 (CH, N**C**HCH$_2$OH), 52.2 (CH_2), 51.2 (CH_2), 46.5 (CH_2), 27.3 (CH_2), 24.1 (CH_2), 22.9 (CH_2); MS (*m/z*, %) 283 (M^+, 2), 252 (17), 141 (13), 110 (92), 82 (100); HRMS calcd for $C_{13}H_{18}NSO_2$ (M^+-CH_2OH): 252.1058. Found: 252.1065.

7.2.7 2-[1-(2-Benzenesulfonyl)ethylpiperidin-2-yl]-ethanol (209)

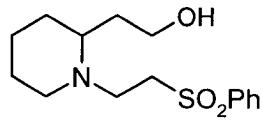

209

The same procedure was followed as for compound **208**, starting with 712 mg (5.52 mmol) of 2-piperidineethanol **(202)** and 0.929 g (5.53 mmol) of sulfone **27**, except that the reaction was refluxed for 2 d. Chromatography afforded 1.559 g (95%) of **209** as a light yellow oil: IR (film) 3532, 1445, 1301, 1138, 1082 cm^{-1}; ^1H NMR (200 MHz) 7.99-7.85 (m, 2 H), 7.74-7.50 (m, 3 H), 3.84-3.55 (m, 2 H), 3.34-2.93 (m, 4 H), 2.91-2.73 (m, 1 H), 2.67-2.46 (m, 1 H), 2.40-2.15 (m, 1 H), 1.89-1.20 (m, 8 H); ^{13}C NMR (50 MHz) δ 139.2 (C), 133.4 (CH), 129.0 (CH), 127.6 (CH), 60.3 (CH_2), 57.6 (CH), 52.7 (CH_2), 50.2 (CH_2), 46.1 (CH_2), 32.0 (CH_2), 28.3 (CH_2), 23.5 (CH_2), 22.2 (CH_2); MS (*m/z*, %) 296 (M^+, 0.6), 252 (31), 110 (100), 82 (93); HRMS calcd for $C_{13}H_{18}NO_2S$ (M^+-C_2H_4OH): 252.1058. Found: 252.1064.

7.2.8 (*S*)-*N*-Benzyl-2-[2-(benzenesulfonyl)ethylamino]propan-1-ol (210)

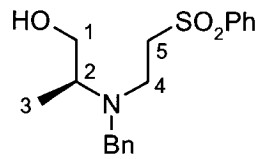

210

The amino alcohol **203** (723 mg, 2.98 mmol), DIPEA (577 mg, 4.47 mmol) and benzyl bromide (612 mg, 3.58 mmol) were refluxed for 4 h in 15 mL of anhydrous acetonitrile. The mixture was concentrated *in vacuo* and chromatographed (50% ethyl acetate-hexanes) to give 781 mg (79%) of **210** as a colourless oil, which solidified upon standing, mp 40-42 °C; IR (film) 3483, 1448, 1299, 1145, 1083 cm^{-1}; ^1H NMR (200 MHz) δ 7.86-7.72 (m, 2 H), 7.70-7.45 (m, 3 H), 7.35-7.15 (m, 5 H), 3.74 (d, J = 13.5 Hz, 1 H), 3.38 (d, J = 13.5 Hz, 1 H) superimposed on 3.39-3.30 (m, 1 H), 3.15-2.74 (m, 6 H), 0.91 (d, J = 6.7 Hz, 3 H, H-3); ^{13}C NMR (50 MHz) δ 138.9 (C), 138.4 (C), 133.3 (CH), 128.9 (CH), 128.4 (CH), 128.1 (CH), 127.3 (CH), 126.9 (CH), 62.8 (CH_2), 56.9 (CH, C-2), 54.4 (CH_2), 53.8 (CH_2), 43.1 (CH_2), 9.4 (CH_3, C-3); MS (*m/z*, %) 332 (M^+-1, 1), 302 (26), 160 (29), 132 (24), 91 (100); HRMS calcd for $C_{17}H_{19}NO_2S$ (M^+-CH_3OH): 301.1137. Found: 301.1134.

7.2.9 (*S*)-*N*-Benzyl-2-[2-(benzenesulfonyl)ethylamino-3-phenyl]propan-1-ol (211)

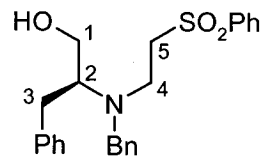

211

The same procedure was followed as for compound **210**, starting with 814 mg (5.39 mmol) of amino alcohol **204**, to give 1.582 g (92%) of **211** as a yellow oil: IR (film) 3496, 3022, 2934, 1447, 1305, 1143, 1084 cm^{-1}; ^1H NMR (200 MHz) δ 7.89-7.78 (m, 2 H), 7.72-7.50 (m, 3 H), 7.37-7.05 (m, 10 H), 3.88 (d, J = 13.5 Hz, 1 H), 3.53 (d, J = 13.3 Hz, 1 H), 3.50-3.38 (m, 2 H), 3.24-2.85 (m, 7 H), 2.44 (dd, J = 13.5, 9.1 Hz, 1 H); ^{13}C NMR (50 MHz) δ 139.0 (C), 138.7 (C), 138.4 (C), 133.5 (CH), 129.1 (CH), 128.7 (CH), 128.6 (CH), 128.5 (CH), 128.3 (CH), 127.5 (CH), 127.2 (CH), 126.0 (CH), 64.2 (CH, C-2), 60.8 (CH_2), 54.7 (CH_2), 54.5 (CH_2), 43.7 (CH_2), 32.4 (CH_2); MS (*m/z*, %) 410 (M^+, 0.3), 287 (65), 186 (50), 133 (90) 91 (100); HRMS calcd for $C_{23}H_{24}NO_2S$ (M^+-CH_2OH): 378.1528. Found: 378.1545.

7.2.10 (*S*)-*N*-Benzyl-2-[2-(benzenesulfonyl)ethylamino]-3-methylbutan-1-ol (212)

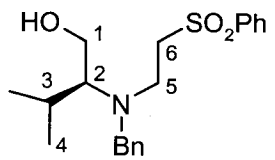

212

The same procedure was followed as for compound **210**, starting with 1.800 g (6.64 mmol) of **205**, to afford 2.220 g (93%) of **212** as a colourless oil: IR (film) 3534, 1445, 1306, 1148, 1086 cm^{-1}; ^1H NMR (200 MHz) δ 7.81-7.69 (m, 2 H), 7.69-7.44 (m 3 H), 7.32-7.17 (m, 5 H), 3.85 (d, J = 13.3 Hz, 1 H), 3.63 (d, J = 13.3 Hz, 1 H) superimposed on 3.75-3.56 (m, 1 H), 3.36 (dd, J = 10.9, 9.9 Hz, 1 H, H-1), 3.26-3.06 (m,

2 H), 3.05-2.77 (m, 3 H), 2.47 (m, 1 H, H-3), 1.94-1.75 (m, 1 H), 1.03 (d, J = 6.7 Hz, 3 H), 0.88 (d, J = 6.7 Hz, 3 H); ^{13}C NMR (50 MHz) δ 139.2 (C), 138.7 (C), 133.2 (CH), 128.8 (CH), 128.5 (CH), 128.1 (CH), 127.3 (CH), 126.9 (CH), 69.4 (CH, C-2), 60.0 (CH_2), 55.1 (CH_2), 55.0 (CH_2), 45.8 (CH_2), 27.9 (CH, C-3), 21.6 (CH_3), 19.8 (CH_3); MS (*m/z*, %) 361 (M^+, 0.7), 330 (19), 239 (17), 132 (31), 91 (100); HRMS calcd for $C_{19}H_{24}NO_2S$ (M^+-CH_2OH): 330.1528. Found: 330.1543.

7.2.11 *N*-Benzyl-2-[2-(benzenesulfonyl)ethylamino]propan-1-ol (213)

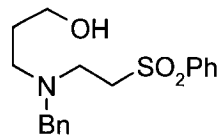

213

The same procedure was followed as for compound **210** starting with 830.1 mg (3.42 mmol) of **206** to afford 1.032 g (91%) of **213** as a colourless oil: IR (film) 3518, 2941, 1443, 1303, 1148, 1080 cm^{-1}; ^{1}H NMR (200 MHz) δ 7.87-7.77 (m, 2 H), 7.70-7.45 (m, 3 H), 7.31-7.10 (m, 5 H), 3.67 (t, J = 5.5 Hz, 2 H, C**H**$_2$O), 3.54 (s, 2 H), 3.31-3.15 (m, 2 H), 2.99-2.82 (m, 2 H), 2.64 (t, J = 6.1 Hz, 2 H), 1.75-1.56 (m, 2 H, C**H**$_2$CH$_2$O); ^{13}C NMR (50 MHz) δ 138.6 (C), 137.3 (C), 133.3 (C), 128.8 (CH), 128.4 (CH), 127.9 (CH), 127.3 (CH), 126.8 (CH), 61.6 (CH_2), 57.9 (CH_2), 52.3 (CH_2), 51.7 (CH_2), 46.2 (CH_2), 28.4 (CH_2); MS (*m/z*, %) 333 (M^+, 1.28), 288 (19), 146 (54), 118 (38), 91 (100); HRMS calcd for $C_{16}H_{18}NO_2S$ (M^+-C_2H_4OH): 288.1058. Found: 288.1057.

7.2.12 (*R*)-*N*-Benzyl-*N*-[2-(benzenesulfonyl)ethyl]-2-chloropropylamine (218)

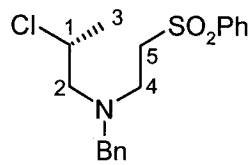

218

Product **210** (2.054 g, 6.17 mmol) and thionyl chloride (1.102 g, 9.26 mmol) were refluxed for 2 h in 30 mL of chloroform. The solution was washed with 1 M aqueous KOH solution, water and brine. The organic layer was dried over $MgSO_4$, concentrated and chromatographed (20% ethyl acetate-hexanes) to afford 2.038 g (94%) of **218** as a light yellow oil; IR (film) 1444, 1308, 1145, 1079 cm^{-1}; ^1H NMR (200 MHz) δ 7.93-7.79 (m, 2 H), 7.69-7.49 (m 3 H), 7.32-7.16 (m, 5 H), 3.93 (m, 1 H, H-1), 3.64 (d, J = 13.7 Hz, 1 H), 3.56 (d, J = 13.7 Hz, 1 H), 3.37-3.17 (m, 2 H), 3.05-2.92 (m, 2 H), 2.67 (m, 2 H), 1.42 (d, J = 6.7 Hz, 3 H, H-3); ^{13}C NMR (50 MHz) δ 139.3 (C), 137.9 (C), 133.6 (CH), 129.2 (CH), 128.8 (CH), 128.3 (CH), 127.8 (CH), 127.3 (CH), 62.5 (CH_2), 59.1 (CH_2), 55.4 (CH, C-1), 53.5 (CH_2), 47.8 (CH_2), 22.9 (CH_3, C-3); MS (*m/z*, %) 351 (M^+, 1), 314 (3), 208 (14), 144 (27), 91 (100); HRMS calcd for $C_{18}H_{22}ClNO_2S$: 351.1060. Found: 351.1042.

7.2.13 (*R*)-*N*-Benzyl-*N*-[2-(benzenesulfonyl)ethyl]-2-chloro-3-methyl-butylamine (219)

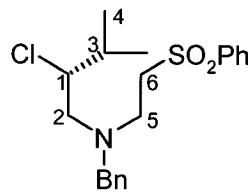

219

The same procedure was followed as for compound **218**, starting with 2.219 g (6.15 mmol) of **212** to afford 2.220 g (95%) of **219** as a colourless solid, mp 53 °C (from chloroform-hexanes); IR (film) 1449, 1305, 1152 cm^{-1}; ^1H NMR (200 MHz) δ 7.98-7.77 (m, 2 H), 7.75-7.43 (m 3 H), 7.29-7.15 (m, 5 H), 3.80 (ddd, J = 7.3, 6.3, 3.3 Hz, 1 H, H-1), 3.62 (d, J = 13.7 Hz, 1 H), 3.54 (d, J = 13.7 Hz, 1 H), 3.34-3.18 (m, 2 H), 3.00-2.92 (m, 2 H), 2.75 (dd, J = 13.8, 6.3 Hz, 1 H, H-2), 2.66 (dd, J = 13.8, 7.2 Hz, 1 H, H-2), 2.14-1.89 (m, 1 H, H-3), 0.96 (d, J = 6.8 Hz, 3 H), 0.78 (d, J = 6.5 Hz, 3 H); ^{13}C NMR (50 MHz) δ 139.2 (C), 137.9 (C), 133.6 (CH), 129.2 (CH), 128.7 (CH), 128.3 (CH), 127.8 (CH), 127.3 (CH), 67.1 (CH, C-1), 59.0 (2x CH_2), 53.3 (CH_2), 47.6 (CH_2), 31.2 (CH, C-3), 20.3 (CH_3),

15.9 (CH_3); MS (*m/z*, %) 379 (M^+, 0.2), 144 (81), 91 (100). Anal. calcd for $C_{20}H_{26}ClNO_2S$: C, 63.22; H, 6.90; N, 3.69. Found: C, 63.11; H, 7.05; N, 3.82.

7.2.14 (*3R,4S*)-*N*-Benzyl-3-benzenesulfonyl-4-methylpyrrolidine (220)

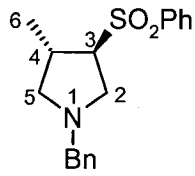

220

The chloroamine **218** (503 mg, 1.43 mmol) was dissolved in 5 mL of THF and added to 2.0 mmol of LDA in 5 mL of THF at -78 °C. The mixture was stirred at -78 °C for 2 h and was then quenched by filtration through neutral alumina. The filtrate was concentrated *in vacuo*, and the residue was chromatographed (15% ethyl acetate-hexanes) to afford 361 mg (80%) of **220** as a yellow oil: IR (film) 1447, 1304, 1146, 1089 cm^{-1}; ^1H NMR (200 MHz) δ 7.96-7.83 (m, 2 H), 7.72-7.50 (m, 3 H), 7.33-7.15 (m, 5 H), 3.62 (d, *J* = 13.2 Hz, 1 H), 3.48 (d, *J* = 13.2 Hz, 1 H), 3.34-3.20 (m, 1 H, H-3), 3.02 (dd, *J* = 10.4, 5.6 Hz, 1 H), 2.87-2.62 (m, 3 H), 2.23 (dd, *J* = 8.2, 5.3 Hz, 1 H), 1.03 (d, *J* = 6.8 Hz, 3 H, H-6); ^{13}C NMR (50 MHz) δ 138.4 (C), 138.2 (C), 133.5 (CH), 129.1 (CH), 128.6 (CH), 128.4 (CH), 128.1 (CH), 127.0 (CH), 70.1 (CH, C-3), 61.3 (CH_2), 59.3 (CH_2), 54.2 (CH_2), 34.5 (CH, C-4), 19.8 (CH_3, C-6); MS (*m/z*, %) 315 (M^+, 1), 173 (27), 158 (100), 145 (27), 91 (64); HRMS calcd for $C_{18}H_{21}NO_2S$: 315.1293. Found: 315.1312.

7.2.15 (*3R,4S*)-3-(Benzenesulfonyl)-*N*,4-dibenzylpyrrolidine (221)

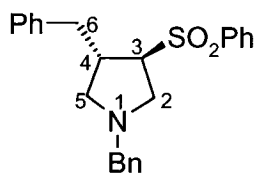

221

A solution of **211** (249 mg, 0.608 mmol) and thionyl chloride (0.11 mL, 1.5 mmol) in 20 mL of chloroform was refluxed for 3 h and and concentrated *in vacuo* (to remove excess thionyl chloride). The yellow residue was dissolved in 5 mL THF and added to a solution of excess LDA (1.8 mmol) in 6 mL of THF. The mixture was stirred at -78 °C for 2 h and at room temperature for 2 h and was then quenched by filtration through neutral alumina. The filtrate was concentrated *in vacuo*, and the residue was chromatographed (14% ethyl acetate-hexanes, then 20% ethyl acetate-hexanes) to afford 188 mg (79%) of **221** as a colourless oil: IR (film) 1446, 1298, 1142, 1082 cm^{-1}; ^1H NMR (200 MHz) δ 7.97-7.78 (m, 2 H), 7.73-7.50 (m, 3 H), 7.33-7.17 (m, 8 H), 7.14-6.94 (m, 2 H), 3.64 (d, *J* = 13.3 Hz, 1 H), 3.49 (d, *J* = 13.3 Hz, 1 H), 3.50-3.36 (m, 1 H, H-3), 3.10-2.52 (m, 6 H), 2.43 (dd, *J* = 9.2, 4.7 Hz, 1 H); ^{13}C NMR (50 MHz) δ 139.2 (C), 138.4 (C), 138.3 (C), 133.6 (CH), 129.2 (CH), 128.8 (CH), 128.7 (CH), 128.4 (CH), 128.3 (CH), 128.2 (CH), 127.1 (CH), 126.3 (CH), 67.9 (CH, C-3), 59.2 (CH_2), 58.5 (CH_2), 53.7 (CH_2), 41.5 (CH, C-4), 40.6 (CH_2); MS (*m/z*, %) 391 (M^+, 0.3), 158 (80), 91 (100); HRMS calcd for $C_{24}H_{25}NO_2S$: 391.1606. Found: 391.1638.

7.2.16 (*3R,4S*)-*N*-Benzyl-3-(benzenesulfonyl)-4-isopropylpyrrolidine (222)

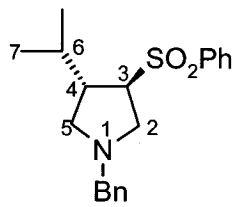

222

The same procedure was followed as for compound **220**, starting with 224 mg (0.589 mmol) of **212**, but using 1.5 equiv of LDA to afford 181 mg (90%) of **222** as a yellow oil: IR (film) 1448, 1306, 1151, 1090 cm^{-1}; ^1H NMR (200 MHz) δ 7.98-7.82 (m, 2 H), 7.73-7.46 (m 3 H), 7.37-7.09 (m, 5 H), 3.58 (d, *J* = 13.2 Hz, 1 H), 3.45 (d, *J* = 13.2 Hz, 1 H) superimposed on 3.49-3.38 (m, 1 H, H-3), 2.98 (dd, *J* = 10.4, 5.0 Hz, 1 H), 2.79-2.60 (m, 2 H), 2.59-2.44 (m, 1 H), 2.35 (dd, *J* = 8.7, 5.2 Hz, 1 H), 1.63 (m, 1 H, H-6), 0.88 (d, *J*

= 6.7 Hz, 3 H), 0.85 (d, J = 6.7 Hz, 3 H); ^{13}C NMR (50 MHz) δ 138.5 (C), 138.4 (C), 133.4 (CH), 128.9 (CH), 128.8 (CH), 128.2 (CH), 128.1 (CH), 126.9 (CH), 66.8 (CH, C-3), 59.3 (CH_2), 56.5 (CH_2), 54.6 (CH_2), 45.6 (CH, C-4), 31.1 (CH, C-6), 21.0 (CH_3), 19.0 (CH_3); MS (*m/z*, %) 343 (M^+, 0.6), 201 (34), 158 (91), 132 (25), 91 (100); HRMS calcd for $C_{20}H_{25}NO_2S$: 343.1606. Found: 343.1613. Anal. calcd for $C_{20}H_{25}NO_2S$: C, 69.93; H, 7.34; N, 4.08. Found: C, 69.54; H, 7.09; N, 4.15.

7.2.17 4-Toluenesulfonic acid 3-[*N*-benzyl-(2-benzenesulfonyl)ethylamino]propyl ester (225)

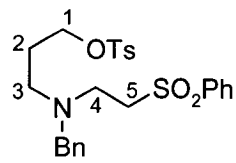

225

The amino alcohol **213** (479 mg, 1.44 mmol) and DMAP (507 mg, 4.16 mmol) were dissolved in 15 mL of chloroform, and 1.5 equiv of TsCl (413 mg, 2.16 mmol) and 2 mL triethylamine were added to the solution, which was then stirred overnight at room temperature, the reaction mixture was poured into 10 mL of water and the aqueous phase was extracted three times with dichlomethane, and the combined organic fractions were dried (Na_2SO_4), concentrated, and chromatographed. Elution with 20% ethyl acetate-hexanes afforded 537 mg (77%) of **225** as a colourless oil, which crystallized from dichloromethane-hexanes to give white crystals: mp 169-170 °C; IR (KBr) 2952, 1444, 1308, 1172, 1146, 1084 cm^{-1}; ^{1}H NMR (200 MHz) δ 7.92-7.69 (m, 4 H), 7.69-7.43 (m, 3 H), 7.42-7.15 (m, 5 H), 7.14-7.01 (m, 2 H), 4.06 (t, J = 6.2 Hz, 2 H, H-1), 3.43 (s, 2 H), 3.25-3.06 (m, 2 H), 2.91-2.71 (m, 2 H), 2.44 (s, 3 H, tolyl Me), 2.51-2.37 (m, 2 H), 1.71 (quintet, J = 6.5 Hz, 2 H, H-2); ^{13}C NMR (50 MHz) δ 144.6 (C), 139.1 (C), 137.8 (C), 133.4 (CH), 132.7 (C), 129.7 (CH), 129.0 (CH), 128.3 (CH), 128.1 (CH), 127.6 (CH), 127.5 (CH), 127.0 (CH), 68.2 (CH_2), 58.0 (CH_2), 52.8 (CH_2), 49.4 (CH_2), 46.5 (CH_2), 26.5 (CH_2, C-2), 21.4 (CH_3, tolyl Me); MS (*m/z*, %) 485 (M^++1, 0.14), 146 (70), 107 (100), 91

(95); Anal. calcd for $C_{28}H_{39}NO_4S$: C, 61.58; H, 5.99; N, 2.87. Found: C, 61.72; H, 6.13; N, 2.79.

7.2.18 (*2S,3R,4R*)-4-(Benzenesulfonyl)-1,2-dimethyl-3-phenylpyrrolidine (226) and its (*2S,3S,4S*) isomer (227)

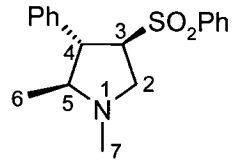

226 and

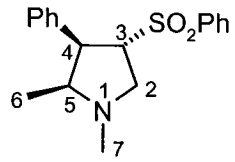

227

A solution of **207** (1.182 g, 3.55 mmol) and thionyl chloride (0.65 mL, 8.9 mmol) in 45 mL of chloroform was refluxed for 3 h and then concentrated *in vacuo*. The residue was dissolved in 10 mL of THF and added to a solution of excess LDA (10.1 mmol) in 10 mL of THF at -78 °C. The mixture was stirred at -78 °C for 2 h and at room temperature for 5 h and was then quenched by filtration through neutral alumina. The filtrate was concentrated *in vacuo*, and the residue was chromatographed (25% ethyl acetate-hexanes, then 35% ethyl acetate-hexanes) to afford 326 mg (29%) of diastereomer **227** as a light yellow oil: IR (film) 1444, 1306, 1148 cm^{-1}; ^1H NMR (200 MHz) δ 7.93-7.74 (m, 2 H), 7.64-7.37 (m 3 H), 7.21-7.08 (m, 3 H), 7.08-6.96 (m, 2 H), 3.84 (m, 1 H, H-5), 3.58 (dd, J = 7.4, 4.3 Hz, 1 H, H-4), 3.48-3.30 (m, 1 H, H-3), 2.88-2.62 (m, 2 H), 2.31 (s, 3 H, H-7), 0.66 (d, J = 6.5 Hz, 3 H, H-6); ^{13}C NMR (50 MHz,) δ 140.7 (C), 138.7 (C), 133.5 (CH), 129.1 (CH), 128.8 (CH), 128.3 (CH), 128.0 (CH), 126.7 (CH), 69.1 (CH), 65.0 (CH), 55.9 (CH_2, C-2), 50.4 (CH), 39.7 (CH_3, C-7), 14.8 (CH_3, C-6); MS (*m/z*, %) 174 (M^+, 3), 156 (37), 128 (19), 115 (100); HRMS calcd for $C_{12}H_{16}N$ (M^+-SO_2Ph): 174.1283. Found: 174.1291.

Continued elution afforded 446 mg (40%) of **226** as a light yellow solid, which crystallized from ethyl acetate-hexanes to afford white crystals: mp 137.5-138 °C (from ethyl acetate-hexanes); IR (film) 1441, 1304, 1145 cm^{-1}; ^1H NMR (200 MHz) δ 7.84-7.70 (m, 2 H), 7.59-7.28 (m 3 H), 7.24-7.04 (m, 3 H), 7.03-6.86 (m, 2 H), 3.82-3.70 (m, 2 H),

3.09 (dd, J = 9.4, 7.4 Hz, 1 H), 2.75 (dd, J = 11.6, 9.9 Hz, 1 H), 2.31 (s, 3 H, H-7), 2.29-2.15 (m, 1 H), 1.00 (d, J = 5.8 Hz, 3 H, H-6); ^{13}C NMR (50 MHz,) δ 139.8 (C), 138.2 (C), 133.4 (CH), 128.9 (CH), 128.5 (CH), 128.4 (CH), 127.7 (CH), 126.9 (CH), 70.2 (CH), 68.5 (CH), 56.2 (CH_2, C-2), 54.6 (CH), 39.6 (CH_3, C-7), 15.9 (CH_3, C-6); MS (*m/z*, %) 174 (M^+, 7), 172 (37), 156 (61), 115 (100); HRMS calcd for $C_{12}H_{16}N$ (M^+-SO_2Ph): 174.1283. Found: 174.1279. Anal. calcd for $C_{18}H_{21}NO_2S$: C, 68.54; H, 6.71; N, 4.44. Found: C, 68.63; H, 6.79; N, 4.48. The X-ray structure of **226** is shown in Fig. 2.7 and additional crystallographic data is given in Appendix I.

7.2.19 (+/-)-2-(Benzenesulfonyl)indolizidine (230)

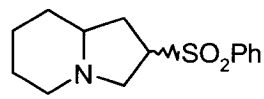

230

A solution of **208** (3.650 g, 12.85 mmol) and 2.34 mL of thionyl chloride (3.82 g, 32.1 mmol) in 30 mL of chloroform was refluxed for 2 h. The solution was washed with 1 M aqueous KOH solution, water and brine. The organic layer was dried over $MgSO_4$, concentrated and chromatographed (20% ethyl acetate-hexanes) to afford 3.370 g (87%) of the corresponding chloroamine **228**, which crystallized from dichloromethane-hexanes to give a light yellow solid: mp 44 °C; IR (film) 1445, 1298, 1144, 1088 cm^{-1}; ^{1}H NMR (200 MHz) δ 7.97-7.83 (m, 2 H), 7.69-7.47 (m, 3 H), 3.54-3.37 (m, 2 H), 3.34-3.21 (m, 2 H), 3.13-2.86 (m, 2 H), 2.70-2.57 (m, 1 H), 2.55-2.40 (m, 1 H), 2.28-2.14 (m, 1 H), 1.66-1.15 (m, 6 H); ^{13}C NMR (50 MHz) δ 139.5 (C), 133.7 (CH), 129.2 (CH), 127.8 (CH), 60.2 (CH), 52.5 (CH_2), 51.3 (CH_2), 47.0 (CH_2), 45.0 (CH_2), 28.8 (CH_2), 25.1 (CH_2), 22.4 (CH_2); MS (*m/z*, %) 301 (M^+, 2), 252 (16), 110 (100), 96 (47), 82 (74). Anal. calcd for $C_{14}H_{20}ClNO_2S$: C, 55.71; H, 6.68; N, 4.64. Found: C, 55.46; H, 6.52; N, 4.57.

The above chloroamine **228** (281 mg, 0.934 mmol) was dissolved in 5 mL of THF and added to 1.60 mmol of LDA in 5 mL of THF at -78 °C. The mixture was stirred at -78 °C for 2 h and at room temperature for another 2 h and was then quenched by filtration

through neutral alumina. The filtrate was concentrated *in vacuo* and the residue was chromatographed (25% ethyl acetate-hexanes, then 33% ethyl acetate-hexanes) to afford 96 mg (39%) of the less polar diastereomer of **230** as a colourless oil: IR (film) 1446, 1304, 1283, 1149, 1086 cm^{-1}; ^1H NMR (200 MHz) δ 7.98-7.81 (m, 2 H), 7.72-7.47 (m, 3 H), 3.67-3.52 (m, 1 H), 3.47 (dd, J = 10.8, 2.5 Hz, 1 H), 2.98 (dt, J = 10.8, 3.1 Hz, 1 H), 2.49-2.30 (m, 1 H), 2.16-1.98 (m, 1 H), 1.99-1.79 (m, 3 H), 1.78-1.61 (m, 2 H), 1.60-1.39 (m, 2 H), 1.24-1.03 (m, 2 H); ^{13}C NMR (50 MHz) δ 138.5 (C), 133.4 (CH), 129.0 (CH), 128.6 (CH), 63.5 (CH), 61.0 (CH), 54.1 (CH_2), 52.0 (CH_2), 32.9 (CH_2), 30.2 (CH_2), 24.7 (CH_2), 23.8 (CH_2); MS (*m/z*, %) 265 (M^+, 0.5), 155 (28), 110 (100), 82 (96); HRMS calcd for $C_{14}H_{19}NO_2S$: 265.1137. Found: 265.1129.

Continued elution (45% ethyl acetate-hexanes) afforded 112 mg (45%) of the more polar diastereomer of **230** as a colourless oil: IR (film) 1442, 1303, 1148, 1083 cm^{-1}; ^1H NMR (200 MHz) δ 7.96-7.80 (m, 2 H), 7.70-7.47 (m, 3 H), 3.78-3.59 (m, 1 H), 3.14 (dd, J = 9.4, 8.3 Hz, 1 H), 3.05-2.92 (m, 1 H), 2.59 (crude t, J = 9.1 Hz, 1 H), 2.33 (ddd, J = 13.3, 6.0, 3.1 Hz, 1 H), 2.14-1.96 (m, 2 H), 1.85-1.57 (m, 4 H), 1.53-0.98 (m, 3 H); ^{13}C NMR (50 MHz) δ 138.8 (C), 133.6 (CH), 129.2 (CH), 128.3 (CH), 63.0 (CH), 60.2 (CH), 54.5 (CH_2), 52.4 (CH_2), 32.5 (CH_2), 30.5 (CH_2), 25.2 (CH_2), 23.8 (CH_2); MS (*m/z*, %) 265 (M^+, 3), 122 (100), 94 (34); HRMS calcd for $C_{14}H_{19}NO_2S$: 265.1137. Found: 265.1139.

7.2.20 (2*S*)-2-[2-(Benzenesulfonyl)-1-methylethylamino]propan-1-ol (239)

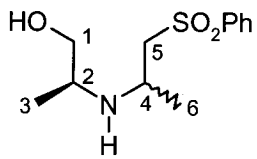

239

A mixture of amino alcohol **196** (289 mg, 3.85 mmol) and sulfone **238** (702 mg, 3.85 mmol) was refluxed for 2 d in 20 mL of xylenes. Chromatography (hexanes:ethyl acetate:methanol = 4:1:0.5) afforded 900 mg (91%) of the corresponding adduct **239** as a mixture of two diastereomers formed in the ratio of ca. 1:1, colourless oil: IR (film) 3408,

1448, 1301, 1144, 1082 cm^{-1}; ^1H NMR (200 MHz, both diastereomers) δ 7.97-7.83 (m, 2 H), 7.72-7.47 (m, 3 H), 3.60-2.99 (m, 5 H), 2.87-2.64 (m, 1 H), 2.18 (br, s, 2 H, NH and OH), 1.23 (d, J = 6.3 Hz), 1.11 (d, J = 6.2 Hz), 1.02 (d, J = 6.3 Hz), 0.98 (d, J = 6.5 Hz), total of signals from δ 1.23-0.98: 6 H; ^{13}C NMR (50 MHz, both diastereomers) δ 139.9 (C), 139.5 (C), 133.7 (CH), 133.5 (CH), 129.2 (CH), 129.1 (CH), 127.6 (CH), 127.5 (CH), 66.0 (CH_2), 65.5 (CH_2), 62.4 (CH_2), 62.2 (CH_2), 51.8 (CH), 51.1 (CH), 46.4 (CH), 45.3 (CH), 22.1 (CH_3), 21.2 (CH_3), 17.9 (CH_3), 16.9 (CH_3); MS (*m/z*, %) 226 (M^+-CH_2OH, 41), 141 (83), 125 (23), 77 (82), 44 (100); HRMS calcd for $C_{11}H_{16}NO_2S$ (M^+-CH_2OH): 226.0902. Found: 226.0905.

7.2.21 (*2S*)-2-[2-(Benzenesulfonyl)-1-methylethylamino-3-phenyl]propan-1-ol (240)

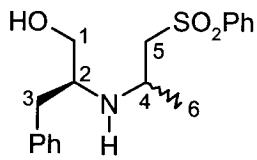

240

The same procedure was followed as for compound **239**, starting with **197** (1.039 g, 6.88 mmol) and **238** (1.250 g, 6.87 mmol) in 25 mL xylenes and the reaction was refluxed for 3 d, affording 1.812 g (87%) of **240** as a yellow oil: IR (film) 3510, 2923, 1444, 1299, 1149, 1082 cm^{-1}; ^1H NMR (200 MHz, mixture of diastereomers) δ 8.01-7.78 (m, 2 H), 7.73-7.51 (m, 3 H), 7.34-7.08 (m, 5 H), 3.64 (dd, J = 11.3 Hz, 3.4 Hz, 1 H), 3.48 (dd, J = 10.7 Hz, 3.8 Hz, 1 H), 3.45-3.23 (m, 2 H), 3.24-2.94 (m, 2 H), 2.93-2.84 (m, 1 H), 2.83-2.55 (m, 2 H), 2.39-1.54 (br, s, 1 H, OH), 1.15 (d, J = 6.3 Hz, 3 H, H-6), 1.04 (d, J = 6.2 Hz, 3 H, H-6); ^{13}C NMR (50 MHz, mixture of diastereomers) δ 139.93, 139.42, 138.32, 138.21, 133.58, 133.43, 129.11, 128.94, 128.91, 128.26, 128.21, 127.47, 126.11, 63.20, 62.75, 62.40, 62.06, 57.64, 57.32, 46.39, 45.66, 38.35, 38.08, 21.41, 21.09; MS (*m/z*, %) 333 (M^+, 3.6), 302 (6), 242 (11), 118 (90), 91 (100); HRMS calcd for $C_{17}H_{20}NO_2S$ (M^+-CH_2OH): 302.1215. Found: 302.1238.

7.2.22 (*2S*)-*N*-Benzyl-2-[2-(benzenesulfonyl)-1-methylethylamino]propan-1-ol (241)

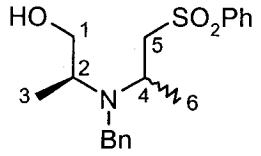

241

The conjugate addition adduct **239** (273 mg, 1.06 mmol) was treated with benzyl bromide as in the preparation of **210** to afford 259 mg (70%) of **241** (mixture of diastereomers) as a colourless oil: IR (film) 3456, 1451, 1303, 1141, 1079 cm^{-1}; ^1H NMR (200 MHz, both diastereomers) δ 7.92-7.13 (m, 10 H), 3.87-3.23 (m, 6 H), 3.08-2.88 (m, 2 H), 1.93 (br, s, 1 H, OH), 1.31 (d, J = 7.0 Hz), 1.20 (d, J = 6.5 Hz), 1.01 (d, J = 6.7 Hz), 0.97 (d, J = 6.5 Hz), total of signals from δ 1.31-0.97: 6 H; ^{13}C NMR (50 MHz, both diastereomers) δ 139.7 (C), 139.6 (C), 139.4 (C), 139.2 (C), 133.7 (CH), 133.5 (CH), 129.4 (CH), 129.2 (2 x CH), 128.6 (2 x CH), 128.5 (CH), 128.4 (CH), 127.7 (CH), 127.6 (CH), 127.1 (CH), 63.9 (CH_2), 63.6 (CH_2), 60.9 (CH_2), 59.7 (CH_2), 55.1 (CH), 53.8 (CH), 49.6 (CH), 49.5 (CH_2), 48.3 (CH), 48.1 (CH_2), 20.4 (CH_3), 17.2 (CH_3), 13.5 (CH_3), 13.2 (CH_3); MS (*m/z*, %) 347 (M^+, 0.5), 316 (19), 91 (100); HRMS calcd for $C_{18}H_{22}NO_2S$ (M^+-CH_2OH): 316.1371. Found: 316.1388.

7.2.23 (*2S*)-*N*-Benzyl-2-[2-(benzenesulfonyl)-1-methylethylamino-3-phenyl] propan-1-ol (242)

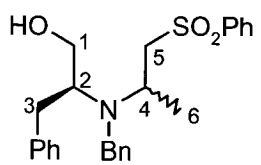

242

The same procedure was followed as for compound **239** starting with 1.442 g (4.156 mmol) of **240** to afford 1.232 g (68%) of **242** as a yellow oil: IR (film) 3470, 2930,

1445, 1399, 1299, 1152, 1083, 1028 cm^{-1}; ^1H NMR (200 MHz, mixture of diastereomers) δ 7.93-7.72 (m, 2 H), 7.71-7.44 (m, 3 H), 7.44-7.16 (m, 8 H), 7.17-7.03 (m, 2 H), 4.06-3.69 (m, 2 H, H-1), 3.69-3.30 (m, 4 H), 3.31-2.62 (m, 4 H), 2.60-2.36 (m, 1H), 1.35 (d, J = 6.8 Hz, 3 H, H-6); ^{13}C NMR (50 MHz, mixture of diastereomers) δ 139.60, 139.48, 139.18, 139.02, 138.87, 138.82, 133.45, 133.35, 129.13, 129.04, 128.87, 128.65, 128.39, 128.24, 127.50, 127.39, 127.00, 126.09, 125.97, 62.33, 61.41, 61.02, 60.82, 60.73, 60.28, 49.82, 48.82, 48.53, 47.80, 35.18, 34.89, 20.07, 17.91; MS (*m/z*, %) 423 (M^+, 0.9), 392 (21), 332 (29), 301 (66), 117 (79), 91 (100); HRMS calcd for $C_{24}H_{26}NO_2S$ (M^+-CH_2OH): 392.1684. Found: 392.1713.

7.2.24 (*2S,3R,4S*)-*N*-Benzyl-3-(benzenesulfonyl)-2,4-dimethylpyrrolidine (243) and its (*2R,3S,4S*) isomer 244

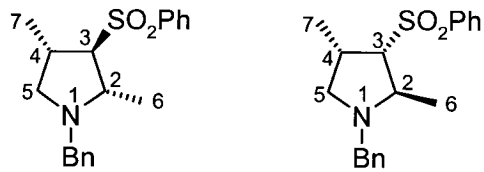

243 and **244**

A solution of **241** (644 mg, 1.86 mmol) and thionyl chloride (0.34 mL, 4.7 mmol) in 25 mL of chloroform was refluxed for 3 h and then concentrated *in vacuo*. The residue was dissolved in 5 mL of THF and added to a solution of excess LDA (5.6 mmol) in 6 mL of THF at -78 °C. The mixture was stirred at -78 °C for 2 h and at room temperature for 2 h, and was then quenched by filtration through neutral alumina. The filtrate was concentrated *in vacuo*, and the residue was chromatographed (14% ethyl acetate-hexanes), to afford 320 mg (43%) of diastereomer **243**. Recrystallization from chloroform-methanol provided pure **243** as light yellow crystals, mp 134-135 °C. IR (KBr) 1442, 1300, 1146, 1082 cm^{-1}; ^1H NMR (200 MHz) δ 8.01-7.84 (m, 2 H), 7.75-7.50 (m, 3 H), 7.39-7.16 (m, 5 H), 3.98 (d, J = 13.3 Hz, 1 H), 3.18 (d, J = 13.3 Hz, 1 H), 3.02 (quintet, J = 6.4 Hz, 1 H, H-2), 2.87 (dd, J = 7.2, 3.8 Hz, 1 H, H-3), 2.66-2.34 (m, 3 H), 1.18 (d, J = 6.0 Hz, 3 H, H-

6), 0.96 (d, J = 6.8 Hz, 3 H, H-7); ^{13}C NMR (50 MHz) δ 138.9 (C), 138.6 (C), 133.6 (CH), 129.2 (CH), 128.6 (CH), 128.4 (CH), 128.1 (CH), 126.9 (CH), 77.4 (CH, C-3), 60.2 (CH, C-2), 59.4 (CH_2), 56.9 (CH_2), 33.3 (CH, C-4), 21.5 (CH_3, C-7), 19.5 (CH_3, C-6); MS (*m/z*, %) 329 (M^+, 2), 187 (38), 172 (90), 146 (70), 91 (100); HRMS calcd for $C_{19}H_{23}NO_2S$: 329.1450. Found: 329.1437. Anal. calcd for $C_{19}H_{23}NO_2S$: C, 69.27; H, 7.04; N, 4.25. Found: C, 69.34; H, 7.10; N, 4.28. The X-ray structure of **243** is shown in Fig. 2.8 and additional crystallographic data is given in Appendix II.

Further chromatography with 20% ethyl acetate-hexanes afforded 62 mg (10%) of **244**, which gave white crystals from ethyl acetate-hexanes, mp 139-142 °C. IR (film) 1445, 1301, 1145, 1082 cm^{-1}; ^{1}H NMR (200 MHz) δ 7.97-7.82 (m, 2 H), 7.72-7.51 (m, 3 H), 7.39-7.19 (m, 5 H), 3.93 (d, J = 12.8 Hz, 1 H), 3.29 (d, J = 12.3 Hz, 1 H) superimposed on 3.36-3.26 (m, 1 H), 3.01 (quintet, J = 5.8 Hz, 1 H), 2.90 (dd, J = 8.4, 5.8 Hz, 1 H), 2.78-2.53 (m, 1 H), 2.40 (dd, J = 10.9, 8.6 Hz, 1 H), 1.39 (d, J = 7.2 Hz, 3 H), 0.77 (d, J = 6.2 Hz, 3 H); ^{13}C NMR (50 MHz) δ 140.3 (C), 139.0 (C), 133.5 (CH), 129.1 (CH), 128.8 (CH), 128.5 (CH), 128.3 (CH), 127.0 (CH), 72.1 (CH, C-2), 61.8 (CH, C-4), 60.8 (CH_2), 58.2 (CH_2), 35.6 (CH, C-4), 20.1 (CH_3), 13.2 (CH_3); MS (*m/z*, %) 329 (M^+, 7), 173 (78), 158 (63), 146 (55), 91 (100). Anal. calcd for $C_{19}H_{23}NO_2S$: C, 69.27; H, 7.04; N, 4.25. Found: C, 68.88; H, 6.82; N, 4.16. The X-ray structure of **244** is shown in Fig. 2.9 and additional crystallographic data is given in Appendix III.

7.2.25 (*2S,3R,4S*)-3-Benzenesulfonyl-1,4-dibenzyl-2-methylpyrrolidine (245) and its isomers 246

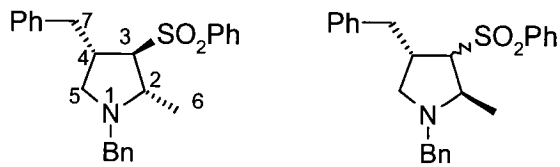

245 and **246**

The same procedure was followed as for compound **243** starting with 336 mg (0.793 mmol) of **242**. Flash chromatography (10% ethyl acetate in hexanes) afforded 161

mg (66%) of the less polar diastereomer **245**. Crystallization from methanol afforded colourless crystals: mp 98-100 °C; IR (film) 2927, 2802, 1449, 1305, 1145 cm^{-1}; ^1H NMR (200 MHz) δ 7.93-7.79 (m, 2 H), 7.70-7.47 (m, 3 H), 7.36-7.26 (m, 5 H), 7.18-7.07 (m, 3 H), 6.92-6.76 (m, 2 H), 4.03 (d, J = 13.2 Hz, 1 H), 3.23 (d, J = 13.2 Hz, 1 H), 3.19-2.92 (m, 2 H), 2.76-2.42 (m, 4 H), 2.42-2.25 (m, 1 H), 1.27 (d, J = 5.8 Hz, 3 H, H-6); ^{13}C NMR (50 MHz): δ 139.06, 138.35, 133.54, 129.18, 128.87, 128.74, 128.53, 128.38, 128.31, 128.13, 126.89, 126.11, 74.69 (C-3), 59.55, 56.85, 56.42, 41.19, 40.44, 20.03 (C-6); MS (*m/z*, %) 405 (M^+, 1), 390 (2.7), 263 (20), 172 (100); HRMS calcd for $C_{24}H_{24}NO_2S$ (M^+-CH_3): 390.1528. Found: 390.1529. The X-ray structure of **245** is shown in Fig. 2.10 and additional crystallographic data is given in Appendix IV.

Further chromatography with 20% ethyl acetate-hexanes afforded 72 mg (22%) of the more polar epimers **246** in ca. 70:30 ratio as a colourless oil: IR (film) 2923, 1443, 1305, 1150, 1084 cm^{-1}; ^1H NMR (200 MHz, mixture of epimers) δ 8.07-7.71 (m, 2 H), 7.70-7.44 (m, 3 H), 7.42-7.00 (m, 10 H), 3.93-3.78 (m, 1 H), 3.01-2.70 (m, 2 H), 3.28-3.01 (m, 2 H), 2.58 (major, dd, J = 10.9 Hz, 8.7 Hz, 1 H), 2.30 (minor, dd, J = 14.4 Hz, 10.2 Hz, 1 H), 2.18-1.98 (m, 1 H), 1.03 (minor, d, J = 5.8 Hz, 3 H), 0.72 (major, d, J = 6.3 Hz, 3 H); ^{13}C NMR (50 MHz) major epimer: δ 140.69, 138.57, 133.65, 129.21, 128.67, 128.55 (2 × C), 128.35, 128.28, 128.21, 127.02, 126.06, 71.99, 61.68, 58.41, 58.14, 42.92, 34.45, 20.29; minor epimer: δ 139.93, 138.21, 133.60, 129.15, 128.99, 128.79, 128.64, 126.19, 68.37, 64.57, 60.50, 55.78, 41.22, 31.61, 21.19; MS (*m/z*, %) 405 (M^+, 0.25), 172 (100); HRMS calcd for $C_{24}H_{24}NO_2S$ (M^+-CH_3): 390.1528. Found: 390.1548.

7.2.26 3-[2-(Benzenesulfonyl)-1-methylethylamino]propan-1-ol (247)

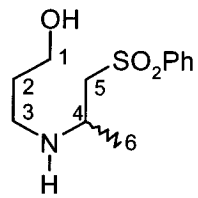

247

The same procedure was followed as for compound **203**, starting with 1.031 g (13.75 mmol) of amino alcohol **199** and 2.368 g (13.01 mmol) of vinyl sulfone **238** in 35 mL of isopropanol, except that the reaction was refluxed for 3 d, to afford 3.216 g (91%) of **247** as a colourless oil: IR (film) 3312, 2935, 1443, 1301, 1148, 1083 cm^{-1}; ^1H NMR (200 MHz) δ 7.96-7.79 (m, 2 H), 7.71-7.48 (m, 3 H), 3.72 (t, J = 5.5 Hz, 2 H, H-1), 3.30-3.13 (m, 2 H), 3.02 (dd, J = 16.6, 7.2 Hz, 1 H), 2.76 (t, J = 5.6 Hz, 2 H, H-3), 1.65 (q, J = 5.6 Hz, 2 H, H-2), 1.18 (d, J = 7.2 Hz, 3 H, H-6); ^{13}C NMR (50 MHz) δ 139.4 (C), 133.6 (CH), 129.1 (CH), 127.4 (CH), 62.3 (CH_2), 61.3 (CH_2), 48.5 (CH, C-4), 45.1 (CH_2, C-3), 31.5 (CH_2, C-2), 20.6 (CH_3, C-6); MS (*m/z*, %) 257 (M^+, 0.1), 198 (20), 141 (25), 77 (41), 59 (100); HRMS calcd for $C_{11}H_{16}NO_3S$ (M^+-CH_3): 242.0851. Found: 242.0856.

7.2.27 *N*-Benzyl-3-[2-(benzenesulfonyl-1-methylethylamino]propan-1-ol (248)

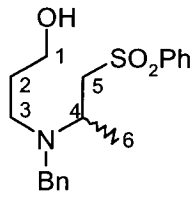

248

The conjugate addition adduct **247** (3.216 g, 12.51 mmol) was treated with benzyl bromide as in the preparation of **210** to afford 3.922 g (82%) of **248** as a colourless oil: IR (film) 3533, 2937, 1449, 1304, 1145, 1083 cm^{-1}; ^1H NMR (200 MHz) δ 7.91-7.79 (m, 2 H), 7.71-7.49 (m, 3 H), 7.31-7.12 (m, 5 H), 3.62 (t, J = 5.5 Hz, 2 H, H-1), 3.58 (d, J = 12.5 Hz, 1 H), 3.36 (d, J = 13.6 Hz, 1 H), 3.50-3.29 (m, 3 H), 3.02 (dd, J = 14.5, 9.2 Hz, 1 H), 2.62-2.40 (m, 2 H), 1.81-1.40 (m, 2 H), 1.27 (d, J = 6.8 Hz, 3 H, H-6); ^{13}C NMR (50 MHz) δ 139.5 (C), 138.2 (C), 133.5 (CH), 129.2 (CH), 128.7 (CH), 128.3 (CH), 127.6 (CH), 127.1 (CH), 62.3 (CH_2, C-1), 58.5 (CH_2), 54.0 (CH_2), 49.2 (CH, C-4), 47.7 (CH_2, C-3), 29.0 (CH_2, C-2), 16.4 (CH_3, C-6); MS (*m/z*, %) 346 (M^+-1, 4), 332 (4), 302 (48), 192 (51), 164 (73), 118 (67), 91 (100); HRMS calcd for $C_{18}H_{22}NO_3S$ (M^+-CH_3): 332.1320. Found: 332.1330.

7.2.28 4-Toluenesulfonic acid 3-[(2-benzenesulfonyl-1-methylethyl)-*N*-benzyl-amino]-propyl ester (249)

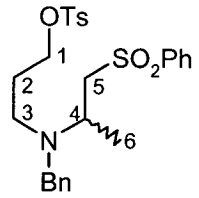

249

The same procedure was followed as for compound **225**, starting with 1.061 g (3.20 mmol) of **248** to afford 1.120 g (73%) of **249** as a light yellow oil, which crystallized from dichloromethane-hexanes to give white crystals: mp 92-94 °C; IR (KBr) 2970, 1447, 1359, 1300, 1178, 1145, 1082 cm^{-1}; ^1H NMR (200 MHz) δ 7.92-7.70 (m, 4 H), 7.70-7.47 (m, 3 H), 7.40-7.04 (m, 7 H), 4.00 (t, J = 6.4 Hz, 2 H, H-1), 3.49 (d, J = 14.2 Hz, 1 H), 3.35 (d, J = 14.3 Hz, 1 H), 3.41-3.20 (m, 2 H), 3.08-2.89 (m, 1 H), 2.45 (s, 3 H, tolyl Me), 2.58-2.24 (m, 2 H), 1.67-1.57 (m, 2 H), 1.18 (d, J = 6.8 Hz, 3H, H-6); ^{13}C NMR (50 MHz) δ 144.6 (C), 139.8 (C), 138.9 (C), 133.5 (CH), 133.0 (C), 129.7 (CH), 129.2 (CH), 128.1 (2 x CH), 127.7 (CH), 127.6 (CH), 126.9 (CH), 68.3 (CH_2, C-1), 59.0 (CH_2), 54.2 (CH_2), 50.1 (CH, C-4), 45.4 (CH_2, C-3), 27.5 (CH_2, C-2), 21.5 (CH_3, tolyl Me), 16.6 (CH_3); MS (*m/z*, %) 501 (M^+, 1.14), 346 (36), 302 (30), 146 (83), 91 (100); HRMS calcd for $C_{19}H_{24}NO_3S$ (M^+-Ts): 346.1477. Found: 346.1478. Anal. calcd for $C_{26}H_{31}NO_5S_2$: C, 62.25; H, 6.23; N, 2.87. Found: C, 61.76; H, 6.63; N, 2.81.

7.2.29 (+/-)-*trans*-*N*-Benzyl-2-methyl-3-(benzenesulfonyl)piperidine (250)

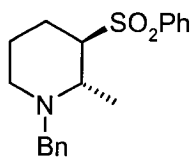

250

The tosylate **249** (242 mg, 0.483 mmol) was dissolved in 4 mL of THF and added to 0.65 mmol of LDA in 5 mL of THF at -78 °C. The mixture was stirred at -78 °C for 2 h and at room temperature for 3 h and was then quenched by filtration through neutral alumina. The filtrate was concentrated *in vacuo*, and the residue was chromatographed (20% ethyl acetate-hexanes) to afford 103 mg (43%) of unreacted **249** and 68 mg (43%; 75% based on the amount of consumed **249**) of **250** as a light yellow oil: IR (film) 2931, 1448, 1300, 1141, 1083 cm^{-1}; ^1H NMR (200 MHz) δ 7.96-7.82 (m, 2 H), 7.68-7.46 (m, 3 H), 7.39-7.21 (m, 5 H), 3.67 (d, J = 13.7 Hz, 1 H), 3.55 (d, J = 14.0 Hz, 1 H), 3.56-3.42 (m, 1 H), 3.04 (q, J = 4.9 Hz, 1 H), 2.65-2.48 (m, 1 H), 2.46-2.32 (m, 1 H), 2.10-1.69 (m, 3 H), 1.54-1.36 (m, 1 H), 1.28 (d, J = 6.7 Hz, Me); ^{13}C NMR (50 MHz) δ 139.2 (C), 139.1 (C), 133.3 (CH), 129.0 (CH), 128.8 (CH), 128.6 (CH), 128.2 (CH), 126.9 (CH), 65.9 (CH, **C**HSO$_2$Ph), 57.4 (CH_2), 53.0 (CH, **C**HMe), 46.1 (CH_2), 21.8 (CH_2), 21.4 (CH_2), 13.2 (CH_3, Me); MS (*m/z*, %) 329 (M^+, 5), 314(12), 186 (90), 172 (79), 160 (75), 91 (100); HRMS calcd for $C_{19}H_{23}NO_2S$: 329.1450. Found: 329.1468.

7.2.30 [1-(2-Benzenesulfonylpropyl)piperidin-2-yl]methanol (252)

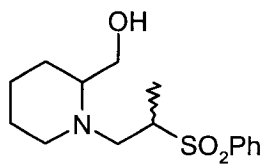

252

A mixture of (2-piperidine)methanol (**201**, 433.6 mg, 3.77 mmol) and sulfone **238** (686 mg, 3.77 mmol) in 25 mL of xylenes was refluxed for 3 d. After removal of solvent *in vacuo*, chromatography (hexanes:ethyl acetate:methanol = 4:1:0.5) afforded 324 mg (29%) of **252** as a mixture of two diastereomers formed in the ratio of 60:40 as a light yellow oil; IR (film) 3501, 1446, 1301, 1142, 1081 cm^{-1}; ^1H NMR (200 MHz, mixture of diasteroisomers) δ 8.00-7.81 (m, 2 H), 7.71-7.46 (m, 3 H), 3.71 (minor isomer, dd, J = 11.6, 4.1 Hz, 1 H), 3.56-3.20 (m, 3 H), 2.94 (major isomer, dd, J = 13.3, 4.9 Hz, 1 H), 2.87-2.63 (m, 2 H), 2.60 (br, s, 1 H, OH), 2.50-2.00 (m, 3 H), 1.70-1.35 (m, 3 H), 1.35-

1.04 (m, 2 H), 1.30 (minor isomer, d, J = 6.8 Hz, 3 H, Me), 1.28 (major isomer, d, J = 6.8 Hz, 3 H, Me); ^{13}C NMR (50 MHz) major diastereomer: δ 137.9 (C), 133.5 (CH), 129.0 (CH), 128.6 (CH), 62.0 (CH_2), 61.4 (CH), 58.7 (CH), 52.9 (CH_2), 50.4 (CH_2), 26.1 (CH_2), 23.2 (CH_2), 22.5 (CH_2), 12.7 (CH_3); minor diastereomer: δ 138.7 (C), 133.4 (CH), 128.9 (CH), 128.5 (CH), 62.0 (CH_2), 61.8 (CH), 58.4 (CH), 54.0 (CH_2), 52.1 (CH_2), 26.3 (CH_2), 23.6 (CH_2), 22.7 (CH_2), 13.0 (CH_3); MS (*m/z*, %) 296 (M^+-1, 1), 266 (18), 124 (100), 96 (58), 82 (80); HRMS calcd for $C_{14}H_{20}NO_2S$ (M^+-CH_2OH): 266.1215. Found: 266.1221.

7.2.31 2-[1-(2-Benzenesulfonylpropyl)piperidin-2-yl]ethanol (253)

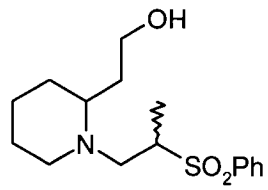

253

2-(2-Piperidine)ethanol (**202**, 808 mg, 6.26 mmol) and sulfone **238** (1.140 g, 6.26 mmol) were refluxed in 25 mL of xylenes for 4 d. After removal of solvent *in vacuo*, chromatography (hexanes-ethyl acetate-methanol = 4:1:0.5) afforded 506 mg (26%) of **253** as a mixture of two diastereomers formed in the ratio of ca. 55:45 as a light yellow oil; IR (film) 3530, 1443, 1305, 1145, 1080 cm^{-1}; ^{1}H NMR (200 MHz, mixture of diasteroisomers) δ 7.96-7.81 (m, 2 H), 7.70-7.48 (m, 3 H), 3.85-3.50 (m, 3 H), 3.42-3.00 (m, 2 H), 3.01-2.70 (m, 1 H), 2.70-2.07 (m, 3 H), 2.07-1.75 (m, 1 H), 1.29 (d, J = 6.8 Hz, 3 H, Me) superimposed on 1.68-1.16 (m, 7 H); ^{13}C NMR (50 MHz) major diastereomer: δ 137.7 (C), 133.5 (CH), 129.0 (CH), 128.6 (CH), 62.0 (CH_2), 59.3 (CH), 58.6 (CH), 52.9 (CH_2), 50.0 (CH_2), 31.5 (CH_2), 26.4 (CH_2), 22.2 (CH_2), 21.0 (CH_2), 12.8 (CH_3, Me); minor diastereomer: δ 137.7 (C), 133.5 (CH), 129.0 (CH), 128.6 (CH), 61.6 (CH_2), 60.1 (CH), 58.8 (CH), 52.7 (CH_2), 48.6 (CH_2), 31.7 (CH_2), 27.5 (CH_2), 22.4 (CH_2), 21.5 (CH_2), 12.6 (CH_3, Me); MS (*m/z*, %) 311 (M^+, 0.12), 266 (3), 124 (100), 82 (17); HRMS calcd for $C_{14}H_{20}NO_2S$ (M^+-C_2H_4OH): 266.1215. Found: 266.1204.

7.2.32 (+/-)-2-(Benzenesulfonyl)-2-methylindolizidine (256)

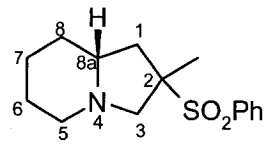

256

A solution of **252** (332 mg, 1.11 mmol) and thionyl chloride (0.26 mL, 3.6 mmol) in 25 mL of chloroform was refluxed for 3 h and then concentrated *in vacuo*. The residue of crude chloroamine **254** was dissolved in 5 mL of THF and added to a solution of excess LDA (3.4 mmol) in 6 mL of THF at -78 °C. The mixture was stirred at -78 °C for 2 h and at room temperature for 6 h, and was then quenched by filtration through neutral alumina. The filtrate was concentrated *in vacuo*, and the residue was chromatographed (25% ethyl acetate-hexanes) to afford 134 mg (43%) of the less polar isomer of **256** as a yellow oil: IR (film) 1443, 1300, 1140 1075 cm^{-1}; ^1H NMR (200 MHz) 7.99-7.85 (m, 2 H), 7.71-7.46 (m, 3 H), 3.69 (d, J = 11.1 Hz, 1 H), 2.85 (dt, J = 10.8, 2.9 Hz, 1 H), 2.21 (dd, J = 12.3, 10.4 Hz, 1 H), 2.03 (d, J = 11.0 Hz, 1 H), 1.98-1.74 (m, 2 H), 1.72-1.58 (m, 3 H), 1.48-1.40 (m, 1 H), 1.43 (s, 3 H, Me), 1.33-1.22 (m, 1 H), 1.17-0.96 (m, 2 H); ^{13}C NMR (50 MHz) δ 136.8 (C), 133.3 (CH), 130.1 (CH), 128.5 (CH), 66.3 (C), 62.5 (CH), 62.4 (CH_2), 52.0 (CH_2), 41.1 (CH_2), 30.2 (CH_2), 24.8 (CH_2), 23.9 (CH_2), 22.8 (CH_3); MS (*m/z*, %) 279 (M^+, 2), 136 (100), 108 (49); HRMS calcd for $C_{15}H_{21}NO_2S$: 279.1293. Found: 279.1313.

Further elution with 30% ethyl acetate-hexanes afforded 88 mg (28%) of the more polar isomer of **256** as a yellow oil: IR (film) 1444, 1300, 1152; 1076 cm^{-1}; ^1H NMR (200 MHz) 7.97-7.87 (m, 2 H), 7.72-7.51 (m, 3 H), 2.97 (d, J = 9.2 Hz, 1 H) superimposed on 3.05-2.91 (m, 1 H), 2.74 (d, J = 9.4 Hz, 1 H), 2.67 (dd, J = 13.3, 6.0 Hz, 1 H), 2.23-2.10 (m, 1 H), 2.04 (td, J = 11.1, 3.4 Hz, 1 H), 1.82-1.70 (m, 2 H), 1.65-1.57 (m, 1 H), 1.48 (s, 3 H, Me), 1.32 (dd, J =13.5, 10.6 Hz, 2 H), 1.22-1.06 (m, 2 H); ^{13}C NMR (50 MHz) δ 136.7 (C), 133.6 (CH), 130.1 (CH), 128.9 (CH), 66.2 (C), 64.6 (CH), 61.8 (CH_2), 52.6 (CH_2), 41.2 (CH_2), 30.8 (CH_2), 25.2 (CH_3), 25.1 (CH_2), 23.9 (CH_2); MS (*m/z*, %) 279 (M^+, 1.4), 136 (100), 108 (76); HRMS calcd for $C_{15}H_{21}NO_2S$: 279.1293. Found: 279.1279.

7.2.33 (+/-)-3-methyl-3-(benzenesulfonyl)quinolizidine (257)

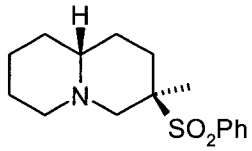

257

The same procedure was followed as for compound **256**, starting with 199 mg (0.640 mmol) of **253** to afford 140 mg (75%) of **257** as a single diastereomer. Crystallization from ethyl acetate-hexanes gave light yellow crystals: mp 127-129 °C; IR (KBr) 1443, 1297, 1147 cm^{-1}; ^1H NMR (200 MHz) δ 7.93-7.80 (m, 2 H), 7.72-7.49 (m, 3 H), 2.80-2.56 (m, 2 H), 2.44 (d, J = 10.6 Hz, 1 H), 2.11-1.86 (m, 2 H), 1.46 (s, 3 H, Me) superimposed on 1.72-1.10 (m, 10 H); ^{13}C NMR (50 MHz) δ 135.4 (C), 133.6 (CH), 130.4 (CH), 128.7 (CH), 62.7 (C), 62.0 (CH), 58.4 (CH_2), 56.6 (CH_2), 32.6 (CH_2), 28.8 (CH_2), 28.7 (CH_2), 25.7 (CH_2), 24.3 (CH_2), 17.6 (CH_3, Me); MS (*m/z*, %) 292 (M^+-1, 1.2), 150 (100), 136 (48), 94 (40); HRMS calcd for $C_{16}H_{23}NO_2S$: 293.1450. Found: 293.1452. Anal. calcd for $C_{16}H_{23}NO_2S$: C, 65.49; H, 7.90; N, 4.77. Found: C, 65.12; H, 8.03; N, 4.71. The X-ray structure of **257** is shown in Fig. 2.12 and additional crystallographic data is given in Appendix V.

7.3 Experiments Pertaining to Chapter 3

7.3.1 Resin 269

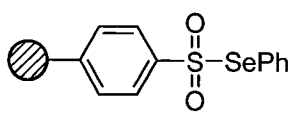

269

Benzeneseleninic acid (**268**, 1.89 g, 10 mmol) was added in portions over 15 min to 2.25 g of a suspension of 3-[4-(hydrazinosulfonyl)phenyl]propionyl AM resin (**84**, NovaBiochem Inc., 1.5 mmol/g) in 20 mL of methanol-THF (1:1) at room temperature.

Evolution of nitrogen was observed. After stirring at room temperature overnight, the mixture was filtered and washed with methanol, THF and ether, and dried under vacuum to afford 2.70 g of the yellow resin **269**: IR (KBr) 1669, 1292, 1119, 1068 cm^{-1}.

7.3.2 3-[4-(1-Hexynylsulfonyl)phenyl]propionyl Resin (271)

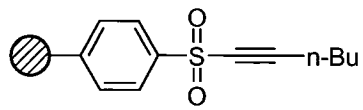

271

1-Hexyne (820 mg, 10.0 mmol), diphenyl diselenide (47 mg, 0.15 mmol) and AIBN (24 mg, 0.15 mmol) were added to a suspension of the resin **269** (1.00 g) in 20 mL of dry benzene. After refluxing for 24 h under nitrogen, the mixture was filtered and washed with benzene, methanol, THF and ether, and then dried under vacuum to afford 1.10 g of the yellow β-seleno vinyl sulfone resin **270**. The resin **270** was then suspended in THF (30 mL) and 30% hydrogen peroxide (3 mL) was added. The mixture was stirred for 2 h at 60 °C. The resin was filtered and washed with water, methanol, THF and ether, and dried under vacuum to afford 821 mg (0.90 mmol/g) of **271**, obtained as a white resin: IR (KBr) 2194, 1650, 1314, 1142, 1083, 1006 cm^{-1}.

7.3.3 (*E*)-1-(*p*-Nitrobenzene)sulfonyl-2-phenylseleno-1-hexene (295)

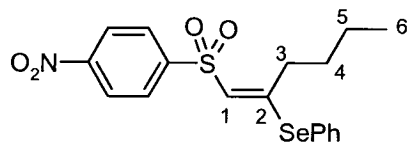

295

1-Hexyne (548 mg, 6.83 mmol) and selenosulfonate **294** (762 mg, 2.23 mmol) were dissolved in 6 mL of chloroform and irradiated for 2 h in a Rayonet reactor equipped with six 300 nm lamps. The solvent was evaporated, and the residue was purified by flash

chromatography (15% ethyl acetate-hexanes) to afford 803 mg (85%) of **295** as a yellow solid: mp 104-106 °C; IR (KBr) 3108, 2957, 1524, 1351, 1308, 1147 cm^{-1}; ^1H NMR (300 MHz) δ 8.33 (d, J = 8.7 Hz, 2 H), 7.96 (d, J = 8.7 Hz, 2 H), 7.58-7.38 (m, 5 H), 5.77 (s, 1 H, H-1), 2.88 (t, J = 8.2 Hz, 2 H, H-3), 1.69-1.55 (m, 2 H), 1.40 (sextet, J = 7.2 Hz, 2 H), 0.92 (t, J = 7.2 Hz, 3 H, H-6); ^{13}C NMR (75 MHz) δ 166.1 (C), 150.1 (C), 148.1 (C), 136.8 (CH), 130.2 (CH), 128.1 (CH), 125.5 (C), 124.3 (CH), 121.0 (CH), 33.2 (CH_2, C-3), 32.4 (CH_2), 22.5 (CH_2), 13.7 (CH_3, C-6); MS (*m/z*, %) 425 (M^+, 55), 383 (28), 239 (20), 157 (50), 81 (100); HRMS calcd for $C_{18}H_{19}NO_4S^{80}Se$: 425.0218.

7.3.4 1-[(4-Aminobenzene)sulfonyl)]-1-hexyne (297) and 1-[(4-Aminobenzene)sulfonyl]-hexan-2-one (298)

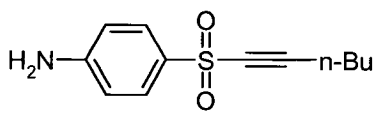

297 and

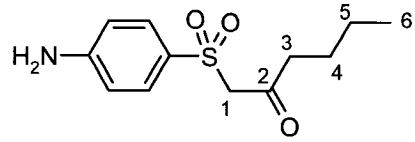

298

β-Seleno vinyl sulfone **295** (500 mg, 1.18 mmol) was dissolved in 20 mL of chloroform. *m*CPBA (672 mg, 77%, 3.0 mmol) was added and the mixture was stirred for 20 min at room temperature. The solution was then washed with 10% aqueous K_2CO_3 solution, water, dried over $MgSO_4$, and concentrated *in vacuo*. The residue was redissolved in 20 mL of chloroform and the mixture was refluxed for 2 h and concentrated *in vacuo*. The residue was purified by flash chromatography (10% ethyl acetate-hexanes) to afford 286 mg (91%) of acetylenic sulfone **296** as a white solid: mp 61-62 °C; ^1H NMR (300 MHz) δ 8.42 (d, J = 8.7 Hz, 2 H), 8.19 (d, J = 8.7 Hz, 2 H), 2.41 (t, J = 6.7 Hz, 2 H), 1.62-1.50 (m, 2 H), 1.44-1.31 (m, 2 H), 0.89 (t, J = 6.7 Hz, 3 H, Me); ^{13}C NMR (75 MHz) δ 150.7, 147.2, 128.6, 124.5, 100.5, 77.1, 28.7, 21.9, 18.7, 13.3 (Me); MS (*m/z*, %) 267 (M^+, 3), 252 (4), 225 (32), 81 (91), 41 (100).

Acetylenic sulfone **296** (286 mg, 1.07 mmol) was dissolved in 15 mL of hot ethanol and 2 mL of aqueous 2 M $Na_2S_2O_4$ solution was added. After refluxing for 9 h, the solvent was concentrated to ca. 2 mL and extracted with dichloromethane (10 mL × 3).

The organic layers were combined, dried over $MgSO_4$, and concentrated *in vacuo*. The residue was purified by flash chromatography (elution with 30% ethyl acetate-hexanes) to afford 61 mg (24%) of the less polar compound **297** as a light yellow oil: IR (film) 3477, 3381, 2960, 2202, 1593, 1310, 1150 cm^{-1}; ^1H NMR (300 MHz) δ 7.72 (d, J = 8.7 Hz, 2 H), 6.70 (d, J = 8.7 Hz, 2 H), 4.62-4.00 (br, s, 2 H, NH_2), 2.33 (t, J = 6.7 Hz, 2 H), 1.60-1.42 (m, 2 H), 1.40-1.31 (m, 2 H), 0.87 (t, J = 7.7 Hz, 3 H); ^{13}C NMR (75 MHz) δ 151.9 (C), 129.6 (C), 129.5 (CH), 113.9 (CH), 95.8 (C), 78.9 (C), 29.0 (CH_2), 21.8 (CH_2), 18.5 (CH_2), 13.3 (CH_3); MS (*m/z*, %) 237 (M^+, 88), 172 (20), 158 (36), 130 (100), 108 (51); HRMS calcd for $C_{12}H_{15}NO_2S$: 237.0824. Found: 237.0805.

Further elution with 40% ethyl acetate-hexanes afforded 123 mg (45%) of the more polar β-keto sulfone **298** as a light yellow solid: mp 90-93 °C; IR (KBr) 3474, 3380, 2933, 1715, 1596, 1299, 1132 cm^{-1}; ^1H NMR (200 MHz) δ 7.59 (d, J = 7.7 Hz, 2 H), 6.68 (d, J = 7.7 Hz, 2 H), 4.50-3.78 (br, 2 H, NH_2), 4.09 (s, 2 H, H-1), 2.68 (t, J = 7.2 Hz, 2 H, H-3), 1.63-1.43 (m, 2 H), 1.38-1.20 (m, 2 H), 0.89 (t, J = 7.2 Hz, 3 H, H-6); ^{13}C NMR (50 MHz) δ 198.8 (C-2), 152.0 (C), 130.4 (CH), 126.5 (C), 113.9 (CH), 67.4 (CH_2, C-1), 44.0 (CH_2, C-3), 25.2 (CH_2), 22.0 (CH_2), 12.7(CH_3, C-6); MS (*m/z*, %) 255 (M^+, 59), 171 (18), 156 (100) 108 (61), 92 (92); HRMS calcd for $C_{12}H_{17}NO_2S$: 255.0929. Found: 255.0912.

7.3.5 1-[(4-Aminobenzene)sulfonyl)]-2-phenylseleno-1-hexene (299)

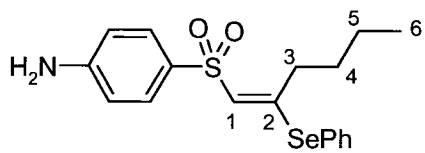

299

β-Seleno vinyl sulfone **295** (2.12 g, 5.00 mmol) was dissolved in 50 mL of hot ethanol and 15 mL of aqueous 2 M $Na_2S_2O_4$ solution was added. After refluxing for 9 h, the solvent was concentrated to ca. 15 mL and extracted with dichloromethane (20 mL × 4). The organic layers were combined, dried over $MgSO_4$, and concentrated *in vacuo*. The residue was purified by flash chromatography (4% chloroform-methanol) to afford 1.492 g (76%) of **299** as a yellow oil: IR (film) 3471, 3370, 2954, 1592, 1297, 1139 cm^{-1}; ^1H

NMR (300 MHz) δ 7.62-7.50 (m, 4 H), 7.50-7.30 (m, 3 H), 6.65 (d, J = 8.7 Hz, 2 H), 5.87 (s, 1 H, H-1), 4.40-3.92 (br, s, 2 H, NH_2), 2.83 (t, J = 7.7 Hz, 2 H, H-3), 1.64-1.49 (m, 2 H), 1.46-1.24 (m, 2 H), 0.90 (t, J = 7.7 Hz, 3 H, H-6); ^{13}C NMR (75 MHz) δ 159.2 (C), 150.7 (C), 136.6 (CH), 130.5 (C), 130.0 (CH), 129.7 (CH), 129.0 (CH), 126.1 (C), 124.8 (CH), 114.1 (CH, C-1), 32.8 (CH_2), 32.0 (CH_2), 22.5 (CH_2), 13.8 (CH_3, C-6); MS (*m/z*, %) 395 (M^+, 18), 289 (10), 238 (31), 156 (100); HRMS calcd for $C_{18}H_{21}NO_2S^{80}Se$: 395.0458. Found: 395.0447.

7.3.6 2-(1-Propynylthio)benzoic acid (312)

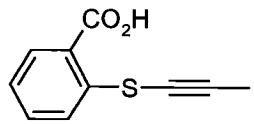

312

Thiosalicylic acid (**310**, 1.54 g, 10 mmol) was dissolved in 35 mL of methanol and 0.5 mL of concentrated HCl was added. The mixture was refluxed for 22 h and the solvent was evaporated and the residue was dissolved in 30 mL of acetone, followed by the addition of 1.52 g (11.0 mmol) of K_2CO_3 at room temperature under an argon atmosphere. The mixture was stirred for 4 h and propargyl bromide (1.30 g, 11.0 mmol) was added slowly to the reaction mixture and stirring was continued for 1 h at room temperature followed by reflux for 16 h. The solvent was removed and the residue was diluted with 10 mL of water. This was extracted with chloroform (15 mL × 3), the extract was washed with 5 mL of water, dried over anhydrous $MgSO_4$, and the solvent removed. The crude product obtained was purified by flash chromatography (15% ethyl acetate-hexanes) to afford 1.42 g (69%, 2 steps) of the corresponding acetylenic sulfide as a white solid: mp 94-96 °C, with a ^1H NMR spectrum in accord with the literature.[165] The resulting solid was stirred with a 5 M methanolic solution of KOH (5 mL) at room temperature for 2 d. After the removal of the solvent under reduced pressure, the yellow solid residue was diluted with 15 mL of water, acidified with concentrated HCl and the white precipitate was filtered and washed with water (10 mL × 3). The light yellow solid was dried under

vacuum to afford 1.122 g of the acetylenic sulfide **312** in 85% yield: mp 156-160 °C; IR (film) 3450-2500, 2200, 1672, 1600, 742 cm^{-1}; ^1H NMR (300 MHz) δ 8.16 (d, J = 7.7 Hz, 1 H), 8.05 (d, J = 7.7 Hz, 1 H), 7.58 (t, J = 8.2 Hz, 1 H), 7.29 (t, J = 7.7 Hz, 1 H), 2.17 (s, 3 H, Me); ^{13}C NMR (75 MHz) δ 171.0 (C), 140.3 (C), 133.8 (C), 132.3 (CH), 127.0 (CH), 125.2 (CH), 124.6 (CH), 97.8 (C), 65.0 (C), 5.4 (CH_3); MS (*m/z*, %) 192 (M^+, 6), 147 (7), 69 (60), 45 (100); HRMS calcd for $C_{10}H_8O_2S$: 192.0245. Found 192.0244.

7.3.7 4-(1-Propynylthio)benzoic acid (315)

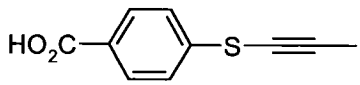

315

Product **315** was prepared from via a similar procedure to that used for **312**. The product **315** was obtained from **314** in 43% yield in 4 overall steps a pale yellow solid: mp 171-174 °C; IR (film) 3434, 1686, 1592, 843, 755 cm^{-1}; ^1H NMR (CD_3COCD_3, 300 MHz) δ 8.05 (d, J = 8.7 Hz, 2 H), 7.50 (d, J = 8.7 Hz, 2 H), 2.16 (s, 3 H, Me); ^{13}C NMR (75 MHz) δ 167.6 (C), 141.5 (C), 131.9 (CH), 130.1 (C), 126.4 (CH), 97.8 (C), 65.0 (C), 5.5 (CH_3); MS (*m/z*, %) 192 (M^+, 100), 147 (65), 71 (31); HRMS calcd for $C_{10}H_8O_2S$: 192.0245. Found 192.0236.

7.3.8 4-(3-Propynylsulfonyl)benzoic acid methyl ester (319)

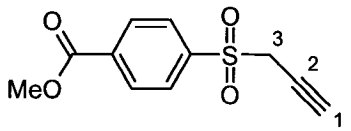

319

Resin **317** (60 mg, 0.93 mmol/g) was refluxed overnight in 5 mL of a mixture of methanol-THF (1:4) containing sodium methoxide (81 mg, 1.5 mmol). The resin was

removed by filtration and was washed with THF, methanol and ether. The filtrate was concentrated to dryness and extracted with dichloromethane. The organic solvent was then filtered and evaporated and the residue was purified by flash chromatography (20% hexanes-ethyl acetate) to afford 7.2 mg (54%) of **319** as a white solid: mp 127-130 °C; IR (KBr) 3283, 3246, 2955, 2129, 1723, 1286 cm^{-1}; ^1H NMR (300 MHz) δ 8.25 (d, J = 8.7 Hz, 2 H), 7.08 (d, J = 8.4 Hz, 2 H), 4.00 (d, J = 2.6 Hz, 2 H, H-3), 3.99 (s, 3 H, OCH_3), 2.38 (t, J = 2.6 Hz, 1 H, H-1); ^{13}C NMR (75 MHz) δ 165.4 (C, carbonyl C), 141.2 (C), 135.4 (C), 130.2 (CH), 129.0 (CH), 76.2 (CH, C-1), 71.2 (C-2), 52.8 (CH_3, OCH_3), 48.3 (CH_2, C-3); MS (*m/z*, %) 238 (M^+, 1.3), 199 (29), 135 (100), 119 (80); HRMS calcd for $C_{11}H_{10}O_4S$: 238.0300. Found: 238.0320.

7.3.9 Preparation of Resin 318 from 315

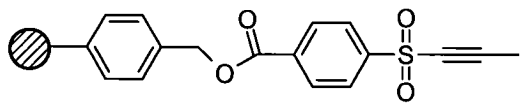

318

To a round-bottom flask charged with Merrifield resin (**64**, 2.00 g, 1.2 mmol/g) and 35 mL of DMF was added **315** (922 mg, 4.8 mmol), cesium carbonate (1.56 g, 4.8 mmol), and potassium iodide (398 mg, 2.4 mmol). The mixture was heated to 90 °C for 28 h. After cooling to room temperature, the resin was filtered and washed with DMF, 1:1 DMF/water, methanol and ether. Drying under vacuum overnight afforded 2.36 g of acetylenic sulfide **320** as a light brown solid. To the suspension of resin **320** (2.356 g) in 35 mL of acetic acid, 30% hydrogen peroxide (2.0 mL, 20 mmol) was added and the mixture was stirred for 20 h under reflux. The resin was filtered and washed with water, THF, dichloromethane, methanol and ether, followed by drying under reduced pressure to afford 2.367 g (0.87 mmol/g) of yellow resin **318**: IR (KBr) 3025, 2915, 2215, 1730, 1331, 1164 cm^{-1}.

7.3.10 *p*-(Bromomethyl)benzenesulfonhydrazide (323)

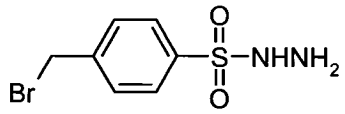

323

p-(Bromomethyl)benzenesulfonyl chloride (**322**, 8.07 g, 30.0 mmol) was dissolved in 120 mL of THF. The stirred mixture was cooled in an ice bath and a solution of hydrazine hydrate (3.30 g, 66.0 mmol) in 3 mL of water was added dropwise. Stirring was continued for 15 min. The mixture was washed with brine, dried over $MgSO_4$, filtered through a Celite pad. The clear filtrate was evaporated under reduced pressure to afford 7.14 g (90%) of **323** as a white solid, mp 156-160 °C (dec.); IR (KBr) 3479, 3330, 1328, 1148 cm^{-1}; ^1H NMR (300 MHz) δ 7.91 (d, J = 8.2 Hz, 2 H), 7.59 (d, J = 8.7 Hz, 2 H), 5.68-5.57 (br, s, 1 H, NH), 4.52 (s, 2 H, $BrCH_2$), 2.18-1.36 (br, s, 2 H, NH_2); ^{13}C NMR (75 MHz) δ 143.6, 136.3, 129.9, 128.7, 31.2. The crude product was used directly in the next step.

7.3.11 *Se*-Phenyl *p*-(bromomethyl)benzeneselenosulfonate (324)

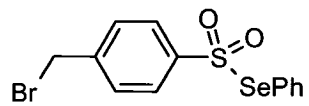

324

The sulfonhydrazide **323** (6.40 g, 24.2 mmol) in 80 mL of methanol was added in portions to benzenseleninic acid (**268**, 4.56 g, 24.1 mmol) over 25 min at 0 °C. Vigorous evolution of nitrogen was observed. The solution gradually turned clear yellow and toward the end of the addition a yellow precipitate formed. After cooling at -20 °C overnight, the product was filtered to afford 8.49 g (90%) of the selenosulfonate **324** as a yellow solid, mp 60-62 °C (from methanol); IR (KBr) 1292, 1128, 745 cm^{-1}; ^1H NMR (300 MHz) δ 7.58-7.32 (m, 9 H), 4.47 (s, 2 H, $BrCH_2$); ^{13}C NMR (75 MHz) δ 144.8, 143.5, 137.2,

131.0, 129.7, 129.3, 127.8, 127.5, 31.3; MS (*m/z*, %) 390 (M^+, 20), 233 (40), 217 (44), 157 (85), 90 (100); HRMS calcd for $C_{13}H_{11}{}^{79}BrO_2S^{80}Se$: 389.8828. Found: 389.8827. Anal. calcd for $C_{13}H_{11}BrO_2SSe$: C, 40.02; H, 2.84. Found: C, 40.08; H, 2.69.

7.3.12 (*E*)-1-[(*p*-Bromomethyl)benzenesulfonyl]-2-phenylseleno-1-hexene (326)

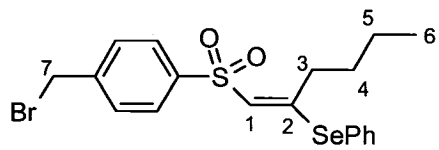

326

1-Hexyne (82 mg, 1.0 mmol) and selenosulfonate **324** (250 mg, 0.641 mmol) were dissolved in 4 mL of chloroform and irradiated for 1 h in a Rayonet reactor equipped with six 300 nm lamps. The solvent was evaporated, and the residue was purified by flash chromatography (15% ethyl acetate-hexanes) to afford 268 mg (88%) of **326** as a pale yellow oil: IR (film) 1317, 1305, 1146, 1085 cm^{-1}; ^1H NMR (300 MHz) δ 7.76 (d, J = 8.2 Hz, 2 H), 7.58-7.47 (m, 4 H), 7.47-7.33 (m, 3 H), 5.83 (s, 1 H, H-1), 4.49 (s, 2 H, H-7), 2.85 (t, J = 7.7 Hz, 2 H, H-3), 1.63-1.51 (m, 2 H), 1.43-1.30 (m, 2 H), 0.91 (t, J = 7.2 Hz, 3 H, H-6); ^{13}C NMR (75 MHz) δ 162.9 (C), 142.8 (C), 142.2 (C), 136.7 (CH), 130.1 (CH), 130.0 (CH), 129.7 (CH), 127.3 (CH), 125.7 (C), 122.8 (CH), 33.0 (CH_2), 32.2 (CH_2), 31.5 (CH_2, C-7), 22.5 (CH_2), 13.7 (CH_3, C-6); MS (*m/z*, %) 472 (M^+, 0.7), 89 (100); HRMS calcd for $C_{19}H_{21}{}^{79}BrO_2S^{80}Se$: 471.9611. Found: 471.9615. Anal. calcd for $C_{19}H_{21}BrO_2SSe$: C, 48.32; H, 4.48. Found: C, 48.46; H, 4.65.

7.3.13 (*E*)-2-[(*p*-Bromomethyl)benzenesulfonyl]-1-phenyl-1-(phenylseleno) ethene (325)

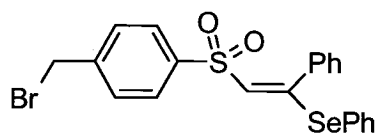

325

The same procedure as for **326** was employed, using phenylacetylene, to afford 90% of **325**: mp 128-129 °C (from ethyl acetate-hexanes); IR (film) 1305, 1273, 1131, 1082 cm^{-1}; ^1H NMR (300 MHz) δ 7.60 (d, J = 7.4 Hz, 2 H), 7.48-7.23 (m, 10 H), 7.16 (d, J = 6.7 Hz, 2 H), 6.18 (s, 1 H, vinyl), 4.43 (s, 2 H, BrC**H**$_2$); ^{13}C NMR (75 MHz) δ 158.3 (C), 142.5 (C), 141.4 (C), 136.5 (CH), 134.3 (C), 130.18 (CH), 130.15 (CH), 129.3 (CH), 129.1 (CH), 128.3 (CH), 127.9 (CH), 127.8 (CH), 126.6 (C), 125.5 (CH), 31.6 (CH_2, Br**C**H$_2$); MS (*m/z*, %) 492 (M^+, 18), 259 (54), 157 (59), 90 (100); HRMS calcd for $C_{21}H_{17}{}^{79}BrO_2S^{80}Se$: 491.9298. Found: 491.9311. Anal. calcd for $C_{21}H_{17}BrO_2SSe$: C, 51.24; H, 3.48. Found: C, 51.11; H, 3.37.

7.3.14 (*E*)-2-[(*p*-Bromomethyl)benzenesulfonyl]-1-phenylseleno-1-trimethylsilylethene (327)

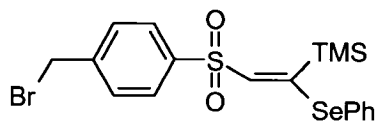

327

The same procedure as for **326** was employed, using trimethylsilylacetylene, to afford 93% of **327**: mp 99-101 °C (from ethyl acetate-hexanes); IR (KBr) 1320, 1304, 1247, 1147, 1085 cm^{-1}; ^1H NMR (300 MHz) δ 7.66 (d, J = 8.2 Hz, 2 H), 7.48 (d, J = 8.2 Hz, 2 H), 7.46-7.32 (m, 5 H), 6.03 (s, 1 H, vinyl), 4.48 (s, 2 H, BrC**H**$_2$), 0.50 (s, 9 H, Si**Me**$_3$); ^{13}C NMR (75 MHz) δ 161.6 (C), 142.7 (C), 141.2 (C), 136.8 (CH), 130.8 (CH), 130.2 (CH), 129.9 (CH), 129.6 (CH), 127.4 (CH), 126.6 (C), 31.5 (CH_2, Br**C**H$_2$), 0.4 (CH_3, $SiMe_3$); MS (*m/z*, %) 488 (M^+, 6), 473 (20), 182 (41), 73 (100); HRMS calcd for $C_{18}H_{21}{}^{79}BrO_2S^{80}SeSi$: 487.9380. Found: 487.9428. Anal. calcd for $C_{18}H_{21}BrO_2SSeSi$: C, 44.27; H, 4.33. Found: C, 44.19; H, 4.23.

7.3.15 Preparation of Resin 304b from 328

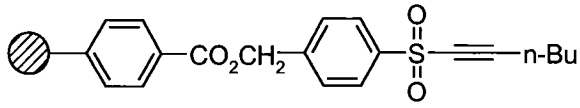

304b

Benzoic acid resin **328** (1.50 g, 0.86 mmol/g), prepared from Merrifield resin (**64**, 1.2 mmol/g), was suspended in 30 mL of DMF under a nitrogen atmosphere. Bromide **326** (1.54 g, 3.21 mmol), cesium iodide (0.78 g, 3.0 mmol) and DIPEA (0.39 g, 3.0 mmol) were added and the suspension was stirred at room temperature for 1 d. The mixture was filtered, washed with water, DMF, dichloromethane, methanol and ether, followed by drying under reduced pressure, to afford a yellow resin. The latter was then suspended in 25 mL of THF and 3.0 mL of 30% hydrogen peroxide were added. The mixture was stirred and heated at 60 °C for 2 h. The resin was filtered and washed with water, THF, dichloromethane, methanol and ether, followed by drying under reduced pressure to afford 1.76 g (0.65 mmol/g) of **304b**, obtained as a white resin: IR (KBr) 2198, 1720, 1599, 1333, 1268, 1160 cm^{-1}.

7.3.16 Preparation of Resins 304a and 304d

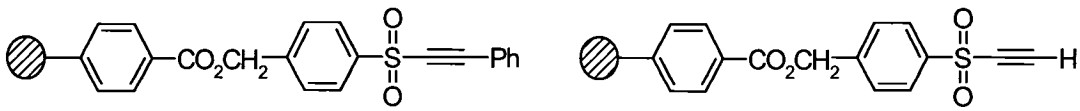

304a and **304d**

Resin **304a** (0.59 mmol/g) was obtained similarly from **328** and **325**: IR (KBr) 2176, 1716, 1599, 1338, 1266, 1153 cm^{-1}.

Resin **304c** was prepared similarly by esterification of **328** (3.00 g, 0.86 mmol/g) with **327**, followed by oxidation and selenoxide elimination conducted as follows. The esterified resin was suspended in 70 mL of chloroform. *m*CPBA (3.36 g, 77%, 15.0 mmol) was added and the mixture was stirred for 10 h at room temperature and then refluxed for

5 h. The resin was filtered, washed with water, 10% aqueous K_2CO_3 solution, water, methanol and dichloromethane to afford 3.54 g of **394c** as a yellow resin: IR (KBr) 2122, 1718, 1598, 1338, 1269, 1162 cm^{-1}. Resin **304c** (3.00 g) was suspended in a mixture of 20 mL of methanol and 20 mL of 30 % aqueous K_2CO_3 solution, and the mixture was stirred at room temperature for 40 h. The resin was filtered, then washed with water, methanol, dichloromethane and ether, followed by drying under reduced pressure, to provide 2.71 g (0.36 mmol/g) of the yellow resin **304d**: IR (KBr), 2119, 1717, 1368, 1270, 1162 cm^{-1}.

7.3.17 1-[(*p*-Hydroxymethyl)benzenesulfonyl]-2-phenylethyne (329)

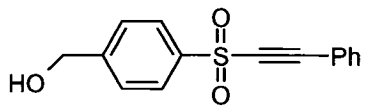

329

To determine the loading, 1.00 g of resin **304a** was hydrolyzed in 20 mL of THF containing 2.0 mL of 5% aqueous LiOH solution at room temperature overnight to give 161 mg (0.59 mmol) of **329** as a pale yellow oil: IR (film) 3419, 2180, 1330, 1156 cm^{-1}; ^1H NMR (300 MHz) δ 8.05 (d, J = 8.2 Hz, 2 H), 7.59 (d, J = 8.7 Hz, 2 H), 7.56-7.43 (m, 3 H), 7.42-7.34 (m, 2 H), 4.84 (s, 2 H, OCH_2), 2.39-1.82 (br, s, 1 H, OH); ^{13}C NMR (75 MHz) δ 147.8, 140.6, 132.7, 131.6, 128.7, 127.7, 127.2, 117.8, 93.5, 85.3, 64.2 (OCH_2). The loading of resin **304a** was determined to be 0.59 mmol/g.

7.3.18 (*p*-Hydroxymethyl)phenylmethyl sulfone (330)

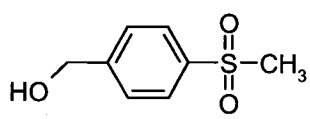

330

Similarly to **329**, 1.00g of resin **304d** was treated to afford 67 mg (0.36 mmol) of **330** as a pale yellow oil: IR (film) 3491, 1303, 1146 cm^{-1}; ^1H NMR (300 MHz) δ 7.86 (d, J = 8.7 Hz, 2 H), 7.54 (d, J = 8.2 Hz, 2 H), 4.79 (s, 2 H, OCH_2), 3.03 (s, 3 H, Me), 2.58-2.17 (br, s, 1 H, OH); ^{13}C NMR (75 MHz) δ 147.4, 139.2, 127.4, 127.2, 64.0 (OCH_2), 44.5 (Me). The loading of resin **304d** was determined to be 0.36 mmol/g.

7.3.19 Preparation of Resin 333

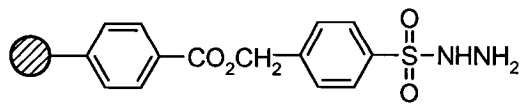

333

Benzoic acid resin **328** (4.00 g, 0.86 mmol/g) was suspended in 50 mL of DMF under nitrogen. Sulfonhydrazide **323** (2.11 g, 7.96 mmol), cesium iodide (2.08 g, 8.00 mmol) and DIPEA (1.03 g, 7.97 mmol) were added and the suspension was stirred at room temperature for 1 d. The solid was filtered, washed with water, DMF, dichloromethane, methanol, dichloromethane and ether, followed by drying under reduced pressure, to yield 4.59 g of **333** as a white resin: IR (KBr), 3365, 3269, 1717, 1335, 1267, 1154 cm^{-1}. Elemental analysis of the resin indicated it to contain 1.88% nitrogen, which corresponds to a loading of 0.67 mmol/g.

7.3.20 Preparation of Resins 304a, 304b, and 304d from Resin 333

Sulfonhydrazide resin **333** (4.00 g, 0.67 mmol/g) was stirred in 30 mL of THF-methanol (1:1). Benzeneseleninic acid (**268**, 1.50 g, 7.9 mmol) was added in portions over 15 min at room temperature. Evolution of nitrogen was observed. After stirring at room temperature overnight, the yellow resin was filtered, washed with methanol, THF and ether, and then dried under vacuum to afford 4.32 g of the corresponding polymer-

supported selenosulfonate. The latter resin (0.80 g), 1-hexyne (0.39 g, 4.8 mmol), diphenyl diselenide (31 mg, 0.10 mmol) and AIBN (16 mg, 0.10 mmol) were refluxed under a nitrogen atmosphere for 24 h in 15 mL of dry benzene. The resulting β-selenovinyl sulfone resin was filtered, washed with benzene, methanol, THF and ether. The product was then suspended in THF (30 mL) and 30% hydrogen peroxide (2.0 mL, 20 mmol) was added at room temperature. The mixture was then stirred for 2 h at 60 °C, and the resin was filtered, washed with water, methanol, THF and ether, and then dried under vacuum to afford 0.77 g (0.67 mmol/g) of **304a**, obtained as a white resin.

The selenosulfonate resin (0.80 g), phenylacetylene (0.41 g, 4.0 mmol), diphenyl diselenide (31 mg, 0.10 mmol) and AIBN (16 mg, 0.10 mmol) were refluxed under a nitrogen atmosphere for 24 h in 15 mL of dry benzene. The resulting β-selenovinyl sulfone resin was filtered, washed with benzene, methanol, THF and ether. The product was then suspended in 20 mL chloroform and *m*CPBA (0.67 g, 77%, 3.0 mmol) was added at room temperature. The mixture was refluxed for 3 h. The resin was filtered, washed with water, 10% aqueous K_2CO_3 solution, water, methanol, THF and ether, and then dried under vacuum to afford 0.76 g (0.59 mmol/g) of **304b** as a white resin.

The selenosulfonate resin (0.80 g), trimethysilylacetylene (0.41 g, 4.2 mmol), diphenyl diselenide (31 mg, 0.10 mmol) and AIBN (16 mg, 0.10 mmol) were refluxed under a nitrogen atmosphere for 24 h in 15 mL of dry benzene. The resulting β-selenovinyl sulfone resin was filtered, washed with benzene, methanol, THF and ether. The product was then suspended in chloroform (20 mL) and *m*CPBA (0.67 g, 77%, 3.0 mmol) was added at room temperature. The mixture was was refluxed for 3 h. The resin was filtered, washed with water, 10% aqueous K_2CO_3 solution, water, methanol, THF and ether. The resulting resin **304c** was then suspended in 10 mL of methanol and 10 mL of 30% aqueous K_2CO_3 solution, and the mixture was stirred at room temperature for 43 h. The resin was filtered, and then washed with water, methanol, dichloromethane and ether, followed by drying under vacuum, to provide 0.70 g (0.47 mmol/g) of **304d** as a yellow resin.

7.3.21 Chloroamine 338

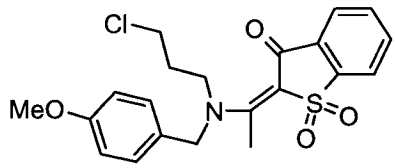

338

The chloroamine **276** was liberated from its hydrochloride salt (125 mg, 0.5 mmol) by treatment with aqueous KOH solution, extraction with dichloromethane, drying ($MgSO_4$), and concentration under reduced pressure at room temperature. A suspension of resin **321** (500 mg, 0.83 mmol/g) and the above free base **276** was refluxed for 2 d in 15 mL of benzene. The resin was filtered and washed with benzene, dichloromethane and ether. The filtrate was concentrated to dryness to afford 101 mg (58%) of crude **338** of ca. 95% purity. The residue was purified by flash chromatography (50% hexanes-ethyl acetate) to afford 88 mg (51%) of **338** as a yellow oil: IR (film) 3001, 2833, 1615, 1547, 1402, 1253, 1138 cm^{-1}; ^1H NMR (300 MHz) δ 7.92-7.84 (m, 2 H), 7.75-7.64 (m, 2 H), 7.17 (d, J = 8.7 Hz, 2 H), 6.90 (d, J = 8.7 Hz, 2 H), 4.72 (s, 2 H, NCH_2Ar), 3.81 (s, 3 H, OCH_3), 3.74-3.64 (m, 2 H), 3.63 (t, J = 5.6 Hz, 2 H), 2.76 (s, 3 H, Me), 2.07 (quintet, J = 6.7 Hz, 2 H, CH_2CH_2Cl); ^{13}C NMR (75 MHz) δ 174.6, 166.1, 159.8, 142.2, 133.5, 133.25, 133.18, 129.4, 126.6, 123.3, 120.0, 114.5, 109.4, 55.3 (2 × C), 41.1 (2 × C), 30.4, 19.4; MS (*m/z*, %) 419 (M^+, 0.8), 250 (4), 209 (9), 121 (100); HRMS calcd for $C_{21}H_{22}ClNO_4S$: 419.0958. Found: 419.0975.

7.3.22 4-3-(Methylenebicyclo[2.2.1]hept-5-ene-2-sulfonyl)benzoic acid methyl ester (339)

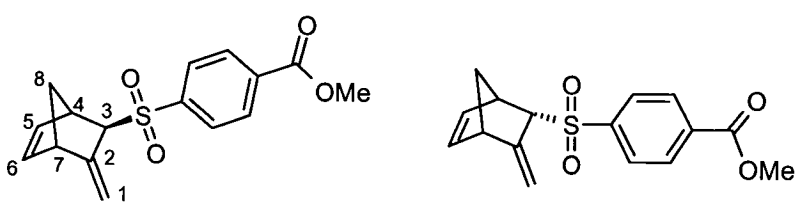

339

A suspension of cyclopentadiene (**335**, 1.0 mL) and resin **318** (400 mg, 0.83 mmol/g) in 10 mL of benzene was refluxed for 40 h and filtered. The resin was washed with benzene and then with dichloromethane, methanol, and ether, followed by drying under reduced pressure to afford 419 mg of resin. The product was cleaved from the resin by refluxing the resin overnight in 10 mL of methanol-THF (1:2) containing sodium methoxide (81 mg, 1.5 mmol). The resin was removed by filtration and was washed with methanol:THF (1:1), THF, methanol and ether. The filtrate was concentrated to dryness and extracted with dichloromethane. The organic solvent was dried over $MgSO_4$, then filtered and evaporated to give 69 mg (66%) of crude **339** with ca. 95% purity. Flash chromatography (25% hexanes-ethyl acetate) afforded 56 mg (54%) of **339** as a colourless oil, which consisted of two epimers formed in a ratio of ca. 10:1. IR (film) 2952, 1729, 1318, 1278, 1147 cm^{-1}; ^1H NMR (300 MHz, mixture of epimers) δ 8.24 (d, J = 8.7 Hz, 2 H), 8.01 (d, J = 8.7 Hz, 2 H), 6.30 (dd, J = 5.6, 3.1 Hz, 1 H, H-5 or H-6), 6.10 (dd, J = 5.6, 3.1 Hz, 1 H, H-5 or H-6), 5.29 (d, J = 2.0 Hz, 1 H, H-1), 5.13 (d, J = 2.0 Hz, 1 H, H-1), 3.98 (s, 3 H, OC**H**$_3$), 3.52 (d, J = 1.6 Hz, 1 H, H-3), 3.30 (s, 1 H), 3.17 (s, 1 H), 2.04 (d, J = 8.7 Hz, 1 H), 1.58-1.50 (m, 1 H); ^{13}C NMR (75 MHz) major epimer: δ 165.8 (C), 143.2 (C), 142.8 (C), 140.3 (CH), 135.7 (CH), 135.0 (C), 130.5 (CH), 129.3 (CH), 111.7 (CH_2, C-1), 67.8 (CH_3, O**C**H_3), 53.0 (CH), 50.9 (CH), 46.6 (CH_2, C-8), 46.0 (CH); ^{13}C NMR (75 MHz) minor epimer: δ 165.8 (C), 143.2 (C), 142.8 (C), 140.3 (CH), 135.6 (CH), 133.2 (C), 130.2 (CH), 129.1 (CH), 110.5 (CH_2), 69.5 (CH_3), 53.0 (CH), 52.5 (CH_2), 50.2 (CH), 45.7 (CH); MS (*m/z*, %) 304 (M^+, 0.5), 273 (3), 121 (27), 105 (100), 77 (57); HRMS calcd for $C_{16}H_{16}O_4S$: 304.0769. Found 304.0769.

7.3.23 2-(3-Methylenebicyclo[2.2.1]hept-5-ene-2-sulfonyl)benzoic acid methyl ester (340)

340

The products **340** were prepared from resin **321** via a similar procedure to that used for **339**. Compounds **340** were obtained with ca. 95% purity as a colourless oil, which consisted of two epimers in the ratio of ca. 6:1. IR (film) 2990, 1734, 1432, 1313, 1292, 1151 cm^{-1}; ^1H NMR (300 MHz, mixture of epimers) δ 8.08-8.04 (m, 1 H), 7.71-7.63 (m, 3 H), 6.31 (dd, J = 5.1, 3.1 Hz, 1 H, H-5 or H-6), 6.12 (dd, J = 5.1, 3.1 Hz, 1 H, H-5 or H-6), 5.28 (d, J = 1.0 Hz, 1 H, H-1), 5.10 (d, J = 1.0 Hz, 1 H, H-1), 4.23 (d, J = 2.0 Hz, 1 H, H-3), 3.96 (s, 3 H, OC**H**$_3$), 3.34 (s, 1 H), 3.19 (s, 1 H), 2.37 (d, J = 8.7 Hz, 1 H), 1.70-1.50 (m, 2 H); ^{13}C NMR (75 MHz) major epimer: δ 167.7 (C), 143.1 (C), 140.0 (CH), 137.9 (C), 135.5 (CH), 133.6 (CH), 133.3 (C), 131.2 (CH), 130.6 (CH), 129.6 (CH), 111.1 (CH_2, C-1), 67.0 (CH), 53.2 (CH_3, O**C**H$_3$), 50.6 (CH), 46.7 (CH_2, C-8), 45.9 (CH); ^{13}C NMR (75 MHz) minor epimer: δ 167.8 (C), 143.8 (C), 138.5 (C), 135.4 (CH), 133.5 (CH), 133.3 (CH), 133.2 (CH), 130.7 (CH), 129.5 (CH), 109.6 (CH_2), 68.5 (CH), 53.2 (CH_3), 52.5 (CH), 49.7 (CH_2), 45.4 (CH); MS (*m/z*, %) 304 (M^+, 8), 273 (34), 183 (46), 152 (46), 121 (85), 105 (97), 79 (100); HRMS calcd for $C_{16}H_{16}O_4S$: 304.0769. Found 304.0751.

7.3.24 4-[(*p*-Methoxycarbonyl)benzenesulfonyl]-3-mesityl-5-methyl-1,2-oxazole (341)

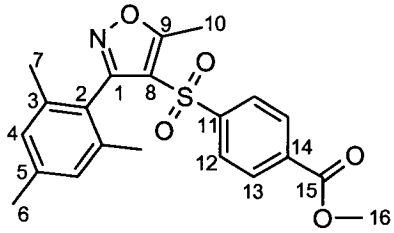

341

A suspension of nitrile *N*-oxide **336** (98 mg, 0.61 mmol) and resin **318** (400 mg, 0.87 mmol/g) in 10 mL of ether was stirred for 48 h and filtered. The resin was washed with ether and then with dichloromethane, methanol, and ether, followed by drying under reduced pressure to afford 430 mg of resin. The crude product **341** was cleaved from the resin by refluxing it in 10 mL of methanol-THF (1:2) containing sodium methoxide (81 mg, 1.5 mmol) overnight. The resin was removed by filtration and was washed with methanol-THF (1:1), THF, methanol and ether. The filtrate was concentrated to dryness

and extracted with dichloromethane. The organic solvent was dried over $MgSO_4$, then filtered and evaporated to give 97 mg (71%) of crude **341** with ca. 95% purity. Flash chromatography (25% hexanes-ethyl acetate) afforded 74 mg (54%) of **341** as a white solid: mp 98-101 °C (from ethyl acetate-hexanes); IR (KBr) 2949, 1729, 1575, 1333, 1278, 1167 cm^{-1}; ^1H NMR (300 MHz) δ 7.98 (d, J = 8.2 Hz, 2 H), 7.46 (d, J = 8.2 Hz, 2 H), 6.84, (s, 2 H, H-4), 3.97 (s, 3 H, H-16), 2.93 (s, 3 H, H-6 or H-10), 2.36 (s, 3 H, H-6 or H-10), 1.69 (s, 6 H, H-7); ^{13}C NMR (75 MHz) δ 174.5 (C-15), 165.4 (C-9), 159.7 (C), 144.2 (C), 140.0 (C), 137.9 (C), 134.6 (C), 129.9 (CH), 128.1 (CH), 127.8 (CH), 122.4 (C), 117.5 (C), 52.7 (CH_3, C-16), 21.2 (CH_3), 19.6 (CH_3), 13.3 (CH_3); MS (*m/z*, %) 399 (M^+, 4), 334 (7), 292 (10), 104 (48), 43 (100); HRMS calcd for $C_{21}H_{21}NO_5S$: 399.1140. Found 399.1161; Anal. Calcd for $C_{12}H_{21}NO_5S$: C, 63.14; H, 5.30; N, 3.51. Found: C, 62.70; H, 5.17; N, 3.40.

7.3.25 3-Mesityl-4-[(*o*-methoxycarbonyl)benzenesulfonyl]-5-methyl-1,2-oxazole (342)

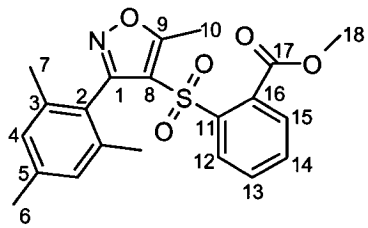

342

The product **342** was prepared from resin **321** via a similar procedure to that used for **341**. Oxazole **342** was obtained in ca. 95% purity as a colourless oil: IR (film) 2962, 1733, 1583, 1325, 1293, 1168 cm^{-1}; ^1H NMR (300 MHz) δ 7.59-7.53 (m, 2 H), 7.19-7.11 (m, 1 H), 6.94 (d, J = 8.7 Hz, 1 H), 6.75 (s, 2 H, H-4), 3.93 (s, 3 H, H-18), 2.89 (s, 3 H, H-6 or H-10), 2.33 (s, 3 H, H-6 or H-10), 1.71 (s, 6 H, H-7); ^{13}C NMR (75 MHz) δ 175.1 (C-17), 159.4 (C-9), 139.6 (C), 138.3 (C), 133.2 (C), 132.8 (C), 130.9 (C), 130.2 (CH), 128.8 (CH), 127.9 (CH), 122.7 (C), 117.5 (C), 53.0 (CH_3, C-18), 21.2 (CH_3), 18.2 (CH_3), 13.5 (CH_3); MS (*m/z*, %) 399 (M^+, 7), 334 (10), 292 (17), 276 (62), 232 (46), 200 (67), 134 (88), 91 (83), 43 (100); HRMS calcd for $C_{21}H_{21}NO_5S$: 399.1140. Found 399.1149.

7.3.26 2-*n*-Butyl-3-(*p*-hydroxymethyl)benzenesulfonyl-1-(*p*-methoxybenzyl)-2,3-dehydropiperidine (343b)

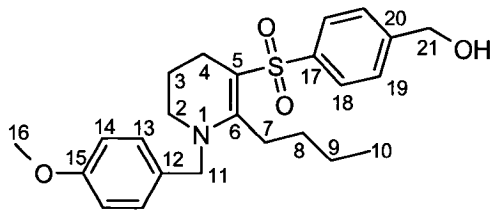

343b

The chloroamine **276** was liberated from its hydrochloride salt (316 mg, 1.26 mmol) by treatment with aqueous KOH solution, extraction with dichloromethane, drying ($MgSO_4$), and concentration under reduced pressure at room temperature. A suspension of resin **304b** (690 mg, 0.65 mmol/g) and the free base **276** was refluxed for 2 d in 20 mL of benzene. The resin was filtered and washed with benzene, dichloromethane, methanol and ether, followed by drying under reduced pressure. The product was suspended in 15 mL of dry THF and 1.0 mmol of LDA in 5 mL of THF was added at -78 °C. The mixture was stirred at -78 °C for 1 h and was then quenched with 1.0 mL of 5% aqueous LiOH solution. The mixture was stirred at room temperature overnight, filtered and washed with THF and ether. The filtrate was concentrated to dryness and the residue was triturated with dichloromethane, washed with water, dried over $MgSO_4$, filtered and evaporated to give 109 mg (57%) of **343b** with ca. 90% purity. Flash chromatography (30% hexanes-ethyl acetate) afforded a pale yellow oil: IR (film) 3442, 1558, 1283, 1252, 1124, 1078 cm^{-1}; ^1H NMR (300 MHz) δ 7.82 (d, J = 8.2 Hz, 2 H), 7.46 (d, J = 8.2 Hz, 2 H), 7.04 (d, J = 8.7 Hz, 2 H), 6.87 (d, J = 8.7 Hz, 2 H), 4.78 (s, 2 H, H-21), 4.33 (s, 2 H, H-11), 3.81 (s, 3 H, H-16), 3.05 (t, J = 6.2 Hz, 2 H, H-2), 2.77 (m, 2 H), 2.50 (t, J = 6.2 Hz, 2 H), 1.79-1.67 (m, 2 H), 1.55-1.22 (m, 4 H), 0.86 (t, J = 7.2 Hz, 3 H, H-10); ^{13}C NMR (75 MHz) δ 159.0 (C), 156.1 (C), 144.7 (C), 144.2 (C), 129.3 (C), 127.6 (CH), 126.8 (CH), 126.4 (CH), 114.2 (CH), 99.7 (C-5), 64.4 (CH_2, C-21), 55.3 (CH_3, C-16), 53.2 (CH_2, C-11), 48.5 (CH_2), 31.6 (CH_2), 28.7 (CH_2), 24.9 (CH_2), 22.9 (CH_2), 21.6 (CH_2), 13.7 (CH_3, C-10); MS (*m/z*, %) 429 (M^+, 0.6), 216 (26), 121 (100); HRMS calcd for $C_{24}H_{31}NO_4S$: 429.1974. Found:

429.1947. Similar procedure was used for the following compounds and the yield and purity are listed in Table 3.2.

7.3.27 3-(*p*-Hydroxymethyl)benzenesulfonyl-1-(*p*-methoxybenzyl)-2-phenyl-2,3-dehydropiperidine (343a)

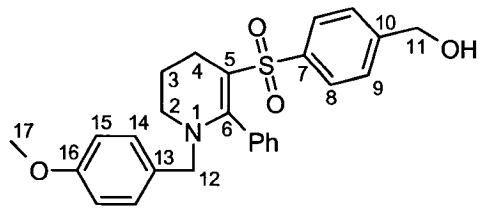

343a

The product **343a** was obtained from **304a** and **276** via a similar procedure to that used to prepare **343b** from **304b**: pale yellow oil: IR (film) 3464, 1355, 1289, 1246, 1138 cm^{-1}; ^1H NMR (300 MHz) δ 7.37 (d, J = 7.7 Hz, 2 H), 7.34-7.21 (m, 5 H), 7.14 (d, J = 7.2 Hz, 2 H), 6.97 (d, J = 8.2 Hz, 2 H), 6.81 (d, J = 8.2 Hz, 2 H), 4.67 (s, 2 H, H-11), 3.83 (s, 2 H, H-12), 3.77 (s, 3 H, H-17), 3.12 (t, J = 5.1 Hz, 2 H, H-2), 2.61 (t, J = 5.9 Hz, 2 H, H-4), 1.81 (quintet, J = 5.6 Hz, 2 H, H-3); ^{13}C NMR (75 MHz) δ 158.9 (C), 154.8 (C), 144.9 (C), 143.0 (C), 134.1 (C), 129.7 (CH), 129.2 (C), 128.7 (CH), 128.3 (CH), 127.7 (CH), 126.6 (CH), 126.3 (CH), 113.9 (CH), 103.9 (C-5), 64.1 (CH_2, C-11), 55.2 (CH_3, C-17), 54.3 (CH_2, C-12), 47.2 (CH_2), 24.4 (CH_2), 21.5 (CH_2); MS (*m/z*, %) 449 (M^+, 2), 156 (7), 121 (100); HRMS calcd for $C_{26}H_{27}NO_4S$: 449.1661. Found: 449.1659.

7.3.28 3-(*p*-Hydroxymethyl)benzenesulfonyl-1-(*p*-methoxybenzyl)-2,3-dehydropiperidine (343d)

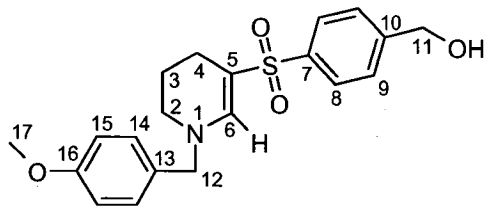

343d

The product **343d** was obtained from **304d** and **276** via a similar procedure to that used to prepare **343b** from **304b**. The product required purification by flash chromatography (30% hexanes-ethyl acetate) to afford **343d** as a pale yellow oil: IR (film) 3478, 1617, 1513, 1358, 1249, 1133 cm^{-1}; ^1H NMR (300 MHz) δ 7.78 (d, J = 8.2 Hz, 2 H), 7.49 (s, 1 H, H-6), 7.45 (d, J = 8.2 Hz, 2 H), 7.12 (d, J = 8.7 Hz, 2 H), 6.88 (d, J = 8.7 Hz, 2 H), 4.76 (s, 2 H, H-11), 4.24 (s, 2 H, H-12), 3.81 (s, 3 H, H-17), 2.93 (t, J = 5.6 Hz, 2 H, H-2), 2.23 (br, s, 1 H, OH), 2.14 (t, J = 6.2 Hz, 2 H, H-4), 1.74 (quintet, J = 5.6 Hz, 2 H, H-3); ^{13}C NMR (75 MHz) δ 159.4 (C), 145.0 (C), 144.3 (C), 141.6 (C), 128.8 (CH), 128.2 (C), 127.0 (CH), 126.9 (CH), 114.2 (CH, C-6), 100.3 (C-5), 64.4 (CH_2, C-11), 59.2 (CH_2, C-12), 55.3 (CH_3, C-17), 44.7 (CH_2, C-2), 20.9 (CH_2), 19.6 (CH_2); MS (*m/z*, %) 373 (M^+, 3), 205 (11), 121 (100); HRMS calcd for $C_{20}H_{23}NO_4S$: 373.1348. Found: 373.1353.

7.3.29 3-(*p*-Hydroxymethyl)benzenesulfonyl-4-phenyl-3,4-dehydroquinolizidine (344a)

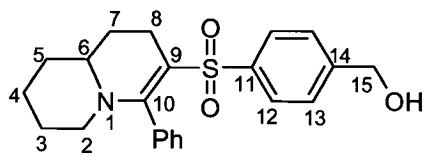

344a

The product **344a** was obtained from **304a** and **334** via a similar procedure to that used to prepare **343a** from **276**: pale yellow oil; IR (film) 3464, 1556, 1282, 1145, 1079 cm^{-1}; ^1H NMR (300 MHz) δ 7.37 (d, J = 8.2 Hz, 2 H), 7.34-7.24 (m, 5 H), 7.11-7.03 (m, 2 H), 4.68 (s, 2 H, H-15), 3.20-3.08 (m, 1 H), 3.00-2.83 (m, 1 H), 2.74-2.38 (m, 2 H), 2.00-1.85 (m, 1 H), 1.84-1.51 (m, 3 H), 1.50-1.28 (m, 4 H), 1.26-1.10 (m, 1 H); ^{13}C NMR (75 MHz) δ 154.7 (C), 144.6 (C), 143.4 (C), 134.7 (C), 129.8 (CH), 129.0 (CH), 128.4 (CH), 127.7 (CH), 127.5 (CH), 126.6 (CH), 126.3 (CH), 103.5 (C-9), 64.3 (CH_2, C-15), 56.7 (CH, C-6), 49.6 (CH_2), 32.5 (CH_2), 28.9 (CH_2), 26.3 (CH_2), 24.3 (CH_2), 21.8 (CH_2); MS (*m/z*, %) 383 (M^+, 36), 212 (81), 210 (100), 105 (43); HRMS calcd for $C_{22}H_{25}NO_3S$: 383.1555. Found: 383.1552.

7.3.30 4-*n*-Butyl-3-(*p*-hydroxymethyl)benzenesulfonyl-3,4-dehydroquinolizidine (344b)

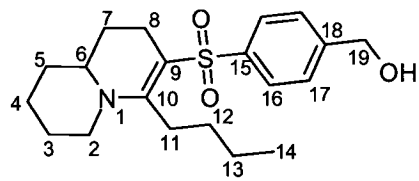

344b

The product **344b** was obtained from **304b** and **334** via a similar procedure to that used to prepare **343b** from **276**: pale yellow oil; IR (film) 3464, 1558, 1272, 1124, 1078 cm^{-1}; ^1H NMR (300 MHz) δ 7.77 (d, J = 8.2 Hz, 2 H), 7.43 (d, J = 8.2 Hz, 2 H), 4.75 (s, 2 H, H-19), 3.81-3.71 (m, 1 H), 3.10-2.97 (m, 1 H), 2.80-2.62 (m, 2 H), 2.54-2.42 (m, 1 H), 1.89-1.76 (m, 2 H), 1.72-1.22 (m, 12 H), 0.86 (t, J = 7.2 Hz, 3 H, H-14); ^{13}C NMR (75 MHz) δ 155.9 (C), 144.7 (C), 144.4 (C), 126.8 (CH), 126.2 (CH), 100.9 (C-9), 64.5 (CH_2, C-19), 57.0 (CH, C-6), 48.2 (CH_2), 32.4 (CH_2), 31.1 (CH_2), 28.7 (CH_2), 28.6 (CH_2), 26.7 (CH_2), 24.5 (CH_2), 22.8 (CH_2), 22.3 (CH_2), 13.8 (CH_3, C-14); MS (*m/z*, %) 363 (M^+, 7), 257 (100), 192 (93), 150 (62). HRMS calcd for $C_{20}H_{29}NO_3S$: 363.1868. Found: 363.1878.

7.3.31 3-(*p*-Hydroxymethyl)benzenesulfonyl-3,4-dehydroquinolizidine (344d)

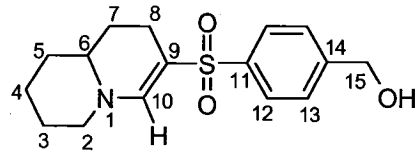

344d

The product **344d** was obtained from **304d** and **334** via a similar procedure to that used to prepare **343d** from **276**: pale yellow oil; IR (film) 3478, 1616, 1513, 1277, 1247, 1132, 1092 cm^{-1}; ^1H NMR (300 MHz) δ 7.77 (d, J = 8.2 Hz, 2 H), 7.44 (d, J = 8.2 Hz, 2 H), 7.18 (s, 1 H, H-10), 4.76 (s, 2 H, H-15), 3.34 (dt, J = 12.3, 2.0 Hz, 1 H, H-2), 3.03 (td, J = 12.3, 3.1 Hz, 1 H, H-2), 2.93-2.82 (m, 1 H), 2.28-2.04 (m, 2 H), 1.98-1.78 (m, 2 H), 1.74-1.16 (m, 6 H); ^{13}C NMR (75 MHz) δ 145.0 (C), 144.9 (CH), 141.3 (C), 127.1 (CH), 126.9 (CH), 101.9 (C-9), 64.4 (CH_2, C-15), 54.0 (CH, C-6), 53.0 (CH_2), 31.5 (CH_2), 28.7 (CH_2), 25.9 (CH_2), 23.9 (CH_2), 19.0 (CH_2); MS (*m/z*, %) 307 (M^+, 7), 136 (23), 83 (24), 43 (100); HRMS calcd for $C_{16}H_{21}NO_3S$: 307.1242. Found: 307.1226.

7.3.32 2-*n*-Butyl-3-(*p*-hydroxymethyl)benzenesulfonylnorbornadiene (345b)

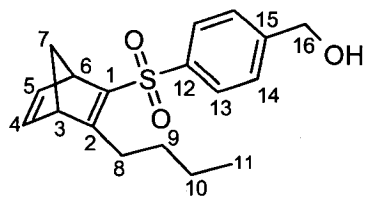

345b

A mixture of cyclopentadiene **(335)** (1.0 mL) and resin **304b** (250 mg, 0.65 mmol/g) in 20 mL of benzene was refluxed for 30 h. The resin was filtered, washed with benzene, dichloromethane, methanol and ether, followed by drying under reduced pressure. The resin was suspended in 10 mL of THF and 1.0 mL of 5% aqueous LiOH was added. The mixture was then stirred at room temperature overnight and filtered, followed

by washing with THF, chloroform and ether. The filtrate was concentrated to dryness and triturated with dichloromethane. The mixture was dried over $MgSO_4$, filtered and evaporated to give 27 mg (52%) of crude **345b** with ca. 95% purity. Flash chromatography (40% hexanes-ethyl acetate) afforded pure **345b** as a colourless oil: IR (film) 3504, 1610, 1308, 1139 cm^{-1}; ^1H NMR (300 MHz) δ 7.77 (d, J = 8.2 Hz, 2 H), 7.50 (d, J = 8.2 Hz, 2 H), 6.54 (s, 2 H, H-4 and H-5), 4.80 (s, 2 H, H-16), 3.69 (s, 1 H), 3.60 (s, 1 H), 3.83-3.70 (m, 2 H), 2.06 (d, J = 6.7 Hz, 2 H), 1.91 (d, J = 6.7 Hz, 2 H), 1.42-1.24 (m, 4 H), 0.94 (t, J = 6.9 Hz, 3 H, H-11); ^{13}C NMR (75 MHz) δ 170.6 (C), 146.1 (C), 144.6 (C), 142.6 (CH), 139.7 (CH), 139.4 (C), 127.5 (CH), 126.9 (CH), 70.6 (CH_2, C-7), 64.3 (CH_2, C-16), 56.4 (CH), 52.3 (CH), 28.9 (CH_2), 28.8 (CH_2), 22.6 (CH_2), 13.9 (CH_3, C-11); MS (*m/z*, %) 318 (M^+, 32), 253 (33), 117 (72), 91 (94), 77 (100); HRMS calcd for $C_{18}H_{22}O_3S$: 318.1290. Found: 318.1275. Similar procedure was used for the following compounds and the yield and purity are listed in Table 3.2.

7.3.33 2-(*p*-Hydroxymethyl)benzenesulfonyl-3-phenylnorbornadiene (345a)

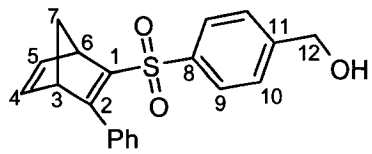

345a

The product **345a** was prepared from resin **304a** via a similar procedure to that used for **345b**: pale yellow oil; IR (film) 3505, 1304, 1144, 1085 cm^{-1}; ^1H NMR (300 MHz) δ 7.56 (d, J = 8.2 Hz, 2 H), 7.46-7.41 (m, 2 H), 7.39-7.32 (m, 5 H), 6.77 (dd, J = 5.1 Hz, 2.6 Hz, 1 H, H-4 or H-5), 6.59 (dd, J = 5.1 Hz, 2.6 Hz, 1 H, H-4 or H-5), 4.73 (s, 2 H, H-12), 3.96 (s, 1 H), 3.87 (s, 1 H), 2.32 (d, J = 6.7 Hz, 1 H, H-7), 2.02 (d, J = 6.7 Hz, 1 H, H-7); ^{13}C NMR (75 MHz) δ 164.7 (C), 146.3 (C), 146.2 (C), 142.8 (CH), 139.5 (CH), 138.5 (C), 133.6 (C), 129.2 (CH), 127.9 (CH), 127.8 (CH), 127.7 (CH), 126.6 (CH), 70.3 (CH_2, C-7), 64.2 (CH_2, C-12), 59.7 (CH), 54.0 (CH); MS (*m/z*, %) 338 (M^+, 5) 273 (13), 167 (100); HRMS calcd for $C_{20}H_{18}O_3S$: 338.0977. Found: 338.0961.

7.3.34 2-(*p*-Hydroxymethyl)benzenesulfonylnorbornadiene (345d)

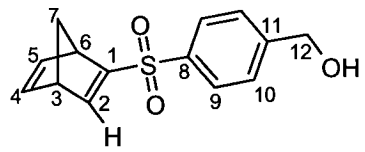

345d

The product **345d** was prepared from resin **304d** via a similar procedure to that used for **345b**. The product solidified on standing, mp 62-65 °C; IR (film) 3505, 1297, 1162, 1141cm^{-1}; ^{1}H NMR (300 MHz) δ 7.71 (d, J = 8.7 Hz, 2 H), 7.48 (d, J = 7.7 Hz, 2 H), 7.48 (s, 1 H, H-2), 6.64-6.56 (m, 2 H, H-4 and H-5), 4.76 (s, 2 H, H-12), 3.79 (s, 1 H), 3.66 (s, 1 H), 2.80-2.30 (br, s, 1 H, OH), 2.16 (d, J = 6.7, 1 H, H-7), 2.07 (d, J = 6.7, 1 H, H-7); ^{13}C NMR (75 MHz) δ 157.3 (C), 153.5 (CH), 147.0 (C), 142.4 (CH), 141.0 (CH), 137.5 (C), 127.9 (CH), 127.0 (CH), 74.0 (CH_2, C-7), 64.0 (CH_2, C-12), 51.5 (CH), 50.8 (CH); MS (*m/z*, %) 262 (M^+, 7), 91 (100); HRMS calcd for $C_{14}H_{14}O_3S$: 262.0664. Found: 262.0673.

7.3.35 5-*n*-Butyl-4-(*p*-hydroxymethyl)benzenesulfonyl-3-mesityl-1,2-oxazole (346b)

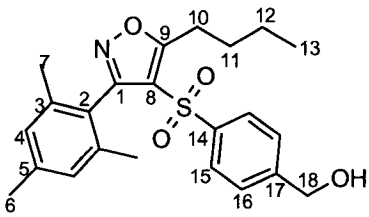

346b

Nitrile *N*-oxide **336** (91 mg, 0.57 mmol) and resin **304b** (300 mg, 0.65 mmol/g) were stirred for 30 h in 10 mL of ether. The resin was filtered and washed with ether, dichloromethane, methanol and ether, followed by drying under reduced pressure. The product was suspended in 10 mL of THF and 1.0 mL of 5% aqueous LiOH was added. The mixture was then stirred at room temperature overnight and filtered, followed by

washing with THF, chloroform and ether. The filtrate was concentrated to dryness and triturated with dichloromethane. The mixture was dried over $MgSO_4$, filtered and evaporated to give 39 mg (48%) of the crude **346b** with ca. 95% purity. Flash chromatography (40% hexanes-ethyl acetate) afforded pure **346b** as a colourless oil: IR (film) 3441, 1570, 1330, 1161, 1134, 1057 cm^{-1}; ^1H NMR (300 MHz) δ 7.36 (d, J = 8.7 Hz, 2 H), 7.31 (d, J = 8.7 Hz, 2 H), 6.83 (s, 2 H, H-4), 4.77 (s, 2 H, H-18), 3.33, (t, J = 7.7 Hz, 2 H, H-10), 2.35 (s, 3 H, H-6), 1.96-1.85 (m, 2 H), 1.70 (s, 6 H, H-7), 1.58-1.46 (m, 2 H), 1.03 (t, J = 7.2 Hz, 3 H, H-13); ^{13}C NMR (75 MHz) δ 177.6 (C), 159.7 (C), 147.0 (C), 139.7 (C), 139.5 (C), 138.1 (C), 128.04 (CH), 128.01 (CH), 126.5 (CH), 122.8 (C), 117.6 (C), 64.1 (CH_2, C-18), 29.8 (CH_2), 26.9 (CH_2), 22.4 (CH_2), 21.3 (CH_3), 19.6 (CH_3), 13.7 (CH_3, C-13); MS (*m/z*, %) 413 (M^+, 40), 242 (46), 186 (59), 158 (90), 41 (100); HRMS calcd for $C_{23}H_{27}NO_4S$: 413.1661. Found 413.1685. Similar procedure was used for the following compounds and the yield and purity are listed in Table 3.2.

7.3.36 4-(*p*-Hydroxymethyl)benzenesulfonyl-3-mesityl-5-phenyl-1,2-oxazole (346a)

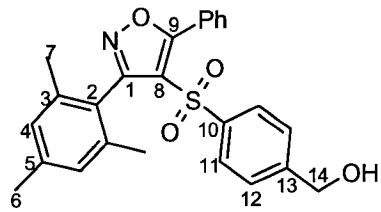

346a

The product **346a** was prepared from resin **304a** via a similar procedure to that used for **346b**, which solidified upon standing: mp 150-153 °C; IR (film) 3437, 1557, 1366, 1327, 1162 cm^{-1}; ^1H NMR (300 MHz) δ 7.99 (dd, J = 8.2, 1.5 Hz, 2 H), 7.64-7.55 (m, 3 H), 7.33 (d, J = 8.2 Hz, 2 H), 7.25 (d, J = 8.7 Hz, 2 H), 6.86 (s, 2 H, H-4), 4.73 (s, 2 H, H-14), 2.36 (s, 3 H, H-6), 1.86 (s, 6 H, H-7); ^{13}C NMR (75 MHz) δ 172.7 (C-9), 160.6 (C), 147.1 (C), 139.8 (C), 139.2 (C), 138.1 (C), 131.9 (C), 130.1 (CH), 128.4 (CH), 128.10 (CH), 128.06 (CH), 126.4 (CH), 125.9 (C), 123.0 (C), 118.3 (C), 64.1 (CH_2, C-14), 21.3 (CH_3), 19.9 (CH_3); MS (*m/z*, %) 433 (M^+, 13), 243 (35), 105 (100), 91 (67), 77 (66); HRMS calcd for $C_{25}H_{23}NO_4S$: 433.1348. Found: 433.1351.

7.3.37 4-(*p*-Hydroxymethyl)benzenesulfonyl-3-mesityl-1,2-oxazole (346d)

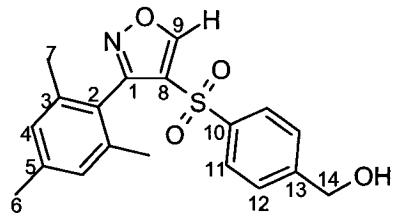

346d

The product **346d** was prepared from resin **304d** via a similar procedure to that used for **346b**, which solidified upon standing: mp 118-122 °C; IR (KBr) 3437, 1341, 1160, 1112 cm^{-1}; ^1H NMR (300 MHz) δ 8.10 (d, J = 8.7 Hz, 2 H), 7.64 (d, J = 8.7 Hz, 2 H), 6.94 (s, 2 H, H-4), 6.90 (s, 1 H, H-9), 4.86 (s, 2 H, H-14), 2.32 (s, 3 H, H-6), 2.09 (s, 6 H, H-7); ^{13}C NMR (75 MHz) δ 167.3 (C), 162.5 (C), 148.6 (C), 139.8 (C), 137.1 (C), 136.9 (C), 128.9 (CH), 128.7 (CH), 127.5 (CH), 123.9 (CH), 109.6 (CH), 64.1 (CH_2, C-14), 21.1 (CH_3), 20.3 (CH_3); MS (*m/z*, %) 357 (M^+, 21), 186 (100), 158 (77); HRMS calcd for $C_{19}H_{19}NO_4S$: 357.1035. Found: 357.1059.

7.3.38 5-Butyl-4-(*p*-hydroxymethyl)benzenesulfonyl-1-methylpyrazole (347b) and 4-Butyl-5-(*p*-hydroxymethyl)benzenesulfonyl-1-methylpyrazole (348b)

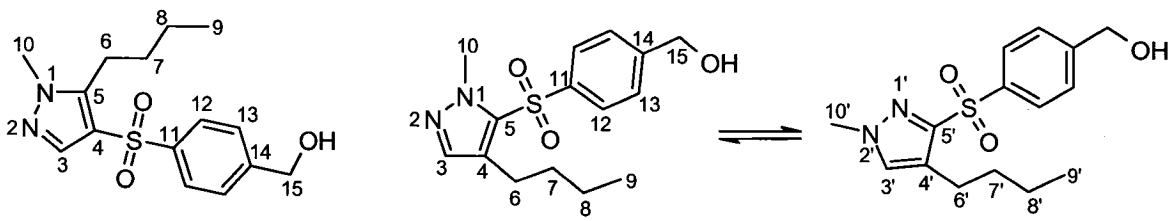

347b and **348b**

To a suspension of resin **304b** (400 mg, 0.65 mmol/g) in 10 mL of ether was added diazomethane (2.0 mmol) in 6 ml of ether dropwise at 0 °C and the mixture was stirred for 26 h. The excess diazomethane was quenched by adding acetic acid. The resin was filtered

and washed with ether and then with dichloromethane, methanol, and ether, followed by drying under reduced pressure to afford 406 mg of the resin. The resin was suspended in 10 mL of THF and 1.0 mL of 5% LiOH aqueous solution was added. The mixture was then stirred at room temperature overnight and filtered, followed by washing with THF, chloroform and ether. The filtrate was concentrated to dryness and extracted with dichloromethane. The organic solvent was dried over $MgSO_4$ and then filtered and evaporated to give 51 mg of crude product, which was purified by flash chromatography (40% hexanes-ethyl acetate) to afford 11 mg (14%) of the less polar regioisomer **347b** as a colourless oil: IR (film) 3399, 2953, 1312, 1156, 1119 cm^{-1}; ^1H NMR (300 MHz) δ 7.87 (d, J = 8.2 Hz, 2 H), 7.55 (d, J = 8.2 Hz, 2 H), 7.35 (s, 1 H, H-3), 4.81 (s, 2 H, H-15), 4.02 (s, 3 H, H-10), 2.77 (t, J = 7.2 Hz, 2 H, H-6), 2.05-1.75 (br, s, 1 H, OH), 2.70-2.55 (m, 2 H), 2.50-2.35 (m, 2 H), 0.95 (t, J = 7.2 Hz, 3 H, H-9); ^{13}C NMR (75 MHz) δ 147.2, 140.3, 138.4, 134.8, 128.0, 127.3, 127.2, 64.1 (C-15), 39.5, 32.6, 23.9, 22.5, 13.9 (C-9); MS (*m/z*, %) 308 (M^+, 6), 279 (16), 266 (56), 201 (32), 137 (37), 95 (100); HRMS calcd for $C_{15}H_{20}N_2O_3S$: 308.1195. Found 308.1196.

Further elution (25% hexanes-ethyl acetate) afforded 34 mg (44%) of the more polar regioisomer **348b** as a colourless oil, which solidified upon standing. Product **348b** consisted of two tautomers formed in a ratio of ca. 2:1; mp 86-89 °C; IR (film) 3383, 2929, 1520, 1308, 1160 cm^{-1}; ^1H NMR (300 MHz, both tautomers) δ 7.89 (d, J = 8.2 Hz, 2 H), 7.84 (s, 1 H, H-3 or H-3′), 7.81 (s, 1 H, H-3 or H-3′), 7.50 (d, J = 7.7 Hz, 2 H), 4.79 (s, 2 H, H-15), 3.86 (s, 3 H, H-10 or H-10′), 3.78 (s, 3 H, H-10 or H-10′), 2.82 (t, J = 7.7 Hz, 2 H, H-6 or H-6′), 2.67 (d, J = 7.7 Hz, 2 H, H-6 or H-6′), 2.15-1.90 (br, s, 1 H, OH), 1.59-1.45 (m, 2 H), 1.43-1.23 (m, 2 H), 0.91 (t, J = 6.7 Hz, 3 H, H-9 or H-9′), 0.88 (t, J = 7.7 Hz, 3 H, H-9 or H-9′); ^{13}C NMR (75 MHz, both tautomers) 152.3, 146.3, 146.2, 145.1, 142.2, 141.8, 139.3, 134.0, 127.8, 127.2, 127.1, 127.0, 126.9, 120.8, 64.2 (C-15), 39.3, 36.7, 30.8, 30.5, 26.3, 24.0, 22.6, 22.5, 13.8, 13.7; MS (*m/z*, %) 308 (M^+, 9), 279 (15), 266 (52), 201 (36), 137 (40), 95 (100); HRMS calcd for $C_{15}H_{20}N_2O_3S$: 308.1195. Found 308.1199.

7.3.39 4-(*p*-Hydroxymethyl)benzenesulfonyl-1-methyl-5-phenylpyrazole (348a)

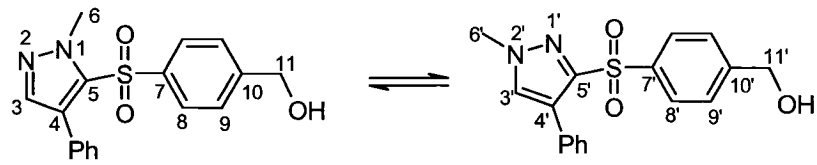

348a

The product **348a** was prepared from resin **304a** via a similar procedure to that used for **347b** and **348b**. Product **348a** was a colourless oil that consisted of two tautomers formed in a ratio of ca. 1.2:1; IR (film) 3397, 2922, 1596, 1307, 1165, 1140 cm^{-1}; ^1H NMR (300 MHz, both tautomers) δ 8.01 (s 1 H, H-3 or H-3′), 7.99 (s, 1 H, H-3 or H-3′), 7.64-7.31(m, 5 H), 7.30-7.15 (m, 4 H), 4.67 (s, 2 H, H-11 or H-11′), 4.66 (s, 2 H, H-11 or H-11′), 3.94 (s, 3 H, H-6 or H-6′), 3.64 (s, 3 H, H-6 or H-6′), 2.75-2.26 (br, s, 1 H, OH); ^{13}C NMR (75 MHz, major tautomer) δ 146.4 (C), 146.3 (C), 141.0 (C), 139.3 (CH), 130.6 (C), 130.1 (CH), 129.2 (CH), 128.5 (CH), 127.15 (CH), 126.5 (CH), 122.3 (C), 64.0 (CH_2), 37.5 (CH_3); ^{13}C NMR (75 MHz, minor tautomer) δ 150.4 (C), 143.9 (C), 140.7 (C), 135.3 (CH), 130.6 (C), 130.2 (CH), 129.0 (CH), 128.1 (CH), 127.21 (CH), 126.6 (CH), 121.8 (C), 64.0 (CH_2), 39.5 (CH_3); MS (*m/z*, %) 328 (M^+, 75), 233 (29), 105 (47), 89 (48), 77 (100); HRMS calcd for $C_{17}H_{16}N_2O_3S$: 328.0882. Found 328.0897.

7.3.40 2-*n*-Butyl-1-(*p*-methoxybenzyl)piperidine (280)

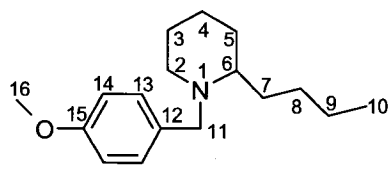

280

Chloroamine **276** was liberated from its hydrochloride salt (217 mg, 0.87 mmol) and added to resin **304b** (600 mg, 0.65 mmol/g) to effect conjugate addition and base-

mediated cyclization as in the case of **343b**, except that LiHMDS was employed instead of LDA. The resulting resin was filtered, washed and dried as in the case of **343b**. It was then suspended in 25 mL of dichloromethane containing $NaCNBH_3$ (375 mg, 5.97 mmol). TFA (0.44 mL, 5.7 mmol) was added dropwise and the mixture was stirred at room temperature for 50 min and refluxed for 50 min. The resin was filtered, washed with aqueous KOH solution, water, methanol, THF and ether, and then dried under vacuum. The product was suspended in 25 mL of dry THF and finely ground 5% sodium amalgam (4.44 g, 9.65 mmol of Na) was added. The mixture was refluxed under nitrogen for 30 h and filtered through a Celite pad, followed by washing with THF. The filtrate was washed with water, dried over $MgSO_4$, filtered and concentrated *in vacuo* to afford 50 mg (46%) of **280** with ca. 90% purity. Flash chromatography (20% ethyl acetate-hexanes) afforded pure **280** as a pale yellow oil: IR (film) 1612, 1509, 1245, 1039 cm^{-1}; ^1H NMR (300 MHz) δ 7.25 (d, J = 8.7 Hz, 2 H), 6.85 (d, J = 8.7 Hz, 2 H), 3.93 (d, J = 13.3 Hz, 1 H, H-11), 3.81 (s, 3 H, H-16), 3.22 (d, J = 12.8 Hz, 1 H, H-11), 2.79-2.70 (m, 1 H), 2.32-2.21 (m, 1 H), 2.09-1.98 (m, 1 H), 1.75-1.22 (m, 12 H), 0.92 (t, J = 6.7 Hz, 3 H, H-10); ^{13}C NMR (75 MHz) δ 158.5 (2 × C), 130.2 (CH), 113.5 (CH), 60.7 (CH, C-6), 56.7 (CH_2, C-11), 55.2 (CH_3, C-16), 51.5 (CH_2), 31.3 (CH_2), 30.1 (CH_2), 27.7 (CH_2), 25.0 (CH_2), 23.6 (CH_2), 23.2 (CH_2), 14.1 (CH_3, C-10); MS (*m/z*, %) 261 (M^+, 0.6), 261 (1.6, M^+-1), 204 (12), 121 (100); HRMS calcd for $C_{17}H_{26}NO$ (M^+- H): 260.2014. Found: 260.2001. Similar procedure was used for compound **349a** and the yield and purity are listed in Table 3.3.

7.3.41 1-(*p*-Methoxybenzyl)-2-phenylpiperidine (349a)

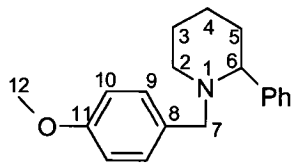

349a

The product **349a** was obtained from **304a** and **276** via a similar procedure to that used to prepare **280** from **304b**: mp 82-83 °C (from hexanes); IR (KBr) 1507, 1247, 1092,

1035 cm^{-1}; ^1H NMR (300 MHz) δ 7.51-7.45 (m, 2 H), 7.42-7.33 (m, 2 H), 7.30-7.20 (m, 1 H), 7.17 (d, J = 8.7 Hz, 2 H), 6.82 (d, J = 8.2 Hz, 2 H), 3.79 (s, 3 H, H-12), 3.76-3.66 (m, 1 H), 3.09 (d, J = 15.0 Hz, 1 H, H-7), 3.02-2.91 (m, 1 H), 2.77 (d, J = 13.4 Hz, 1 H, H-7), 1.93 (m, 1 H), 1.82-1.70 (m, 2 H), 1.67-1.48 (m, 3 H), 1.46-1.27 (m, 1 H); ^{13}C NMR (75 MHz) δ 158.3 (C-11), 145.8(C), 131.7 (C), 129.8 (CH), 128.45 (CH), 128.39 (CH), 127.4 (CH), 126.8 (CH), 113.44 (CH), 113.37 (CH), 69.1 (CH_3, C-12), 59.0 (CH, C-6), 55.2 (CH_2), 53.1 (CH_2), 37.0 (CH_2), 26.0 (CH_2), 25.2 (CH_2); MS (*m/z*, %) 281 (M^+, 12), 204 (22), 160 (11), 121 (100); HRMS calcd for $C_{19}H_{23}NO$: 281.1780. Found: 281.1784.

7.3.42 1-Hydroxy-3-imino-3-mesityl-1-phenyl-1-propene (352)

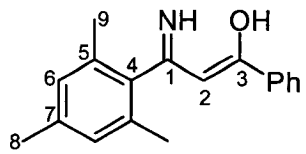

352

The cycloaddition of **346** with resin **304a** was performed as in the preparation of **346a** and subsequent desulfonylation was performed with 5% sodium amalgam in THF as in the preparation of **349a**. The crude product was purified by flash chromatography (30% ethyl acetate-hexanes) to afford **352** (34%) as a colourless oil: IR (KBr) 3337, 1595, 1599, 1529, 1320, 1289 cm^{-1}; ^1H NMR (300 MHz) δ 10.51-10.28 (br, s, 1 H, NH), 7.91 (dd, J = 7.9, 1.2 Hz, 2 H), 7.50-7.37 (m, 3 H), 6.93 (s, 2 H, H-6), 5.79 (d, J = 1.0 Hz, 1 H, H-2), 5.22-5.10 (br, s, 1 H, OH), 2.34 (s, 6 H, H-9), 2.33 (s, 3 H, H-8); ^{13}C NMR (75 MHz) δ 190.1 (C-3), 163.6 (C-1), 140.1 (C), 138.5 (C), 135.1 (C), 134.9 (C), 131.0 (CH), 128.3 (CH), 128.2 (CH), 127.2 (CH), 93.6 (CH, C-2), 21.1 (CH_3), 19.3 (CH_3); MS (*m/z*, %) 265 (34, M^+), 250 (85), 236 (25), 146 (35), 121 (39), 105 (100). HRMS calcd for $C_{18}H_{19}NO$: 265.1467. Found: 265.1489.

7.4 Experiments Pertaining to Chapter 4

7.4.1 2-Butyl-1,4-diphenyl-3-(*p*-toluenesulfonyl)-oxabenzonorbornadiene (353)

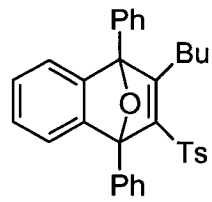

353

A solution of diphenylisobenzofuran (**110**, 567 mg, 2.10 mmol) and 1-(*p*-toluenesulfonyl)-1-hexyne (**1a**, 472 mg, 2.00 mmol) in 4.5 mL of toluene was heated in a sealed V-vial at 109 °C for 1 d. The mixture was concentrated under reduced pressure and separated by flash chromatography (elution with 10% ethyl acetate-hexanes) to afford 806 mg (80%) of the cycloadduct **353** as a light yellow oil. Crystallization from ethyl acetate-hexanes gave white crystals: mp 159-164 °C; IR (KBr) 1600, 1452, 1317, 1146 cm^{-1}; ^1H NMR (300 MHz) δ 7.88-7.78 (m, 4 H), 7.63-7.44 (m, 5 H), 7.36-7.29 (m, 3 H), 7.15-7.06 (m, 4 H), 6.99 (d, J = 8.2 Hz, 2 H), 2.94 (ddd, J = 12.3, 10.5, 5.3 Hz, 1 H), 2.66 (ddd, J = 12.0, 10.5, 4.3 Hz, 1 H), 2.34 (s, 3 H, tolyl Me), 1.36-0.98 (m, 4 H), 0.80 (t, J = 7.2 Hz, 3 H, Me); ^{13}C NMR (75 MHz) δ 171.8 (C), 149.7 (C), 148.2 (C), 147.9 (C), 143.4 (C), 137.9 (C), 134.0 (C), 133.5 (C), 129.0 (CH), 128.6 (CH), 128.5 (CH), 128.3 (CH), 128.1 (CH), 127.7 (CH), 127.2 (CH), 126.6 (CH), 125.9 (CH), 125.4 (CH), 121.4 (CH), 120.9 (CH), 93.4 (C), 91.6 (C), 30.1 (CH_2), 26.5 (CH_2), 22.7 (CH_2), 21.5 (CH_3, tolyl Me), 13.6 (CH_3, Me); MS (*m/z*, %) 506 (M^+, 0.4), 350 (100), 270 (99), 105 (98), 77 (73); HRMS calcd for $C_{33}H_{30}O_3S$: 506.1916. Found 50.1961. Anal. Calcd for $C_{33}H_{30}O_3S$: C, 78.23; H, 5.97. Found: C, 77.89; H, 5.76. The X-ray structure of **353** is shown in Fig. 4.1 and additional crystallographic data is given in Appendix VI.

7.4.2 1,2,4-Triphenyl-3-(*p*-toluenesulfonyl)-oxabenzonorbornadiene (354)

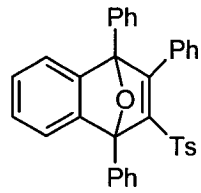

354

A solution of **110** (567 mg, 2.10 mmol) and 1-phenyl-2-(p-toluenesulfonyl)ethyne (**1b**, 512 mg, 2.00 mmol) in 4.5 mL of toluene was heated in a sealed V-vial at 124 °C for 42 h. The reaction mixture was concentrated under reduced pressure and separated by flash chromatography (elution with 40% pentane-dichloromethane) to afford 852 mg (81%) of **354** as a light yellow oil. Crystallization from methanol gave white crystals: mp 200-202 °C; IR (KBr) 1595, 1450, 1312, 1304, 1143 cm^{-1}; ^1H NMR (300 MHz) δ 8.05 (d, J = 6.7 Hz, 2 H), 7.81 (d, J = 6.7 Hz, 1 H), 7.57-7.37 (m, 5 H), 7.34-7.21 (m, 6 H), 7.16 (d, J = 7.2 Hz, 1 H), 7.09 (d, J = 8.2 Hz, 1 H), 7.07 (d, J = 7.2 Hz, 1 H), 6.89 (d, J = 7.2 Hz, 2 H), 6.71-6.62 (m, 4 H), 2.17 (s, 3 H, tolyl Me); ^{13}C NMR (75 MHz) δ 167.1 (C), 153.4 (C), 149.9 (C), 149.6 (C), 143.2 (C), 136.9 (C), 133.9 (C), 132.5 (C), 132.2 (C), 129.33 (CH), 129.32 (CH), 129.2 (CH), 128.9 (CH), 128.8 (CH), 128.39 (CH), 128.37 (CH), 128.2 (CH), 127.7 (CH), 127.3 (CH), 126.1 (CH), 125.7 (CH), 123.3 (CH), 122.3 (CH), 95.7 (C), 95.4 (C), 21.5 (CH_3, tolyl Me); MS (*m/z*, %) 526 (M^+, 0.2), 510 (0.7), 371 (100), 270 (78); HRMS calcd for $C_{35}H_{26}O_3S$: 526.1603. Found 526.1628; Anal. Calcd for $C_{35}H_{26}O_3S$: C, 79.82; H, 4.98. Found: C, 79.60; H, 4.98.

7.4.3 2-*n*-Butyl-2,4-diphenyl-3-(*p*-toluenesulfonyl)-2*H*-naphthalen-1-one (355) and 2-(*E*-1-Butenyl)-1,4-diphenyl-3-(*p*-toluenesulfonyl)naphthalene (356)

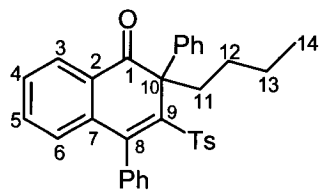

355

and

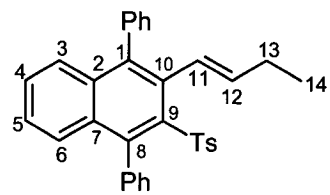

356

A solution of **353** (342 mg, 0.676 mmol) in 4 mL of xylenes was heated in a sealed V-vial at 152 °C for 60 h. The mixture was concentrated under reduced pressure to afford a colourless oil that was separated by flash chromatography (elution with 50% pentane-dichloromethane) to afford 149 mg (45%) of **356** as a colourless oil: IR (film) 1595, 1440, 1321, 1150 cm^{-1}; ^1H NMR (300 MHz) δ 7.54-7.30 (m, 14 H), 7.22-7.14 (m, 2 H), 7.12 (d, J = 8.2 Hz, 2 H), 6.42 (dt, J = 16.1, 1.5 Hz, 1 H, H-11), 4.93 (dt, J = 16.1, 6.7 Hz, 1 H, H-12), 2.36 (s, 3 H, tolyl Me), 1.80-1.68 (m, 2 H), 0.56 (t, J = 7.2 Hz, 3 H, H-14); ^{13}C NMR (75 MHz) δ 142.8 (C), 142.0 (C), 141.1 (C), 140.7 (C), 139.9 (CH), 139.3 (C), 137.7 (C), 135.9 (C), 134.34 (C), 134.30 (C), 132.5 (C), 130.9 (CH), 130.3 (CH), 128.8 (CH), 128.31 (CH), 128.26 (CH), 128.0 (CH), 127.5 (CH), 127.4 (CH), 127.2 (CH), 126.92 (CH), 126.88 (CH), 126.34 (CH), 126.26 (CH), 26.2 (CH_2), 21.5 (CH_3, tolyl Me), 12.6 (CH_3, C-14); MS (*m/z*, %) 488 (M^+, 94), 459 (11), 381 (81), 302 (97), 119 (71), 105 (100); HRMS calcd for $C_{33}H_{28}O_2S$: 488.1810. Found 488.1820.

Further elution (50% pentane-dichloromethane) provided 164 mg (48%) of **355** as a light yellow oil. Crystallization from ethyl acetate-hexanes gave white crystals: mp 186-188 °C; IR (KBr) 1677, 1594, 1447, 1315, 1301, 1137 cm^{-1}; ^1H NMR (300 MHz) δ 8.17-8.11 (m, 1 H), 7.51-7.29 (m, 10 H), 6.97 (td, J = 7.2 Hz, 1.6 Hz, 1 H), 6.84 (d, J = 8.2 Hz, 2 H), 6.71-6.66 (m, 1 H), 6.61 (d, J = 8.2 Hz, 2 H), 6.52 (d, J = 7.7 Hz, 1 H), 3.37 (td, J = 12.8 Hz, 4.1 Hz, 1 H, H-11), 3.01 (td, J = 12.8 Hz, 4.1 Hz, 1 H, H-11), 2.30 (s, 3 H, tolyl Me), 1.92-1.75 (m, 1 H), 1.58-1.42 (m, 2 H), 1.19-1.04 (m, 1 H), 0.96 (t, J = 7.2 Hz, 3 H, H-14); ^{13}C NMR (75 MHz) δ 198.4 (C-1), 148.1 (C), 144.2 (C), 142.7 (C), 141.1(C), 139.6 (C), 137.9 (C), 134.7 (CH), 134.1 (C), 131.9 (CH), 130.6 (CH), 130.2 (CH), 129.2 (CH), 128.7 (CH), 128.6 (CH), 128.3 (C), 128.1 (CH), 127.9 (CH), 127.8(CH), 127.5 (CH), 127.4 (CH), 127.2 (CH), 126.8 (CH), 60.2 (C-10), 36.3 (CH_2), 26.9 (CH_2), 23.2 (CH_2), 21.4 (CH_3, tolyl Me), 13.9 (CH_3, C-14); MS (*m/z*, %) 506 (M^+, 0.6), 449 (25), 350 (100), 306 (58), 294 (99), 264 (78), 218 (100), 91 (100); HRMS calcd for $C_{33}H_{30}O_3S$: 506.1916. Found 506.1937; Anal. Calcd for $C_{33}H_{30}O_3S$: C, 78.23; H, 5.97. Found: C, 77.92; H, 5.96. The X-ray structure of **355** is shown in Fig. 4.2 and additional crystallographic data is given in Appendix VII.

7.4.4 2,2,4-Triphenyl-3-(*p*-toluenesulfonyl)-2*H*-naphthalen-1-one (357) and 1,1,4-Triphenyl-3-(*p*-toluenesulfonyl)-1*H*-naphthalen-2-one (358)

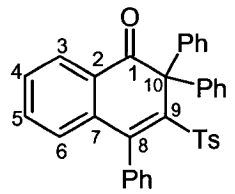

357

and

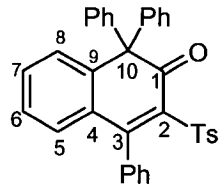

358

A solution of **354** (150 mg, 0.285 mmol) in 4 mL of xylenes was heated in a sealed V-vial at 155 °C for 60 h. The solution was cooled to room temperature, the reaction mixture was concentrated under reduced pressure, and the residue was triturated with hot methanol and filtered. The white solid was washed with methanol and dried to afford 41 mg (27%) of **357**, obtained as white crystals: mp 294.5-295.5 °C (from dichloromethane-methanol); IR (KBr) 1680, 1590, 1449, 1323, 1151 cm^{-1}; ^1H NMR (300 MHz) δ 8.03-7.98 (m, 1 H), 7.80-7.73 (m, 4 H), 7.47-7.29 (m, 11 H), 7.12 (d, J = 7.2 Hz, 2 H), 6.73 (d, J = 8.2 Hz, 2 H), 6.71-6.65 (m, 1 H), 6.00 (d, J = 8.7 Hz, 2 H), 2.26 (s, 3 H, tolyl Me); ^{13}C NMR (75 MHz) δ 198.2 (C-1), 147.9 (C), 145.5 (C), 143.0 (C), 139.2(C), 139.1 (C), 137.9 (C), 134.7 (CH), 134.5 (C), 131.1 (CH), 130.8 (CH), 130.7 (CH), 129.2 (CH), 128.3 (CH), 128.12 (CH), 128.07 (CH), 128.03 (CH), 127.98 (C), 127.8(CH), 127.7 (CH), 66.8 (C-10), 21.4 (CH_3, tolyl Me); MS (*m/z*, %) 371 (M^+-Ts, 100), 309 (12), 293 (13), 265 (15); Anal. Calcd for $C_{35}H_{26}O_3S$: C, 79.82; H, 4.98. Found: C, 80.13; H, 4.96. The X-ray structure of **357** is shown in Fig. 4.3 and additional crystallographic data is given in Appendix VIII.

The methanol filtrate was concentrated under reduced pressure and purified by flash chromatography on silica gel (elution with 20% pentane-dichloromethane) to afford 84 mg (56%) of **358**, obtained as yellow crystals: mp 187-193 °C (from methanol); IR (KBr) 1700, 1684, 1443, 1321, 1148 cm^{-1}; ^1H NMR (300 MHz) δ 7.47-7.40 (m, 3 H), 7.39-7.16 (m, 12 H), 7.04 (d, J = 8.2 Hz, 2 H), 6.95 (dd, J = 8.2, 1.5 Hz, 1 H), 6.82-6.76 (m, 4 H), 6.73 (dd, J = 7.7, 1.5 Hz, 1 H), 2.39 (s, 3 H, tolyl Me); ^{13}C NMR (75 MHz) δ 195.0 (C-1), 156.3 (C), 144.2 (C), 143.4 (C), 139.2(C), 137.5 (C), 134.8 (C), 134.3 (C), 132.2 (C), 131.5 (CH), 131.4 (CH), 131.2 (CH), 130.2 (CH), 129.0 (CH), 128.8 (CH),

128.7 (CH), 128.2 (CH), 128.1 (CH), 127.9 (CH), 127.72 (CH), 127.68 (CH), 69.6 (C-10), 21.5 (CH_3, tolyl Me); MS (*m/z*, %) 526 (M^+, 0.5), 371 (58), 330 (100), 265 (40); HRMS calcd for $C_{35}H_{26}O_3S$: 526.1603. Found 526.1635; Anal. Calcd for $C_{35}H_{26}O_3S$: C, 79.82; H, 4.98. Found: C, 79.68; H, 5.25. The X-ray structure of **358** is shown in Fig. 4.4 and additional crystallographic data is given in Appendix IX.

7.4.5 2-Butyl-1,4-diphenyl-3-(*p*-toluenesulfonyl)naphthalene (367)

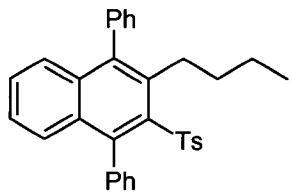

367

Product **356** (89 mg, 0.18 mmol) was dissolved in 8 mL of methanol and palladium hydroxide on charcoal (64 mg, 20% weight on C) was added. The mixture was hydrogenated at 1 atmosphere for 4 d. After filtration of the mixture through a pad of Celite, the methanol was evaporated and the residue was separated by flash chromatography (elution with 40% pentane-dichloromethane) to afford 78 mg (88%) of **367** as a colourless oil: IR (film) 1598, 1439, 1316, 1151 cm^{-1}; ^1H NMR (300 MHz) δ 7.57-7.42 (m, 3 H), 7.40-7.17 (m, 11 H), 7.17-7.07 (m, 4 H), 3.09-2.98 (m, 2 H), 2.38 (s, 3 H, tolyl Me), 1.50-1.38 (m, 2 H), 1.08 (sextet, J = 7.2 Hz, 2 H), 0.65 (t, J = 7.2 Hz, 3 H, Me); ^{13}C NMR (75 MHz) δ 142.7, 142.6, 141.7, 139.0, 137.6, 137.1, 136.2, 134.7, 132.1, 130.9, 130.3, 129.2, 128.4, 128.2, 128.0, 127.5, 127.2, 127.1, 126.5, 126.2, 125.9, 34.1, 31.6, 23.1, 21.5 (tolyl Me), 13.4; MS (*m/z*, %) 490 (M^+, 53), 455 (100), 426 (31), 305 (28), 291 (53), 215 (34); HRMS calcd for $C_{33}H_{28}O_2S$: 490.1967. Found 490.1989.

7.4.6 2,3,7-Triphenyl-6-(*p*-toluenesulfonyl)-4,5-benzoxepin (377) and 1-Benzoyl-1,2-diphenyl-3-(*p*-toluenesulfonyl)-1*H*-indene (378)

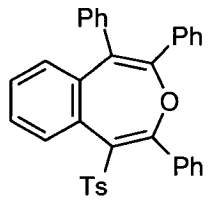

377 and

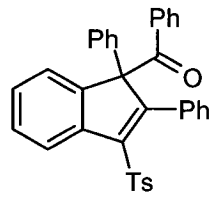

378

A solution of **354** (203 mg, 0.386 mmol) in 4 mL of dichloromethane was irradiated for 2 d in a Rayonet reactor equipped with six 300 nm lamps. The solvent was evaporated, and the residue was purified by flash chromatography (elution with 14% ethyl acetate-hexanes) to afford 103 mg (51%) of benzoxepin **377**, obtained as white crystals: 225-227 mp °C (from hexanes-ethyl acetate); IR (KBr) 1595, 1442, 1318, 1148 cm^{-1}; ^1H NMR (300 MHz) δ 8.27 (d, J = 8.1 Hz, 1 H), 7.47 (d, J = 8.7 Hz, 2 H), 7.42-7.08 (m, 17 H), 6.75 (d, J = 8.2 Hz, 1 H), 6.56 (d, J = 7.2 Hz, 2 H), 2.39 (s, 3 H, tolyl Me); ^{13}C NMR (75 MHz) δ 173.6 (C), 155.8 (C), 143.4 (C), 139.0 (C), 138.7 (C), 138.5 (C), 136.0 (C), 134.0 (C), 133.4 (C), 131.2 (CH), 131.1 (CH), 131.0 (CH), 130.2 (C), 129.5 (CH), 129.1 (CH), 129.0 (CH), 128.6 (CH), 128.1 (CH), 128.0 (CH), 127.9 (CH), 127.8 (C), 127.7 (CH), 127.5 (CH), 127.4 (CH), 126.8 (CH), 21.5 (CH_3, tolyl Me); MS (*m/z*, %) 526 (M^+, 1.2), 372 (27), 343 (26), 265 (31), 105 (100); Anal. Calcd for $C_{35}H_{26}O_3S$: C, 79.82; H, 4.98. Found: C, 79.62; H, 4.94. The X-ray structure of **377** is shown in Fig. 4.5 and the additional crystallographic data is given in Appendix X.

Further elution (15% ethyl acetate-hexanes) afforded 85 mg (42%) of exocyclic ketone **378** as white crystals: mp 133-134 °C (from ethyl acetate-hexanes); IR (KBr) 1670, 1443, 1323, 1148 cm^{-1}; ^1H NMR (300 MHz) δ 8.33 (d, J = 7.7 Hz, 1 H), 7.59-7.52 (m, 1 H), 7.54 (d, J = 8.2 Hz, 2 H), 7.45-7.28 (m, 5 H), 7.26-6.98 (m, 10 H), 6.59 (dd, J = 8.2, 1.0 Hz, 2 H), 6.30 (dd, J = 8.2, 1.0 Hz, 2 H), 2.40 (s, 3 H, tolyl Me); ^{13}C NMR (75 MHz) δ 196.1 (C, **C**OPh), 160.4 (C), 144.2 (C), 143.4 (C), 140.7 (C), 140.1 (C), 138.1 (C), 137.5 (C), 136.5 (C), 132.5 (CH), 132.4 (C), 129.8 (CH), 129.4 (CH), 129.2 (CH), 129.1 (CH), 128.8 (CH), 128.3 (CH), 128.2 (CH), 128.0 (CH), 127.9 (CH), 127.8 (CH), 127.6 (CH),

126.8 (CH), 125.7 (CH), 124.0 (CH), 79.6 (C, PhCCOPh), 21.6 (CH_3, tolyl Me); MS (*m/z*, %) 526 (M^+, 0.7), 371 (73), 343 (10), 265 (53), 105 (100); HRMS calcd for $C_{35}H_{26}O_3S$: 526.1603. Found 526.1590; Anal. Calcd for $C_{35}H_{26}O_3S$: C, 79.82; H, 4.98. Found: C, 79.47; H, 4.81. For correlations of COSY, HMQC and HMBC, see Tables 4.1 and 4.2.

7.5 Experiments Pertaining to Chapter 5

7.5.1 (*1S,2S*)-*N*-(2-Hydroxy-1-methylbut-3-enyl)benzamide (418)

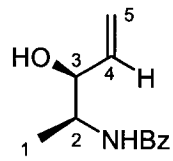

418

To a stirred solution of methyl ester **419** (14.49 g, 70.0 mmol) in 150 mL of dichloromethane at -78 °C under argon was added dropwise 70 mL of a 1.5 M solution of DIBALH in toluene, and the mixture was stirred for 1 h at -78 °C. Then, 210 mL of 1.0 M solution of vinylmagnesium bromide in THF (210 mmol) was added via canula to the above solution at -78 °C. The mixture was allowed to warm to -20 °C and to stir at this temperature for 2 d. The mixture was made acidic with 10% of HCl at 0 °C and extracted with dichloromethane (50 mL × 4). The combined organic layers was washed with water, brine, dried over $MgSO_4$ and evaporated *in vacuo* to afford a yellow oil residue, which was purified by flash chromatography over silica gel (60% ethyl acetate-hexanes) to give 9.498 g (66%) of allyl alcohol **418** as white crystals: mp 97-98 °C (from ethyl acetate-hexanes); IR (KBr) 3298, 2974, 1634, 1541, 1032 cm^{-1}; ^1H NMR (300 MHz) δ 7.79-7.70 (m, 2 H), 7.55-7.36 (m, 3 H), 6.64-6.51 (br, s, 1 H, NH), 5.91 (ddd, J = 16.9, 11.8, 5.6, Hz, 1 H, H-4), 5.36-5.27 (m, 1 H), 5.22-5.16 (m, 1H), 4.28-4.13 (m, 2 H), 3.31-3.10 (br, s, 1 H, OH), 1.30 (d, J = 6.7 Hz, 3 H, H-1); ^{13}C NMR (75 MHz) δ 167.8 (C), 138.1 (CH), 134.4 (C), 131.4 (CH), 128.5 (CH), 126.9 (CH), 116.4 (CH_2, C-5), 75.5 (CH, C-3), 49.7

(CH, C-2), 17.5 (CH_3, C-1); MS (*m/z*, %) 206 (M^++1, 0.3), 187 (0.8), 148 (77), 105 (100), 77 (35); Anal. Calcd for $C_{12}H_{15}NO_2$: C, 70.22; H, 7.37; N, 6.82. Found: C, 69.94; H, 7.31; N, 6.76. $[\alpha]^{22}_D$ = - 21.8 (*c* 0.444, $CHCl_3$).

7.5.2 (*1S,2S*)-*N*-(2-Benzyloxy-1-methylbut-3-enyl)benzamide (420)

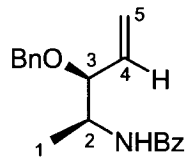

420

The allyl alcohol **418** (9.498 g, 46.3 mmol) dissolved in 50 mL of dry THF was added to a stirred suspension of NaH (3.60 g, 60%, 90 mmol) in dry THF (100 mL) at 0 °C. After 1 h, benzyl bromide (17.10 g, 100 mmol) was added and the reaction was allowed to warm to room temperature under argon. After 1 d, the mixture was washed with water, 10% aqueous $NaHCO_3$, dried over $MgSO_4$ and evaporated *in vacuo* to afford a yellow oil, which was purified by flash chromatography (20% ethyl acetate-hexanes) to give 10.89 g (80%) of allylic benzyl ether **420** as a white solid: mp 77-78 °C (from ethyl acetate-hexanes); IR (KBr) 3289, 2979, 1636, 1552, 1339, 1099 cm^{-1}; ^1H NMR (300 MHz) δ 7.81-7.70 (m, 2 H), 7.55-7.29 (m, 8 H), 6.46 (d, *J* = 8.7 Hz, 1 H, NH), 5.93-5.79 (m, 1 H, H-4), 5.37 (s, 1 H), 5.33 (dd, *J* = 5.1, 1.6 Hz, 1 H), 4.70 (d, *J* = 11.8 Hz, 1 H), 4.43 (d, *J* = 11.8 Hz, 1 H), 4.42-4.33 (m, 1 H), 3.88 (dd, *J* = 7.7, 3.0 Hz, 1 H, H-3), 1.32 (d, *J* = 6.7 Hz, 3 H, H-1); ^{13}C NMR (75 MHz) δ 166.7 (C), 138.0 (C), 135.4 (CH), 134.7 (C), 131.2 (CH), 128.34 (CH), 128.28 (CH), 127.8 (CH), 127.6 (CH), 126.8 (CH), 118.9 (CH_2, C-5), 81.6 (CH, C-3), 70.4 (CH_2), 48.5 (CH, C-2), 17.6 (CH_3, C-1); MS (*m/z*, %) 296 (M^++1, 0.4), 204 (4), 187 (6), 174 (29), 148 (62), 105 (100), 91 (63); HRMS calcd for $C_{14}H_{12}NO_2$ (M^+-Bn): 204.1025. Found: 204.1022. Anal. Calcd for $C_{19}H_{21}NO_2$: C, 77.26; H, 7.17; N, 4.74. Found: C, 76.99; H, 7.07; N, 4.74. $[\alpha]^{22}_D$ = - 6.2 (*c* 0.50, $CHCl_3$).

7.5.3 (*2R,3S*)-3-Benzylamino-2-benzyloxybutan-1-ol (422)

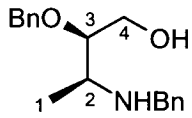

422

NMO (9.00 g, 72.6 mmol) and OsO_4, (30 mL, 2.5% solution in *t*-BuOH) were added to a solution of 0.5 M **420** (137 mL, 68.4 mmol) in acetone and the mixture was stirred at room temperature for 5 min. Sodium periodate (20 g, 93 mmol in 200 mL of water) was added to the above reaction mixture with a white precipitate forming during the course of the reaction. The progress of the reaction was monitored by TLC which indicated that the majority of the starting material was consumed within 10 h. Sodium thiosulfate (300 mg, 1.90 mmol) was added to the reaction mixture and stirring was continued for another 2 h. The mixture was filtered and the filtrate was reduced to ca. 200 mL *in vacuo* and the aqueous solution was extracted with chloroform (70 mL × 3), dried over $MgSO_4$, and evaporated *in vacuo* to give 16.093 g (80%) of the corresponding aldehyde **421** as a colourless oil, which was used in the next step without further purification: ^{1}H NMR (300 MHz) δ 9.71 (s, 1 H), 7.78-7.69 (m, 2 H), 7.55-7.29 (m, 8 H), 6.53 (d, J = 8.2 Hz, 1 H), 4.85 (d, J = 11.8 Hz, 1 H), 4.63 (d, J = 11.8 Hz, 1 H), 4.85-4.73 (m, 1 H), 3.95 (d, J = 2.6 Hz, 1 H), 1.35 (d, J = 6.7 Hz, 3 H); ^{13}C NMR (75 MHz) δ 201.9 (CH), 166.8 (C), 138.0 (C), 134.0 (C), 131.6 (CH), 128.6 (CH), 128.5 (CH), 128.32 (CH), 128.27 (CH), 126.9 (CH), 84.7 (CH), 73.0 (CH_2), 45.2 (CH), 17.4 (CH_3); MS (*m/z*, %) 298 (M^++1, 1.7), 268 (6), 148 (52), 105 (100), 91 (63); HRMS calcd for $C_{18}H_{19}NO_3$: 297.1365. Found 297.1388. $[\alpha]^{22}_D$ = - 23.8 (*c* 0.50, $CHCl_3$).

A solution of the above aldehyde **421** (6.849 g, 23.06 mmol) in THF (100 mL) was added slowly to a stirring suspension of LAH (3.80 g, 100 mmol) in 300 mL of THF at 0 °C. The resulting suspension was then refluxed for 10 h and cooled to 0 °C, and water (3 mL), 20% of aqueous NaOH (10 mL), water (20 mL) were sequentially added. The resulting mixture was allowed to warm to room temperature, stirred for another 30 min, followed by filtration through a Celite pad, and the filtrate was dried over $MgSO_4$ and evaporated to give a colourless oil. The oily residue was purified by flash chromatography

(65% ethyl acetate-hexanes) to afford 5.849 g (89 %) of amino alcohol **422** as a colourless oil: IR (KBr) 3315, 2869, 1496, 1451, 1093, 736, 697 cm^{-1}; ^1H NMR (300 MHz) δ 7.40-7.23 (m, 10 H), 4.74 (d, J = 11.8 Hz, 1 H), 4.50 (d, J = 11.8 Hz, 1 H), 4.04 (dd, J = 11.8, 4.6 Hz, 1 H, H-4), 3.89 (d, J = 12.8 Hz, 1 H), 3.76 (dd, J = 11.8, 2.6 Hz, 1 H, H-4), 3.74 (d, J = 12.8 Hz, 1 H), 3.42-3.37 (m, 1 H), 3.07 (dq, J = 6.7, 3.1 Hz, 1 H, H-2), 1.24 (d, J = 6.7 Hz, 3 H, H-1); ^{13}C NMR (75 MHz) δ 139.4 (C), 138.3 (C), 128.5 (CH), 128.3 (CH), 128.2 (CH), 127.7 (CH), 127.6 (CH), 127.1 (CH), 78.8 (CH, C-3), 71.2 (CH_2), 62.8 (CH_2), 55.8 (CH, C-2), 51.0 (CH_2), 16.1 (CH_3); MS (*m/z,* %) 286 (M^++1, 9), 254 (22), 176 (33), 134 (100), 91 (88); ESI 286 $(M+H)^+$; HRMS calcd for $C_{17}H_{20}NO$ (M^+-CH_2OH): 254.1545. Found 254.1555. $[\alpha]^{22}_D$ = + 50.0 (*c* 2.01, $CHCl_3$).

7.5.4 (*2R,3S*)-3-Benzylamino-2-benzyloxy-1-chlorobutane (190)

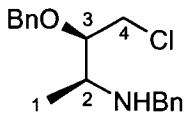

190

Amino alcohol **422** (2.149 g, 7.54 mmol) and thionyl chloride (1.102 g, 9.26 mmol) were heated at 48 °C for 3 d in 40 mL of chloroform. The solution was washed with 1 M aqueous KOH solution, water and brine. The organic layer was dried over $MgSO_4$, concentrated *in vacuo* and chromatographed (30% ethyl acetate-hexanes) to afford 1.805 g (79%) of chloroamine **190** as a yellow oil: IR (film) 3325, 2964, 2870, 1494, 1451, 1091, 739, 699 cm^{-1}; ^1H NMR (300 MHz) δ 7.47-7.25 (m, 10 H), 4.80 (d, J = 12.8 Hz, 1 H), 4.60 (d, J = 11.3 Hz, 1 H), 3.93 (dd, J = 11.3, 4.6 Hz, 1 H, H-4), 3.92 (d, J = 12.8 Hz, 1 H), 3.73 (d, J = 12.8 Hz, 1 H), 3.70 (dd, J = 11.3, 5.1Hz, 1 H, H-4), 3.58 (q, J = 5.1 Hz, 1 H, H-3), 3.03 (m, 1H), 1.81-1.64 (br, 1 H, NH), 1.18 (d, J = 6.7 Hz, 3 H, H-1); ^{13}C NMR (75 MHz) δ 140.2 (C), 137.9 (C), 128.34 (CH), 128.27 (CH), 128.0 (CH), 127.9 (CH), 127.8 (CH), 126.8 (CH), 82.8 (CH, C-3), 73.1 (CH_2), 53.5 (CH, C-2), 51.2 (CH_2), 43.8 (CH_2), 16.0 (CH_3, C-1); MS (*m/z,* %) 224 (0.9), 176 (28), 134 (34), 120 (32), 91

(100); ESI 304 $(M+H)^+$; HRMS calcd for $C_{17}H_{20}NO$ (M^+-CH_2Cl): 254.1545. Found 254.1532. $[\alpha]^{22}_D = +37.9$ (*c* , 0.96 $CHCl_3$).

7.5.5 Enamine sulfone 426

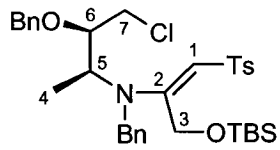

426

Chloroamine **190** (2.381 g, 7.86 mmol) was added to a solution of **191** (2.801 g, 8.65 mmol) in 50 mL of dry methanol. The solution was stirred at room temperature for 20 h, then concentrated *in vacuo* to give a yellow oil. The residue was chromatographed over silica gel using 20% ethyl acetate-hexane to give 3.869 g (79 %) of the Michael addition product **426** as a pale yellow oil, which crystallized from ethyl acetate-hexanes. Pure **426** was obtained as fine white crystals: mp 106-107.5 °C (from ethyl acetate-hexanes); IR (KBr) 2927, 2857, 1557, 1284, 1255, 1130, 1086, 839 cm^{-1}; ^1H NMR (300 MHz) δ 7.46-7.31 (m, 7 H), 7.22-7.17 (m, 3 H), 7.11-7.03 (m, 4 H), 5.37 (d, *J* = 13.0 Hz, 1 H, H-3), 4.85 (s, 1 H, H-1), 4.68 (d, *J* = 11.8 Hz, 1 H), 4.55 (t, *J* = 7.2 Hz, 1 H), 4.47 (d, *J* = 13.0 Hz, 1 H, H-3), 4.40 (d, *J* = 11.8 Hz, 1 H), 4.32 (d, *J* = 16.9 Hz, 1 H), 3.93 (d, *J* = 16.9 Hz, 1 H), 3.85-3.76 (m, 1 H), 3.58-3.50 (m, 2 H), 2.36 (s, 3 H, tolyl Me), 1.24 (d, *J* = 7.2 Hz, 3 H, H-4), 0.85 (s, 9 H, *t*-Bu), 0.07 (s, 3 H, SiC**H**$_3$), 0.03 (s, 3 H, SiC**H**$_3$); ^{13}C NMR (75 MHz) δ 158.1 (C), 142.9 (C), 141.7 (C), 137.0 (C), 136.2 (C), 129.0 (CH), 128.6 (CH), 128.5 (CH), 128.4 (CH), 128.1 (CH), 126.8 (CH), 126.1 (CH), 125.9 (CH), 99.3 (CH, C-1), 79.1 (CH, C-6), 72.1 (CH_2), 55.8 (CH_2), 55.1 (CH, C-5), 47.4 (CH_2), 43.1 (CH_2), 25.6 (CH_3), 21.3 (CH_3, tolyl Me), 17.9 (C), 15.4 (CH_3), -5.6 (CH_3), -5.7 (CH_3); MS (*m/z,* %) 627 (M^+, 5), 591 (1.1), 458 (63), 444 (32), 188 (30), 149 (65), 91 (100); HRMS calcd for $C_{26}H_{37}NO_2Si^{35}Cl$ (M^+-CH_2Ts): 458.2282. Found 458.2304; Anal. Calcd for $C_{34}H_{46}ClNO_4SSi$: C, 64.99; H, 7.38; N, 2.23. Found: C, 65.06; H, 7.30; N, 2.06. $[\alpha]^{22}_D = +149.1$ (*c* 0.34, $CHCl_3$).

7.5.6 (*5S,6S*)-*N*-Benzyl-5-benzyloxy-2-(*t*-butyldimethylsilyloxymethyl)-6-methyl-3-(*p*-toluenesulfonyl)-2,3-dehydropiperidine (189)

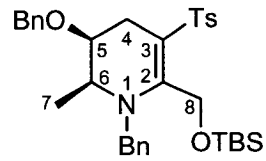

189

Sulfone **426** (3.135 g, 5.0 mmol) was dissolved in 20 mL of dry THF and cooled to -78 °C under argon. A solution of LDA (10.0 mmol) in 30 mL of dry THF was added via syringe over 5 min. The resulting orange solution was stirred at -78 °C for 4 min and was then filtered through neutral alumina. The alumina was washed with THF (15 mL × 2) and the clear filtrate was concentrated *in vacuo*. Compound **189** was obtained as a colourless oil without further purification (2.689 g, 4.55 mmol, 91%): IR (film) 2935, 2854, 1568, 1360, 1296, 1141, 837 cm^{-1}; ^1H NMR (300 MHz) δ 7.80 (d, *J* = 8.4 Hz, 2 H), 7.38-7.21 (m, 8 H), 7.20-7.09 (m, 4 H), 5.45 (d, *J* = 12.8 Hz, 1 H, H-8), 4.99 (d, *J* = 16.4 Hz, 1 H), 4.59 (d, *J* = 12.8 Hz, 1 H, H-8), 4.39 (d, *J* = 11.8 Hz, 1 H), 4.34 (d, *J* = 11.8 Hz, 1 H), 4.22 (d, *J* = 16.4 Hz, 1 H), 3.58-3.48 (m, 1 H), 3.38-3.27 (m, 1 H), 2.86 (dd, *J* =16.4 Hz, 6.2 Hz, 1 H, H-4), 2.43 (s, 3 H, tolyl Me), 2.16 (dd, *J* =16.4 Hz, 10.5 Hz, 1 H, H-4), 0.92 (d, *J* = 6.6 Hz, 3 H, H-7), 0.92 (s, 9 H, *t*-Bu), 0.14 (s, 3 H, $SiCH_3$), 0.13 (s, 3 H, $SiCH_3$); ^{13}C NMR (75 MHz) δ 150.7 (C), 142.5 (C), 141.1 (C), 138.1 (C), 138.0 (C), 129.5 (CH), 128.9 (CH), 128.5 (CH), 127.8 (CH), 127.69 (CH), 126.67 (CH), 127.2 (CH), 126.6 (CH), 99.6 (C-3), 72.6 (CH, C-5), 70.7 (CH_2, C-8), 56.3 (CH_2), 53.6 (CH, C-6), 53.0 (CH_2), 27.0 (CH_2, C-4), 26.0 (CH_3), 21.6 (CH_3, tolyl Me), 18.3 (C), 11.2 (CH_3), -5.1 (CH_3), -5.3 (CH_3); MS (*m/z*, %) 591 (M^+, 2), 534 (7), 303 (26), 213 (40), 149 (81), 91 (100); HRMS calcd for $C_{30}H_{36}NO_4SSi$ (M^+-C_4H_9): 534.2134. Found 534.2147. $[\alpha]^{22}_D$ = + 127.5 (*c* 0.9, $CHCl_3$).

7.5.7 (*5S,6S*)-*N*-Benzyl-5-benzyloxy-2-hydroxymethyl-6-methyl-3-(*p*-toluenesulfonyl)-2,3-dehydropiperidine (429)

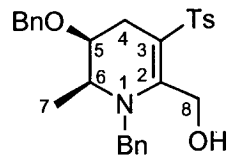

429

Compound **189** (632 mg, 1.07 mmol) was dissolved in 4 mL of THF, cooled to 0°C and treated with 1.0 M TBAF in THF (1.5 mL, 1.5 mmol). The solution was stirred at room temperature for 2 h and washed with brine (10 mL × 2), dried and concentrated *in vacuo*. The residue was chromatographed over silica gel using 35% ethyl acetate-hexane as eluent to give 464 mg (91%) of free alcohol **429** as a white solid: mp 97-98 °C (from ethyl acetate-hexanes); IR (KBr) 3500, 2935, 1597, 1454, 1289, 1118 cm^{-1}; ^1H NMR (CD_3COCD_3, 300 MHz) δ 7.77 (d, J = 8.2 Hz, 2 H), 7.45-7.10 (m, 12 H), 5.01 (d, J = 14.6 Hz, 1 H, H-8), 4.94 (d, J = 14.6 Hz, 1 H, H-8), 4.52-4.34 (m, 4 H), 4.13-3.86 (br, s, 1 H, OH), 3.62-3.46 (m, 2 H), 2.75 (dd, J = 16.2, 6.2 Hz, 1 H, H-4), 2.41 (s, 3 H, tolyl Me), 2.22 (dd, J = 16.2, 10.6 Hz, 1 H, H-4), 0.91 (d, J = 6.7 Hz, 3 H, H-7); ^{13}C NMR (75 MHz) δ 152.8 (C), 143.4 (C), 142.8 (C), 139.4 (C), 130.4 (CH), 129.6 (CH), 129.2 (CH), 128.5 (CH), 128.4 (CH), 128.3 (CH), 128.2 (CH), 127.2 (CH), 101.3 (C-3), 73.5 (CH, C-5), 71.2 (CH_2, C-8), 56.8 (CH_2), 54.5 (CH, C-6), 53.4 (CH_2), 27.8 (CH_2, C-4), 21.5 (CH_3, tolyl Me), 11.4 (CH_3); ESI 478 $(M+H)^+$, 500 $(M+Na)^+$; Anal. Calcd for $C_{28}H_{31}NO_4S$: C, 70.41; H, 6.54; N, 2.93. Found: C, 70.71; H, 6.12; N, 2.73. $[\alpha]^{22}_D$ = + 177 (*c* 0.44, acetone). The X-ray structure of **429** is shown in Fig. 5.1 and additional crystallographic data is given in Appendix XI.

7.5.8 (*2S,3S,5S,6S*)-*N*-Benzyl-5-benzyloxy-2-hydroxymethyl-6-methyl-3-(*p*-toluenesulfonyl)-piperidine (432)

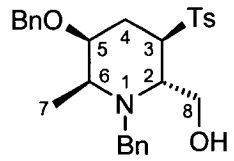

432

Trifluoroacetic acid (0.80 mL, 10 mmol) was added dropwise to a suspension of alcohol **429** obtained above (464 mg, 0.973 mmol) and sodium cyanoborohydride (668 mg, 10.6 mmol) in 15 mL of dichloromethane at 0 °C, and the mixture was stirred at 0 °C for 1 h, then at room temperature for another 1 h. It was washed with aqueous KOH solution, dried over $MgSO_4$, and concentrated *in vacuo* to provide a light yellow oil, which was purified by flash chromatography (45% ethyl acetate-hexanes) to afford 20 mg (4%) of the less polar byproducts as a clear oil that consisted of an inseparable mixture of **430** and **431**. Further elution with 55% ethyl acetate-hexanes afford 391 mg (84%) of 2,6-*trans* piperidine **432** as a colourless oil: IR (film) 3411, 2876, 1597, 1494, 1316, 1145 cm^{-1}; ^1H NMR (400 MHz) δ 7.75 (d, J = 8.1 Hz, 2 H), 7.39-7.31 (m, 5 H), 7.30-7.16 (m, 5 H), 7.04-7.00 (m, 2 H), 4.53 (d, J = 11.9 Hz, 1 H), 4.34 (d, J = 11.9 Hz, 1 H), 4.17 (d, J = 14.3 Hz, 1 H), 3.84-3.71 (m, 3 H), 3.58 (s, 1 H, H-5), 3.43 (d, J = 14.3 Hz, 1 H), 3.18-3.07 (m, 2 H, H-2 and H-6), 2.98-2.79 (br, s, 1 H, OH), 2.49 (s, 3 H, tolyl Me), 2.40 (d, J = 13.9 Hz, 1 H, H-4), 2.02 (dt, J = 13.7, 2.5 Hz, 1 H, H-4), 3.12 (d, J = 6.7 Hz, 3 H, H-7); ^{13}C NMR (100 MHz) δ 144.8 (C), 139.5 (C), 138.0 (C), 134.9 (C), 130.0 (CH), 128.7 (CH), 128.38 (CH), 128.36 (CH), 128.2 (CH), 127.6 (CH), 127.3 (CH), 127.1 (CH), 76.0 (CH, C-5), 71.5 (CH_2, C-8), 55.5 (CH_2), 54.5 (CH), 53.6 (CH), 51.8 (CH_2), 50.2 (CH), 23.6 (CH_2, C-4), 21.6 (CH_3, tolyl Me), 16.2 (CH_3, C-7); MS (*m/z*, %) 448 (M^+-CH_2OH, 76), 388 (7), 293 (17), 187 (30), 91 (100); HRMS calcd for $C_{27}H_{30}NO_3S$ (M^+-CH_2OH): 448.1946. Found 448.1982. $[\alpha]^{22}_D$ = - 62.1 (*c* 1.24, $CHCl_3$).

7.5.9 (*2S,3S,6R*)-*N*-Benzyl-3-benzyloxy-6-(hydroxymethyl)-2-methylpiperidine (187)

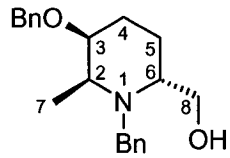

187

Sulfone **432** (314 mg, 0.655 mmol) was suspended in 15 mL of dry THF and finely ground 5% sodium amalgam (4.44 g, 9.65 mmol of Na) was added. The mixture was refluxed under nitrogen for 22 h and filtered through a Celite pad, followed by washing with THF (10 mL × 2). The filtrate was concentrated *in vacuo* to provide a yellow oil, which was purified by flash chromatography (elution with 55% ethyl acetate-hexanes) to afford 179 mg (84%) of **187** as a colourless oil: IR (KBr) 3424, 2929, 1495, 1452, 1375, 1071 cm^{-1}; ^1H NMR (400 MHz) δ 7.38-7.18 (m, 10 H), 4.51 (d, J = 12.0 Hz, 1 H), 4.42 (d, J = 12.0 Hz, 1 H), 3.88 (d, J = 14.2 Hz, 1 H), 3.78 (d, J = 14.2 Hz, 1 H), 3.61 (dd, J = 11.0 Hz, 4.4 Hz, 1 H, H-8), 3.55-3.47 (m, 2 H), 3.23 (dq, J = 13.4 Hz, 3.8 Hz, 1 H, H-2), 2.84 (dt, J = 13.1 Hz, 4.4 Hz, 1 H, H-6), 2.42-2.02 (br, s, 1 H, OH), 1.86-1.70 (m, 3 H), 1.59-1.43 (m, 1 H), 1.12 (d, J = 6.8 Hz, 3 H, H-7); ^{13}C NMR (100 MHz) δ 140.2 (C), 138.8 (C), 128.5 (CH), 128.28 (CH), 128.26 (CH), 127.4 (CH), 127.3 (CH), 127.0 (CH), 76.3 (CH, C-3), 70.3 (CH_2, C-8), 61.7 (CH_2), 54.6 (CH, C-6), 52.8 (CH_2), 52.1 (CH, C-2), 24.2 (CH_2), 23.0 (CH_2, C-5), 8.6 (CH_3, C-7); MS (*m/z,* %) 324 (M^+-H, 1), 310 (1), 294 (100), 234 (57), 91 (100); HRMS calcd for $C_{20}H_{24}NO$ (M^+-CH_2OH): 294.1858. Found 294.1838. $[\alpha]^{22}_D$ = - 16.0 (*c* 0.21, $CHCl_3$). The ^{13} C NMR for compound **187** suffers from quadrupolar boadending of signals. The signals corresponding to C-7 and C-5 are very small and broad.

7.5.10 (*5S,6S*)-*N*-Benzyl-5-benzyloxy-2-formyl-6-methyl-2,3-dehydropiperidine (439)

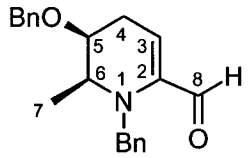

439

Compound **189** (591 mg, 1.0 mmol) was dissolved in 8 mL of chloroform-methanol (5:2), and treated with 1.0 mL of concentrated HCl under argon. The solution was stirred at room temperature for 1 d and washed with saturated aqueous $KHCO_3$ solution. The aqueous layer was extracted with chloroform (10 mL × 2). The combined organic layers were dried over $MgSO_4$ and concentrated. The residue was purified by flash chromatography (18% ethyl acetate-hexanes) to give 263 mg (82%) of aldehyde **439** as a pale yellow oil: IR (KBr) 2974, 2931, 2733, 1685, 1458, 1361 cm^{-1}; ^1H NMR (300 MHz) δ 9.24 (s, 1 H, H-8), 7.41-7.20 (m, 10 H), 5.69 (dd, J = 5.1, 3.1 Hz, 1H, H-3), 4.49 (d, J = 12.0 Hz, 1 H), 4.40 (d, J = 12.0 Hz, 1 H), 4.39 (d, J = 14.9 Hz, 1 H), 4.31 (d, J = 14.9 Hz, 1 H), 3.46 (ddd, J = 10.3, 6.2, 4.6 Hz, 1 H, H-5), 3.33-3.23 (m, 1 H, H-6), 2.53 (dt, J = 13.3, 6.1 Hz, 1H, H-4), 2.27 (ddd, J = 13.3, 10.2, 3.1 Hz, 1 H, H-4), 0.89 (d, J = 6.7 Hz, 3 H, H-7); ^{13}C NMR (75 MHz) δ 190.3 (CH, C-8), 143.5 (C), 139.2 (C), 138.2 (C), 128.33 (CH), 128.30 (CH), 128.26 (CH), 127.6 (CH), 127.5 (CH), 127.1 (CH), 125.4 (CH), 71.4 (CH, C-5), 70.5 (CH_2), 54.2 (CH, C-6), 52.4 (CH_2), 27.0 (CH_2, C-4), 11.0 (CH_3, C-7); MS (*m/z,* %) 321 (M^+, 28), 230 (28), 215 (30), 186 (26), 110 (70), 91 (100); HRMS calcd for $C_{21}H_{23}NO_2$: 321.1729. Found 321.1715. $[\alpha]^{22}_D$ = - 70.2 (*c* 1.20, $CHCl_3$).

7.5.11 Preparation of 187 from 439 by Stereoselective Reduction

Concentrated HCl (1.0 mL) was added dropwise to a suspension of aldehyde **439** (263 mg, 0.82 mmol) and sodium cyanoborohydride (601 mg, 9.54 mmol) in 15 mL of dichloromethane at -10 °C, and the mixture was stirred at 0 °C for 10 h, then at room temperature for 2 h. The mixture was washed with 10 mL of aqueous 20% KOH solution,

dried ($MgSO_4$), and concentrated *in vacuo* to provide a light yellow oil, which was purified by flash chromatography (elusion with 55% ethyl acetate-hexanes) to afford 200 mg (75%) of **187** as a colourless oil. The product was identical to that prepared in section **7.5.9**.

7.5.12 (*2S,3S,6R*)-12-(*N*-Benzyl-3-benzyloxy-2-methylpiperidin-6-yl)dodec-11-en-1-ol (415)

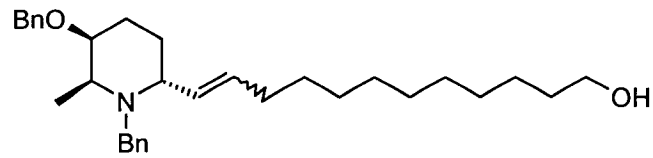

415

To a solution of oxalyl chloride (114 mg, 0.90 mmol) in dry dichloromethane (4 mL) at -78 °C was added a solution of DMSO (140 mg, 0.90 mmol) in dichloromethane (2 mL). After 10 min, a solution of alcohol **187** (202 mg, 0.62 mmol) in dichloromethane (2 mL) was added. The mixture was allowed to stir for 45 min at -65 °C, and then triethylamine (182 mg, 1.8 mmol) was added. After the mixture was stirred for 20 min at -65 °C, it was warmed to room temperature for 1 h. The mixture was quenched with 10% of aqueous $NaHCO_3$ and then extracted with dichloromethane (10 mL × 3). The organic layers were combined and dried over $MgSO_4$, followed by filtration. The filtrate was evaporated *in vacuo* to afford 200 mg of aldehyde **445** as a yellow oil, which was used immediately without further purification.

A mixture of 11-bromo-1-undecanol (452 mg, 1.8 mmol) and triphenylphosphine (471 mg, 1.8 mmol) was heated under reflux in acetonitrile (5 mL) for 26 h. After the solution was cooled to room temperature, the solvent was removed under vacuum and the residue was washed with diethyl ether to remove excess alkyl bromide. THF (10 mL) was added and the mixture was sonicated. The precipitated phosphonium salt was filtered and dried to afford 631 mg (66%) of a white solid. The phosphonium salt was suspended in 8.0 mL of THF and cooled to -78 °C. A solution of *n*-BuLi (2.38 M in hexane, 1.03 mL, 2.46 mmol) was added dropwise and the mixture was stirred for 45 min at -78 °C and then

stirred for 1 h at room temperature. The resulting ylide **446** solution was cooled to -78 °C and aldehyde **445** obtained above (200 mg, 6.19 mmol), in THF (5 mL) was added. After the mixture was stirred at -78 °C for 2 h, it was warmed to 0 °C for 1 h, and stirred for an additional 2 h at room temperature. The reaction was quenched with water (10 mL) and the solution was extracted with dichloromethane (20 mL × 3). The combined organic layers were dried over $MgSO_4$ and concentrated. The residue was purified by flash chromatography (elution with 30% ethyl acetate-hexanes) to give 204 mg (69%) of olefin **415** *(cis/trans* = 9:1) as colourless oil: IR (KBr) 3363 (br, OH), 2926, 2849, 1705, 1453, 1372, 1075, 733, 697 cm^{-1}; ^1H NMR (300 MHz, mixture of geometrical isomers) δ 7.37-7.14 (m, 10 H), 7.66-7.50 (m, 1 H), 5.43 (dt, *J* = 10.8, 7.2 Hz, 1 H), 5.23 (t, *J* = 10.8 Hz, 1 H), 4.41 (d, *J* = 11.8 Hz, 1 H), 4.36 (d, *J* = 11.8 Hz, 1 H),4.00 (d, *J* = 13.8 Hz, 1 H), 3.65 (t, *J* = 6.7 Hz, 1 H), 3.64 (t, *J* = 6.5 Hz, 1 H), 3.56-3.43 (m, 1 H), 3.38 (d, *J* = 14.3 Hz, 1 H), 3.28-3.15 (m, 1 H), 2.16-2.02 (m, 2 H), 2.01-1.90 (m, 1 H), 1.86-1.70 (m, 1 H), 1.69-1.48 (m, 3 H), 1.47-1.16 (m, 16 H), 0.99 (d, *J* = 6.7 Hz, 3 H), 0.96 (d, *J* = 7.2 Hz, 3 H); ^{13}C NMR (75 MHz, major *cis* isomer) δ 140.5 (C), 138.8 (C), 133.6 (CH), 131.3 (CH), 128.3 (CH), 128.2 (CH), 128.1 (CH), 127.5 (CH), 127.3 (CH), 126.5 (CH), 77.6 (CH) 69.9 (CH_2), 63.1 (CH_2), 53.8 (CH_2), 51.02 (CH), 50.96 (CH), 32.8 (CH_2), 31.6 (CH_2), 29.6 (CH_2), 29.53 (CH_2), 29.48 (CH_2), 29.43 (CH_2), 29.38 (CH_2), 29.24 (CH_2), 27.7 (CH_2), 25.7 (CH_2), 24.7 (CH_2), 3.0 (CH_3); MS (*m/z,* %) 477 (M^+, 4), 462 (8), 386 (15), 294 (16), 134 (69), 91 (100); HRMS calcd for $C_{32}H_{47}NO_2$: 477.3607. Found 477.3579.

7.5.13 (-)-Julifloridine (151)

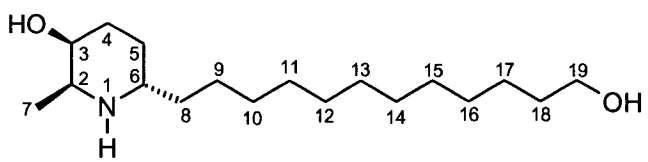

151

To a stirred solution of olefin **415** (112 mg, 0.29 mmol) in 14 mL of ethyl acetate was added palladium hydroxide (50 mg, 20% on C), and the resulting suspension was stirred under a hydrogen atmosphere at 45 °C and 400 psi for 10 h. The catalyst was

filtered through a Celite pad, and the filtrate was evaporated to give a colourless oil (92 mg), which was used directly in the next step.

The above oil was dissolved in 5.0 mL of THF and cooled to -78 °C, a dry ice-acetone condenser was added to the flask and ammonia (*ca.* 15 mL) was condensed in it. Freshly cut sodium (368 mg, 16.0 mmol) was added while stirring, to afford a dark purple solution, which was stirred for 30 min at -78 °C. The mixture was warmed to -30 °C and stirred under reflux for 3 h. Solid ammonium chloride was added until the colour disappeared and then the mixture was warmed to room temperature in a water bath. Stirring was continued until evolution of ammonia ceased, then 10 mL of water was added. The mixture was transferred to a separatory funnel and the aqueous phase was extracted with ether (15 mL × 3), the combined organic phase was dried over potassium carbonate, filtered and concentrated under reduced pressure. The oily residue was purified by flash chromatography (gradient 2.5:2.5:95 to 10:10:80 AcOH/MeOH/CH_2Cl_2) and the fractions containing **151** [R_f= 0.28; (10:10:80 AcOH/MeOH/CH_2Cl_2)] were collected in an Erlenmeyer flask. The flask was cooled to 0 °C with an ice bath and 10 M NaOH was added until the pH was strongly basic. Extraction with dichlormethane, drying with K_2CO_3, filtration and evaporation of the solvent afforded 30 mg (62%) of (-)-julifloridine **(151)** as a white solid. mp: 81-83.5 °C, lit.[135] 82-83 °C, lit.[132] 85-87.5 °C; IR (KBr) 3424 (br, OH and NH), 3385, 3271, 2924, 2850, 1456, 1364, 1096 cm^{-1}; ^1H NMR (400 MHz) δ 3.70-3.58 (quintet, J = 3.0 Hz, 1 H, H-3), 3.64 (t, J = 6.7 Hz, 2 H, H-19), 3.13 (dq, J = 6.5, 2.8 Hz, 1 H, H-2), 2.82 (quintet, J = 5.8 Hz, 1 H, H-6), 2.22-1.90 (br, s, 3 H, OH and NH), 1.94-1.84 (m, 1 H), 1.76-1.60 (m, 2 H), 1.58-1.44 (m, 3 H), 1.40-1.20 (m, 20 H), 1.09 (d, J = 6.6 Hz, 3 H, H-7); ^{13}C NMR (100 MHz) δ 68.8 (CH), 63.1 (CH_2), 50.4 (CH), 49.6 (CH), 32.8 (2 × CH_2), 29.7 (CH_2), 29.6 (CH_2), 29.5 (5 × CH_2), 29.4 (CH_2), 27.5 (CH_2), 26.6 (CH_2), 25.7 (CH_2), 15.9 (CH_3); MS (*m/z,* %) 300 (M^++1, 29), 204 (10), 114 (100); HRMS calcd for $C_{18}H_{37}NO_2$: 299.2824. Found 299.2847. $[\alpha]^{22}_D$ = - 8.2 (*c* 0.34, MeOH), lit.[135] of (+)-julifloridine: $[\alpha]^{20}_D$ = + 7.3 (*c* 0.23, MeOH), lit.[132] of (+)-julifloridine: $[\alpha]^{25}_D$ = + 18 (*c* 0.84, MeOH). The ^{13}C NMR for compound (-)-julifloridine **(151)** suffers from extensive quadrupolar boadending of signals. Thus, the signals corresponding to C-2, C-5 and C-6 are very small and broad. The signal corresponding to C-7 is missing entirely. These signals were observed, however, in the DEPT135 spectrum.

References

1. For general reviews of sulfone chemistry, see: (a) Simpkins, N. S. *Sulphones in Organic Synthesis*; Pergamon Press, Oxford, UK, **1993**. (b) *The Chemistry of Sulphones and Sulphoxides*, ed. Patai, S.; Rappoport, Z.; Stirling, C. J. M. Wiley, Chichester, UK, **1988**. (c) Block, E. *Reactions of Organosulfur Compounds*, Academic Press, New York, **1978**. For acetylenic and allenic sulfones, see: (d) Back, T. G. *Tetrahedron* **2001**, *57*, 5263.
2. Nájera, C.; Yus, M. *Tetrahedron* **1999**, 55, 10547.
3. (a) Back, T. G.; Collins, S. *Tetrahedron Lett.* **1981**, *22*, 5111. (b) Back, T. G.; Collins, S. *J. Org. Chem.* **1981**, *46*, 3249. (c) Back, T. G.; Collins, S.; Kerr, R. G. *J. Org. Chem.* **1983**, *48*, 3077. (d) Back, T. G.; Collins, S.; Gokhale, U.; Law, K. W. *J. Org. Chem.* **1983**, *48*, 4776. (e) Back, T. G.; Krishna, M. J. *J. Org. Chem.* **1987**, *52*, 4265. (f) Back, T. G.; Krishna, M. V.; Muralidharan, K. R. *J. Org. Chem.* **1989**, *54*, 4146.
4. Back, T. G.; Collins, S.; Krishna, M. V. *Can. J. Chem.* **1987**, *65*, 38.
5. (a) McDowell, S. T.; Stirling, C. J. M. *J. Chem. Soc. (B)* **1967**, 351. (b) McMullen, C. H.; Stirling, C. J. M. *J. Chem. Soc. (B)* **1966**, 1217. (c) Pink, R. C.; Spratt, R.; Stirling, C. J. M. *J. Chem. Soc.* **1965**, 5714. (d) Stirling, C. J. M. *J. Chem. Soc.* **1964**, 5863.
6. (a) Truce, W. E.; Brady, D. G. *J. Org. Chem.* **1966**, *31*, 3543. (b) Truce, W. E.; Markley, L. D. *J. Org. Chem.* **1970**, *35*, 3275. (c) Truce, W. E.; Onken, D. W. *J. Org. Chem.* **1975**, *40*, 3200.
7. (a) McMullen, C. H.; Stirling, C. J. M. *J. Chem. Soc. (B)* **1966**, 1217. (b) Pink, R. C.; Spratt, R.; Stirling, C. J. M. *J. Chem. Soc.* **1965**, 5714. (c) Stirling, C. J. M. *J. Chem. Soc.* **1964**, 5863.
8. For a review of sulfone-stabilized anions, see: Block, E. *Reactions of Organosulfur Compounds*, Academic Press, New York, **1978**, Ch. 2.
9. Alonso, D. A.; Costa, D. A.; Mancheno, B.; Najera, C. *Tetrahedron* **1997**, *53*, 4791.
10. Corey, E. J.; Chaykovsky, M. *J. Am. Chem. Soc.* **1964**, *86*, 1639.
11. Brown, A. C.; Carpino, L. A. *J. Org. Chem.* **1985**, *50*, 1749.

12. (a) Miyaoka, H.; Tamura, M.; Yamada, Y. *Tetrahedron Lett.* **1998**, *39*, 621. (b) Bintz-Giudicelli, C.; Weymann, O. i. p.; Uguen, D.; De Cian, A.; Fischer, J. *Tetrahedron Lett.* **1997**, *38*, 2841. (c) Kato, M.; Watanabe, M.; Vogler, B.; Awen, B. Z.; Masuda, Y.; Tooyama, Y.; Yoshikoshi, A. *J. Org. Chem.* **1991**, *56*, 7071.
13. (a) Back, T. G.; Nakajima, K. *Org. Lett.* **1999**, *1*, 261. (b) Back, T. G.; Nakajima, K. *J. Org. Chem.* **2000**, *65*, 4543. (c) Back, T. G.; Nakajima, K. *J. Org. Chem.* **1998**, *63*, 6566.
14. Back, T. G.; Hamilton, M. D. *Org. Lett.* **2002**, *4*, 1779.
15. Back, T. G.; Hamilton, M. D. Lim, V. J. J.; Parvez, M. *J. Org. Chem.* **2005**, *70*, 967.
16. Back, T. G.; Parvez, M.; Wulff, J. E. *J. Org. Chem.* **2003**, *68*, 2223.
17. El Sayed, K.; Al-Said, M. S.; El-Feraly, F. S.; Ross, S. A. *J. Nat. Prod.* **2000**, *63*, 995.
18. Simpkins, N. S. *Tetrahedron* **1990**, *46*, 6951.
19. Paquette, L. A.; Carr, R. V. C. *Org. Syntheses* **1986**, *64*, 157.
20. Brace, N. O. *J. Org. Chem.* **1993**, *58*, 4506.
21. Asscher, M.; Vofsi, D. *J. Chem. Soc.* **1964**, 4962.
22. Liu, L. K.; Chi, Y.; Jen, K. Y. *J. Org. Chem.* **1980**, *45*, 406.
23. Hopkins, P. B.; Fuchs, P. L. *J. Org. Chem.* **1978**, *43*, 1208.
24. Schmidt, G. H.; Garrat, D. G. in *Chemistry of Double-bounded Functional Groups,* Patai, S. (Ed.), Wiley, London, **1977**, Part 2, Ch. 9.
25. Back, T. G.; Collins, S. *Tetrahedron Lett.* **1980**, *21*, 2215.
26. Gancarz, R. A.; Kice, J. L. *J. Org. Chem.* **1981**, *46*, 4899.
27. Inomata, K.; Kobayashi, T.; Sasaoka, S.; Kinoshita H.; Kotake, H. *Chem. Lett.* **1986**, 289.
28. Bongini, A.; Savoia. D.; Ronchi, A. U. *J. Organomet. Chem.* **1976**, *112*, 1.
29. Posner, G. H.; Brunelle, D. J. *J. Org. Chem.* **1972**, *37*, 3547.
30. (a) Craig, D.; Ley, S. V.; Simpkins, N. S.; Whitham, C. H.; Prior, M. J. *J. Chem. Soc., Perkin Trans. 1* **1985**, 1949. (b) Vollhardt, J.; Gais. H. J.; Lukas. K. L. *Angew. Chem. Int. Ed.* **1985**, *24,* 696.
31. Fiandanese, V.; Marchese, G.; Naso, F. *Tetrahedron Lett.* **1978**, *8,* 513.

32. Block, E.; Aslam, M. *Tetrahedron* **1988**, *44*, 281.
33. Grela, K.; Bieniek, M. *Tetrahedron Lett.* **2001**, *42*, 6425.
34. McDowell, S. T.; Stirling, C. J. M. *J. Chem. Soc. (B)* **1967**, 343.
35. Harman, P. R.; Fuchs, P. L. *J. Org. Chem.* **1983**, *48*, 914.
36. Benedetti, F.; Fabrissin, S.; Risaliti, A. *Tetrahedron* **1984**, *40*, 977.
37. Takaki, K.; Nakagawa, K.; Negoro, K. *J. Org. Chem.* **1980**, *45*, 4789.
38. Hayakawa, K.; Nishiyama, N.; Kanematsu, K. *J. Org. Chem.* **1985**, *50*, 512.
39. Fuchs, P. L.; Pasquato, P. L. *Chem. Rev.* **1986**, *86*, 903.
40. McDowell, S. T.; Stirling, C. J. M. *J. Chem. Soc. (B)* **1967**, 348.
41. For general reviews of SPOS, see: Dörwald, F. Z. *Organic Synthesis on Solid Phase: Supports, Linkers, Reactions* Wiley-VCH, Weinheim, **2000**.
42. Ley, S. V.; Baxendale, I. R.; Bream, R. N.; Jackson, P. S.; Leach, A. G.; Longbottom, D. A.; Nesi, M.; Scott, J. S.; Storer, R. I.; Taylor, S. J. *J. Chem. Soc., Perkin Trans. 1*, **2000**, 3815.
43. For general reviews of combinatorial chemistry, see: *Handbook of Combinatorial Chemistry*, ed. Nicolaou, K. C.; Hanko, R.; Hartwig, W. Wiley-VCH, Weinheim, **2002**, vol. 1.
44. Merrifield, R. B. *J. Am. Chem. Soc.* **1963**, *85*, 2149.
45. Letsinger, R. L.; Kornet, M. J. *J. Am. Chem. Soc.* **1963**, *85*, 3045.
46. (a) Brown, R. C. D. *J. Chem. Soc., Perkin Trans. 1* **1998**, 3293. (b) Hermkens, P. H. H.; Ottenheijm, H. C. J.; Rees, D. C. *Tetrahedron* **1997**, *53*, 5643.
47. Mukherjee, A. K.; Ghosh, A. C. *Int. J. Info. Technol. Management* **2002**, *4*, 345.
48. Flory, P. J. *Principles of Polymer Chemistry*; Cornell University Press: Ithaca, NY, **1953**.
49. Vaino, A. R.; Janda, K. D. *J. Comb. Chem.* **2000**, *2*, 579.
50. *Handbook of Combinatorial Chemistry*, ed. Nicolaou, K. C.; Hanko, R.; Hartwig, W. Wiley-VCH, Weinheim, **2002**, vol. 1, Ch. 2.
51. (a) Flynn, D.L.; Crich, J. Z.; Devraj, R. V.; Hockerman, S. L.; Parlow, J. J.; South, M. S.; Woodard. S. *J. Am. Chem. Soc.* **1997**, *119*, 4874. (b) Chen J.; Dixon, B. R.;

Dumas, J.; Brittelli, D. *Tetrahedron Lett.* **1999**, *40*, 9195. (c) Shapiro, R.H. *Org. React.* **1979**, *23*, 405.

52. (a) Yu, Z.; Alesso, S.; Pears, D.; Worthington, P. A.; Luke, R. W. A.; Bradley, M. *Tetrahedron Lett.* **2000**, *41*, 8963. (b) Schön, U.; Messinger, J.; Merayo, N.; Juszkiewicz, G.; Kirschning, A. *Synlett* **2003**, 983.
53. Pickup, S.; Blum, F. D.; Ford, W. T.; Periyasami, M. *J. Am. Chem. Soc.* **1986**, *108,* 3987.
54. Fréchet, J. M. J. *Tetrahedron* **1981**, *37*, 663.
55. Brown, A. R.; Hermkens, P. H. H.; Ottenheijm, H. C. J.; Rees, D. C. *Synlett.* **1998**, 817.
56. Maclean, D.; Baldwin, J. J.; Ivanov, V. T.; Kato, Y.; Shaw, A.; Schneider, P.; Gordon, E. M. *Pure Appl. Chem.* **1999**, *71*, 2349.
57. Gordon, K.; Balasubramanian, S. *J. Chem. Technol. Biotechnol.* **1999**, *74*, 835.
58. Guillier,F.; Orain, D.; Bradley, M. *Chem. Rev.* **2000**, *100*, 2091.
59. Ajayaghosh, A.; Pillai, V. N. R. *Tetrahedron* **1988**, *44*, 6661.
60. Pietta, P. G.; Cavallo, P. F.; Takahashi, K.; Marshall, G. R. *J. Org. Chem.* **1974**, *39*, 44.
61. Fyles, T. M.; Leznoff, C. C. *Can. J. Chem.* **1976**, *54*, 935.
62. Holte, P.; Thijs, L.; Zwanenburg, B. *Tetrahedron Lett.* **1998**, *39*, 7407.
63. Zikos, C. C.; Ferderigos, N. G. *Tetrahedron Lett.* **1994**, *35,* 1767.
64. Rich, D. H.; Gurwara, S. K. *J. Am. Chem. Soc.* **1975**, *97,* 1575.
65. Wang, S. S. *J. Am. Chem. Soc.* **1973**, *95*, 1328.
66. Mergler, M.; Tanner, R.; Gosteli, J.; Grogg, P. *Tetrahedron Lett.* **1988**, *29*, 4005.
67. Stranix, B. R.; Liu, H. Q.; Darling, G. D. *J. Org. Chem.* **1997**, *62*, 6183.
68. *Handbook of Combinatorial Chemistry*, ed. Nicolaou, K. C.; Hanko, R.; Hartwig, W. Wiley-VCH, Weinheim, **2002**, vol. 1 Ch. 4.
69. (a) Thompson, L. A. Ellman, J. A. *Tetrahedron Lett.* **1994**, *35*, 9333. (b) Lezenoff, C. C.; Greenberg, S. *Can. J. Chem.* **1976**, *54*, 3824. (c) Huwe, C. M.; Kunzer, H. *Tetrahedron Lett.* **1999**, *40*, 683.
70. Boehm,T. L.; Showalter, H. D. H. *J. Org. Chem.* **1996**, *61*, 6498.

71. Chao, H. G.; Bernatowicz, M. S.; Matsueda, G. R. *J. Org. Chem.* **1993**, *58*, 2640.

72. Chao, H. G.; Bernatowicz, M. S.; Reiss, P. D.; Klimas, C. E.; Matsueda, G. R. *J. Am. Chem. Soc.* **1994**, *116*, 1746.

73. Timar, Z.; Gallagher, I. E. *Tetrahedron Lett.* **2000**, *41*, 3173.

74. Nicolaou, K. C.; Pastor, J.; Barluenga, S.; Winssinger, N. *Chem. Commun.* **1998**, 1947.

75. Ruhland, T.; Andersen, K.; Pedersen, H. *J. Org. Chem.* **1998**, *63*, 9204.

76. (a) Frechet, J. M. J.; Nuyens, L. J.; Seymour, E. *J. Am. Chem. Soc.* **1979**, *101*, 432. (b) Pourbaix, C.; Carreaux, F.; Carboni, B.; Deleuze, H. *Chem. Commun.* **2000**, 1275. (c) Burgess, W. Li. K. *Tetrahedron Lett.* **1999**, *40*, 6527. (d) Gravel, M.; Thompson, K. A.; Zak, M.; Bérubé, C.; Hall, D. G. *J. Org. Chem.* **2002**, *67*, 3.

77. Nicolaou, K. C.; Winssinger, N. Pastor, J.; Murphy, F. *Angew. Chem. Int. Ed.* **1998**, *37*, 2534.

78. Marshall, D. L.; Liener, I. E. *J. Org. Chem.* **1970**, *35*, 867.

79. Patek, M.; Lebi, M. *Tetrahedron Lett.* **1991**, *32*, 3891.

80. Spivey, A. C.; Diaper, C. M.; Adams, H.; Rudge, A. J. *J. Org. Chem.* **2000**, *65*, 5253.

81. Guthrie, E. J.; Macritchie, J.; Hartley, R. C. *Tetrahedron Lett.* **2000**, *41*, 4987.

82. Kamogawa, H.; Kanzawa, A.; Kadoya, M; Naito, T.; Nanasawa, M. M. *Bull. Chem. Soc. Jpn.* **1983**, *56*, 762.

83. Jung, K. W.; Zhao, X. Y.; Janda, K. D.; *Tetrahedron* **1997**, *53*, 6645.

84. Jin, S. J.; Holub, D. P.; Wustrow, D. J. *Tetrahedron Lett.* **1998**, *39*, 3651.

85. Waugh, J. S. In *NMR and Biochemistry*; Opella, S. J., Lu, P., Eds.; Marcel Dekker: New York, **1980**, 203.

86. Giralt, E.; Rizo, J.; Pedroso, E. *Tetrahedron* **1984**, 40, 4141.

87. Ford, W. T.; Balakrishnan, T. *Macromolecules* **1981**, *14*, 284.

88. Kiefer, P. A. *Drugs Future* **1998**, *23*, 301.

89. (a) Chen, C.; Randall, L. A. A.; Miller, R. B.; Jones, A. D.; Kurth, M. J. *J. Am. Chem. Soc.* **1994**, *116*, 2261. (b) Hauske, J. R.; Dorff, P. *Tetrahedron Lett.* **1995**, *36*, 1589.

90. Haskins, N. J.; Hunter, D. J.; Organ, A. J.; Rahman, S. S.; Thom, C. *Rapid Commun. Mass Spectrom.* **1995**, *9*, 1437.

91. Dörwald, F. Z. *Organic Synthesis on Solid Phase: Supports, Linkers, Reactions*, Wiley-VCH, Weinheim, **2000**, Ch. 2.
92. Gordon, K.; Balasubramanian, S. *J. Chem. Technol. Biotechnol.* **1999**, *74*, 835.
93. Morphy, J. R.; Rankovic, Z.; Rees, D. C. *Tetrahedron Lett.* **1996**, *37*, 3209.
94. Brown, A. R.; Rees, D. C.; Rankovic, Z.; Morphy, J. R. *J. Am. Chem. Soc.* **1997**, *119*, 3288.
95. (a) Kroll, F. E. K.; Morphy, R.; Rees D.; Gani, D. *Tetrahedron Lett.* **1997**, *38*, 8573. (b) Heinonen, P.; onggberg, H. *Tetrahedron Lett.* **1997**, *38*, 8569. (c) Wang, G.; Yao, S. Q. *Org. Lett.* **2003**, *5*, 4437.
96. Fruchtel, J. S.; Jung, G. *Angew. Chem. Int. Ed.* **1996**, *35*, 17.
97. D'herde, J. N.; De Clercq, P. J. *Tetrahedron Lett.* **2003**, *44*, 6657.
98. Li, W.; Chen, Y.; Lam, Y. *Tetrahedron Lett.* **2004**, *45*, 6545.
99. Nicolaou, K. C.; Snyder, S. A.; Bigot, A.; Turner, N. J. *Angew. Chem. Int. Ed.* **2000**, *39*, 1093.
100. Arvanitis, E. A.; Craig, D.; Timm, A. *ARKIVOC* **2002**, IX, 19.
101. Connors, R. V.; Zhang, A. J.; Shuttleworth, S. J. *Tetrahedron Lett.* **2002**, *43*, 6661.
102. Wu, T. Y. H.; Schultz, P. G. *Org. Lett.* **2002**, *4*, 4033.
103. Posner, G. H.; Brunelle, D. J. *J. Org. Chem.* **1972**, *37*, 3547.
104. Wang, G.; Mahesh, U.; Chen, G. Y. J.; Yao, S. Q. *Org. Lett.* **2003**, *5*, 737.
105. For reviews of the reactions, synthesis and applications of benzofurans, including isobenzofurans, see: (a) Heaney, H.; Ahn, J. S. in *Comprehensive Heterocyclic Chemistry II*, Bird, C. W. (Ed.), Elsevier, Oxford, **1996**, Ch. 2.06, pp. 297-350. (b) Friedrichsen, W. in *Comprehensive Heterocyclic Chemistry II*, Bird, C. W. (Ed.), Elsevier, Oxford, **1996**, Ch. 2.07, pp. 351-393. (c) Keay, B. A.; Dibble, P. W. in *Comprehensive Heterocyclic Chemistry II*, Bird, C. W. (Ed.), Elsevier, Oxford, **1996**, Ch. 2.08, pp. 395-436.
106. Wittig, G.; Krebs, A. *Chem. Ber.* **1961**, *94*, 3260.
107. Wittig, G.; Weinlich, J.; Wilson, E. R. *Chem. Ber.* **1965**, *98*, 458.
108. Gribble, G. W.; Kelly, W. J.; Sibi, M. P. *Synthesis* **1982**, 143.
109. (a) Reddy, G. S.; Bhatt, M. V. *Tetrahedron Lett.* **1980**, *21*. 3627. (b) Wittig, G.;

Pohlke, R. *Chem. Ber.* **1961**, *94*, 3276.

110. (a) Beringer, F. M.; Huang, S. J. J. *Org. Chem.* **1964**, *29*, 445. (b) Feldman, K. S.; Ruckle, R. E., Jr.; Ensel, S. M.; Weinreb, P. H. *Tetrahedron Lett.* **1992**, *33*, 7101.
111. Wittig, G.; Mayer, U. *Chem. Ber.* **1963**, *96*, 329.
112. Komatsu, K.; Aonuma, S.; Jinbu, Y.; Tsuji, R.; Hirosawa, C.; Takeuchi, K. *J. Org. Chem.* **1991**, *56*, 195.
113. Kitamura, T.; Kotani, M.; Yokoyama, T.; Fujiwara, Y. *J. Org. Chem.* **1999**, *64*, 680.
114. (a) Pummerer, R. *Ber.* **1909**, *42*, 2282. (b) Pummerer, R. *Ber.* **1910**, *43*, 1401.
115. DeLucchi, O.; Miotti, U.; Modena, G. *Org. Reactions,* Paquette, L. A., Ed.; John Wiley: **1991**, Ch. 3, pp 157-184.
116. Cochran, J. E.; Padwa, A. *Tetrahedron Lett.* **1995**, *36*, 3495.
117. Lee, G. A.; Huang, A. N.; Chen, C. S.; Li, Y. C.; Jann, Y. C. *J. Org. Chem.* **1997**, *62*, 3355.
118. (a) Hanack, M.; Massa, F. *Tetrahedron Lett.* **1977**, *18*, 661. (b) Massa, F.; Hanack, M.; Subramanian, L. R. *J. Fluorine Chem.* **1982**, *19*, 601.
119. (a) Strunz, G. M.; Findlay, J. A. In *The Alkaloids*, ed. Brossi, A. Academic Press: New York, **1985**, Vol. 26, p. 89-174. (b) Fodor, G. B.; Colasanti, B. The Pyridine and Piperidine Alkaloids: Chemistry and Pharmacology. In *Alkaloids*: *Chemical and Biological Perspectives*; ed. Pelletier, S. W. Wiley-Interscience, New York, **1985**, Vol. 3, pp. 1-90. (c) Laschat, S.; Dickner, T. *Synthesis* **2000**, *13*, 1781.
120. Peraza, P. S.; Vallado, M. R.; Loeza, W. B.; Mena-Rejón, G. J.; Quijano, L. *Fitoterapia* **2000**, *76*, 690.
121. Bolzani; V. S.; Gunatilaka, A. A. L.; Kingston, D. G. I. *Tetrahedron* **1995**, *51*, 5929.
122. Kirtikar, K. R.; Basu, B. D. *Indian Medicinal Plants* Leader Press, Allahbad, **1935**, vol. 2, 910.
123. Siddiqui, S.; Murthi, S. *J. Sci. Ind. Res.* **1948**, *7b*, 188.
124. Merzabani, M. M. El.; Aaser, A. A.; Attia, M. A.; Duweini, A. K. Al; Ghazal, A. M. *Planta Med.* **1979**, *36*, 150.
125. Ahmad, A., Khan, K. A.; Ahmad, V. U.; Qazi, S. *Planta Med*, **1986**, *4*, 285.

126. Aqeel, A., Khursheed, A. K. Viqaruddin A, Sabiha Q. *Arzneimittel Forschung* **1989**, *39*, 652.

127. Ahmad, V. U.; Basha, A.; Haque, *W. Z. Naturforsch., B: Anorg. Chem., Org. Chem.* **1978**, *33B,* 347.

128. Paterne, M.; Brown, *E. C. R. Seances Acad. Sci., Ser. 2* **1983**, *296,* 433.

129. Ahmad, V. U.; Qazi, *S. Z. Naturforsch., B: Anorg. Chem., Org. Chem.* **1983**, *38B,* 660.

130. Datwyler, P.; Ott-Longoni, R.; Schopp, E.; Hesse, M. *Helv. Chim. Acta* **1981**, *64*, 1959.

131. Nakano, H.; Nakajima, E.; Fujii, Y.; Shigemori, H. Hasegawa, K. *Plant Growth Regulation* **2004**, *44*, 207.

132. Kiguchi, T.; Shirakawa, M.; Honda, R.; Ninomiya, I.; Naito, T. *Tetrahedron* **1998**, *54*, 15589.

133. Shimizu, T.; Hiramura, S.; Nakata, T. *Tetrahedron Lett.* **1996**, *37,* 6145.

134. Barton, D. H. R.; McCombie, *S. W. J. Chem. Soc., Perkin Trans. 1* **1975**, 1574.

135. Lemire, A.; Charette, A. B. *Org. Lett.* **2005**, *7*, 2747.

136. Charette, A. B.; Grenon, M.; Lemire, A.; Pourashraf, M.; Martel, J. *J. Am. Chem. Soc.* **2001**, *123*, 11829.

137. Hamilton, M. D. M.Sc. Thesis, University of Calgary, **2002**.

138. (a) Giovvannini, R. Petrini, M. *Synlett.* **1998**, 90. (b) Eisch, J. J.; Galle, J. E. *J. Org. Chem.* **1998**, *45*, 4534. (c) Katherine E. B.; Anthony L. C.; Peter D. K.; Christopher J. *Tetrahedron lett.* **2002**, *43*, 135.

139. Hsiao, Y.; Hegedus, L. S. *J. Org. Chem.* **1997**, *62*, 3586.

140. Brace, N. O. *J. Org. Chem.* **1993**, *58*, 4506.

141. Dey, S.; Kumbhare, L. B.; Jain, V. K.; Schurr, T.; Kaim, W.; Klein, A.; Belaj, F. *Eur. J. Inorg. Chem.* **2004**, 4510.

142. (a) Coldham, I.; Hufton, R. *Tetrahedron* **1996**, *52*, 12541. (b) Di Cesare, P.; Bouzard, D.; Essiz, M.; Jacquet, J. P.; Ledoussal, B.; Kiechel, J. R.; Remuzon, P.; Kessler, R. E.; Fung-Tomc, J.; Desiderio, J. *J. Med. Chem.* **1992**, *35*, 4205.

143. Chelucci, G.; Saba, A. *Angew. Chem. Int. Ed.* **1995**, *34*, 78.

144. Padwa, A.; Kline, D. N.; Murphree, S. S.; Yeske, P. E. *J. Org. Chem.* **1992**, *57*, 298.

145. (a) Miller, B. *Advanced Organic Chemistry – Reactions and Mechanisms*; Prentice Hall: Upper Saddle River, New Jersey, **1998**, pp. 177-181. (b) Crist, D. R.; Leonard, N. J. *Angew. Chem. Int. Ed.* **1969**, *8*, 962.

146. (a) Fuson, R. C.; Zirkle, C. L. *J. Am. Chem. Soc.* **1948**, *70*, 2760. (b) Kerwin, J. F.; Ullyot, G. E.; Fuson, R. C.; Zirkle, C. L. *J. Am. Chem. Soc.* **1947**, *69*, 2961. (c) Schultz, E. M.; Sprague, J. M. *J. Am. Chem. Soc.* **1948**, *70*, 48.

147. Dieter, R. K.; Deo, N.; Lagu, B.; Dieter, J. W. *J. Org. Chem.* **1992**, *57*, 1663.

148. Back, T. G.; Chau, J. H. L.; Codding, P. W.; Gladstone, P. L.; Jones, D. H.; Morzycki, J. W.; Roszak, A. W. *J. Org. Chem.* **1992**, *57*, 4110.

149. Evans, D. A.; Mitch, C. H. *Tetrahedron Lett.* **1982**, *23*, 285.

150. For some earlier studies of elimination-addition reactions involves bis-sulfones similar to **261**, see: Kader, A. T.; Stirling, C. J. M. *J. Chem. Soc.* **1962**, 3686.

151. Reich, H. J.; Peake, S. L. *J. Am. Chem. Soc.* **1978**, *100*, 4888.

152. Trost, B. M.; Arndt, H. C.; Strege, P. E.; Vehoeven, T. R. *Tetrahedron Lett.* **1976**, *17*, 3477.

153. Angier, R. B.; Smith, A. *J. Org. Chem.* **1956**, *21*, 1540.

154. Qian, H.; Huang, X. *Tetrahedron Lett.* **2002**, *43*, 1059.

155. Psiorz, H. M.; Bomhard, A.; Hauel, N.; Narr, B.; Noll, K.; Lillie, C.; Kobinger, W.; Daemmgen, *J. Eur. Pat. Appl.* **1988**, EP 292840.

156. Norton, T. R.; Seibert, R. A.; Benson, A. A.; Bergstrom, F. W. *J. Am. Chem. Soc.* **1946**, *68*, 1572.

157. Zhong, H. M.; Greco, M. N.; Maryanoff, B. E. *J. Org. Chem.* **1997**, *62*, 9326.

158. Sonogashira, K.; Tohda, Y.; Hagihara, N. *Tetrahedron Lett.*, **1975**, *16*, 4467.

159. Fairlamb, I. J. S.; Bäuerlein, P. S.; Marrison, L. R.; Dickinson, J. M. *Chem. Commun.* **2003**, 632.

160. Liu, L. K.; Chi, Y.; Jen, K. Y. *J. Org. Chem.* **1980**, *45*, 406.

161. Venkataraman, G. *Indian Acad. Sci. Sect. A* **1945**, *21*, 34.

162. Reid, W. *J. Am. Chem. Soc.* **1923**, *45*, 2411.

163. Nandi, B.; Kundu, N. G. *J. Chem. Soc., Perkin Trans. 1,* **2001**, 1649.

164. Hollinshead, S. P. *Tetrahedron Lett.* **1996**, *37*, 9157.

165. Iwata, N.; Morioka, T.; Kobayashi, T.; Asada, T.; Kinoshita, H.; Inomata, K. *Bull. Chem. Soc. Jpn.* **1992**, *65*, 1379.

166. Wong, S. C.; Green, G. D. J.; Shaw. E. *J. Med. Chem.* **1978**, *21*, 456.

167. Morales, G. A.; Corbett, J. W.; DeGrado, W. F. *J. Org. Chem.* **1998**, *63*, 1172.

168. Beebe X.; Schore, N. E.; Kurth, M. J. *J. Org. Chem.* **1995**, *60*, 4196.

169. Bell, M. L.; Chiechi, R. C.; Johnson, C. A.; Kimball, D. B.; Matzger, A. J. W.; Wan, B.; Weakley, T. J. R.; Haley, M. M. *Tetrahedron* **2001**, *57*, 3507.

170. Grundmann, C.; Richter, R. *J. Org. Chem.* **1968**, *33*, 476.

171. For a recent review, see: Nicolaou, K. C.; Synder, S. A.; Montagnon, T.; Vassilikogiannakis. G. *Angew. Chem. Int. Ed.* **2002**, *41*, 1668.

172. Lee, S. W.; Fuchs, P. L. *Tetrahedron Lett.* **1991**, *32*, 2861.

173. Pearson, W. H.; Walavalkar, R. *Tetrahedron* **2001**, *57*, 5081.

174. Baumgartel O.; Szeimies G. *Chem. Ber.* **1983**, *116*, 2180.

175. For lead references and a discussion of the migratory aptitudes of various types of substituents, see: Smith, M. B.; March, J. in *March's Advanced Organic Chemistry: Reactions, Mechanisms and Structure*, 5th edn, Wiley, New York, **2001**, pp. 1384.

176. For the oxidation of other polycyclic arenes with peracids see: Lewis, S. N. in *Oxidation*, Augustine, R. L. (ed.), Dekker, New York, **1969**, vol. 1, p. 235-236.

177. Carey, F. A.; Sundberg, R. J. in *Advanced Organic Chemistry. Part A: Reactions, Mechanisms and Structure*, 3th edn, Kluwer/Plenum, New York, **1993**, pp. 215.

178. (a) Prinzbach, H.; Arguëlles, M.; Druckrey, E. *Angew. Chem. Int. Ed.* **1966**, *5*, 1039. (b) Vogel, P.; Willhalm, B.; Prinzbach, H. *Helv. Chim. Acta* **1969**, *52*, 584. (c) Tochtermann, W.; Olsson, G. *Chem. Rev.* **1989**, *89*, 1203. (d) Tochtermann, W.; Timm, H.; Diekmann, J. *Tetrahedron Lett.* **1977**, *18*, 4311. (e) Tochtermann, W.; Köhn, H. *Chem. Ber.* **1980**, *113*, 3249.

179. Haselbach, E; Martin, H. -D. *Helv. Chim. Acta* **1974**, *57*, 472.

180. Prinzbach, H.; Babsch, H. *Angew. Chem. Int. Ed.* **1975**, *14*, 753.

181. Schleyer, P.; Williams, E. J.; Blanchard, K. R. *J. Am. Chem. Soc.* **1970**, *92*, 2377.

182. Huisgen, R. *Angew. Chem. Int. Ed.* **1980**, *19*, 947.

183. Cockroft, R. D.; Waali, E. E.; Rhoads, S. J. *Tetrahedron Lett.* **1970**, *11*, 3539.

184. (a) Balani, S. K.; Brannigan, I. N.; Boyd, D. R.; Sharma, N. D.; Hempenstall, F.; Smith, A. *J. Chem. Soc., Perkin Trans. 1* **2001**, 1091. (b) Boyd, D. R.; Agarwal, S. K.; Balani, S. K.; Dunlop, R.; Gadaginamath, G. S.; O'Kane, G. A.; Sharma, N. D.; Jennings, W. B.; Yagi, H.; Jerina, D. M. *J. Chem. Soc., Chem. Commun.* **1987**, 1633. (c) Shudo, K.; Okamoto, T. *Chem. Pharm. Bull.* **1973**, *21*, 2809.

185. Vogel, E.; Günther, H. *Angew. Chem. Int. Ed.* **1967**, *6*, 385.

186. (a) Dimroth, K.; Pohl, G. *Angew. Chem.* **1961**, *73*, 436. (b) Ziegler, G. R.; Hammond, G. S. *J. Amer. Chem. Soc.* **1968**, *90*, 513. (c) Jeffrey, A. M.; Jerina, D. M. *J. Amer. Chem. Soc.* **1972**, *94*, 4048.

187. Zimmerman, H. E.; Schuster, D. I. *J. Am. Chem. Soc.* **1961**, *83*, 4486.

188. (a) Schultz, A. G.; Reilly, J. *J. Am. Chem. Soc.* **1992**, *114*, 5068. (b) Zimmerman, H. E.; Pasteris, R. J. *J. Org. Chem.* **1980**, *45*, 4864. (c) Schuster, D. I. *Acc. Chem. Res.* **1978**, *11*, 65. For a different point of view, see: (d) Gómez, I.; Olivella, S.; Reguero, M.; Riera, A.; Solé, A. *J. Am. Chem. Soc.* **2002**, *124*, 15375.

189. (a) Sczostak, A.; Sönnichsen, F.; Tochtermann, W.; Peters, E.-M.; Peters, K.; Schnering, H. G. *Tetrahedron Lett.* **1985**, *26*, 5677. (b) Tochtermann, W.; Olsson, G.; Sczostak, A.; Sonnichsen, F.; Frauenrath, H.; Runsink, J.; Peters, E.-M.; Peters, K.; vonSchnering, H. G. *Chem. Ber.* **1989**, *122*, 199.

190. Paquette, L. A.; Barrett, J. H.; Spitz, R. P.; Pitcher, R. *J. Am. Chem. Soc.* **1965**, *87*, 3417.

191. Tobe, Y.; Iseki, T.; Kakiuchi, K.; Odaira, Y. *Tetrahedron Lett.* **1984**, *25*, 3895.

192. Ibuka, T.; Habashita, H.; Otaka, A.; Oguchi, Y.; Uyehara, T.; Yamamoto, Y. *J. Org. Chem.* **1991**, *56*, 4370.

193. Cram, D. J.; Whon, D. R. *J. Am. Chem. Soc.* **1963**, *86,* 1246.

194. Stevens, R. V. *Acc. Chem. Res.* **1984**, *17*, 289.

195. Toyooka, N.; Yoshida, Y.; Yotsui, Y.; Momose, T. *J. Org. Chem.* **1999**, *64*, 4914.

196. Johnson, F. *Chem. Rev.* **1968**, *68*, 375.

197. Omura, K.; Swern, D. *Tetrahedron* **1978**, *34*, 1651.

198. Lermer, L.; Neeland, E. G.; Ounsworth, J. P.; Sims, R. J.; Tischler, S. A.; Weiler, L.

Can. J. Chem. **1992**, *70*, 1427.

199. Back, T. G.; Yang, K.; Krouse, H. R. *J. Org. Chem.* **1992**, *57*, 1986.

Appendix I X-Ray Crystallographic Data for 226

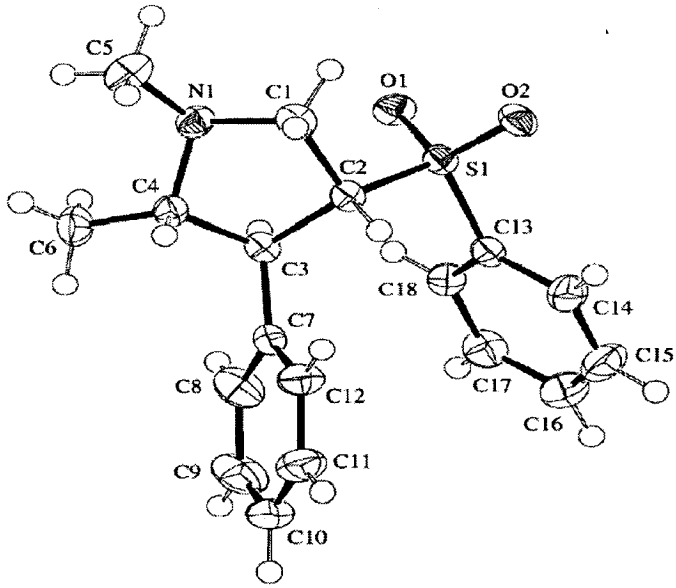

Experimental:

A colorless prismatic crystal of $C_{18}H_{21}NO_2S$ was coated with Paratone 8277 oil (Exxon) and mounted on a glass fiber. All measurements were made on a Nonius KappaCCD diffractometer with graphite monochromated Mo-Kα radiation. Cell constants obtained from the refinement[1] of 19110 reflections in the range $3.0 < \theta < 27.5°$ corresponded to a primitive monoclinic cell; details of crystal data and structure refinement have been provided in Table 1. The space group was uniquely determined from the systematic absences. The data were collected[2] at a temperature of 173(2) K using ω and φ scans to a maximum θ value of 27.5°. The data were corrected for Lorentz and polarization effects and for absorption using multi-scan method[1]. Since the crystal did not show any sign of decay during data collection a decay correction was deemed unnecessary.

The structure was solved by the direct methods[3] and expanded using Fourier techniques.[4] There are two independent molecules in the asymmetric unit. The non-hydrogen atoms were refined anisotropically. Hydrogen atoms were included at geometrically idealized positions and were not refined. The final cycle of full-matrix least-squares refinement using SHELXL97[5] converged (largest parameter shift was 0.00 times its esd) with unweighted and weighted agreement factors, R = 0.0425 and wR = 0.0812 (all data), respectively, and goodness of fit, S = 1.030. The absolute structure was established by the Flack method[6] with the absolute configuration at the chiral centers: C2, C2' (R), C3, C3' (S) and C4, C4' (S). The Flack parameter for the inverted structure was 1.00(5). Therefore, the inverted structure was rejected as the one present in the crystal. The weighting scheme was based on counting statistics and the final difference Fourier map was essentially featureless. The figure was plotted with the aid of ORTEPII.[7]

Table 1. Crystal data and structure refinement for **226**

Empirical formula	$C_{18}H_{21}NO_2S$	
Formula weight	315.42	
Temperature	173(2) K	
Wavelength	0.71073 Å	
Crystal system	Monoclinic	
Space group	$P2_1$	
Unit cell dimensions	a = 8.682(2) Å	α = 90°.
	b = 10.123(2) Å	β = 93.99(2)°.
	c = 18.874(5) Å	γ = 90°.
Volume	1654.8(7) $Å^3$	
Z	4	
Density (calculated)	1.266 Mg/m^3	
Absorption coefficient	0.202 mm^{-1}	
F(000)	672	
Crystal size	0.20 x 0.18 x 0.10 mm^3	
Theta range for data collection	5.9 to 27.5°.	
Index ranges	-11<=h<=10, -15<=k<=15, -24<=l<=24	
Reflections collected	19110	
Independent reflections	7234 [R(int) = 0.034]	
Completeness to theta = 27.5°	97.8 %	
Absorption correction	Multi-scan method	
Max. and min. transmission	0.9801 and 0.9607	
Refinement method	Full-matrix least-squares on F^2	
Data / restraints / parameters	7234 / 1 / 397	
Goodness-of-fit on F^2	1.030	
Final R indices [I>2sigma(I)]	R1 = 0.0425, wR2 = 0.0725	
R indices (all data)	R1 = 0.0716, wR2 = 0.0812	
Largest diff. peak and hole	0.235 and -0.302 $e.Å^{-3}$	

Atomic coordinates and equivalent isotropic displacement parameters, anisotropic displacement parameters as well as bond lengths, bond angles and torsion angles are available via the Internet at http://pubs.acs.org.

Appendix II X-Ray Crystallographic Data for 243

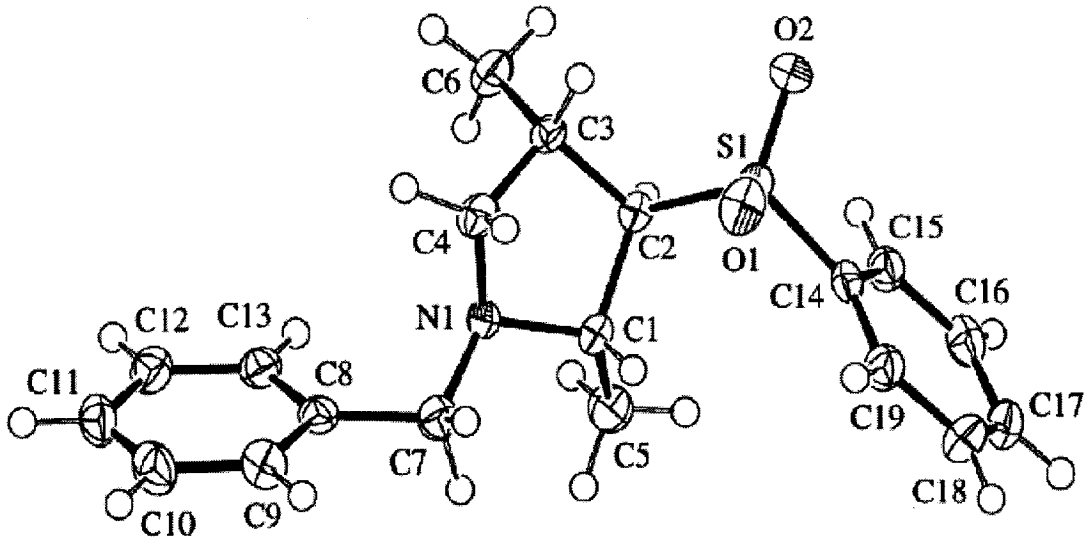

Experimental:

A colorless prismatic crystal of $C_{19}H_{23}NO_2S$ was coated with Paratone 8277 oil (Exxon) and mounted on a glass fiber. All measurements were made on a Nonius KappaCCD diffractometer with graphite monochromated Mo-Kα radiation. Cell constants obtained from the refinement[1] of 9074 reflections in the range $6.0 < \theta < 27.6°$ corresponded to a primitive monoclinic cell; details of crystal data and structure refinement have been provided in Table 1. The space group was uniquely determined from the systematic absences. The data were collected[2] at a temperature of 173(2) K using ω and φ scans to a maximum θ value of 27.6°. The data were corrected for Lorentz and polarization effects and for absorption using multi-scan method[1]. Since the crystal did not show any sign of decay during data collection a decay correction was deemed unnecessary.

The structure was solved by the direct methods[3] and expanded using Fourier techniques.[4] The non-hydrogen atoms were refined anisotropically. Hydrogen atoms were included at geometrically idealized positions and were not refined. The final cycle of full-matrix least-squares refinement using SHELXL97[5] converged (largest parameter shift was 0.00 times its esd) with unweighted and weighted agreement factors, R = 0.0505 and wR = 0.1086 (all data), respectively, and goodness of fit, S = 0.955. The absolute structure was established by the Flack method[6] with the absolute configuration at the chiral centers: C1 (S), C2 (R) and C3 (S). The Flack parameter for the inverted structure was 1.01(9). Therefore, the inverted structure was rejected as the one present in the crystal. The weighting scheme was based on counting statistics and the final difference Fourier map was essentially featureless. The figure was plotted with the aid of ORTEPII.[7]

Table 1. Crystal data and structure refinement for **243**

Empirical formula	$C_{19}H_{23}NO_2S$
Formula weight	329.44
Temperature	173(2) K
Wavelength	0.71073 Å
Crystal system	Orthorhombic
Space group	$P2_12_12_1$
Unit cell dimensions	a = 5.7550(12) Å
	b = 39.7980(13) Å
	c = 7.712(4) Å
Volume	1766.3(9) $Å^3$
Z	4
Density (calculated)	1.239 Mg/m^3
Absorption coefficient	0.192 mm^{-1}
F(000)	704
Crystal size	0.18 x 0.18 x 0.17 mm^3
Theta range for data collection	6.0 to 27.6°.
Index ranges	-6<=h<=7, -51<=k<=51, -10<=l<=9
Reflections collected	9074
Independent reflections	4004 [R(int) = 0.083]
Completeness to theta = 27.6°	98.1 %
Absorption correction	Multi-scan method
Max. and min. transmission	0.9680 and 0.9662
Refinement method	Full-matrix least-squares on F^2
Data / restraints / parameters	4004 / 0 / 208
Goodness-of-fit on F^2	0.955
Final R indices [I>2sigma(I)]	R1 = 0.0505, wR2 = 0.0889
R indices (all data)	R1 = 0.1177, wR2 = 0.1086
Absolute structure parameter	-0.01(9)
Largest diff. peak and hole	0.227 and -0.306 $e.Å^{-3}$

Atomic coordinates and equivalent isotropic displacement parameters, anisotropic displacement parameters as well as bond lengths, bond angles and torsion angles are available via the Internet at http://pubs.acs.org.

Appendix III X-Ray Crystallographic Data for 244

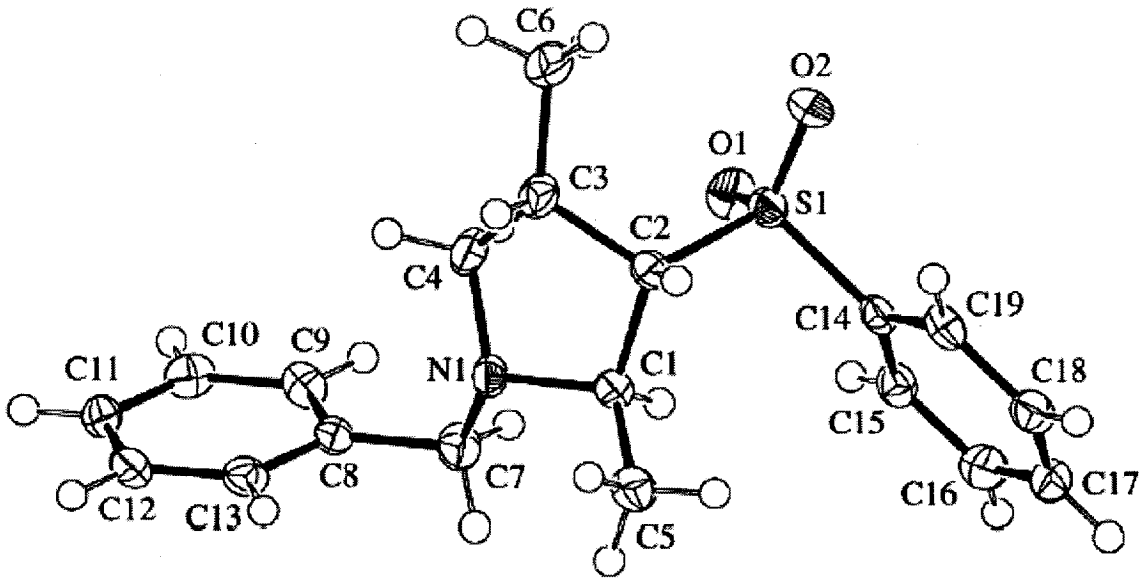

Experimental:

A colorless prismatic crystal of $C_{19}H_{23}NO_2S$ was coated with Paratone 8277 oil (Exxon) and mounted on a glass fiber. All measurements were made on a Nonius KappaCCD diffractometer with graphite monochromated Mo-Kα radiation. Cell constants obtained from the refinement[1] of 10194 reflections in the range $1.0 < \theta < 27.6°$ corresponded to a primitive monoclinic cell; details of crystal data and structure refinement have been provided in Table 1. The space group was uniquely determined from the systematic absences. The data were collected[2] at a temperature of 173(2) K using ω and φ scans to a maximum θ value of 27.6°. The data were corrected for Lorentz and polarization effects and for absorption using multi-scan method[1]. Since the crystal did not show any sign of decay during data collection a decay correction was deemed unnecessary.

The structure was solved by the direct methods[3] and expanded using Fourier techniques.[4] The non-hydrogen atoms were refined anisotropically. Hydrogen atoms were included at geometrically idealized positions and were not refined. The final cycle of full-matrix least-squares refinement using SHELXL97[5] converged (largest parameter shift was 0.00 times its esd) with unweighted and weighted agreement factors, R = 0.0524 and wR = 0.0954 (all data), respectively, and goodness of fit, S = 1.009. The absolute structure was established by the Flack method[6] with the absolute configuration at the chiral centers: C1 (R), C2 (S) and C3 (S). The Flack parameter for the inverted structure was 1.07(10). Therefore, the inverted structure was rejected as the one present in the crystal. The weighting scheme was based on counting statistics and the final difference Fourier map was essentially featureless. The figure was plotted with the aid of ORTEPII.[7]

Table 1. Crystal data and structure refinement for **244**

Empirical formula	$C_{19}H_{23}NO_2S$
Formula weight	329.44
Temperature	173(2) K
Wavelength	0.71073 Å
Crystal system	Orthorhombic
Space group	$P2_12_12_1$
Unit cell dimensions	a = 5.6376(4) Å
	b = 15.1734(10) Å
	c = 20.0417(8) Å
Volume	1714.50(18) $Å^3$
Z	4
Density (calculated)	1.276 Mg/m^3
Absorption coefficient	0.198 mm^{-1}
F(000)	704
Crystal size	0.20 x 0.18 x 0.18 mm^3
Theta range for data collection	6.0 to 27.6°.
Index ranges	-7<=h<=6, -17<=k<=19, -26<=l<=22
Reflections collected	10194
Independent reflections	3871 [R(int) = 0.088]
Completeness to theta = 27.6°	97.8 %
Absorption correction	Multi-scan method
Max. and min. transmission	0.9652 and 0.9614
Refinement method	Full-matrix least-squares on F^2
Data / restraints / parameters	3871 / 0 / 208
Goodness-of-fit on F^2	1.009
Final R indices [I>2sigma(I)]	R1 = 0.0524, wR2 = 0.0796
R indices (all data)	R1 = 0.1219, wR2 = 0.0954
Absolute structure parameter	-0.08(10)
Largest diff. peak and hole	0.226 and -0.292 $e.Å^{-3}$

Atomic coordinates and equivalent isotropic displacement parameters, anisotropic displacement parameters as well as bond lengths, bond angles and torsion angles are available via the Internet at http://pubs.acs.org.

Appendix IV X-Ray Crystallographic Data for 245

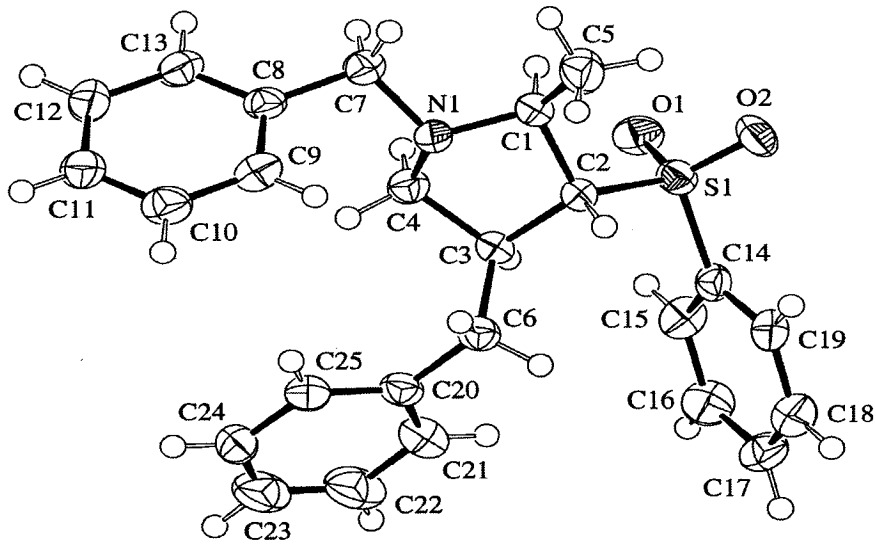

Experimental:

A colorless prismatic crystal of $C_{25}H_{27}NO_2S$ was coated with Paratone 8277 oil (Exxon) and mounted on a glass fiber. All measurements were made on a Nonius KappaCCD diffractometer with graphite monochromated Mo-Kα radiation. Cell constants obtained from the refinement[1] of 5039 reflections in the range $3.6 < \theta < 27.5°$ corresponded to a primitive monoclinic cell; details of crystal data and structure refinement have been provided in Table 1. The space group was uniquely determined from the systematic absences. The data were collected[2] at a temperature of 173(2) K using ω and φ scans to a maximum θ value of 27.5°. The data were corrected for Lorentz and polarization effects and for absorption using multi-scan method[1]. Since the crystal did not show any sign of decay during data collection a decay correction was deemed unnecessary.

The structure was solved by the direct methods[3] and expanded using Fourier techniques.[4] The non-hydrogen atoms were refined anisotropically. Hydrogen atoms were included at geometrically idealized positions and were not refined. The final cycle of full-matrix least-squares refinement using SHELXL97[5] converged with unweighted and weighted agreement factors, R = 0.049 and wR = 0.105 (all data), respectively, and goodness of fit, S = 0.99. The absolute structure was established by the Flack method[6] with the absolute configuration at the chiral centers: C1 (S), C2 (R) and C3 (S). The Flack parameter for the inverted structure was 0.95(8). Therefore, the inverted structure was rejected as the one present in the crystal. The weighting scheme was based on counting statistics and the final difference Fourier map was essentially featureless. The figures were plotted with the aid of ORTEPII.[7]

Table 1. Crystal data and structure refinement for **245**

Empirical formula	$C_{25}H_{27}NO_2S$	
Formula weight	405.54	
Temperature	173(2) K	
Wavelength	0.71073 Å	
Crystal system	Monoclinicic	
Space group	$P2_1$	
Unit cell dimensions	a = 11.491(4) Å	α = 90°.
	b = 8.753(4) Å	β = 94.916(14)°.
	c = 11.720(5) Å	γ = 90°.
Volume	1117.0(8) $Å^3$	
Z	4	
Density (calculated)	1.206 Mg/m^3	
Absorption coefficient	0.17 mm^{-1}	
F(000)	432	
Crystal size	0.22 x 0.16 x 0.04 mm^3	
Theta range for data collection	3.6 to 27.5°.	
Index ranges	-14<=h<=14, -11<=k<=11, -15<=l<=15	
Reflections collected	5035	
Independent reflections	5035 [R(int) = 0.00]	
Completeness to theta = 27.6°	99.3 %	
Absorption correction	Multi-scan method	
Max. and min. transmission	0.993 and 0.965	
Refinement method	Full-matrix least-squares on F^2	
Data / restraints / parameters	5035 / 1 / 262	
Goodness-of-fit on F^2	0.99	
Final R indices [I>2sigma(I)]	R1 = 0.049, wR2 = 0.087	
R indices (all data)	R1 = 0.115, wR2 = 0.105	
Absolute structure parameter	0.04(7)	
Largest diff. peak and hole	0.20 and -0.27 e.$Å^{-3}$	

Table 2. Atomic coordinates (x 10^4) and equivalent isotropic displacement parameters ($Å^2$x 10^3) for **245**. U(eq) is defined as one third of the trace of the orthogonalized U^{ij} tensor

Atom	x	y	z	U(eq)
S(1)	2071(1)	4057(1)	4743(1)	34(1)
O(1)	3165(2)	4985(2)	5201(2)	42(1)
O(2)	1039(2)	4354(2)	5160(1)	41(1)
N(1)	1465(2)	5815(2)	1569(2)	32(1)
C(1)	1165(2)	5804(3)	2694(2)	32(1)
C(2)	1551(2)	4171(3)	3140(2)	29(1)
C(3)	2561(2)	3699(3)	2592(2)	28(1)
C(4)	2689(2)	5133(3)	1898(2)	34(1)
C(5)	-169(3)	6183(4)	2517(3)	48(1)
C(6)	2176(3)	2295(3)	1776(2)	34(1)
C(7)	1387(3)	7290(3)	981(2)	39(1)
C(8)	1558(3)	7134(3)	-244(2)	33(1)
C(9)	969(3)	5968(3)	-1021(3)	40(1)
C(10)	1132(3)	5817(4)	-2141(3)	45(1)
C(11)	1852(3)	6832(3)	-2500(3)	45(1)
C(12)	2425(3)	7992(4)	-1740(3)	50(1)
C(13)	2286(3)	8129(3)	-613(3)	43(1)
C(14)	2501(3)	2124(3)	5027(2)	32(1)
C(15)	3729(3)	1717(4)	5353(2)	40(1)
C(16)	4038(3)	178(4)	5507(3)	48(1)
C(17)	3141(3)	-934(4)	5348(2)	45(1)
C(18)	1925(3)	-503(3)	5031(2)	43(1)
C(19)	1594(3)	1028(3)	4872(2)	35(1)
C(20)	3177(2)	1743(3)	1296(2)	34(1)
C(21)	4140(3)	871(4)	2015(3)	47(1)
C(22)	5067(3)	359(4)	1612(3)	62(1)
C(23)	5048(4)	710(4)	463(4)	66(1)
C(24)	4113(4)	1583(4)	-273(3)	58(1)
C(25)	3171(3)	2097(3)	148(3)	44(1)

Table 3. Bond lengths [Å] and angles [°] for **245**

S(1)-O(2)	1.4435(17)
S(1)-O(1)	1.448(2)
S(1)-C(14)	1.765(3)
S(1)-C(2)	1.782(2)
N(1)-C(7)	1.452(3)
N(1)-C(4)	1.461(3)
N(1)-C(1)	1.465(3)
C(1)-C(5)	1.516(4)
C(1)-C(2)	1.538(4)
C(2)-C(3)	1.552(3)
C(3)-C(4)	1.527(3)
C(3)-C(6)	1.533(3)
C(6)-C(20)	1.512(3)
C(7)-C(8)	1.516(3)
C(8)-C(13)	1.370(4)
C(8)-C(9)	1.391(4)
C(9)-C(10)	1.390(4)
C(10)-C(11)	1.369(4)
C(11)-C(12)	1.372(4)
C(12)-C(13)	1.386(4)
C(14)-C(15)	1.385(4)
C(14)-C(19)	1.385(4)
C(15)-C(16)	1.391(4)
C(16)-C(17)	1.386(4)
C(17)-C(18)	1.379(4)
C(18)-C(19)	1.389(4)
C(20)-C(25)	1.378(4)
C(20)-C(21)	1.387(4)
C(21)-C(22)	1.371(4)
C(22)-C(23)	1.374(5)
C(23)-C(24)	1.375(5)
C(24)-C(25)	1.400(4)
O(2)-S(1)-O(1)	118.83(12)

O(2)-S(1)-C(14)	108.66(12)
O(1)-S(1)-C(14)	108.08(13)
O(2)-S(1)-C(2)	108.17(11)
O(1)-S(1)-C(2)	108.59(12)
C(14)-S(1)-C(2)	103.43(12)
C(7)-N(1)-C(4)	113.4(2)
C(7)-N(1)-C(1)	115.9(2)
C(4)-N(1)-C(1)	104.1(2)
N(1)-C(1)-C(5)	113.2(2)
N(1)-C(1)-C(2)	100.80(19)
C(5)-C(1)-C(2)	114.7(2)
C(1)-C(2)-C(3)	106.19(19)
C(1)-C(2)-S(1)	111.96(17)
C(3)-C(2)-S(1)	112.20(17)
C(4)-C(3)-C(6)	112.6(2)
C(4)-C(3)-C(2)	102.3(2)
C(6)-C(3)-C(2)	111.5(2)
N(1)-C(4)-C(3)	103.2(2)
C(20)-C(6)-C(3)	112.7(2)
N(1)-C(7)-C(8)	111.3(2)
C(13)-C(8)-C(9)	118.6(2)
C(13)-C(8)-C(7)	121.2(3)
C(9)-C(8)-C(7)	120.2(2)
C(10)-C(9)-C(8)	120.2(3)
C(11)-C(10)-C(9)	120.4(3)
C(10)-C(11)-C(12)	119.5(3)
C(11)-C(12)-C(13)	120.3(3)
C(8)-C(13)-C(12)	120.9(3)
C(15)-C(14)-C(19)	121.1(3)
C(15)-C(14)-S(1)	119.8(2)
C(19)-C(14)-S(1)	119.0(2)
C(14)-C(15)-C(16)	118.7(3)
C(17)-C(16)-C(15)	121.0(3)
C(18)-C(17)-C(16)	119.4(3)
C(17)-C(18)-C(19)	120.7(3)
C(14)-C(19)-C(18)	119.2(3)

C(25)-C(20)-C(21)	118.1(3)
C(25)-C(20)-C(6)	121.7(3)
C(21)-C(20)-C(6)	120.2(3)
C(22)-C(21)-C(20)	121.8(3)
C(21)-C(22)-C(23)	119.6(3)
C(22)-C(23)-C(24)	120.3(3)
C(23)-C(24)-C(25)	119.6(3)
C(20)-C(25)-C(24)	120.6(3)

Table 4. Anisotropic displacement parameters ($Å^2 x\ 10^3$) for **245**. The anisotropic displacement factor exponent takes the form:
$-2\pi^2[\ h^2 a^{*2} U^{11} + ... + 2\ h\ k\ a^*\ b^*\ U^{12}\ ]$

Atom	U^{11}	U^{22}	U^{33}	U^{23}	U^{13}	U^{12}
S(1)	38(1)	33(1)	30(1)	-3(1)	12(1)	2(1)
O(1)	42(1)	38(1)	40(1)	-7(1)	5(1)	-7(1)
O(2)	45(1)	50(1)	35(1)	0(1)	21(1)	13(1)
N(1)	38(1)	28(1)	35(1)	4(1)	17(1)	5(1)
C(1)	39(2)	30(2)	31(2)	-1(1)	14(1)	2(1)
C(2)	33(1)	28(1)	28(1)	-1(1)	12(1)	-1(1)
C(3)	28(2)	28(2)	27(1)	-3(1)	9(1)	1(1)
C(4)	37(2)	29(2)	34(2)	-1(1)	11(1)	-2(1)
C(5)	46(2)	52(2)	53(2)	12(2)	25(2)	14(2)
C(6)	35(2)	31(2)	39(2)	-6(1)	14(1)	-3(1)
C(7)	54(2)	29(2)	35(2)	3(1)	17(2)	5(2)
C(8)	42(2)	26(2)	30(1)	2(1)	8(1)	5(1)
C(9)	42(2)	33(2)	42(2)	3(1)	8(1)	-3(2)
C(10)	56(2)	37(2)	35(2)	-2(1)	6(2)	1(2)
C(11)	65(2)	36(2)	34(2)	2(2)	17(2)	3(2)
C(12)	73(2)	42(2)	42(2)	0(2)	28(2)	-9(2)
C(13)	61(2)	28(2)	42(2)	0(1)	18(2)	-5(2)
C(14)	36(2)	35(2)	26(1)	5(1)	12(1)	2(1)
C(15)	32(2)	41(2)	45(2)	4(2)	7(1)	-3(2)

C(16)	36(2)	51(2)	56(2)	7(2)	12(2)	11(2)
C(17)	52(2)	34(2)	51(2)	11(2)	17(2)	7(2)
C(18)	43(2)	42(2)	44(2)	3(1)	13(2)	-4(2)
C(19)	34(2)	42(2)	31(2)	6(1)	13(1)	0(2)
C(20)	37(2)	29(2)	37(2)	-8(1)	13(1)	-3(1)
C(21)	48(2)	49(2)	48(2)	-9(2)	19(2)	2(2)
C(22)	54(2)	55(2)	82(3)	-11(2)	29(2)	11(2)
C(23)	61(2)	49(2)	106(3)	-20(2)	53(2)	-7(2)
C(24)	89(3)	38(2)	70(2)	-14(2)	56(2)	-20(2)
C(25)	61(2)	30(2)	45(2)	-9(1)	24(2)	-8(2)

Table 5. Hydrogen coordinates (x 10^4) and isotropic displacement parameters ($Å^2$x 10^3) for **245**

Atom	x	y	z	U(eq)
H(1)	1704	6552	3270	39
H(2)	829	3477	2818	35
H(3)	3349	3490	3249	33
H(4A)	3317	5832	2411	40
H(4B)	2912	4869	1173	40
H(5A)	-313	6164	3297	58
H(5B)	-699	5427	1979	58
H(5C)	-357	7203	2160	58
H(6A)	1954	1458	2237	41
H(6B)	1438	2550	1091	41
H(7A)	2027	7977	1492	47
H(7B)	576	7754	885	47
H(9)	454	5272	-785	48
H(10)	741	5005	-2660	54
H(11)	1953	6735	-3269	54
H(12)	2920	8704	-1988	60
H(13)	2702	8924	-88	51
H(15)	4348	2475	5469	49
H(16)	4876	-117	5724	58

H(17)	3361	-1983	5458	54
H(18)	1306	-1261	4920	52
H(19)	755	1321	4659	42
H(21)	4158	620	2809	57
H(22)	5718	-235	2123	75
H(23)	5683	348	177	79
H(24)	4107	1837	-1063	70
H(25)	2522	2695	-362	53

Table 6. Torsion angles [°] for **245**

C(7)-N(1)-C(1)-C(5)	65.9(3)
C(4)-N(1)-C(1)-C(5)	-168.9(2)
C(7)-N(1)-C(1)-C(2)	-171.0(2)
C(4)-N(1)-C(1)-C(2)	-45.9(2)
N(1)-C(1)-C(2)-C(3)	26.4(3)
C(5)-C(1)-C(2)-C(3)	148.3(2)
N(1)-C(1)-C(2)-S(1)	149.15(17)
C(5)-C(1)-C(2)-S(1)	-88.9(2)
O(2)-S(1)-C(2)-C(1)	66.8(2)
O(1)-S(1)-C(2)-C(1)	-63.4(2)
C(14)-S(1)-C(2)-C(1)	-178.09(18)
O(2)-S(1)-C(2)-C(3)	-173.92(17)
O(1)-S(1)-C(2)-C(3)	55.8(2)
C(14)-S(1)-C(2)-C(3)	-58.8(2)
C(1)-C(2)-C(3)-C(4)	1.3(3)
S(1)-C(2)-C(3)-C(4)	-121.3(2)
C(1)-C(2)-C(3)-C(6)	-119.2(2)
S(1)-C(2)-C(3)-C(6)	118.1(2)
C(7)-N(1)-C(4)-C(3)	174.9(2)
C(1)-N(1)-C(4)-C(3)	48.2(2)
C(6)-C(3)-C(4)-N(1)	90.9(2)
C(2)-C(3)-C(4)-N(1)	-28.9(2)
C(4)-C(3)-C(6)-C(20)	69.5(3)
C(2)-C(3)-C(6)-C(20)	-176.1(2)

C(4)-N(1)-C(7)-C(8)	66.9(3)
C(1)-N(1)-C(7)-C(8)	-172.8(2)
N(1)-C(7)-C(8)-C(13)	-136.2(3)
N(1)-C(7)-C(8)-C(9)	43.9(4)
C(13)-C(8)-C(9)-C(10)	0.5(4)
C(7)-C(8)-C(9)-C(10)	-179.5(3)
C(8)-C(9)-C(10)-C(11)	-1.3(4)
C(9)-C(10)-C(11)-C(12)	0.8(5)
C(10)-C(11)-C(12)-C(13)	0.5(5)
C(9)-C(8)-C(13)-C(12)	0.8(4)
C(7)-C(8)-C(13)-C(12)	-179.1(3)
C(11)-C(12)-C(13)-C(8)	-1.3(5)
O(2)-S(1)-C(14)-C(15)	-144.4(2)
O(1)-S(1)-C(14)-C(15)	-14.2(2)
C(2)-S(1)-C(14)-C(15)	100.8(2)
O(2)-S(1)-C(14)-C(19)	38.2(2)
O(1)-S(1)-C(14)-C(19)	168.40(19)
C(2)-S(1)-C(14)-C(19)	-76.6(2)
C(19)-C(14)-C(15)-C(16)	0.9(4)
S(1)-C(14)-C(15)-C(16)	-176.5(2)
C(14)-C(15)-C(16)-C(17)	-0.5(4)
C(15)-C(16)-C(17)-C(18)	0.1(4)
C(16)-C(17)-C(18)-C(19)	-0.1(4)
C(15)-C(14)-C(19)-C(18)	-0.9(4)
S(1)-C(14)-C(19)-C(18)	176.5(2)
C(17)-C(18)-C(19)-C(14)	0.5(4)
C(3)-C(6)-C(20)-C(25)	-100.0(3)
C(3)-C(6)-C(20)-C(21)	79.4(3)
C(25)-C(20)-C(21)-C(22)	-0.2(5)
C(6)-C(20)-C(21)-C(22)	-179.6(3)
C(20)-C(21)-C(22)-C(23)	-0.2(5)
C(21)-C(22)-C(23)-C(24)	0.7(5)
C(22)-C(23)-C(24)-C(25)	-0.8(5)
C(21)-C(20)-C(25)-C(24)	0.1(4)
C(6)-C(20)-C(25)-C(24)	179.5(3)
C(23)-C(24)-C(25)-C(20)	0.4(5)

Appendix V X-Ray Crystallographic Data for 257

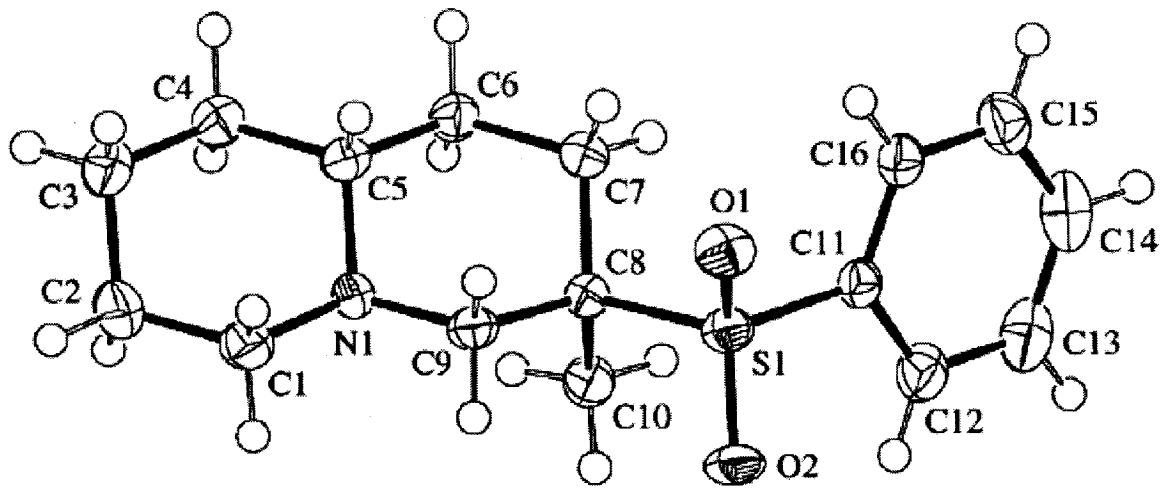

Experimental:

A colorless prismatic crystal of $C_{16}H_{23}NO_2S$ was coated with Paratone 8277 oil (Exxon) and mounted on a glass fiber. All measurements were made on a Nonius KappaCCD diffractometer with graphite monochromated Mo-Kα radiation. Cell constants obtained from the refinement[1] of 6614 reflections in the range $3.4 < \theta < 27.5°$ corresponded to a primitive monoclinic cell; details of crystal data and structure refinement have been provided in Table 1. The space group was uniquely determined from the systematic absences. The data were collected[2] at a temperature of 173(2) K using ω and φ scans to a maximum θ value of 27.5°. The data were corrected for Lorentz and polarization effects and for absorption using multi-scan method[1]. Since the crystal did not show any sign of decay during data collection a decay correction was deemed unnecessary.

The structure was solved by the direct methods[3] and expanded using Fourier techniques.[4] There are two independent molecules in the asymmetric unit. The non-hydrogen atoms were refined anisotropically. Hydrogen atoms were included at geometrically idealized positions and were not refined. The final cycle of full-matrix least-squares refinement using SHELXL97[5] converged (largest parameter shift was 0.00 times its esd) with unweighted and weighted agreement factors, R = 0.049 and wR = 0.114 (all data), respectively, and goodness of fit, S = 0.95. The weighting scheme was based on counting statistics and the final difference Fourier map was essentially featureless. The figure was plotted with the aid of ORTEPII.[7]

Table 1. Crystal data and structure refinement for **257**

Empirical formula	$C_{16}H_{23}NO_2S$
Formula weight	293.41
Temperature	173(2) K
Wavelength	0.71073 Å
Crystal system	Orthorhombic
Space group	$P2_1/n$
Unit cell dimensions	a = 11.310(4) Å
	b = 12.234(5) Å β = 106.815(17)°.
	c = 11.597(6) Å
Volume	1536.0(11) $Å^3$
Z	4
Density (calculated)	1.269 Mg/m^3
Absorption coefficient	0.21 mm^{-1}
F(000)	632
Crystal size	0.10 x 0.08 x 0.08 mm^3
Theta range for data collection	3.4 to 27.5°.
Index ranges	-14<=h<=14, -15<=k<=15, -15<=l<=15
Reflections collected	6614
Independent reflections	3503 [R(int) = 0.0953]
Completeness to theta = 27.5°	99.5 %
Absorption correction	Multi-scan method
Max. and min. transmission	0.983 and 0.979
Refinement method	Full-matrix least-squares on F^2
Data / restraints / parameters	3503 / 0 / 181
Goodness-of-fit on F^2	0.95
Final R indices [I>2sigma(I)]	R1 = 0.049, wR2 = 0.088
R indices (all data)	R1 = 0.151, wR2 = 0.114
Largest diff. peak and hole	0.25 and -0.33 $e.Å^{-3}$

Atomic coordinates and equivalent isotropic displacement parameters, anisotropic displacement parameters as well as bond lengths, bond angles and torsion angles are available via the Internet at http://pubs.acs.org.

Appendix VI X-Ray Crystallographic Data for 353

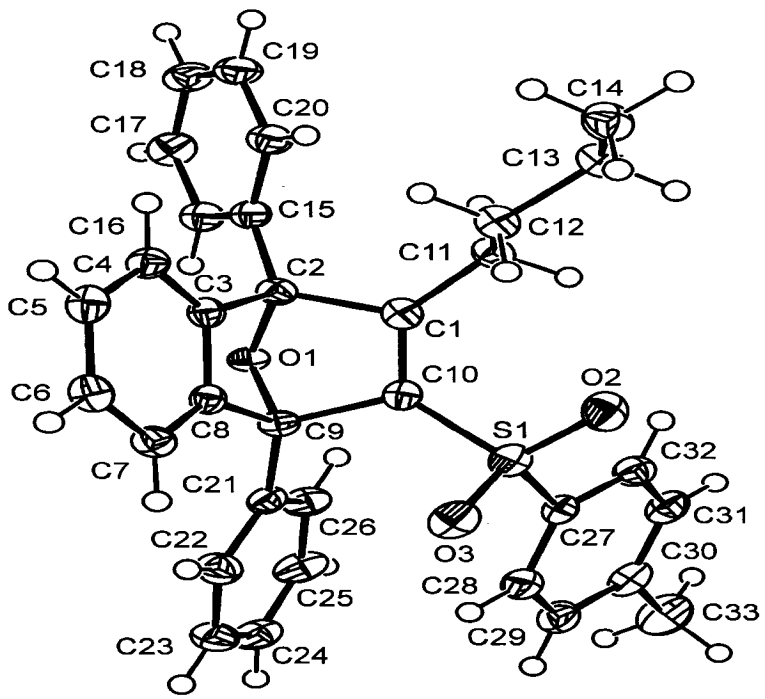

Experimental:

A colorless prismatic crystal of $C_{33}H_{30}O_3S$ was coated with Paratone 8277 oil (Exxon) and mounted on a glass fiber. All measurements were made on a Nonius KappaCCD diffractometer with graphite monochromated Mo-Kα radiation. Cell constants obtained from the refinement[1] of 11313 reflections in the range $3.0 < \theta < 27.5°$ corresponded to a primitive monoclinic cell; details of crystal data and structure refinement have been provided in Table 1. The space group was uniquely determined from the systematic absences. The data were collected[2] at a temperature of 123(2) K using ω and φ scans to a maximum θ value of 27.5°. The data were corrected for Lorentz and polarization effects and for absorption using multi-scan method[1]. Since the crystal did not show any sign of decay during data collection a decay correction was deemed unnecessary.

The structure was solved by the direct methods[3] and expanded using Fourier techniques.[4] The non-hydrogen atoms were refined anisotropically. Hydrogen atoms were located from a difference map, were included at geometrically idealized positions and were not refined except for the one bonded to N1 that was allowed to refine. The final cycle of full-matrix least-squares refinement using SHELXL97[5] converged with unweighted and weighted agreement factors, R = 0.043 and wR = 0.110 (all data), respectively, and goodness of fit, S = 1.01. The weighting scheme was based on counting statistics and the final difference map was free of any chemically significant features. The figure was plotted with the aid of ORTEPII.[7]

Table 1. Crystal data and structure refinement for **353**

Empirical formula	$C_{33}H_{30}O_3S$	
Formula weight	506.63	
Temperature	123(2) K	
Wavelength	0.71073 Å	
Crystal system	Monoclinic	
Space group	$P2_1/c$	
Unit cell dimensions	a = 8.1665(12) Å	α = 90°.
	b = 12.191(3) Å	β = 94.916(14)°.
	c = 25.975(6) Å	γ = 90°.
Volume	2576.5(9) $Å^3$	
Z	4	
Density (calculated)	1.306 Mg/m^3	
Absorption coefficient	0.160 mm^{-1}	
F(000)	1072	
Crystal size	0.18 x 0.11 x 0.07 mm^3	
Theta range for data collection	3.0 to 27.5°.	
Index ranges	-10<=h<=10, -15<=k<=15, -33<=l<=33	
Reflections collected	11313	
Independent reflections	5883 [R(int) = 0.034]	
Completeness to theta = 27.5°	99.7 %	
Absorption correction	Multi-scan method	
Max. and min. transmission	0.989 and 0.972	
Refinement method	Full-matrix least-squares on F^2	
Data / restraints / parameters	5883 / 0 / 336	
Goodness-of-fit on F^2	1.01	
Final R indices [I>2sigma(I)]	R1 = 0.043, wR2 = 0.096	
R indices (all data)	R1 = 0.072, wR2 = 0.110	
Largest diff. peak and hole	0.21 and -0.43 $e.Å^{-3}$	

Atomic coordinates and equivalent isotropic displacement parameters, anisotropic displacement parameters as well as bond lengths, bond angles and torsion angles are available via the Internet at http://pubs.acs.org.

Appendix VII X-Ray Crystallographic Data for 355

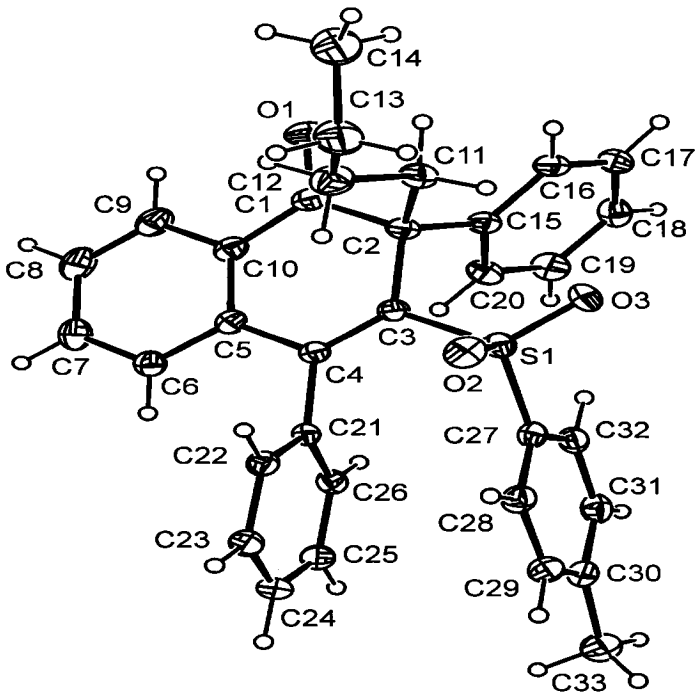

Experimental:

A colorless prismatic crystal of $C_{33}H_{30}O_3S$ was coated with Paratone 8277 oil (Exxon) and mounted on a glass fiber. All measurements were made on a Nonius KappaCCD diffractometer with graphite monochromated Mo-Kα radiation. Cell constants obtained from the refinement[1] of 22252 reflections in the range $3.6 < \theta < 27.5°$ corresponded to a primitive monoclinic cell; details of crystal data and structure refinement have been provided in Table 1. The space group was uniquely determined from the systematic absences. The data were collected[2] at a temperature of 173(2) K using ω and φ scans to a maximum θ value of 27.5°. The data were corrected for Lorentz and polarization effects and for absorption using multi-scan method[1]. Since the crystal did not show any sign of decay during data collection a decay correction was deemed unnecessary.

The structure was solved by the direct methods[3] and expanded using Fourier techniques.[4] The non-hydrogen atoms were refined anisotropically. C13 and C14 of the butyl group were disordered over two sites with equal site occupancy factors. Hydrogen atoms were located from a difference map, were included at geometrically idealized positions and were not refined except for the one bonded to N1 that was allowed to refine. The final cycle of full-matrix least-squares refinement using SHELXL97[5] converged with unweighted and weighted agreement factors, R = 0.049 and wR = 0.132 (all data), respectively, and goodness of fit, S = 1.02. The weighting scheme was based on counting statistics and the final difference map was free of any chemically significant features. The figure was plotted with the aid of ORTEPII.[7]

Table 1. Crystal data and structure refinement for **355**

Empirical formula	$C_{33}H_{30}O_3S$	
Formula weight	506.63	
Temperature	173(2) K	
Wavelength	0.71073 Å	
Crystal system	Monoclinic	
Space group	$P2_1/n$	
Unit cell dimensions	a = 13.398(3) Å	α = 90°.
	b = 10.800(3) Å	β = 91.853(15)°.
	c = 18.235(4) Å	γ = 90°.
Volume	2637.2(11) $Å^3$	
Z	4	
Density (calculated)	1.276 Mg/m^3	
Absorption coefficient	0.156 mm^{-1}	
F(000)	1072	
Crystal size	0.18 x 0.16 x 0.14 mm^3	
Theta range for data collection	3.6 to 27.5°.	
Index ranges	-17<=h<=16, -14<=k<=14, -23<=l<=23	
Reflections collected	22252	
Independent reflections	6028 [R(int) = 0.062]	
Completeness to theta = 27.5°	99.6 %	
Absorption correction	Multi-scan method	
Max. and min. transmission	0.979 and 0.973	
Refinement method	Full-matrix least-squares on F^2	
Data / restraints / parameters	6028 / 0 / 341	
Goodness-of-fit on F^2	1.02	
Final R indices [I>2sigma(I)]	R1 = 0.049, wR2 = 0.111	
R indices (all data)	R1 = 0.088, wR2 = 0.132	
Largest diff. peak and hole	0.24 and -0.44 e.$Å^{-3}$	

Atomic coordinates and equivalent isotropic displacement parameters, anisotropic displacement parameters as well as bond lengths, bond angles and torsion angles are available via the Internet at http://pubs.acs.org.

Appendix VIII X-Ray Crystallographic Data for 357

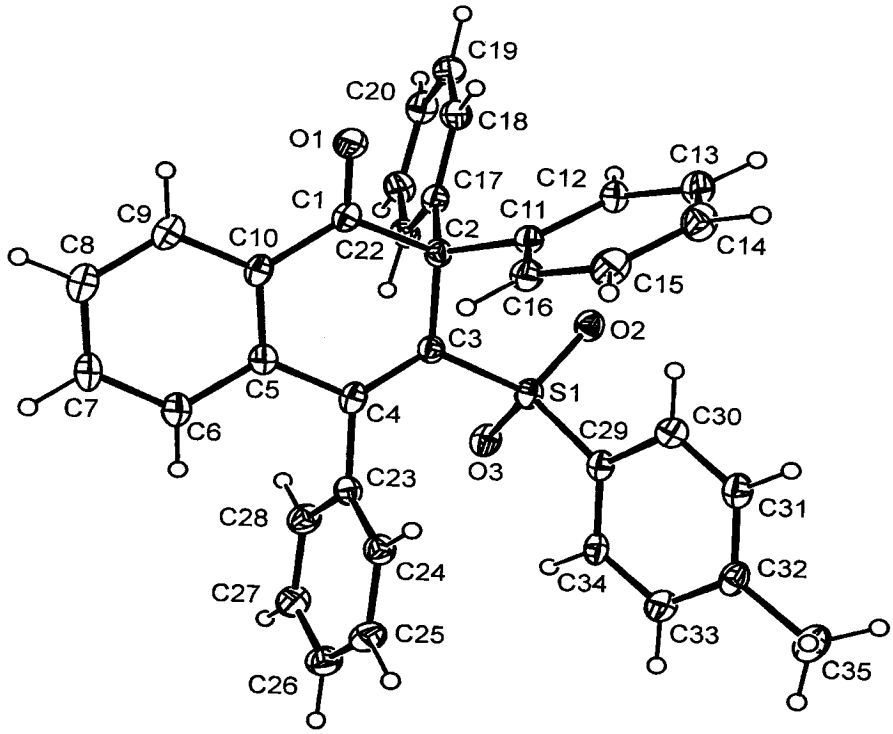

Experimental:

A colorless prismatic crystal of $C_{35}H_{26}O_3S$ was coated with Paratone 8277 oil (Exxon) and mounted on a glass fiber. All measurements were made on a Nonius KappaCCD diffractometer with graphite monochromated Mo-Kα radiation. Cell constants obtained from the refinement[1] of 10990 reflections in the range $1.9 < \theta < 27.3°$ corresponded to a primitive monoclinic cell; details of crystal data and structure refinement have been provided in Table 1. The space group was uniquely determined from the systematic absences. The data were collected[2] at a temperature of 173(2) K using ω and φ scans to a maximum θ value of 27.3°. The data were corrected for Lorentz and polarization effects and for absorption using multi-scan method[1]. Since the crystal did not show any sign of decay during data collection a decay correction was deemed unnecessary.

The structure was solved by the direct methods[3] and expanded using Fourier techniques.[4] The non-hydrogen atoms were refined anisotropically. Hydrogen atoms were included at geometrically idealized positions and were not refined. The final cycle of full-matrix least-squares refinement using SHELXL97[5] converged with unweighted and weighted agreement factors, R = 0.120, and goodness of fit, S = 1.03. The weighting scheme was based on counting statistics and the final difference map was free of any chemically significant features. The figure was plotted with the aid of ORTEPII.[7]

Table 1. Crystal data and structure refinement for **357**

Empirical formula	$C_{35}H_{26}O_3S$	
Formula weight	526.62	
Temperature	173(2) K	
Wavelength	0.71073 Å	
Crystal system	Triclinic	
Space group	P -1	
Unit cell dimensions	a = 10.838(8) Å	α= 109.08(4)°.
	b = 11.321(8) Å	β= 94.84(4)°.
	c = 11.438(7) Å	γ = 95.86(3)°.
Volume	1309.0(16) $Å^3$	
Z	2	
Density (calculated)	1.336 Mg/m^3	
Absorption coefficient	0.160 mm^{-1}	
F(000)	552	
Crystal size	0.14 x 0.12 x 0.06 mm^3	
Theta range for data collection	1.9 to 27.3°.	
Index ranges	-13<=h<=13, -14<=k<=14, -14<=l<=14	
Reflections collected	10990	
Independent reflections	5843 [R(int) = 0.047]	
Completeness to theta = 27.3°	98.9 %	
Absorption correction	Multi-scan method	
Max. and min. transmission	0.9905 and 0.9779	
Refinement method	Full-matrix least-squares on F^2	
Data / restraints / parameters	5843 / 0 / 353	
Goodness-of-fit on F^2	1.03	
Final R indices [I>2sigma(I)]	R1 = 0.120, wR2 = 0.356	
R indices (all data)	R1 = 0.154, wR2 = 0.376	
Extinction coefficient	0.058(9)	
Largest diff. peak and hole	1.02 and -0.48 $e.Å^{-3}$	

Atomic coordinates and equivalent isotropic displacement parameters, anisotropic displacement parameters as well as bond lengths, bond angles and torsion angles are available via the Internet at http://pubs.acs.org.

Appendix IX X-Ray Crystallographic Data for 358

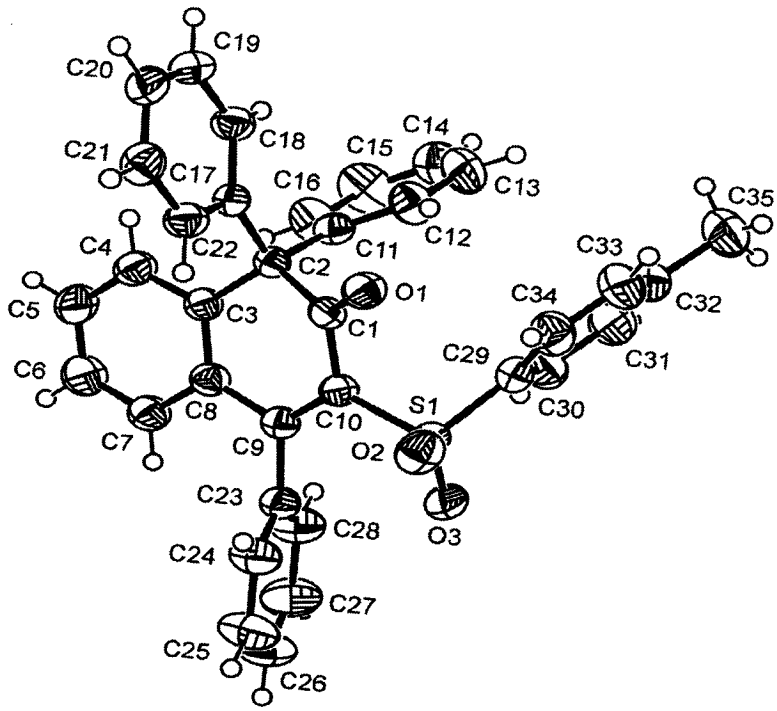

Experimental:

A colorless prismatic crystal of $C_{35}H_{26}O_3S$ was coated with Paratone 8277 oil (Exxon) and mounted on a glass fiber. All measurements were made on a Nonius KappaCCD diffractometer with graphite monochromated Mo-Kα radiation. Cell constants obtained from the refinement[1] of 9219 reflections in the range $3.4 < \theta < 25.3°$ corresponded to a primitive monoclinic cell; details of crystal data and structure refinement have been provided in Table 1. The space group was uniquely determined from the systematic absences. The data were collected[2] at a temperature of 293(2) K using ω and φ scans to a maximum θ value of 25.3°. The data were corrected for Lorentz and polarization effects and for absorption using multi-scan method[1]. Since the crystal did not show any sign of decay during data collection a decay correction was deemed unnecessary.

The structure was solved by the direct methods[3] and expanded using Fourier techniques.[4] The non-hydrogen atoms were refined anisotropically. Hydrogen atoms were located from a difference map, were included at geometrically idealized positions and were not refined. The final cycle of full-matrix least-squares refinement using SHELXL97[5] converged with unweighted and weighted agreement factors, R = 0.046 and wR = 0.120 (all data), respectively, and goodness of fit, S = 1.01. The weighting scheme was based on counting statistics and the final difference map was free of any chemically significant features. The figure was plotted with the aid of ORTEPII.[7]

Table 1. Crystal data and structure refinement for **358**

Empirical formula	$C_{35}H_{26}O_3S$	
Formula weight	526.62	
Temperature	293(2) K	
Wavelength	0.71073 Å	
Crystal system	Triclinic	
Space group	P -1	
Unit cell dimensions	a = 10.228(4) Å	α = 76.54(2)°.
	b = 10.607(3) Å	β = 87.73(2)°.
	c = 14.554(5) Å	γ = 62.90(2)°.
Volume	1363.0(8) $Å^3$	
Z	2	
Density (calculated)	1.283 Mg/m^3	
Absorption coefficient	0.154 mm^{-1}	
F(000)	552	
Crystal size	0.20 x 0.10 x 0.08 mm^3	
Theta range for data collection	3.4 to 25.3°.	
Index ranges	-12<=h<=11, -12<=k<=12, -17<=l<=17	
Reflections collected	9219	
Independent reflections	4892 [R(int) = 0.041]	
Completeness to theta = 27.3°	99.1 %	
Absorption correction	Multi-scan method	
Max. and min. transmission	0.988 and 0.970	
Refinement method	Full-matrix least-squares on F^2	
Data / restraints / parameters	4892 / 0 / 353	
Goodness-of-fit on F^2	1.03	
Final R indices [I>2sigma(I)]	R1 = 0.046, wR2 = 0.101	
R indices (all data)	R1 = 0.085, wR2 = 0.120	
Largest diff. peak and hole	0.17 and -0.29 $e.Å^{-3}$	

Atomic coordinates and equivalent isotropic displacement parameters, anisotropic displacement parameters as well as bond lengths, bond angles and torsion angles are available via the Internet at http://pubs.acs.org.

Appendix X X-Ray Crystallographic Data for 377

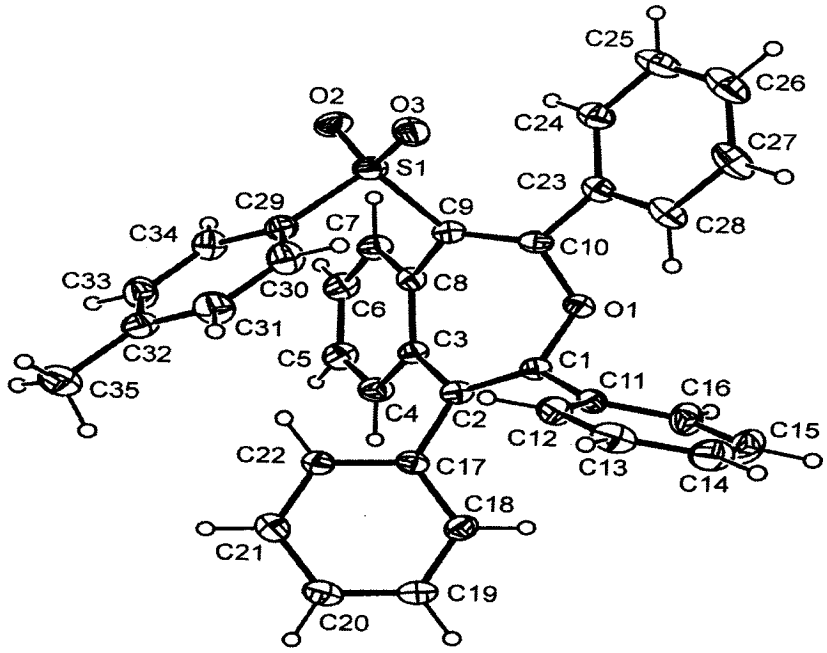

Experimental:

A colorless prismatic crystal of $C_{35}H_{26}O_3S$ was coated with Paratone 8277 oil (Exxon) and mounted on a glass fiber. All measurements were made on a Nonius KappaCCD diffractometer with graphite monochromated Mo-Kα radiation. Cell constants obtained from the refinement[1] of 8974 reflections in the range $3.5 < \theta < 25.0°$ corresponded to a primitive monoclinic cell; details of crystal data and structure refinement have been provided in Table 1. The space group was uniquely determined from the systematic absences. The data were collected[2] at a temperature of 173(2) K using ω and φ scans to a maximum θ value of 25.0°. The data were corrected for Lorentz and polarization effects and for absorption using multi-scan method[1]. Since the crystal did not show any sign of decay during data collection a decay correction was deemed unnecessary.

The structure was solved by the direct methods[3] and expanded using Fourier techniques.[4] The non-hydrogen atoms were refined anisotropically. Hydrogen atoms were included at geometrically idealized positions and were not refined. The final cycle of full-matrix least-squares refinement using SHELXL97[5] converged with unweighted and weighted agreement factors, R = 0.049 and wR = 0.118 (all data), respectively, and goodness of fit, S = 1.01. The absolute structure was established by the Flack method[6]. The Flack parameter for the inverted structure was 0.93(10). Therefore, the inverted structure was rejected as the one present in the crystal. The weighting scheme was based on counting statistics and the final difference Fourier map was essentially featureless. The figure was plotted with the aid of ORTEPII.[7]

Table 1. Crystal data and structure refinement for **377**

Empirical formula	$C_{35}H_{26}O_3S$	
Formula weight	526.62	
Temperature	173(2) K	
Wavelength	0.71073 Å	
Crystal system	Orthorhombic	
Space group	$Pca2_1$	
Unit cell dimensions	a = 14.174(2) Å	α= 90°.
	b = 13.068(2) Å	β= 90°.
	c = 14.911(3) Å	γ = 90°.
Volume	2761.9(8) $Å^3$	
Z	4	
Density (calculated)	1.266 Mg/m^3	
Absorption coefficient	0.152 mm^{-1}	
F(000)	1104	
Crystal size	0.12 x 0.06 x 0.04 mm^3	
Theta range for data collection	3.5 to 25.0°.	
Index ranges	-16<=h<=16, -15<=k<=15, -17<=l<=16	
Reflections collected	8974	
Independent reflections	4775 [R(int) = 0.0627]	
Completeness to theta = 25.0°	99.5 %	
Absorption correction	Multi-scan method	
Max. and min. transmission	0.994 and 0.982	
Refinement method	Full-matrix least-squares on F^2	
Data / restraints / parameters	4775 / 1 / 352	
Goodness-of-fit on F^2	1.01	
Final R indices [I>2sigma(I)]	R1 = 0.049, wR2 = 0.100	
R indices (all data)	R1 = 0.091, wR2 = 0.118	
Absolute structure parameter	-0.07(10)	
Largest diff. peak and hole	0.18 and -0.27 $e.Å^{-3}$	

Atomic coordinates and equivalent isotropic displacement parameters, anisotropic displacement parameters as well as bond lengths, bond angles and torsion angles are available via the Internet at http://pubs.acs.org.

Appendix XI X-Ray Crystallographic Data for 429

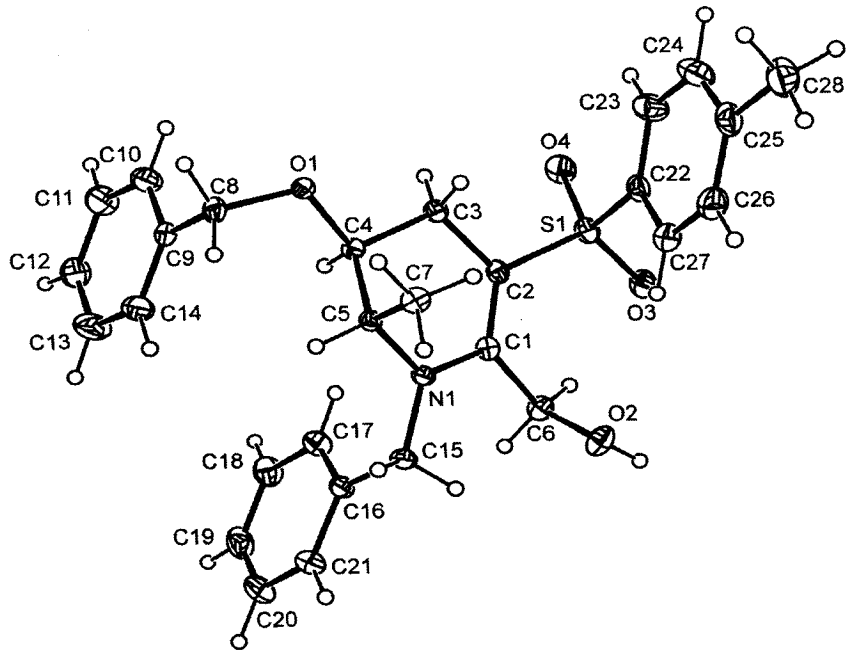

Experimental:

A colorless prismatic crystal of $C_{28}H_{31}NO_4S$ was coated with Paratone 8277 oil (Exxon) and mounted on a glass fiber. All measurements were made on a Nonius KappaCCD diffractometer with graphite monochromated Mo-Kα radiation. Cell constants obtained from the refinement[1] of 5640 reflections in the range $3.6 < \theta < 27.5°$ corresponded to a primitive monoclinic cell; details of crystal data and structure refinement have been provided in Table 1. The space group was uniquely determined from the systematic absences. The data were collected[2] at a temperature of 173(2) K using ω and φ scans to a maximum θ value of 27.5°. The data were corrected for Lorentz and polarization effects and for absorption using multi-scan method[1]. Since the crystal did not show any sign of decay during data collection a decay correction was deemed unnecessary.

The structure was solved by the direct methods[3] and expanded using Fourier techniques.[4] The non-hydrogen atoms were refined anisotropically. Hydrogen atoms were included at geometrically idealized positions and were not refined. The final cycle of full-matrix least-squares refinement using SHELXL97[5] converged with unweighted and weighted agreement factors, R = 0.045 and wR = 0.105 (all data), respectively, and goodness of fit, S = 1.03. The absolute structure was established by the Flack method[6]. The Flack parameter for the inverted structure was 0.97(7). Therefore, the inverted structure was rejected as the one present in the crystal. The weighting scheme was based on counting statistics and the final difference Fourier map was essentially featureless. The figure was plotted with the aid of ORTEPII.[7]

Table 1. Crystal data and structure refinement for **429**

Empirical formula	$C_{28}H_{31}NO_4S$
Formula weight	447.60
Temperature	173(2) K
Wavelength	0.71073 Å
Crystal system	Orthorhombic
Space group	$P2_12_12_1$
Unit cell dimensions	a = 8.458(2) Å α= 90°.
	b = 16.354(7) Å β= 90°.
	c = 17.9917) Å γ = 90°.
Volume	2488.6(16) $Å^3$
Z	4
Density (calculated)	1.275 Mg/m^3
Absorption coefficient	0.164 mm^{-1}
F(000)	1016
Crystal size	0.26 x 0.14 x 0.12 mm^3
Theta range for data collection	3.6 to 27.5°.
Index ranges	-10<=h<=10, -21<=k<=21, -23<=l<=23
Reflections collected	5640
Independent reflections	5640 [R(int) = 0.00]
Completeness to theta = 27.6°	99.2 %
Absorption correction	Multi-scan method
Max. and min. transmission	0.981 and 0.959
Refinement method	Full-matrix least-squares on F^2
Data / restraints / parameters	5640 / 0 / 308
Goodness-of-fit on F^2	1.03
Final R indices [I>2sigma(I)]	R1 = 0.045, wR2 = 0.095
R indices (all data)	R1 = 0.063, wR2 = 0.105
Absolute structure parameter	0.03(7)
Largest diff. peak and hole	0.23 and -0.31 $e.Å^{-3}$

Table 2. Atomic coordinates (x 10^4) and equivalent isotropic displacement parameters ($Å^2$x 10^3) for **429**. U(eq) is defined as one third of the trace of the orthogonalized U^{ij} tensor.

Atom	x	y	z	U(eq)
S(1)	2422(1)	7024(1)	2755(1)	29(1)
O(1)	7124(2)	5218(1)	2267(1)	24(1)
O(2)	5072(2)	8938(1)	2775(1)	37(1)
O(3)	1776(2)	7841(1)	2713(1)	39(1)
O(4)	1495(2)	6374(1)	2431(1)	40(1)
N(1)	6896(2)	7487(1)	2186(1)	22(1)
C(1)	5305(2)	7600(1)	2262(1)	23(1)
C(2)	4340(2)	6949(1)	2413(1)	24(1)
C(3)	4922(2)	6075(1)	2438(1)	26(1)
C(4)	6539(2)	6017(1)	2086(1)	22(1)
C(5)	7614(2)	6697(1)	2374(1)	21(1)
C(6)	4717(2)	8459(1)	2137(1)	29(1)
C(7)	7931(2)	6634(1)	3209(1)	28(1)
C(8)	8612(2)	4998(1)	1919(1)	28(1)
C(9)	8544(2)	5018(1)	1084(1)	28(1)
C(10)	7640(3)	4451(2)	707(1)	41(1)
C(11)	7598(3)	4447(2)	-64(1)	48(1)
C(12)	8464(3)	5011(2)	-465(2)	48(1)
C(13)	9366(4)	5576(2)	-89(2)	57(1)
C(14)	9396(3)	5579(2)	682(1)	43(1)
C(15)	7990(2)	8137(1)	1963(1)	26(1)
C(16)	8241(2)	8206(1)	1131(1)	27(1)
C(17)	7360(3)	7778(1)	621(1)	35(1)
C(18)	7574(3)	7886(2)	-141(1)	42(1)
C(19)	8704(3)	8422(2)	-394(2)	46(1)
C(20)	9630(3)	8839(2)	105(2)	51(1)
C(21)	9412(3)	8733(2)	867(1)	40(1)
C(22)	2663(3)	6785(1)	3711(1)	31(1)
C(23)	1922(3)	6109(2)	4018(2)	44(1)
C(24)	2110(3)	5955(2)	4776(2)	49(1)

C(25)	3041(3)	6446(2)	5225(1)	41(1)
C(26)	3799(3)	7102(2)	4902(1)	44(1)
C(27)	3629(3)	7280(2)	4155(1)	38(1)
C(28)	3194(4)	6261(2)	6039(1)	55(1)

Table 3. Bond lengths [Å] and angles [°] for **429**.

S(1)-O(4)	1.4444(17)
S(1)-O(3)	1.4464(17)
S(1)-C(2)	1.7391(19)
S(1)-C(22)	1.774(2)
O(1)-C(4)	1.434(2)
O(1)-C(8)	1.451(2)
O(2)-C(6)	1.423(3)
O(2)-H(2)	0.8400
N(1)-C(1)	1.365(3)
N(1)-C(15)	1.466(2)
N(1)-C(5)	1.466(2)
C(1)-C(2)	1.368(3)
C(1)-C(6)	1.507(3)
C(2)-C(3)	1.513(3)
C(3)-C(4)	1.511(3)
C(3)-H(3A)	0.9599
C(3)-H(3B)	0.9600
C(4)-C(5)	1.529(3)
C(4)-H(4)	0.9600
C(5)-C(7)	1.528(3)
C(5)-H(5)	0.9600
C(6)-H(6A)	0.9599
C(6)-H(6B)	0.9599
C(7)-H(7A)	0.9599
C(7)-H(7B)	0.9600
C(7)-H(7C)	0.9600
C(8)-C(9)	1.505(3)
C(8)-H(8A)	0.9600

C(8)-H(8B)	0.9600
C(9)-C(14)	1.373(3)
C(9)-C(10)	1.380(3)
C(10)-C(11)	1.387(3)
C(10)-H(10)	0.9600
C(11)-C(12)	1.382(4)
C(11)-H(11)	0.9600
C(12)-C(13)	1.376(4)
C(12)-H(12)	0.9600
C(13)-C(14)	1.388(4)
C(13)-H(13)	0.9599
C(14)-H(14)	0.9599
C(15)-C(16)	1.516(3)
C(15)-H(15A)	0.9600
C(15)-H(15B)	0.9600
C(16)-C(17)	1.374(3)
C(16)-C(21)	1.395(3)
C(17)-C(18)	1.393(3)
C(17)-H(17)	0.9599
C(18)-C(19)	1.375(4)
C(18)-H(18)	0.9600
C(19)-C(20)	1.374(4)
C(19)-H(19)	0.9601
C(20)-C(21)	1.394(4)
C(20)-H(20)	0.9600
C(21)-H(21)	0.9600
C(22)-C(23)	1.386(3)
C(22)-C(27)	1.400(3)
C(23)-C(24)	1.396(4)
C(23)-H(23)	0.9600
C(24)-C(25)	1.385(4)
C(24)-H(24)	0.9599
C(25)-C(26)	1.377(4)
C(25)-C(28)	1.502(4)
C(26)-C(27)	1.384(3)
C(26)-H(26)	0.9601

C(27)-H(27)	0.9600
C(28)-H(28A)	0.9600
C(28)-H(28B)	0.9599
C(28)-H(28C)	0.9600

O(4)-S(1)-O(3)	116.99(10)
O(4)-S(1)-C(2)	108.17(10)
O(3)-S(1)-C(2)	113.50(10)
O(4)-S(1)-C(22)	107.00(11)
O(3)-S(1)-C(22)	107.29(10)
C(2)-S(1)-C(22)	102.73(10)
C(4)-O(1)-C(8)	115.34(15)
C(6)-O(2)-H(2)	109.5
C(1)-N(1)-C(15)	123.44(17)
C(1)-N(1)-C(5)	120.29(16)
C(15)-N(1)-C(5)	116.17(15)
N(1)-C(1)-C(2)	120.18(18)
N(1)-C(1)-C(6)	115.90(17)
C(2)-C(1)-C(6)	123.87(17)
C(1)-C(2)-C(3)	123.13(17)
C(1)-C(2)-S(1)	124.90(16)
C(3)-C(2)-S(1)	111.05(14)
C(4)-C(3)-C(2)	109.98(16)
C(4)-C(3)-H(3A)	109.4
C(2)-C(3)-H(3A)	109.3
C(4)-C(3)-H(3B)	109.0
C(2)-C(3)-H(3B)	109.6
H(3A)-C(3)-H(3B)	109.5
O(1)-C(4)-C(3)	105.93(15)
O(1)-C(4)-C(5)	112.40(15)
C(3)-C(4)-C(5)	110.51(16)
O(1)-C(4)-H(4)	110.4
C(3)-C(4)-H(4)	109.2
C(5)-C(4)-H(4)	108.4
N(1)-C(5)-C(7)	111.05(16)
N(1)-C(5)-C(4)	108.43(15)

C(7)-C(5)-C(4)	112.87(16)
N(1)-C(5)-H(5)	108.2
C(7)-C(5)-H(5)	106.3
C(4)-C(5)-H(5)	109.9
O(2)-C(6)-C(1)	108.89(16)
O(2)-C(6)-H(6A)	110.0
C(1)-C(6)-H(6A)	109.7
O(2)-C(6)-H(6B)	110.0
C(1)-C(6)-H(6B)	108.8
H(6A)-C(6)-H(6B)	109.5
C(5)-C(7)-H(7A)	109.0
C(5)-C(7)-H(7B)	109.7
H(7A)-C(7)-H(7B)	109.5
C(5)-C(7)-H(7C)	109.7
H(7A)-C(7)-H(7C)	109.5
H(7B)-C(7)-H(7C)	109.5
O(1)-C(8)-C(9)	113.05(16)
O(1)-C(8)-H(8A)	109.2
C(9)-C(8)-H(8A)	107.5
O(1)-C(8)-H(8B)	109.6
C(9)-C(8)-H(8B)	108.0
H(8A)-C(8)-H(8B)	109.5
C(14)-C(9)-C(10)	118.8(2)
C(14)-C(9)-C(8)	121.4(2)
C(10)-C(9)-C(8)	119.8(2)
C(9)-C(10)-C(11)	120.6(2)
C(9)-C(10)-H(10)	119.5
C(11)-C(10)-H(10)	119.9
C(12)-C(11)-C(10)	120.4(2)
C(12)-C(11)-H(11)	119.1
C(10)-C(11)-H(11)	120.5
C(13)-C(12)-C(11)	119.0(2)
C(13)-C(12)-H(12)	121.5
C(11)-C(12)-H(12)	119.4
C(12)-C(13)-C(14)	120.3(3)
C(12)-C(13)-H(13)	120.1

C(14)-C(13)-H(13)	119.6
C(9)-C(14)-C(13)	120.9(2)
C(9)-C(14)-H(14)	119.9
C(13)-C(14)-H(14)	119.2
N(1)-C(15)-C(16)	114.38(17)
N(1)-C(15)-H(15A)	109.2
C(16)-C(15)-H(15A)	107.1
N(1)-C(15)-H(15B)	109.3
C(16)-C(15)-H(15B)	107.3
H(15A)-C(15)-H(15B)	109.5
C(17)-C(16)-C(21)	118.2(2)
C(17)-C(16)-C(15)	123.04(19)
C(21)-C(16)-C(15)	118.7(2)
C(16)-C(17)-C(18)	121.4(2)
C(16)-C(17)-H(17)	119.9
C(18)-C(17)-H(17)	118.7
C(19)-C(18)-C(17)	119.8(2)
C(19)-C(18)-H(18)	120.7
C(17)-C(18)-H(18)	119.4
C(20)-C(19)-C(18)	119.7(2)
C(20)-C(19)-H(19)	119.2
C(18)-C(19)-H(19)	121.1
C(19)-C(20)-C(21)	120.4(2)
C(19)-C(20)-H(20)	119.8
C(21)-C(20)-H(20)	119.8
C(20)-C(21)-C(16)	120.3(2)
C(20)-C(21)-H(21)	119.9
C(16)-C(21)-H(21)	119.8
C(23)-C(22)-C(27)	119.8(2)
C(23)-C(22)-S(1)	120.66(19)
C(27)-C(22)-S(1)	119.55(17)
C(22)-C(23)-C(24)	118.9(2)
C(22)-C(23)-H(23)	120.5
C(24)-C(23)-H(23)	120.6
C(25)-C(24)-C(23)	121.9(2)
C(25)-C(24)-H(24)	118.2

C(23)-C(24)-H(24)	119.8
C(26)-C(25)-C(24)	118.1(2)
C(26)-C(25)-C(28)	121.8(3)
C(24)-C(25)-C(28)	120.0(2)
C(25)-C(26)-C(27)	121.7(2)
C(25)-C(26)-H(26)	120.1
C(27)-C(26)-H(26)	118.2
C(26)-C(27)-C(22)	119.6(2)
C(26)-C(27)-H(27)	120.1
C(22)-C(27)-H(27)	120.3
C(25)-C(28)-H(28A)	109.5
C(25)-C(28)-H(28B)	109.6
H(28A)-C(28)-H(28B)	109.5
C(25)-C(28)-H(28C)	109.3
H(28A)-C(28)-H(28C)	109.5
H(28B)-C(28)-H(28C)	109.5

Table 4. Anisotropic displacement parameters ($Å^2 x\ 10^3$) for **429**.
The anisotropic displacement factor exponent takes the form:

$$-2\pi^2[\ h^2 a^{*2} U^{11} + ... + 2\ h\ k\ a^*\ b^*\ U^{12}\ ]$$

Atom	U^{11}	U^{22}	U^{33}	U^{23}	U^{13}	U^{12}
S(1)	16(1)	36(1)	36(1)	0(1)	0(1)	2(1)
O(1)	23(1)	21(1)	29(1)	3(1)	3(1)	2(1)
O(2)	36(1)	31(1)	44(1)	-11(1)	-7(1)	9(1)
O(3)	26(1)	40(1)	51(1)	4(1)	4(1)	12(1)
O(4)	21(1)	49(1)	51(1)	-9(1)	-4(1)	-8(1)
N(1)	19(1)	21(1)	26(1)	4(1)	2(1)	0(1)
C(1)	21(1)	27(1)	19(1)	1(1)	-3(1)	3(1)
C(2)	16(1)	29(1)	27(1)	1(1)	1(1)	3(1)
C(3)	19(1)	25(1)	34(1)	1(1)	2(1)	0(1)
C(4)	20(1)	22(1)	23(1)	2(1)	-2(1)	2(1)
C(5)	19(1)	21(1)	23(1)	2(1)	2(1)	1(1)
C(6)	27(1)	28(1)	31(1)	2(1)	-3(1)	5(1)

C(7)	28(1)	30(1)	26(1)	1(1)	-7(1)	1(1)
C(8)	22(1)	28(1)	34(1)	-2(1)	3(1)	5(1)
C(9)	26(1)	24(1)	32(1)	-4(1)	6(1)	2(1)
C(10)	48(1)	38(1)	35(1)	-3(1)	10(1)	-13(1)
C(11)	56(2)	50(2)	38(1)	-14(1)	5(1)	-15(1)
C(12)	64(2)	48(2)	31(1)	-6(1)	13(1)	-2(1)
C(13)	78(2)	51(2)	41(2)	0(1)	20(1)	-21(2)
C(14)	49(2)	38(1)	42(2)	-3(1)	11(1)	-12(1)
C(15)	25(1)	23(1)	30(1)	4(1)	1(1)	-3(1)
C(16)	24(1)	25(1)	32(1)	5(1)	5(1)	1(1)
C(17)	34(1)	39(1)	31(1)	4(1)	2(1)	-4(1)
C(18)	46(1)	50(2)	31(1)	2(1)	2(1)	3(1)
C(19)	54(2)	51(2)	34(1)	10(1)	17(1)	11(1)
C(20)	53(2)	49(2)	49(2)	9(1)	25(1)	-7(1)
C(21)	39(1)	37(1)	44(1)	3(1)	11(1)	-9(1)
C(22)	23(1)	35(1)	35(1)	0(1)	8(1)	6(1)
C(23)	30(1)	45(2)	55(2)	7(1)	-1(1)	-9(1)
C(24)	43(2)	52(2)	53(2)	21(1)	11(1)	-2(1)
C(25)	40(1)	45(2)	40(1)	4(1)	11(1)	15(1)
C(26)	55(2)	42(2)	35(1)	-8(1)	3(1)	0(1)
C(27)	43(1)	35(1)	35(1)	-5(1)	5(1)	0(1)
C(28)	66(2)	58(2)	42(2)	8(1)	14(1)	22(2)

Table 5. Hydrogen coordinates (x 10^4) and isotropic displacement parameters ($Å^2$x 10^3) for **429**.

Atom	x	y	z	U(eq)
H(2)	4483	9352	2784	55
H(3A)	4197	5731	2172	31
H(3B)	4989	5896	2945	31
H(4)	6438	6076	1557	26
H(5)	8627	6667	2135	25
H(6A)	3596	8451	2054	34
H(6B)	5238	8681	1709	34

H(7A)	8395	6111	3314	34
H(7B)	8644	7060	3358	34
H(7C)	6955	6688	3477	34
H(8A)	8892	4451	2064	34
H(8B)	9423	5370	2077	34
H(10)	7030	4060	982	49
H(11)	6959	4056	-325	58
H(12)	8451	4989	-998	57
H(13)	9955	5980	-360	68
H(14)	10041	5974	935	52
H(15A)	9006	8038	2183	31
H(15B)	7590	8654	2132	31
H(17)	6582	7392	788	41
H(18)	6926	7585	-483	50
H(19)	8863	8509	-917	55
H(20)	10429	9208	-71	61
H(21)	10065	9026	1213	48
H(23)	1282	5757	3716	52
H(24)	1618	5484	4995	59
H(26)	4462	7451	5197	53
H(27)	4172	7740	3943	45
H(28A)	3855	6666	6270	66
H(28B)	2168	6269	6267	66
H(28C)	3660	5731	6101	66

Table 6. Torsion angles [°] for $C_{28}H_{31}NO_4S$.

C(15)-N(1)-C(1)-C(2)	174.65(18)
C(5)-N(1)-C(1)-C(2)	-9.3(3)
C(15)-N(1)-C(1)-C(6)	-2.8(3)
C(5)-N(1)-C(1)-C(6)	173.30(17)
N(1)-C(1)-C(2)-C(3)	-5.4(3)
C(6)-C(1)-C(2)-C(3)	171.77(19)
N(1)-C(1)-C(2)-S(1)	162.66(16)
C(6)-C(1)-C(2)-S(1)	-20.1(3)

O(4)-S(1)-C(2)-C(1)	144.93(18)
O(3)-S(1)-C(2)-C(1)	13.4(2)
C(22)-S(1)-C(2)-C(1)	-102.14(19)
O(4)-S(1)-C(2)-C(3)	-45.74(17)
O(3)-S(1)-C(2)-C(3)	-177.31(15)
C(22)-S(1)-C(2)-C(3)	67.19(16)
C(1)-C(2)-C(3)-C(4)	-14.7(3)
S(1)-C(2)-C(3)-C(4)	175.79(13)
C(8)-O(1)-C(4)-C(3)	174.12(16)
C(8)-O(1)-C(4)-C(5)	-65.1(2)
C(2)-C(3)-C(4)-O(1)	168.63(16)
C(2)-C(3)-C(4)-C(5)	46.6(2)
C(1)-N(1)-C(5)-C(7)	-83.0(2)
C(15)-N(1)-C(5)-C(7)	93.4(2)
C(1)-N(1)-C(5)-C(4)	41.6(2)
C(15)-N(1)-C(5)-C(4)	-142.09(17)
O(1)-C(4)-C(5)-N(1)	-178.11(15)
C(3)-C(4)-C(5)-N(1)	-60.0(2)
O(1)-C(4)-C(5)-C(7)	-54.6(2)
C(3)-C(4)-C(5)-C(7)	63.5(2)
N(1)-C(1)-C(6)-O(2)	-76.9(2)
C(2)-C(1)-C(6)-O(2)	105.8(2)
C(4)-O(1)-C(8)-C(9)	-59.1(2)
O(1)-C(8)-C(9)-C(14)	113.4(2)
O(1)-C(8)-C(9)-C(10)	-68.2(3)
C(14)-C(9)-C(10)-C(11)	0.2(4)
C(8)-C(9)-C(10)-C(11)	-178.2(2)
C(9)-C(10)-C(11)-C(12)	0.1(4)
C(10)-C(11)-C(12)-C(13)	-0.1(4)
C(11)-C(12)-C(13)-C(14)	-0.3(5)
C(10)-C(9)-C(14)-C(13)	-0.6(4)
C(8)-C(9)-C(14)-C(13)	177.8(2)
C(12)-C(13)-C(14)-C(9)	0.7(5)
C(1)-N(1)-C(15)-C(16)	-90.0(2)
C(5)-N(1)-C(15)-C(16)	93.8(2)
N(1)-C(15)-C(16)-C(17)	8.8(3)

N(1)-C(15)-C(16)-C(21)	-171.73(19)
C(21)-C(16)-C(17)-C(18)	-2.6(3)
C(15)-C(16)-C(17)-C(18)	176.9(2)
C(16)-C(17)-C(18)-C(19)	1.0(4)
C(17)-C(18)-C(19)-C(20)	0.9(4)
C(18)-C(19)-C(20)-C(21)	-1.1(4)
C(19)-C(20)-C(21)-C(16)	-0.6(4)
C(17)-C(16)-C(21)-C(20)	2.4(4)
C(15)-C(16)-C(21)-C(20)	-177.1(2)
O(4)-S(1)-C(22)-C(23)	-4.3(2)
O(3)-S(1)-C(22)-C(23)	122.05(19)
C(2)-S(1)-C(22)-C(23)	-118.1(2)
O(4)-S(1)-C(22)-C(27)	174.90(17)
O(3)-S(1)-C(22)-C(27)	-58.8(2)
C(2)-S(1)-C(22)-C(27)	61.1(2)
C(27)-C(22)-C(23)-C(24)	2.4(3)
S(1)-C(22)-C(23)-C(24)	-178.40(19)
C(22)-C(23)-C(24)-C(25)	-1.4(4)
C(23)-C(24)-C(25)-C(26)	-0.3(4)
C(23)-C(24)-C(25)-C(28)	179.3(2)
C(24)-C(25)-C(26)-C(27)	1.0(4)
C(28)-C(25)-C(26)-C(27)	-178.6(2)
C(25)-C(26)-C(27)-C(22)	0.0(4)
C(23)-C(22)-C(27)-C(26)	-1.8(3)
S(1)-C(22)-C(27)-C(26)	179.08(18)

Table 7. Hydrogen bonds for **429** [Å and °].

D-H...A	d(D-H)	d(H...A)	d(D...A)	<(DHA)
O(2)-H(2)...O(1)#1	0.84	1.97	2.800(2)	171.7

Symmetry transformations used to generate equivalent atoms:
#1 -x+1,y+1/2,-z+1/2

References for appendices:

1. Otwinowski, Z. & Minor, W. (1997). "Processing of X-ray Diffraction Data Collected in Oscillation Mode", *Methods in Enzymology*, Volume 276: Macromolecular Crystallograpy, part A, p. 307-326, C.W. Carter, Jr. & R.M. Sweet, Eds., Academic Press.
2. Hooft, R. (1998). *COLLECT*: Users Manual, Nonius B.V., Delft. The Netherlands.
3. Altomare, A., Cascarano, M., Giacovazzo, C.& Guagliardi, A. (1993). Completion and Refinement of Crystal Structures with SIR92. J. Appl. Cryst., **26**, 343-350.
4. Beurskens, P.T., Admiraal, G., Beurskens, G., Bosman, W.P., de Gelder, R., Israel, R. & Smits, J.M.M. (1994). The *DIRDIF-94* program system, Technical Report of the Crystallography Laboratory, University of Nijmegen, The Netherlands.
5. Sheldrick, G.M. (1997). *SHELXL97*- A Program for Refinement of Crystal Structures, University of Göttingen, Germany.
6. Flack, H. D. (1983). Acta Cryst. A39, 876.
7. Johnson, C.K. (1976). ORTEPII. Report ORNL-5138. Oak Ridge National Laboratory, Tennessee, USA.

Appendix XII Publications and Presentations

Research Publications:

(1) Back, T. G., Parvez, M., and Zhai, H., Rearrangements of the Diels-Alder Cycloaddition Products Obtained from Acetylenic Sulfones and 1,3-Diphenylisobenzofuran, *J. Org. Chem.* **2006**, *71*, 5254. I completed all of the synthetic research for this publication, under the supervision of Professor Back. Most of the results presented in Chapter 4 of this thesis were included in this article. Dr. Parvez solved five crystal structures for this work, which were useful in identifying the various products. The body of the manuscript was written by Professor Back. I wrote the experimental portion of this work, and also assembled the supporting information.

(2) Back, T. G., and Zhai, H., Cyclizations and Cycloadditions of Acetylenic Sulfones on Solid Supports, *Chem. Commun.* **2006**, *3*, 326. I completed all of the synthetic research for this publication, under the supervision of Professor Back. This was our preliminary communication of the results presented in Chapter 3 of this thesis, and focus on the first preparation of polymer-supported acetylenic sulfones, along with their applications to cyclizations. The body of the manuscript was written by Professor Back. I wrote the experimental portion of this work, and also assembled the supporting information.

(3) Back, T. G., Parvez, M., and Zhai, H., Stereospecific Rearrangements during the Synthesis of Pyrrolidines and Related Heterocycles from Cyclizations of Amino Alcohols with Vinyl Sulfones, *J. Org. Chem.* **2003**, *68*, 9389. I completed all of the synthetic research for this publication, under the supervision of Professor Back. Most of the results presented in Chapter 2 of this thesis were included in this article. Dr. Parvez solved four crystal structures for this work, which were useful in characterizing the various products. The body of the manuscript was written by Professor Back. I wrote the experimental portion of this work, and also assembled the supporting information.

Conference Presentations:

(1) Lecture: H. Zhai and T. G. Back, *Synthesis of Nitrogen Hetercycles Using Unsaturated Sulfones.* Presented at the Canadian Society for Chemistry's 2005 National Meeting, Saskatoon, SA on June 1, 2005. I conducted all of the research for this presentation, under the supervision of Professor Back.

(2) Poster: H. Zhai and T. G. Back, *Synthesis of Nitrogen Hetercycles Using Unsaturated Sulfones.* Presented at the second Banff Symposium on Organic Chemistry, Banff, AB on November 11, 2005. I conducted all of the research for this presentation, under the supervision of Professor Back.